Evaluación de desempeño de estrategias descentralizadas de operación de redes de distribución para la gestión de recursos energéticos distribuidos

Presentado por

Iván David Serna Suárez

Trabajo de grado para optar por el título de

Doctor en Ingeniería: Área Eléctrica

Director

Gilberto Carrillo Caicedo

Doctor Ingeniero Industrial

Codirector

Gabriel Ordóñez Plata

Doctor Ingeniero Industrial

Universidad Industrial de Santander

Facultad de Ingenierías Fisicomecánicas

Escuela de Ingenierías Eléctrica,

Electrónica y de Telecomunicaciones

Doctorado en Ingeniería: Área Eléctrica

Bucaramanga

2019

I may have wasted all those years
They're not worth their time in tears
I may have spent too long in darkness
In the warmth of my fears
And as I walk through all my myths
Rising and sinking like the waves
With my thoughts wrapped around me
Through a trial of tears
[...]

Still awake
I continue to move along
Cultivating my own nonsense
[...]

Still awake
Bringing change,
bringing movement, bringing life
A silent prayer,
thrown away, disappearing in the air
Rising
Sinking
Raining deep inside me
Nowhere to turn
I look for a way back home
It's raining, raining
Raining deep in heaven

–John Myung

Al pequeño corazón de bufonsita
que es ahora parte de mi alma,
y el cual nació del cálido amor que
una hermosa flor de primavera
brindó a una inerte quimera sin rumbo.

–Iván

Agradecimientos

Fácilmente podría llenar un documento con la misma extensión de esta tesis tan solo agradeciendo a todos aquellos que estuvieron apoyándome durante este proceso. Lamentablemente, sólo podré dar crédito a aquellos que por ahora se me vienen a la mente. Me disculpo entonces si he dejado a alguien sin su respectivo reconocimiento, la emoción del momento no ayuda a mejorar la memoria.

Quisiera darle en primer lugar mis agradecimientos a las personas mayormente afectadas por este trabajo, esto es, a mi amada flor de primavera, Margarita, y a mi amada corazoncita, Cordelita. Ellas realmente se han llevado la peor parte hasta la fecha. Afortunadamente, ambas son mujeres muy fuertes y pese a los desplantes y ausencias, creo yo que aún me quieren. Realmente me considero una persona muy afortunada por ser el receptáculo de tanto cariño.

Siguiendo con los parias de este proceso, no queda duda que los otros que han sufrido, esta vez quizás por mi terquedad, son los profesores Gilberto Carrillo y Gabriel Ordóñez. Tal vez la paciencia les llegó porque recuerdan que tan testarudo puede ser alguien cuando se encuentra trabajando en la tesis de doctorado. Como sea, no he podido tener mejor suerte y honor al tener la oportunidad de ser dirigido por estos dos grandes de la ingeniería eléctrica colombiana.

Las olas de la vida en ocasiones elevan, y en ocasiones, hunden. Durante mi estadía en Holanda del Sur, no hay duda que me encontraba a los pies de un tsunami. Por fortuna, mi contacto para realizar la pasantía fue Germán, una persona sumamente brillante y además de una calidad humana igualmente excepcional. Supongo que en este caso aquellos con tal inteligencia y calor humano se atraen, ya que el profesor Mathijs *comparte estas características con él. Los dos fueron estupendos tutores durante mi estadía en el Reino de los Países Bajos; muy comprensivos, pero más importante aún, muy críticos sobre aquello que les presentaba. Les he quedado en deuda a ellos, y en general a Holanda. Con mi florecita rockera siempre hablamos del momento en el que podremos tener nuestra revancha y retribuir un poco a estas dos maravillosas personas, y a ese gran Reino.*

Tras bambalinas, el profesor Johann, César y Óscar estuvieron siempre muy atentos a colaborarme en lo que necesité. Aprovecho entonces para agradecerles a ellos también, ya que su ayuda fue clave para poder finalizar mi tesis de manera exitosa. Además, quisiera aprovechar para agradecer el compromiso con el cual mis evaluadores (el profesor Tomás, Juan José, César, Óscar y Javier) tomaron el trabajo de revisar mi tesis. Todos sus comentarios fueron muy acertados, y adicionalmente, durante la defensa, gracias a sus preguntas creo que pude dar una visión muy completa de mi trabajo.

Terminando con los agradecimientos a mis maestros, quisiera confesar aquí que lloré la caída del Titán de Colombia. Me percaté lo importante que había sido en mi vida cuando me llené de tristeza al saber que jamás podría escuchar más sus consejos e historias. Gracias a él desde muy temprana edad supe que en verdad si algo se quiere hay que luchar, que hay aves negras por doquier; me enseñó a navegar por un mar de sed, a ser fiel a la promesa, a ser como el aire, ser como el fuego, ser agua y tierra, ser símbolo y huella; a brindar por ser humano, a nunca mentirme. Y aunque ya tengo los ojos cansados, seguiré su consejo, y no me detendré, pues aún faltan muchos sueños por alcanzar. Gracias maestro, gracias Titán.

Demasiada nostalgia me invade, el tiempo se acaba y debo ya cerrar. Doy gracias a todos mis viejos y nuevos compañeros en la Universidad Industrial de Santander; a todos mis pupilos por su confianza; a mis compañeros en la Universidad de Santander, y a todos aquellos que he conocido en este camino. A mis padres, que no dejan de brindarme su cariño pese a lo ingrato que a veces soy. A mi familia biológica y a aquella familia que me ha abierto las puertas de su hogar, por estar siempre dispuestos a brindarme afecto y comprensión cuando más lo necesito. Y finalmente, a todos mis maestros muertos y en vida que a través del arte me han enseñado a navegar por este profundo y abismal océano que es la vida.

Contents

List of Figures

List of Tables

LIST OF APPENDICES

RESUMEN

TÍTULO:

Evaluación de desempeño de estrategias descentralizadas de operación de redes de distribución para la gestión de recursos energéticos distribuidos.[1]

AUTOR:

Iván David Serna Suárez[2]

PALABRAS CLAVE:

Redes de distribución activas, recursos energéticos distribuidos, sistemas de gestión de la energía, energía renovable.

DESCRIPCIÓN:

El aumento de la penetración de la energía solar fotovoltaica plantea varios desafíos para el funcionamiento de las redes de distribución, principalmente porque una alta penetración de este recurso podría causar problemas de confiabilidad. Por lo tanto, para explotar eficientemente estos recursos energéticos distribuidos (DERs), se ha propuesto una transición hacia una operación "Activa" de las redes de distribución. Entre los desafíos para implementar lo que se llama un "Sistema de Distribución Activo" (ADN), esta tesis se enfoca en la programación óptima de los DER, específicamente, en la solución del flujo de potencia óptimo (ACOPF) trifásico relacionado con este problema. En este último, el estado del arte a menudo se limita a modelos unifilares e ignora algunas características claves de las redes de distribución. Además, recientes avances en la optimización convexa plantean la posibilidad de descentralizar completamente la toma de decisiones en los ADN, lo que podría aumentar la resiliencia y la escalabilidad de la red. Para comprender los límites de las soluciones del ACOPF trifásico y evaluar el desempeño de las estrategias descentralizadas en los ADN, se presenta un estudio exhaustivo sobre la programación óptima de DERs en redes de distribución desbalanceadas. Además, se presenta un novedoso algoritmo para resolver el ACOPF trifásico como una secuencia de problemas de optimización cuadráticos restringidos cuadráticamente. Dicha formulación puede resolver el problema de programación óptima de DERs de manera centralizada o descentralizada, conlleva a un menor desbalance en el voltaje y un menor tiempo de cálculo que su contraparte no lineal. Además, converge a un punto factible para el problema primal de la formulación no lineal, sin mayores sacrificios en optimalidad. Gracias al estudio, se presentan algunas ideas clave sobre cuándo y por qué incluir modelos trifásicos, y la relación entre las funciones objetivo del problema, los contraflujos de potencia y la capacidad máxima en la red para albergar DERs.

[1] Trabajo de grado.

[2] Facultad de Ingenierías Físico-Mecánicas. Escuela de Ingenierías Eléctrica, Electrónica y de Telecomunicaciones. Director: Gilberto Carrillo Caicedo. Codirector: Gabriel Ordóñez Plata.

ABSTRACT

TITLE:

Performance evaluation of decentralized operation strategies of power distribution networks for distributed energy resource management [3]

AUTHOR:

Iván David Serna Suárez[4]

KEY WORDS:

Active Distribution Networks, Distributed Energy Resources, Energy Management Systems, Renewable Energy.

DESCRIPTION:

The increase of solar photovoltaic penetration poses several challenges for distribution network operation, mainly because such high penetration might cause reliability problems. Thus, to efficiently exploit these Distributed Energy Resources (DERs), a transition towards an "Active" operation of distribution networks has been proposed. Among the challenges to implement what is called an "Active Distribution System" (ADN), this thesis focuses on the optimal resource allocation of DERs, specifically, on the solution of the 3-phase optimal power flow (ACOPF) related to this problem. On the latter, the current state-of-the-art often is limited to one-line equivalent models, and it ignores some key characteristics of power distribution networks. Furthermore, recent advances in convex optimization pose a question about the possibility of fully decentralize the decision making in ADNs, thus increasing the resiliency and scalability of the network. To understand the limits of the 3-phase ACOPF solutions and to evaluate the performance of decentralized strategies in ADNs, it is presented a comprehensive study on optimal DER scheduling in unbalanced distribution networks. Additionally, it is presented a novel algorithm to solve the 3-phase ACOPF as a Sequence of convex Quadratically Constrained Quadratic Programs. Such formulation can solve the DER allocation problem in a centralized or decentralized way, it leads to a lower voltage unbalance and computation time than its non-linear counterpart. Also, it converges to a primal feasible point for the non-linear formulation without major sacrifices on optimal DER active power injections. From the comprehensive study, it is presented some key insights on when and why to include 3-phase models, and the relationship between the problem objective functions, the reversed power flows and the maximum DER capacity in the network.

[3] Research work.

[4] Faculty of Physical-Mechanic Engieneering. School of Electrical, Electronical and Telecommunications Engineering. Advisor: Gilberto Carrillo Caicedo. Co-advisor: Gabriel Ordóñez Plata.

INTRODUCTION

This chapter presents the context, motivation, problem, and questions of the research. For this sake, it is briefly described the electric power system structure, the effects of the inclusion of distributed energy resources in power distribution networks and the role of active distribution networks as a technological framework for exploiting them efficiently. Afterward, the research problem and questions are presented, to then give an outline of the document.

Electric power systems

The energy supply chain consists of three stages: 1) Generation, where the energy is transformed from one type (e.g., chemical energy in fossil fuels, kinetic energy of the wind, or potential energy of water in a dam) to electrical energy; 2) Transmission, where the energy is transported across long distances to reach the consumption centers; 3) Distribution, where the energy is delivered to the customers. Figure 1 presents a simplified version of these stages and how they are connected.

Figure 1: Simplified description of the electric power system. Adapted from (Brown, 2009) and (Algarni, 2009).

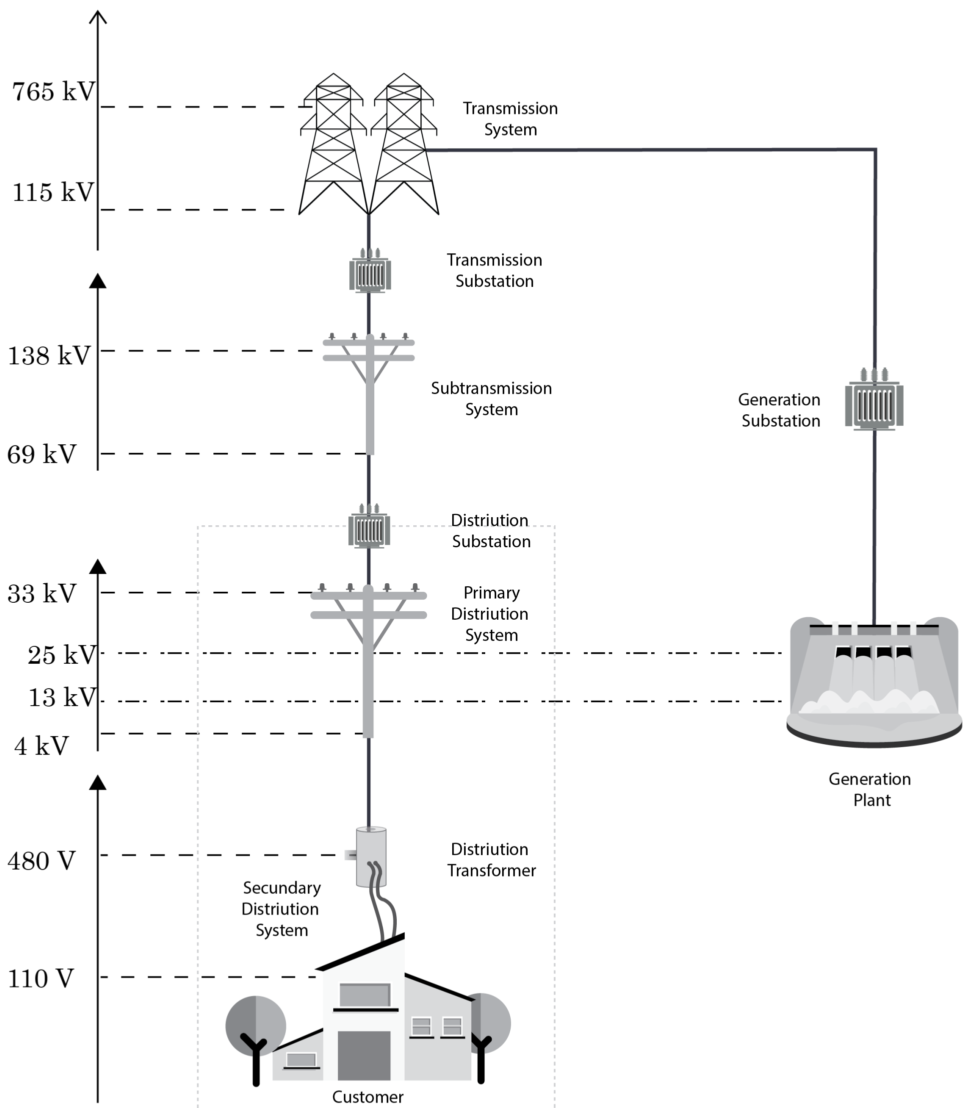

Broadly speaking, the infrastructure needed consists of generation plants and substations; transmission lines, transformer substations, and switching stations; and distribution lines, substations, and switching equipment. How these elements are built and interact are defined in a planning step usually with a scope of minimum a couple of years and maximum one decade or two. After they are built, electrical energy systems must be adjusted and maintained. These actions are defined in a planning step usually with a scope of minimum a couple of months and maximum one year.

Once electrical energy systems are built, they must be continually monitored and adapted as needed. Therefore, the electrical energy system must be under careful surveillance to achieve its main goal, which is to supply the customers' electrical energy needs. Real-time control and operation of the electric system are performed by system operators located in control centers. Their main goal is to monitor and coordinate each of the interventions needed to satisfy the electrical energy demand.

A control center in a transmission system is constantly monitoring power injections, for example, to maintain the voltage magnitude at each node within the recommended limits and to maintain always the required balance between generated and consumed power. A short-term planning stage spanning from a couple of days to a couple of weeks is needed to achieve this. The main idea is as follows: Given a forecast of the energy consumption and the energy available for each generation connected in the system for a given period of time, a decision making process is run to known the set of feasible power injections needed to satisfy the energy demand. So, one of the inputs that control center personnel need is the power injections for each available generation plant connected to the network, i.e., the power generation schedule.

A few decades ago, a control center in a distribution system would not have to deal with generation scheduling, however, due to the increase of local generation, power distribution networks are in a transition towards a more dynamic scenario, where energy is not only consumed but also generated.

The focus of this document is on the importance of a proper control reference for local generation power injections in a power distribution network, i.e., on the importance of Distributed Energy Resource (DER) scheduling in power distribution networks.

Distributed energy resources

A Distributed Energy Resource (DER) can be defined as any source of electric power not directly connected to a bulk power system, thus, it includes local generation (e.g. from a renewable energy source) and storage systems as well (Standars Coordinating Committee, 2018). Note that a Plug-In Electrical Vehicle can behave as a DER when used in the Vehicle-to-Grid operation mode (in contrast, it behaves as a controllable load if Grid-to-Vehicle operation mode is used instead). Also note that, for a DER to be considered as such, some energy conversion process (e.g., electrical, thermal, chemical, mechanical or radiation energy to electrical energy) must be undertaken. With this in mind, all equipment traditionally used to improve the power and service quality of the electrical energy distribution (e.g., capacitor banks, uninterruptible power sources, and custom power devices) usually are not treated as DERs; Table 1 presents some typical generation considered as DER.

Table 1: Typical power distribution network Distributed Energy Resources.

Conversion (Chowdhury et al., 2009)	*Storage* (Diaz-Gonzalez et al., 2012)
Wind energy conversion systems	Pumped hydro
Solar Photovoltaic systems	Compressed air
Small-scale hydroelectric systems	Electrical
Biomass conversion systems	Hydrogen
Microturbines	Flywheel
Fuel cell conversion systems	Supercapacitors
Diesel generation plants	Magnetic (superconducting coils)

Integration of DERs to the power distribution network allows them to supply the electrical energy needs locally. As a consequence, intensive use of the bulk transportation system can be avoided; moreover, these kinds of devices provide the required flexibility to change demand profiles –from the network operator point of view and without changing the total consumed energy.

The addition of DERs to the energy chain in a power distribution network has been of special interest not only because of their technological or environmental appeal but also because of the benefits system participants can get. For example, an independent Distribution Network Operator (DNO) could use a combination of DERs to reduce the losses in the system or to reduce the system congestion on high demand hours, thus allowing some distribution network upgrades to be deferred in time (Quezada et al., 2006; Gil and Joos, 2008), whereas a retailer with several DERs may use them to provide ancillary services or to make some profit by taking advantage of daily energy price variations (Gil and Joos, 2008; C6.19, 2014; C6.11, 2011). Moreover, as the number of network participants increases, the need for a Distribution Market Operator (DMO) becomes evident. In turn, this motivates the creation of the Distribution System Operator (DSO), i.e., an agent that include the functions of the DNO and the DMO (Katiraei et al., 2008; C6.19, 2014). Further details on DER benefits and distribution system agents can be found in Annex A.

The addition of DERs to the energy chain also motivates the creation of the *prosumer*, i.e., a consumer with the capability of injecting power to the network; the *demand response*, i.e., the capability of a demand to react to electricity price changes or to any other external signal of choice; and the *virtual power plant*, i.e., a set of coordinated DERs (scattered through the network) able to supply services in the network as it were a single entity (C6.11, 2011; Bahramirad et al., 2016; Saboori et al., 2011); the latter is similar to the microgrid definition (Lasseter, 2002), being the main difference that, unlike virtual power plants, the power injections of microgrid DERs can be considered to be concentrated at one node.

Nevertheless, in exchange for these benefits, the load predictability is lost, either by the inclusion of supply uncertainty that comes with some renewable resources or by the increase of freedom that customers/retailers can obtain thanks to storage devices. This increase in uncertainty makes the operation of power distribution networks harder. Actually, studies on the inclusion of uncertainty in power distribution networks with renewable generation is a very challenging topic (Capitanescu, 2016), and the discussion about how DERs and local demand should be aggregated to assure a reliable operation under such uncertain conditions is just beginning (Loukarakis et al., 2015b).

Besides, because distribution networks are operated with a radial topology, reverse flows (i.e., power flowing from the network to the header) from DERs may cause protection and regulation device malfunctioning (Mortazavi et al., 2015). A direct solution to this problem is to add a protection device where the local generation is connected to the network, but even for simple cases, a new coordination scheme must be designed to assure the correct behavior of the entire protection system (Che et al., 2014; Laaksonen, 2010). Hence, legacy power distribution networks must evolve to include DERs without losing system reliability (Lopes et al., 2007).

Active Distribution Networks

One possible solution to tackle the uncertainty and reliability issue that comes with the integration of DERs is to change the way the power distribution network is operated: from a passive and one-directional (radial) flow perspective to an active and bi-directional flow perspective. An Active Distribution System (ADN) can be described through three key characteristics: Activeness itself, and automatic and coordinated behavior.

First, for a distribution network to be considered as «active» the system must be able to handle the changes that are occurring over a given time window. Specifically, this document is interested in power injection changes over a day of operation due to variations in the electrical generation (from DERs) or demand. So, for example, for a time window of one day, a power distribution network with automatic on load tap changer can be considered as «active».

This example brings to the picture the second key characteristic of an ADN: The autonomous behavior. Of course, an on load tap changer is not designed to handle the constant variations produced by changes in power injections of some kind of DERs (Dall'Anese and Simonetto, 2018); moreover, such variations increase the maintenance costs, thus incurring in operational inefficiencies and inducing unsafe operating conditions (Hossain et al., 2016).

At this point, it is worth noting that some «activeness» can be added to the distribution network by implementing the usual active measures to solve power quality problems, e.g., custom power device and active filter deployment. However, these measures cannot solve the problems arising due to bi-directional power flows.

To cope with bi-directional power flows, it is needed the third characteristic: coordinated behavior. Therefore, an ADN can handle bi-directional power flows by coordinating DER power injections, thus, making them also responsible for system support (C6.11, 2011) while increasing network reliability and resiliency.

In conclusion, because local energy resources require automatic and coordinated actions to be taken in few minutes –due to the increase in the uncertainty (Lopes et al., 2007; Gill et al., 2014; Siano et al., 2010), an Active Distribution Network (ADN) can be defined as a power distribution network that can handle pervasive energy resources (C6.11, 2011). Among the crucial ADN enabling technologies are then the power electronics (for power injection flexibility), and adequate metering and communication infrastructure (for equipment coordination) (C6.11, 2011).

Some of the most common functionalities of ADNs are Voltage-VAR control, peak load shaving and/or shifting, automatic network reconfiguration, fault ride through of local generation and coordinated dispatch of DERs (C6.11, 2011). This document is focused on the latter problem, i.e., on how to compute the control set-point for each DER power injection in a distribution network.

Operation strategies

The component of an ADN in charge of computing the control set-point for each DER power injection is called Energy Management System (EMS) –A detailed description of Active Distribution System's EMS can be found in Annex B. Formally, an EMS is «[...] a collection of control strategies and operational practices, together with the hardware and software to accomplish the objectives of energy management.» (Kirkham et al., 1981). Keeping it simple, the present document is interested in how to compute the control set-point for each DER power injection. Any software or hardware implementation of a fully functional EMS is out of the scope.

Now, let us define an operating point as the set of values that each DER must follow to guarantee a feasible allocation of the available energy resources. The efficiency of the operating point is assured by using a formal decision making strategy, often related but not limited to the solution of an optimization problem (see Annex B). To compute an efficient operating point there are two main strategies:

Centralized operation strategy Calculations are made using all information available in the network. Once a solution is attained, set-points are broadcast to its respective DER. Here, even if calculations are made in parallel, a central computation element has to recollect and broadcast all the information. In this sense, DERs are being controlled by the central computation element; this kind of strategy is sometimes known as *hierarchical control* (Bhaskara and Chowdhury, 2012, p.3).

Decentralized operation strategy Calculations are made using local information and coordination rules; information is usually privately known by each DER or set of DERs, while the coordination rules specify how and what information must be exchanged. For this kind of strategy set-points can be calculated concurrently, and since every DER (or set of DERs) calculates its own operating point based on local measurements of physical variables, this kind of strategy is sometimes known as *autonomous control* (Bhaskara and Chowdhury, 2012, p.3).

For both operation strategies, the EMS needs at least three control layers to coordinate DERs in an ADN (Figure 2 shows a hierarchical representation of the ADN control layers, Figure 3 depicts a one-line representation of an ADN with its control layers, and Table 2 summarizes each of the controllers usual functionalities).

Figure 2: Hierarchical representation of ADN's control layers.

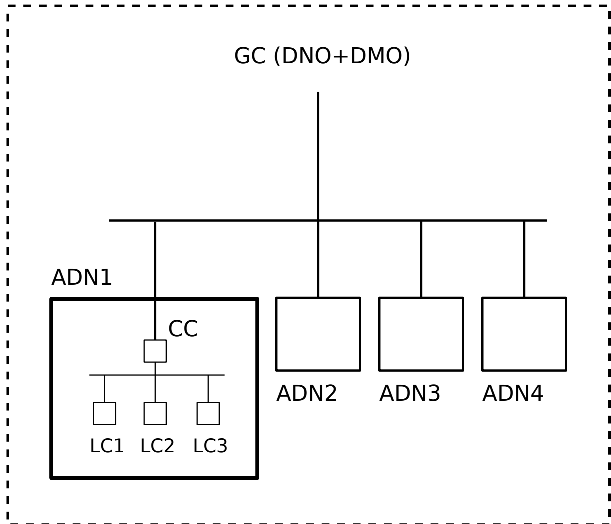

In the deepest layer is the Local Controller (LC), in the middle layer is the Central Controller (CC), and in the highest layer is the Global Controller (GC) which includes the functions of the Distribution Network Operator (DNO) and the Distribution Market Operator (DMO). Adapted from (Katiraei et al., 2008).

Figure 3: One-line representation of the control layers of an Active Distribution Network (ADN).

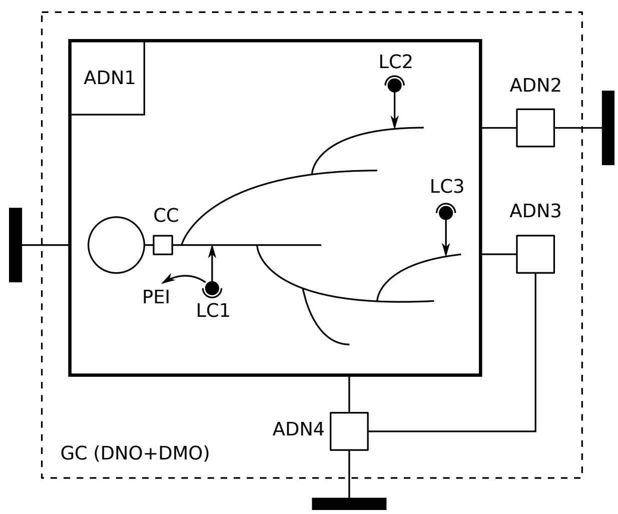

The deepest layer is the Local Controller (LC), which use a Power Electronic Interface (PEI) to give flexibility and fast response to its embedded functions; then is the Central Controller (CC); and on the highest layer, it is the Global Controller (GC) which includes the functions of the Distribution Network Operator (DNO) and the Distribution Market Operator (DMO). Black rectangles are connections to the transmission system.

Local controller This is the deepest control layer. Its main function is to control all relevant physical variables at the Point of Common Coupling (PCC), i.e., the electrical point of connection with the network. The control of the physical variables given a set-point is done through a DER Interface, which has as a main characteristic the flexibility, e.g.

in a power distribution network, the DER Interface is the so-called Power Electronic Interface (PEI) (Katiraei et al., 2008). For both types of operation strategies, the Local Controller (LC) uses local measures and the given set point to control the physical variables without any interaction with other LC nor control layer (Chowdhury et al., 2009, p.6). In contrast, how the local controller acquires the set-point depends on the strategy: with a *centralized operation strategy*, the LC operating point is communicated from the upper control layer; whilst in a *decentralized operation strategy*, the LC set point is updated by running a local decision process and by sharing information with other LCs. In the latter case, if there is no LC to communicate such information, the local set-point will always tend to a local efficient operating point, otherwise, an efficient operating point for all the connected neighbors will be sought (Katiraei et al., 2008, p.63). Such operating points are a consequence of additional functions embedded in the LC and can be used to accomplish specific tasks, e.g. load tracking, demand side management, storage system management or energy bidding.

Central controller This is the middle control layer. With a centralized operation strategy, the Central Controller (CC) communicates to each local controller in the ADN all relevant information for efficient operation, such as the operation set-point and the price of the energy resources (Katiraei et al., 2008, p.63). For a decentralized operation strategy, the latter is not needed. Nevertheless, for both strategies, the set-points are computed according to the network and DER characteristics, and according to the upper layer guidelines (e.g., the objective function to be minimized). Additionally, the CC must (Chowdhury et al., 2009, p.8):

- Run system diagnostics with the available information –retrieved from local controllers and measure at the header of the network.
- Ensure coordinated operation with the transmission system or other ADNs –maintaining the power exchange according to prior agreements.

Global controller This is the upper control layer. It is composed by a Distribution Network Operator (DNO) and a Distribution Market Operator (DMO) (Katiraei et al., 2008, p.62). The DNO coordinates the operation of several ADNs in an area by adjusting the operating point at network header of each ADN or by establishing the operation requirements, for example, to assure a secure transmission system operation or to assure a reliable operation for each of the ADNs in the area. On the other hand, the DMO takes care of the market functions of each ADN in the area, moreover, it also acts as an intermediary between the central energy pool and each ADN. In general, the DMO gives operational and administrative support for every transaction in the area. Note that all information exchanged between the global controller and an ADN is done through the central controller.

Table 2: ADN functions according to the type of controller and for each operation strategy.

Controller	Operation strategy	
	Centralized	Decentralized
Local	Control of the physical variables, load tracking, fault ride through of local generation.	Control of the physical variables, load tracking, fault ride through of local generation, Voltage-VAR control, peak load shaving and/or shifting, demand side management, storage system management (in general coordinated dispatch of DERs and controllable loads), and energy bidding.
Central	Power distribution system diagnosis and coordinated operation with the transmission system and other ADNs, Voltage-VAR control, peak load shaving and/or shifting, demand side management, storage system management (in general coordinated dispatch of DERs and controllable loads), and energy bidding.	Power distribution system diagnosis and coordinated operation with the transmission system and other ADNs.
Global	Operational requirements definition and broadcasting, and operational and administrative support for every electrical energy transaction in a given area.	Operational requirements definition and broadcasting, and operational and administrative support for every electrical energy transaction in a given area.

Still there is no consensus on which of the two operation strategies (centralized or decentralized) must be used to efficiently allocate the local energy resources of ADNs. For example, typical disadvantages of fully centralized controls are high communication requirements and information privacy problems. Also, as this kind of control needs all information to be gathered by a single entity, there can be problems with the reliability and the efficiency of the operation if the main communication with such entity were broken (Binetti et al., 2014; Gharavi et al., 2015).

In this context, the deployment of decentralized controls to manage DERs in an ADNs seems to be a promising alternative. For example, a decentralized operation strategy would always try to find an efficient allocation of the total energy available for the set of subsystems that are sharing information in the ADN (Kulasekera et al., 2011; McArthur et al., 2007b). Therefore, if one ADN subsystem cannot send information to the other subsystems, this isolated subsystem will allocate efficiently its available energy resources automatically and without any further changes in the communication protocol nor the local controller logic; while the remaining subsystems would try to efficiently allocate the remaining energy resources –also automatically and without changes in the communication protocol nor the local controller logic. Such events must be implemented in advance in a centralized operation in order to obtain a similar outcome. Hence, decentralized controls can be considered as more resilient and scalable than the centralized controls.

In addition to this remarkable difference, decentralized operation strategies can take advantage of the structure of power distribution systems to allow local DERs connected to the network to have plug-and-play functionality. This further increases the network scalability (Capitanescu, 2016), i.e., decentralized controls can handle the growth of electrical networks with little changes on the core computations. Moreover, akin to centralized approaches, these strategies can be adapted to handle energy resources uncertainty (Bazrafshan and Gatsis, 2016; Zhang and Giannakis, 2015) and can be easily coupled with other functions of power distribution networks as system protection (Pipattanasomporn et al., 2009), risk analysis (Capitanescu, 2016), reactive power management on unbalanced systems (Robbins and Dominguez-Garcia, 2015; Zheng et al., 2016) and market clearing (Zhang and Giannakis, 2015; Loukarakis et al., 2015a,b; Zheng et al., 2015). Therefore, decentralized operation strategies can be used to find an efficient allocation of local energy resources, thus increasing the resilience and scalability of ADNs.

Problem formulation

Current (passive) measures that have been developed to handle high DER penetration in legacy power distribution networks (like those based on load-to-generation ratio limits in circuits, thermal limits of equipment, voltage magnitude limits and aggregated short-circuit capacity in circuits) do not seem to adequately predict network use (C6.24, 2014), furthermore, such passive measures can result in counterproductive outcomes. For example, given a small voltage violation, on/off strategies implemented to avoid voltage rise may cause a total loss of DER generation (Ferreira et al., 2013). Moreover, because of the increase in the duty cycle, such abrupt change in local generation may diminish durability and increase maintenance costs of automatic on load tap changers and static voltage regulators (Hossain et al., 2016). In general, actual planning practices for distribution network design could impose a barrier for further development of renewable energy and non-conventional loads (C6.19, 2014). Thus, distribution networks require decision making strategies able to find proper set-point for DER power injections to fully exploit local energy resources (Katiraei et al., 2008; Chowdhury et al., 2009; C6.24, 2014).

An Active Distribution Network's (ADN) Energy Management System (EMS) can handle this decision making process. Besides, a decentralized operation strategy seems to be a very suitable choice to allocate energy resources in an ADN, because of the inherently distributed nature of DERs and the added resiliency that offer this type of operation strategies.

Amidst the available alternatives to computing the set-points for DER power injections (see sections B.3.2 and B.3.3), mathematical programming appears as a very strong alternative. The reason is twofold:

1. Convex Programming problems can be solved very efficiently with the current techniques (Grant et al., 2006). Moreover, advances in convex programming have extended the range of non-linear problems that can be solved as convex programs (Madani et al., 2016; Lesieutre et al., 2011; Madani et al., 2015; Coffrin et al., 2016).[5] This may enable EMSs to efficiently allocate energy resources within a few minutes, a very important requirement due to the uncertainty in the power injections of some kinds of DERs.

2. Interactions between local controllers given a decentralized operation strategy can lead to intractable behavior if not well designed. Furthermore, to prove that the resulting allocation exploits efficiently the available energy resources could be challenging (Wooldridge, 2009). As a way to design tractable interactions and to assure the efficiency of the allocation, it can be used a decentralized solution based on mathematical programming. How local controllers interact can be derived directly from the decomposition technique used; and in case of using a dual decomposition technique, the al-

[5] For example, using Second Order Cone Programming or Semidefinite Programming, one could find a convex model that leads to an exact approximation of a non-linear model, i.e., a convex model that yields the same answer than the non-linear model.

location efficiency can be assured for convex optimization problems because convex problems have zero duality gap[6], i.e., the solution of the dual and primal problem are the same.

A decentralized solution also may be derived by taking advantage of the primal problem structure. However, when applied to the ADN energy allocation problem, proposed models are non-convex, therefore, the attained optimum is often limited to specific cases (Christakou et al., 2017a; Mhanna et al., 2018). This lack of a formal proof for a general case is just a consequence of the complexity of the problem being solved.

Dual and primal decomposition for power distribution networks have been already applied to one-line equivalents of distribution networks and transmission networks, nevertheless, such models may ignore the following three features of distribution networks:

1. *The 3-phase set of voltage and currents are unbalanced*, as a consequence, higher active power losses are expected, furthermore, beyond the recommended minimum, system unbalance might be harmful to any device connected to the network (Liao and Milanovic, 2017).

2. *The R/X ratio in distribution lines is greater than the R/X ratio in transmission lines*, as a consequence, system losses cannot be neglected, moreover, approximations based on the high dependency between voltage angle (magnitude) and active (reactive) power must be taken carefully.

3. *The load models depend on the connection and steady state voltage variations*, e.g., to characterize a distribution load one must clarify the number of phases at which is connected (one-phase, two-phase, three-phase load); how it is connected to the network (phase-to-ground, phase-to-phase, *wye* or *delta*); and how it behaves to changes in steady state voltage (constant impedance, constant current, or constant power). Furthermore, a load with a mixture of these three basic types is called a ZIP load.

Assuming that the high R/X ratio is not a problem, modeling only one phase might be useful for almost balanced distribution networks. However, as long as there is enough unbalance, one-line equivalents cannot describe the behavior of the elements causing the unbalance nor the consequences of such unbalance to the network.

As a conclusion, since a single-phase Alternating Current Optimal Power Flow (ACOPF) might not be enough for analyzing ADN behavior, a 3-phase Alternating Current Optimal

[6]Given that the Slater's constraint qualification holds (which is often the case), i.e., that for at least one feasible point all inequalities are strictly satisfied. Slater's condition is a sufficient (although not necessary) condition for strong duality of convex problems.

Power Flow (3ϕ-ACOPF)[7] is needed to cope with all characteristics of ADNs, and in turn, an exact convex approximation of the 3ϕ-ACOPF is required to guarantee the convergence and tractability of the decentralized computation of DER power injection set-points; but, *Is it possible to derive a decentralized operation strategy for optimal allocation of local energy resources in power distribution networks based on a convex approximation of the* 3ϕ-ACOPF *problem?*

Research goals and questions

This document main motivation is to analyze how to compute the set-points for DER power injections in a decentralized way using mathematical programming and considering all three key features of power distribution systems presented in the previous section (see page 30). Two research goals are proposed to achieve this:

(G-I) To characterize the decentralized decision taking for distributed energy resource allocation in an active power distribution network.

(G-II) To propose a comparative analysis of decentralized strategies for distributed energy resource allocation in an active power distribution network.

With the first goal, it is expected to identify the core components of a decentralized set-point computation, whereas, with the second goal, it is expected to compare the resulting allocation from a decentralized method against a centralized method.

Now, to compute the set-point in a decentralized way using mathematical programming, it is necessary to find a convex solution for the 3ϕ-ACOPF or/and to exploit somehow the problem structure. With this in mind, two main questions guide the discussion here presented on optimal power flow for distribution networks and its decentralized solution:

(Q-I) What are the limits and characteristics of the 3ϕ-ACOPF?

(Q-II) Is it possible to have an exact convex relaxation of a 3ϕ-ACOPF?

The first question helps to answer the latter, and in turn, the second question is the key to formulate a decentralized solution for 3ϕ-ACOPF.

[7] Objective functions for this optimization problem depend heavily on the network participant to be analyzed, although often are focused more on the DNO, e.g., load curtailment minimization to safely operate the network and optimal reactive dispatch for losses minimization (Zheng et al., 2016; Bruno et al., 2011). Also, it is common to see photovoltaic energy curtailment minimization (Meng et al., 2017; Su et al., 2014) as an objective.

Outline

This document has two preliminary chapters and three parts. The preliminary chapters are composed of this chapter and chapter one:

Chapter 1 presents a state-of-the-art on optimal power flow for distribution networks. The main goal of this chapter is to see to what extent (Q-I) and (Q-II) has been already answered and to settle the bases from which goal (G-I) could be developed. So, first are presented the non-linear formulations that are used to solve the 3ϕ-ACOPF –including some ideas from transmission network ACOPF. Then, solutions based on quadratic non-convex and convex programming are presented, along with some decentralized solutions to the ACOPF based on mathematical programming. The chapter closes with a discussion about what is lacking the current literature, what does it tell us about the path to choose when formulating a 3ϕ-ACOPF, and how this may help to answer (Q-I) and (Q-II) and achieve goals (G-I) and (G-II).

The first part is devoted to non-linear modeling and scheduling of DERs and it ranges from chapter two to three:

Chapter 2 describes a non-linear model for the 3ϕ-ACOPF. The main goal of this chapter is to present a mathematical model that accounts for all three distribution network key features presented in the previous section (see page 30). This chapter contribution is a 3ϕ-ACOPF formulation that allows the inclusion of constant impedance and constant current load models as linear constraints, thus moving away from the polynomial ZIP model (common in the Current Injection Method formulations) without losing the capability of including a ZIP load. Besides, the presented formulation includes node voltage and current injections as decision variables, hence, allowing the inclusion of *delta* loads without the need of *wye* equivalents. Moreover, storage systems are included without the need of discrete variables. Overall, this model is a three-phase extension of the non-linear formulation in (Castillo et al., 2016b) and the storage model in (Gill et al., 2014).

Chapter 3 presents a discussion on optimal DER scheduling. The main goal of this chapter is to clarify some of the open problems regarding the effect of DERs in distribution networks and related to (Q-I). This chapter main contribution is an analysis of individual and combined effects of photovoltaic curtailment and storage dispatch on power distribution networks for several objectives and under perfectly balanced and unbalanced conditions. All DER schedules for each of the 144 cases are computed by solving an instance of the 3ϕ-ACOPF described in chapter 2. The main conclusions from this study are: (1) the objective function chosen is very important to assure the "almost balanced" conditions needed for some 3ϕ-ACOPF formulations; (2) the similarities between the answers given by balanced and unbalanced models depend mainly on DER penetration; and (3) the system unbalance can be larger than the recommended minimum for high DER penetrations, however, a lower unbalance solution can be found without major sacrifices in the optimal power injections.

The second part is composed by chapter four and five, and it presents how can be derived an exact convex approximation for the 3ϕ-ACOPF and its applications:

Chapter 4 describes a novel convex formulation to solve the 3ϕ-ACOPF as a Sequence of Convex Quadratically Constrained Quadratic Programs. The main goal of this chapter is to present a novel mathematical model that can answer (Q-II), therefore, this chapter contribution is the novel convex formulation for the 3ϕ-ACOPF that accounts explicitly for all three distribution network key features presented in the previous section (see page 30).

Chapter 5 presents two applications of the novel formulation from chapter 4. The main goal of this chapter is to quantify the performance of the centralized and decentralized solutions of the 3ϕ-ACOPF using the novel formulation presented in chapter 4. Therefore, this chapter contributions are twofold: In first place, It is shown that the proposed formulation can compute a DER schedule that is a primal feasible point for the non-linear formulation. Also, it is shown that the presented formulation is computationally more efficient than the IP method used as reference, and that it implicitly leads to a lower voltage unbalance. In second place, it is explained how such formulation can help to design a decentralized operation strategy for optimal DER scheduling. The fundamental elements of a decentralized solution are explained comparing the scaled form of the Alternating Direction Method of Multipliers (ADMM) with methods in the reviewed literature, achieving then goal (G-I). Later, a decentralized operation strategy is designed and tested against the two centralized methods already presented in previous chapters to compare their performance, achieving then goal (G-II).

The third and final part is composed of the chapter 6, the bibliography and the appendices. Chapter 6 summarizes all the contributions and consequences of this research as well as some concluding remarks about optimal power flow for distribution networks and its solution. Also, there are presented some questions left for future researches. Finally, a survey on ADN EMSs and benefits are left as annexes, as well as the result of the power flow for each tested feeder used.

FURTHER READING

The following references can be consulted to get a detailed description of each of the topics briefly described in this chapter: For a concise introduction to electrical system basics please refer to (Blume, 2007). For a description of the infrastructure and a gentle introduction to electric power planning please refer to (Brown, 2009; Mazer, 2007; Seifi and Sepasian, 2011). For a description of power distribution network planning please refer to (Willis, 2004). For a description of some distributed energy resources and a complete list and description of each of the functions of active distribution networks, please refer to (Chowdhury et al., 2009; C6.11, 2011). For a description of storage technology please refer to (Diaz-Gonzalez et al., 2012). For a comprehensive study of the regulation and planning challenges that the electric power sector is facing with the inclusion of distributed energy resources please refer to (Perez-Arriaga et al., 2016). For a description of the functions of power distribution network's control centers please refer to (Brown, 2009; Blume, 2007). For a description of each of the elements related to power system operation and analysis, please refer to (Gomez-Exposito et al., 2018). For a comprehensive survey on ADN definitions and functionalities please refer to (C6.11, 2011), while a deeper insight of the planning challenges for ADNs can be consulted in (C6.19, 2014).

RELATED OUTCOMES

The following undergraduate and graduate degree projects at «Universidad Industrial de Santander», conferences and publications are part of the outcomes of this research:

Undergraduate (UG) and graduate (G) thesis

1. (UG) Economic dispatch including losses solution through iterative negotiations between market agents (Solución al despacho económico con pérdidas mediante negociaciones iterativas entre los agentes del mercado). By Carlos Julio Caicedo Sanchez and Diego Quintero Herrera.

2. (UG) Research seminar: Software tools for micro-grid analysis (Seminario de investigación herramientas software para el análisis de micro-redes). By Ana Maria Cruz Rosas, Joan Gerardo Ortega Garzón and John Mauricio Moreno Niño.

3. (UG) Evaluation of the non-cooperative game theory for the analysis of energy auctions in a micro-grid (Evaluación de la aplicación de la teoria de juegos no cooperativos para el análisis de subastas de energía en una micro-red). By Tatiana Alejandra Quintero Barrera and Andrés Felipe Pérez Quiroga.

4. (UG) Implementation guide of the IEC61970 standard for the information management in power distribution networks (Guía de implementación del estándar IEC61970 para el manejo de la información de sistemas de distribución de energía). By Édinson Enrique Sánchez Galán and Aura Milena Rueda Díaz.

5. (UG) Renewable energy resource project evaluation based on Data Enveloped Analysis (Evaluación de proyectos para el aprovechamiento de fuentes no convencionales de energía utilizando el análisis envolvente de datos). By Holman Andrés Chaparro Flórez and Nixon Adrian Barón Suárez.

6. (UG) Heuristic evaluation for the optimal management of local energy resources in a power distribution system (Evaluación de heurísticas para la gestión óptima de recursos energéticos locales en un sistema de distribución). By Anderson López Chaverra.

7. (UG) Analysis and modeling of the electricity price for the management of local energy resources (Análisis y modelado del precio de la energía eléctrica para la administración de recursos energéticos locales). By Rolando Andrés Rincón Saravia and Alberth Andrés Paba Álvarez.

8. (G) Guide for the short-term forecast of electricity demand: Case «Santander» (Guía para el cálculo del pronóstico a corto plazo de la demanda de energía eléctrica: caso Santander. By Aura Milena Rueda Diaz and Édinson Enrique Sánchez Galán.

Conferences

1. SERNA SUÁREZ, Iván David. CARRILLO CAICEDO, Gilberto. ORDÓÑEZ PLATA, Gabriel. Financial and environmental benefits of active distribution networks. SICEL/2017, Bucaramanga, Colombia, November, 2017.

2. SERNA SUÁREZ, Iván David. CARRILLO CAICEDO, Gilberto. ORDÓÑEZ PLATA, Gabriel. A semi-decentralized solution for the economic dispatch with transmission losses using a JASON-based multiagent system. 12th International Conference on the European Energy Market—EEM15, Lisbon, Portugal, May 2015.

3. SERNA SUÁREZ, Iván David. CARRILLO CAICEDO, Gilberto. ORDÓÑEZ PLATA, Gabriel. Microgrid's Energy Management Systems: A Survey. 12th International Conference on the European Energy Market—EEM15, Lisbon, Portugal, May 2015.

4. SERNA SUÁREZ, Iván David. PETIT SUÁREZ, Johann Farith. ORDÓÑEZ PLATA, Gabriel. CARRILLO CAICEDO, Gilberto. Storage system scheduling effects on the life of lead-acid batteries. IEEE PES Innovative Smart Grid Technologies Latin America (ISGT LATAM), October 2015.

Publications

1. SERNA SUÁREZ, Iván David. CARRILLO CAICEDO, Gilberto. ORDÓÑEZ PLATA, Gabriel. Financial and eviromental benefits of active distribution networks. In: Revista UIS ingenierías. Vol. 17, No 2. (2018); p. 55-64. Facultad de Ingenierías Fisicomecánicas, Universidad Industrial de Santander. ISSN: 1657-4583 (Impreso)/ 2145-8456 (Web).

2. SERNA SUÁREZ, Iván David. CARRILLO CAICEDO, Gilberto. MORALES ESPAÑA, Germán Andrés. DE WEERDT, Mathijs. ORDÓÑEZ PLATA, Gabriel. A Convex Approximation for Optimal DER Scheduling on Unbalanced Power Distribution Networks. In: Revista DYNA. Approved Feb/2019. ISSN: 0012-7353 (Impreso)/ 2346-2183 (Web).

3. SERNA SUÁREZ, Iván David. CARRILLO CAICEDO, Gilberto. MORALES ESPAÑA, Germán Andrés. DE WEERDT, Mathijs. ORDÓÑEZ PLATA, Gabriel. Optimal DER Scheduling consequences in Unbalanced Distribution Networks. Draft.

4. SERNA SUÁREZ, Iván David. CARRILLO CAICEDO, Gilberto. MORALES ESPAÑA, Germán Andrés. DE WEERDT, Mathijs. ORDÓÑEZ PLATA, Gabriel. Scaled ADMM for Three-phase Alternating Current Optimal Power Flow. Draft.

CHAPTER 1

ALTERNATING CURRENT OPTIMAL POWER FLOW

This chapter presents a state-of-the-art on optimal power flow for distribution networks, the key component to compute DER power injection set-points in Active Distribution Networks. This chapter starts in section 1.1 with some basic notions about the Alternating Current Optimal Power Flow (ACOPF), interior point algorithms, and dual decomposition. In section 1.2 are discussed some ideas from transmission network ACOPF that give some hints for distribution network modeling; as well as some formulations based on legacy three-phase power flow solvers and interior point algorithms. In section 1.3 are discussed some formulations based on quadratic and convex programming, while in section 1.4 there is a description of some decentralized formulations for solving the ACOPF. The chapter ends in section 1.5 with some concluding remarks and observations about how far the research questions and goals have been already answered or achieved, respectively.

1.1 Introduction

As a way to fully and efficiently exploit the energy resources in a power transmission system, the decision making has evolved from the classic economic dispatch, where only variable costs of generation are taken into account, to more complex problems that, for example, may include start and shut-down costs and ramp constraints of power generation, line outages and/or stochastic behavior of renewable sources. In contrast, for decades power distribution networks take for granted the available energy, and so, decision making was focused on network reconfiguration, reliability or equipment location.

The arrival of the Distributed Energy Resources (DERs) has increased the interest in how to fully and efficiently exploit DERs in a power distribution network. The similarities between the problems that have been solved for generation dispatch in transmission systems and the problems to be solved for power distribution DER scheduling are evident. However, solutions developed for generation dispatch in transmission systems cannot be applied directly to power distribution systems. Hence, the current challenge is in how to adapt decades of knowledge in transmission system operation to this new environment.

Active Distribution Networks (ADNs) is a technological framework that promises to efficiently manage DERs in a power distribution network. None of this will be remotely possible without advances in power electronics and wireless communications. This two elements combined give power distribution systems the required «activeness» to cope with the uncertainty and dynamism of DERs.

At the core of the ADNs is a decision making unit in charge of computing the set-points for each DER power injection (for a detailed description see annex B). This decision making can be stated as a mathematical programming problem:

$$\begin{aligned}
&\min_{x}\ f\left(x\right)\\
\text{s.t.}&\\
&h_k\left(x\right)=0,\ \forall k\in\{1,2,\dots K\}\\
&g_m\left(x\right)\leqslant 0,\ \forall m\in\{1,2,\dots M\}
\end{aligned}$$

Where, $x\in\mathbb{R}^n$ are the problem decision variables, $f\left(x\right)$ is a scalar valued function called the objective function, $h\left(x\right)=\left[h_1\left(x\right)\ h_2\left(x\right)\ \dots h_K\left(x\right)\right]^T$ is a vector valued function with the equality equations/constraints in each of its components and $g\left(x\right)=\left[g_1\left(x\right)\ g_2\left(x\right)\ \dots g_M\left(x\right)\right]^T$ is a vector valued function with the inequality equations/constraints in each of its components. If $f\left(x\right)$ is a convex function and the feasible region of the problem (which is defined by $h(x)$ and $g\left(x\right)$) is convex, then the decision making becomes a convex optimization problem.

Current convex optimization problems can be solved in polynomial time and they can be used to derive decentralized solutions, therefore, mathematical programming can provide fast and resilient solutions. As an example, in Frame 1 is briefly described some characteristics of optimization problem answers.

When applied to ADNs, these four components usually have the following characteristics:

x — Decision variables usually are: applied voltage and injected current at each node. From this variables other decision variables can be derived, e.g., injected active or reactive power, current or apparent power flowing through a line.

$f(x)$ — Objective functions depend on the application, for example, if some pricing scheme is needed, objective functions are related to minimizing total variable costs of producing energy; if an optimal allocation of equipment is being solved, the objective function might include fixed costs. Other common objective functions are maximizing power injections from a renewable resource, minimizing reactive power consumption or minimizing line active power losses.

$h(x)$ — Equality constraints are often related but not limited to balance equations. In power distribution networks these balance equations are related to the Kirchhoff Current Law and can be used to describe the distribution line model. Additionally, equality constraints are used to define other decision variables, and in general, to describe the equipment model as a function of some set of decision variables. For example, given a complex voltage $v = u + jw$ and current $i = \iota + jy$, active power can be defined as $p = u\iota + wy$.

$g(x)$ — Inequality constraints are related to system operational limits or equipment technical limits. As an example of a system operational limit, the magnitude of the node voltage in a distribution network usually is at most 5% higher than the nominal voltage and at least 5% lower than the nominal voltage. As an example of a technical limit on equipment, the total energy delivered by a storage system cannot be more than the storage system capacity.

Frame 1. PRIMAL PROBLEM

Consider the following optimization problem:

$$\min \{C_T\}$$
$$\text{s.t.}$$
$$P_1 + P_2 = D$$

Where, $C_T = C_1(P_1) + C_2(P_2)$; C_g are the generation costs of unit g, with $g = \{1, 2\}$; P_g is the energy delivered by each unit in MWh and D is the energy demand to be attended also in MWh. The parameters for a problem instance are described in Table 3, while the solution is depicted in Figure 4.

Table 3: Problem instance data

Generation costs of unit 1 (g_1)	$C_1 = 9P_1^2 + 1200P_1 + 40000$ [$]
Generation costs of unit 2 (g_2)	$C_2 = 25P_2^2 + 1200P_2 + 14400$ [$]
Demand	$D = 100$ [MWh]

Figure 4: Problem instance solution.

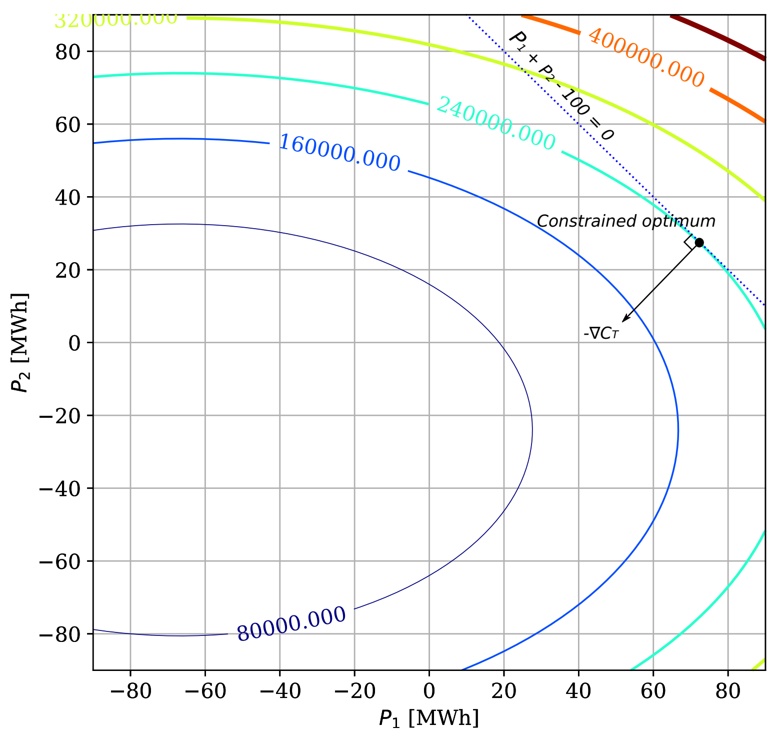

Note that the solution occurs at the (smallest) objective function level curve that is tangent to the constraint set (the line $P_1 + P_2 - 100 = 0$ in this case). In general a function gradient is always perpendicular to its level curves, and the solution is attained on a feasible point such that the objective function gradient is the linear combination of the active constraint gradients, i.e., the gradients of the objective function and the active constraints are linearly dependent (Conejo et al., 2006, chap. 4). In this example, since there is only one equality constraint the gradient of the objective function and the equality constraint are on the same line; when there is more than one constraint binding the problem, the negative of the objective function gradient would be on the plane defined by the gradients of the active constraints. These conditions are formally stated later in equations (1.1.1) to 1.1.5.

When including the line models, the optimization problem is called an Optimal Power Flow (OPF) problem. The non-linear formulation of the optimal power flow is the Alternating Current Optimal Power Flow (ACOPF), while the linear formulation is called the Direct Current Optimal Power Flow (DCOPF). The latter consider all voltage magnitudes equal to the nominal voltage through all the network; additionally, it assumes angle differences between adjacent nodes very small; and line active power losses equal to zero. The first and latter assumption makes impossible to use the DCOPF formulation in power distribution networks. This is why the ACOPF formulation is preferred, and, being a non-linear problem, usually is solved using Interior Point Methods.

1.1.1 Interior point methods. Bellow are presented the equations to derive the search direction for a general optimization problem with the primal-dual interior point method. For feasible point search and some history on the interior point methods please refer to (Torres, 1998; Boyd and Vandenberghe, 2009). Interior point methods are used to solve optimization problems of the form:

$$\begin{aligned}
&\min_{x} \ f(x) \\
\text{s.t.}& \\
&h_k(x) = 0,\ \forall k \in \{1, 2, \ldots K\} \\
&g_m(x) \leqslant 0,\ \forall m \in \{1, 2, \ldots M\}
\end{aligned}$$

Where $x \in \mathbb{R}^n$ is a column vector, moreover, all functions are scalar functions, e.g.,$h_k : \mathbb{R}^n \to \mathbb{R}$ and $g_m : \mathbb{R}^n \to \mathbb{R}$. The feasible region defined by the K equality constraints and the M inequality constraints can be represented by a set $\mathcal{R}$, so the problem can also be written as:

$$\min_{x} f(x)$$

$$\text{s.t.}$$

$$x \in \mathcal{R}$$

If the problem has a solution, the optimal primal $(x^\star)$ and dual $(u^\star, \omega^\star)$ variables satisfy the Karush-Kuhn-Tucker (KKT) conditions:

$$\nabla f(x^\star) + \sum_{k=1}^{K} u_k^\star \nabla h_k(x^\star) + \sum_{m=1}^{M} \omega_m^\star \nabla g_m(x^\star) = 0 \tag{1.1.1}$$

$$h_k(x^\star) = 0, \; \forall k \in \{1, 2, \dots K\} \tag{1.1.2}$$

$$g_m(x^\star) \leqslant 0, \; \forall m \in \{1, 2, \dots M\} \tag{1.1.3}$$

$$\omega_m^\star \geqslant 0, \; \forall m \in \{1, 2, \dots M\} \tag{1.1.4}$$

$$\omega_m^\star g_m(x^\star) = 0, \; \forall m \in \{1, 2, \dots M\} \tag{1.1.5}$$

Where the equations (1.1.1) are often called the *stationarity conditions*, equations (1.1.2) and (1.1.3) are called the *primal feasibility conditions*, equations (1.1.4) are called the *dual feasibility conditions,* and equations (1.1.5) are called the *complementary slackness conditions*. When strong duality holds, the complementary slackness condition and the dual feasibility condition assure that only active inequalities appear in equations (1.1.3). Also, note that the problem Lagrangian is equal to:

$$\mathcal{L}(x, u, \omega) = f(x) + \sum_{k=1}^{K} u_k h_k(x) + \sum_{m=1}^{M} \omega_m g_m(x)$$

So the stationary conditions can be also written as:

$$\nabla_x \mathcal{L}(x^\star, u^\star, \omega^\star) = 0$$

In order to find the optimum, interior point methods solve a modified version of the KKT conditions with Newton methods. Namely, the problem residuals are given by:

$$\begin{aligned} r^d &= \nabla f(x) + \sum_{k=1}^{K} u_k \nabla h_k(x) + \sum_{m=1}^{M} \omega_m \nabla g_m(x) \\ r_m^c &= \omega_m g_m(x) - w, \; \forall m \in \{1, 2, \dots M\} \\ r_k^p &= h_k(x), \; \forall k \in \{1, 2, \dots K\} \end{aligned}$$

Where r^d is the dual residual, r^c is the central path residual, r^p is the primal residual and w is a small enough constant. Therefore, a Newton step can be computed by solving:

$$\begin{bmatrix} L & G^T & H^T \\ \Omega G & \gamma & 0 \\ H & 0 & 0 \end{bmatrix} \begin{bmatrix} \Delta x \\ \Delta \omega \\ \Delta u \end{bmatrix} = - \begin{bmatrix} r^d \\ r^c \\ r^p \end{bmatrix} \tag{1.1.6}$$

Where,

L	$\nabla^2_{xx}\mathcal{L}(x, u, \omega) = \nabla^2 f(x) + \sum_{k=1}^{K} u_k \nabla^2 h_k(x) + \sum_{m=1}^{M} \omega_m \nabla^2 g_m(x)$, is the Hessian of the Lagrangian function with respect to the variable x.
G	$\begin{bmatrix} \nabla g_1 & \nabla g_2 & \ldots & \nabla g_M \end{bmatrix}^T$ is the Jacobian matrix for the inequality constraints.
H	$\begin{bmatrix} \nabla h_1 & \nabla h_2 & \ldots & \nabla h_K \end{bmatrix}^T$ is the Jacobian matrix for the equality constraints.
γ	diag. $\left\{ \begin{bmatrix} g_1 & g_2 & \ldots & g_m \end{bmatrix} \right\}$ is the diagonal matrix of the inequality constraints.
Ω	diag. $\left\{ \begin{bmatrix} \omega_1 & \omega_2 & \ldots & \omega_m \end{bmatrix} \right\}$ is the diagonal matrix of the Lagrange multipliers of the inequality constraints.

There are four remarks about finding the Newton step with equation 1.1.6:

1. The parameter w is used to keep the search direction far from the problem boundaries in early iterations; otherwise, the solution algorithm might be too slow.

2. The elimination of variable Δu increase the algorithm efficiency. This is because the resulting system of equations is smaller and, depending on the problem structure, this may improve the effectiveness of matrix factoring techniques. If after the block elimination of variables Δu the resulting system of equations is ill-conditioned, partial pivoting and/or problem scaling can be applied to improve the solution computation.

3. The resulting search direction often violate conditions (1.1.4) and (1.1.5). To avoid this the resulting Newton step is modified, so the solution feasibility is enforced. Usually, this is included in the line search subroutine of the solution algorithm. Moreover, often the *duality measure* or *surrogate duality gap* (which is equal to $\sum_{m=1}^{M} \omega_m g_m(x)$) is used to control the answer precision and feasibility in each step (Boyd and Vandenberghe, 2009).

4. The convergence guarantees of interior point methods are mainly for convex optimization problems. In contrast, non-convex optimization problems have not such guarantees. Nevertheless, it seems that the interior point methods converge if the problem primal and dual solutions are equal, i.e., if the problem has zero duality gap (Erseghe, 2014).

> Added to the fact that this kind of methods solves in polynomial time many kinds of convex optimization problems, they might be considered as a powerful tool for solving non-convex optimization problems.

Having a zero duality gap is a useful problem property because, depending on the problem structure, the dual problem solution can be computed as a coordinated group of smaller and independent optimization problems, thus allowing the decision maker to transform the solution computation from a centralized to a decentralized scheme –An example of an optimization problem with zero duality gap is shown in Frame 2. The allocation problem to be solved in an ADN has a structure that allows the application of this kind of decentralized solutions, therefore, dual decomposition is a relevant tool to design resilient DER schedules in ADNs.

Frame 2. DUAL PROBLEM

For a given optimization problem, the primal problem is defined as:

$$\min_{x} f(x)$$

s.t.

$$h_k(x) = 0,\ \forall k \in \{1, 2, \dots K\}$$

$$g_m(x) \leqslant 0,\ \forall m \in \{1, 2, \dots M\}$$

Whereas the dual problem is defined in terms of the dual function:

$$\psi(u, \omega) = \inf_{x \in \mathcal{R}} \left\{ f(x) + \sum_{k=1}^{K} u_k h_k(x) + \sum_{m=1}^{M} \omega_m g_m(x) \right\}$$

Thus, the dual problem can be stated as:

$$\max_{u,\omega} \psi(u, \omega)$$

s.t.

$$\omega_m^\star \geqslant 0,\ \forall m \in \{1, 2, \dots M\}$$

For the example presented in Frame 1, the dual function equals to:

$$\psi(u) = 54400 - 100u - \frac{17}{450}(u + 1200)^2\ [\$]$$

And the dual problem has $u^\star = -2523.53\,[\$/\mathrm{MWh}]$ as an answer. Values for P_1 and P_2 are easily recovered from the solution of the optimization problem implicit in the dual function:

$$P_1 = -\frac{600 + u^{\star}/2}{9} = 73.53\,\mathrm{MWh}$$
$$P_2 = -\frac{600 + u^{\star}/2}{25} = 26.47\,\mathrm{MWh}$$

Three remarks can be done at this point:

1. From equation (1.1.1), since at the solution point the objective function gradient and the equality constraint gradient are pointing to the same direction (see Figure 4), the dual variable u must be negative at the optimum.

2. A marginal decrease in the demanded energy causes a decrease in the objective function equal to 2523.53 \$/MWh, which in turn, it is equal to the negative of the optimal dual variable. That is, this dual variable is telling how much costed the last MWh for the given demand, i.e., in this case, it corresponds to the electricity price. In general, dual variables are a sensitivity measure on how much the objective function changes given a perturbation in the parameters of the corresponding constraint. Dual variables related to equality constraints are usually referred as the problem «prices» whereas dual variables related to inequality constraints are usually referred as the problem «shadow prices».

3. From Figure 5, it is clear that the primal and dual optimum are the same; however, note also that non-optimal values of the dual function are always less than the primal objective optimum, i.e., the dual function always gives a lower bound of the primal objective optimum. Moreover, solving the dual problem is equivalent to find the highest lower bound for the primal problem.

Figure 5: Primal objective function for feasible pairs of P_1 and P_2 and dual function values for the problem instance in Frame 1.

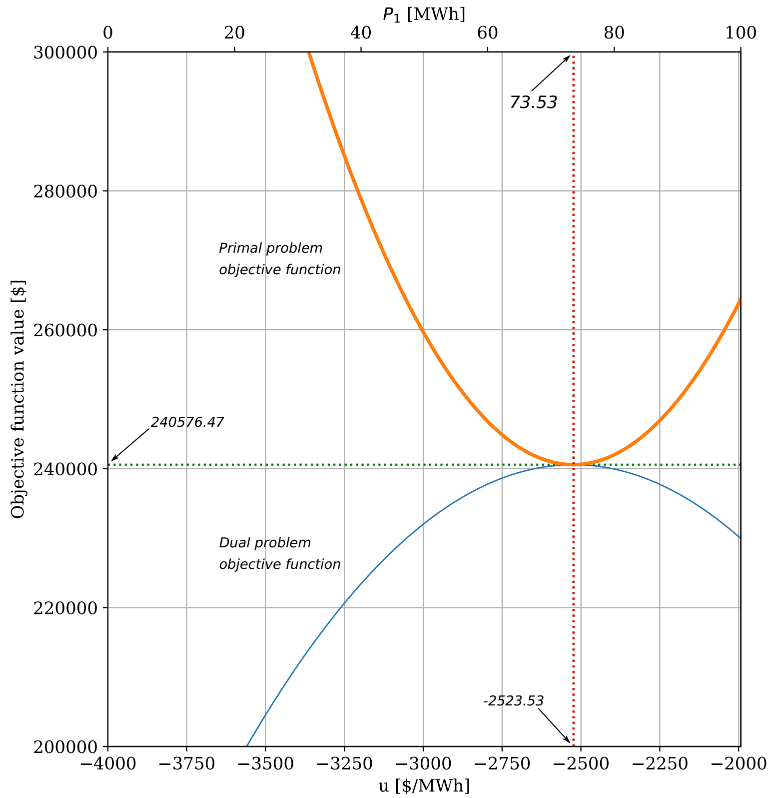

1.1.2 Dual decomposition. In this section is presented how the dual problem can be decomposed in order to solve the primal problem in a decentralized fashion, mainly based in (Boyd et al., 2010; Parikh and Boyd, 2013). Let us begin with a simple equality constrained optimization problem:

$$\min_{x} f(x) \quad \text{s.t.} \quad Ax = b \tag{1.1.7}$$

Where, $x, b \in \mathbb{R}^n$, $A \in \mathbb{R}^{m \times n}$ and $f : \mathbb{R}^n \to \mathbb{R}$ is a convex function. The Lagrangian for this problem is:

$$\mathcal{L}(x, u) = f(x) + u^T (Ax - b)$$

Note that $u \in \mathbb{R}^m$ is the column vector of Lagrange multipliers.

Dual Ascent Optimization problem defined by equations (1.1.7) can be solved using the dual ascent iterations:

$$\begin{aligned} x^{k+1} &:= \arg\min_x \mathcal{L}\left(x, u^k\right) \\ u^{k+1} &:= u^k + \rho\left(Ax^{k+1} - b\right) \end{aligned}$$

Where k is the iteration number. Note that the term $Ax^{k+1} - b$ corresponds to the equality constraint residual in the kth iteration. For a separable objective function, the Lagrangian function is also separable, i.e., for each element $e \in E$ there is a Lagrangian:

$$\mathcal{L}_e\left(x_e, u\right) = f_e\left(x\right) + u^T r_e\left(x\right)$$

Where, $f = \sum_{e \in E} f_e\left(x_e\right)$ and $r_e\left(x\right) = A_e x_e - b_e$. So the dual ascent steps become:

$$\begin{aligned} x_e^{k+1} &:= \arg\min_{x_e} \mathcal{L}\left(x_e, u^k\right) \\ u^{k+1} &:= u^k + \rho \sum_{e \in E} r_e^k\left(x^{k+1}\right) \end{aligned}$$

Where $r_e^k\left(x^{k+1}\right) = A_e x_e^{k+1} - b_e$. These steps are usually interpreted as follows: First, the current value for u^k is broadcast for each element e. Each element finds its optimal output given this value, and then all residuals are gathered to update the value of the Lagrange multiplier. Note that in this case, the dual ascent method is what is usually called a Walrasian Auction (Conejo et al., 2006).

Method of Multipliers Consider the augmented Lagrangian of the problem defined by equations (1.1.7):

$$\hat{\mathcal{L}}\left(x, u\right) = f\left(x\right) + u^T r\left(x\right) + \frac{\rho}{2}\left\|r\left(x\right)\right\|_2^2$$

Where, $\left\|\cdot\right\|_2$ is the norm 2 operator. The *Method of Multipliers* consists in applying the dual ascent method to the augmented Lagrangian. Adding the quadratic term to the Lagrangian improves the algorithm convergence properties and increase its robustness (Boyd et al., 2010). However, given a separable objective function $f = \sum_{e \in E} f_e\left(x_e\right)$, the Lagrangian is not separable.

Alternating Direction Method of Multipliers Decoupling variables with the *Method of Multipliers* requires an extra step: Instead of solving the problem given by equations (1.1.7), find a problem formulation that has the following structure:

$$\min_{x,y} g(x) + h(y) \tag{1.1.8}$$
$$\text{s.t}$$
$$Ax + By = c$$

Then, the augmented Lagrangian is:

$$\hat{\mathcal{L}}(x, y, u) = g(x) + h(y) + u^T r(x, y) + \frac{\rho}{2} \|r(x, y)\|_2^2$$

With $r(x, y) = Ax + By - c$. The *Method of Multipliers* steps are then:

$$\begin{aligned} x^{k+1}, y^{k+1} &:= \arg\min_{x,y} \mathcal{L}\left(x, y, u^k\right) \\ u^{k+1} &:= u^k + \rho r^k \left(x^{k+1}, y^{k+1}\right) \end{aligned}$$

With this new structure, primal variables can be updated in an alternating fashion, i.e.:

$$\begin{aligned} x^{k+1} &:= \arg\min_{x} \mathcal{L}\left(x, y^k, u^k\right) \\ y^{k+1} &:= \arg\min_{y} \mathcal{L}\left(x^{k+1}, y, u^k\right) \\ u^{k+1} &:= u^k + \rho r^k \left(x^{k+1}, y^{k+1}\right) \end{aligned}$$

These are the Alternating Direction Method of Multipliers (ADMM) steps. In general, the algorithm stops when the primal and dual residuals are small enough, i.e., $\left\|r^k\right\|_2 < \epsilon_p$ and $\left\|s^k\right\| = \left\|\rho A^T B\left(y^k - y^{k+1}\right)\right\|_2 < \epsilon_d$, respectively, given the required tolerances ϵ_p and ϵ_d.

Application to power distribution networks Power distribution network optimal power flow can be formulated as presented in (1.1.8) by applying the indicator function pattern (Sun et al., 2013; Erseghe, 2014; Zheng et al., 2015; Robbins and Dominguez-Garcia, 2015; Loukarakis et al., 2015a). First, let us define $\mathcal{R}$ as the feasible set for the optimization problem:

$$\begin{aligned} &\min_{x} \; f(x) \\ &\text{s.t. } \; x \in \mathcal{R} \end{aligned} \tag{1.1.9}$$

Therefore, the problem can be reformulated as:

$$\begin{aligned} \min_{x,\varkappa} \; & f(x) + g(\varkappa) \\ \text{s.t.} \; & x - \varkappa = 0 \end{aligned} \tag{1.1.10}$$

Where $\varkappa$ is a duplicate vector of x, and $g(\varkappa)$ is the indicator function of the feasible set $\mathcal{R}$, i.e.:

$$g(\varkappa) = \begin{cases} 0, & \varkappa \in \mathcal{R} \\ \infty, & \varkappa \notin \mathcal{R} \end{cases}$$

Then, the augmented Lagrangian is:

$$\hat{\mathcal{L}}(x, \varkappa, u) = f(x) + g(\varkappa) + u^T(x - \varkappa) + \frac{\rho}{2}\|x - \varkappa\|_2^2$$

And the application of the dual ascent method lead to the following steps:

$$\begin{aligned} x^{k+1} &:= \arg\min_x \left\{ f(x) + g\left(\varkappa^k\right) + u^T\left(x - \varkappa^k\right) + \frac{\rho}{2}\left\|x - \varkappa^k\right\|_2^2 \right\} \\ \varkappa^{k+1} &:= \arg\min_{\varkappa} \left\{ f\left(x^{k+1}\right) + g(\varkappa) + u^T\left(x^{k+1} - \varkappa\right) + \frac{\rho}{2}\left\|x^{k+1} - \varkappa\right\|_2^2 \right\} \\ u^{k+1} &:= u^k + \rho\left(x^{k+1} - \varkappa^{k+1}\right) \end{aligned}$$

Let us abuse of notation and define $r(x) = r_x = x - \varkappa^k$, $r(\varkappa) = r_\varkappa = x^{k+1} - \varkappa$, and also let us define $r^k(x, \varkappa) = r^k = x^{k+1} - \varkappa^{k+1}$, so the dual ascent steps can be rewritten as:

$$\begin{aligned} x^{k+1} &:= \arg\min_x \left\{ f(x) + g\left(\varkappa^k\right) + u^T r_x + \frac{\rho}{2}\|r_x\|_2^2 \right\} \\ \varkappa^{k+1} &:= \arg\min_{\varkappa} \left\{ f\left(x^{k+1}\right) + g(\varkappa) + u^T r_\varkappa + \frac{\rho}{2}\|r_\varkappa\|_2^2 \right\} \\ u^{k+1} &:= u^k + \rho r^k \end{aligned}$$

These are the steps usually reported in the technical literature, however, there is a cleaner and intuitive way for stating the ADMM steps for power distribution networks. Note that, since $\|a + b\|_2^2 = \|a\|_2^2 + \|b\|_2^2 + 2a^T b$, then:

$$u^T r + \frac{\rho}{2}\|r\|_2^2 = \frac{\rho}{2}\left\|r + \frac{1}{\rho}u\right\|_2^2 - \frac{\rho}{2}\left\|\frac{1}{\rho}u\right\|_2^2 \tag{1.1.11}$$

Therefore, applying equation (1.1.11), dual ascent steps can be written in what is called the "scaled form":

$$\begin{aligned} x^{k+1} &:= \arg\min_x \left\{ f(x) + g\left(\varkappa^k\right) + \frac{\rho}{2}\left\|r_x + \mu^k\right\|_2^2 - \frac{\rho}{2}\left\|\mu^k\right\|_2^2 \right\} \\ \varkappa^{k+1} &:= \arg\min_{\varkappa} \left\{ f\left(x^{k+1}\right) + g(\varkappa) + \frac{\rho}{2}\left\|r_\varkappa + \mu^k\right\|_2^2 - \frac{\rho}{2}\left\|\mu^k\right\|_2^2 \right\} \\ \mu^{k+1} &:= \mu^k + r^k \end{aligned}$$

Where μ=u/ρ is the scaled Lagrange multiplier. These steps can be further be simplified by removing the constant term $(\rho/2)\left\|\mu^k\right\|_2^2$ and by remembering that $g(\varkappa)$ is an indicator function of the set $\mathcal{R}$:

$$\begin{aligned}
x^{k+1} &:= \arg\min_{x} \left\{ f(x) + \frac{\rho}{2}\left\|r_x + \mu^k\right\|_2^2 \right\},\ \varkappa^k \in \mathcal{R} \\
\varkappa^{k+1} &:= \arg\min_{\varkappa} \left\{ g(\varkappa) + \frac{\rho}{2}\left\|r_\varkappa + \mu^k\right\|_2^2 \right\} \\
\mu^{k+1} &:= \mu^k + r^k
\end{aligned}$$

Finally, let us introduce the "proximal operator":

$$\mathrm{prox}_{f,\rho}(x) = \arg\min_{y} \left\{ f(y) + \frac{\rho}{2}\|y - x\|_2^2 \right\}$$

Which can be though as the nearest point to x that also minimize f. And the "projection operator":

$$\mathrm{proj}_{\mathcal{R}}(x) = \arg\min_{y} \{\|y - x\| : y \in \mathcal{R}\}$$

Which is the nearest point to x in the set $\mathcal{R}$. So the dual ascend steps become:

$$x^{k+1} := \mathrm{prox}_{f,\rho}\left(\varkappa^k - \mu^k\right),\ \varkappa^k \in \mathcal{R} \tag{1.1.12}$$

$$\varkappa^{k+1} := \mathrm{proj}_{\mathcal{R}}\left(x^{k+1} + \mu^k\right) \tag{1.1.13}$$

$$\mu^{k+1} := \mu^k + r^k \tag{1.1.14}$$

To see the ADMM in action please refer to the example in Frame 3.

Frame 3. ALTERNATING DIRECTION METHODS OF MULTIPLIERS APPLICATION EXAMPLE

Consider the following optimization problem:

$$\min \{C_1(P_1) + C_2(P_2)\}$$

s.t.

$$P_1 + P_2 = D$$

Where, C_g are the generation costs of plant g, with $g = \{1, 2\}$; P_g is the energy delivered by each plant in MWh and D is the energy demand to be attended. Figure 6 present a solution for a problem instance. Observe that, akin to gradient methods, as the algorithm reaches the problem optimum the number of iterations to make a given improvement increases (see Figure 7). In Table 4 are compared the solutions obtained by a centralized solution (6 iterations) and a decentralized solution (81 iterations). Value of ρ is set to 5, as (Loukarakis et al., 2015a) suggests.

Figure 6: Decentralized solution for example 3 for $\rho = 5$.

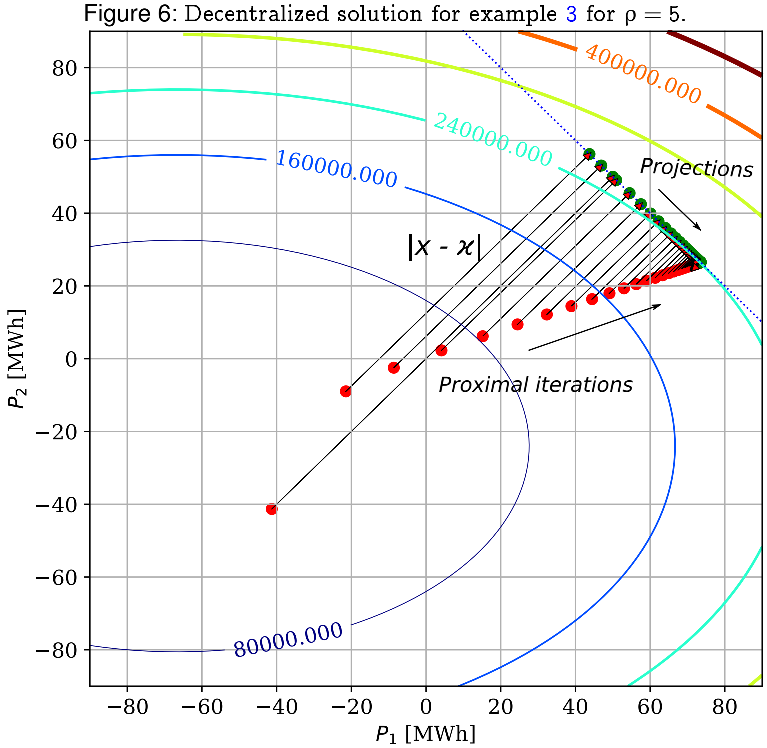

Table 4: Comparison between centralized and decentralized solutions. All tolerances adjusted to $\epsilon_{\text{tol.}} = 1 \times 10^{-4}$ and with a $\rho = 5$.

	Centralized	Decentralized
$P_1^\star$ [MWh]	73.52941	73.52935
$P_2^\star$ [MWh]	26.47059	26.47065
$\pi^\star$ [\$/MWh]	2523.529	2523.527
$C_1^\star + C_2^\star$	240576.5	240576.1

For this specific case, the number of iterations can be reduced from 81 to 42 by choosing $\rho = 10$ (See Figure 8), furthermore, from Figure 8 it is evident that beyond a given tolerance, the algorithm oscillates around 1×10^{-3} and 1×10^{-5}. Also note that for both cases, with a couple of iterations more and with the primal residual as stopping criteria solely, the final answer might be improved by an order of magnitude. Therefore, tuning ρ parameter is crucial to avoid algorithm inefficiencies.

Figure 7: Decentralized solution residuals for $\rho = 5$.

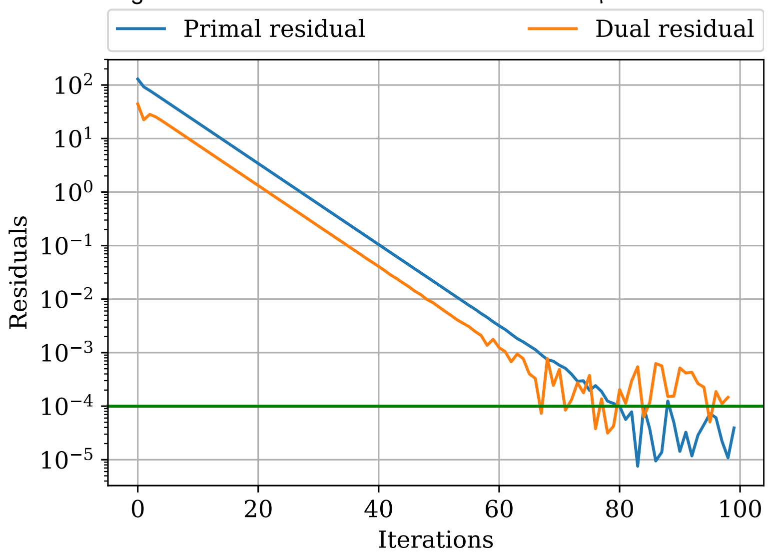

Figure 8: Decentralized solution residuals for $\rho = 10$.

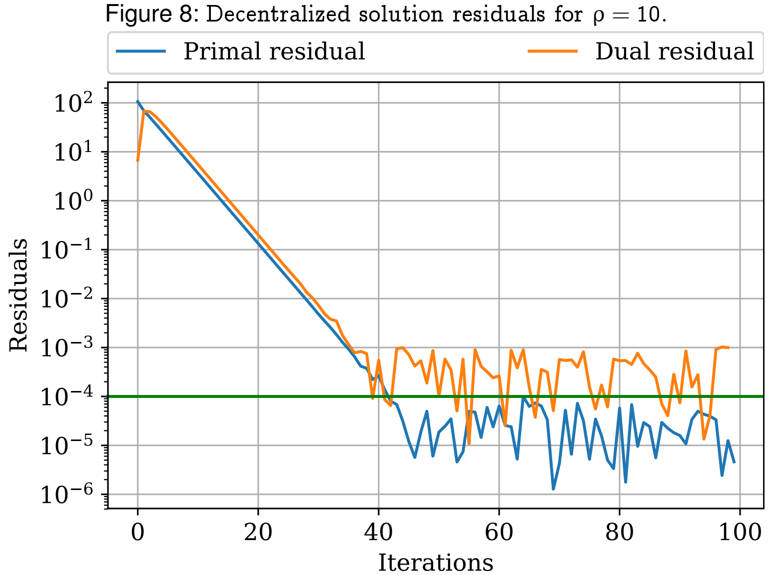

1.2 Non-linear formulations

Transmission networks are balanced systems with R/X ratios lower than their distribution network counterparts, moreover, they have a single type of load: the constant power load.

Thus, the Alternating Current Optimal Power Flow (ACOPF) used for transmission systems is not appropriate to find the optimal Distributed Energy Resource (DER) schedules in a distribution network. However, some key ideas can be borrowed from advances in ACOPF. For example, in (Castillo et al., 2016b) a single-phase ACOPF using cartesian components for each complex value is solved. There, the Kirchhoff Current Law is used to declare the energy balance at each node, and a first order Taylor approximation is used to declare the injected power at each node, and to declare the node voltage (and line current) upper limits. This problem is solved as a sequence of Linear Programs and it also can be extended to solve the Unit Commitment problem for transmission systems (Castillo et al., 2016a). A closer look to this formulation reveals that the cartesian formulation allows the inclusion of constant current and constant impedance load models as linear constraints. This might lead to some computation performance and convergence improvements (Jiang et al., 2009). Furthermore, it makes unnecessary the use of polynomial ZIP load model, and thus, their approximations (Wang et al., 2017b; Ahmadi et al., 2016).

Before moving forward it worth mentioning that with just a three-phase power flow solver one can compute a 3ϕ-ACOPF solution. For example, in (Bruno et al., 2011) a three-phase power flow solution is used to find a proper search direction for the 3ϕ-ACOPF; and in (Borghetti et al., 2010) the 3ϕ-ACOPF is transformed into a Mix-Integer Linear Program using network sensitivities computed from a three-phase power flow. Additionally to these black-box approaches to solve the 3ϕ-ACOPF, nowadays there are also optimal power flow solvers for distribution networks. Often these solvers are based on the Current Injection Method (CIM) formulation and compute the solution with Interior Point (IP) methods (Meng et al., 2017; Araujo et al., 2013; Penido et al., 2008; Garcia et al., 2000), as presented in Frame 4. Now, although CIM-IP can solve the 3ϕ-ACOPF efficiently, there are important advances on convex optimization that directly affects power distribution network analysis.

Frame 4. CURRENT INJECTION METHOD

In transmission systems the Kirchhoff Current Law (KCL) is enforced through a power balance in each node. However, in distribution systems the KCL is applied directly. So, for a single time period:

$$I = YV \tag{1.2.1}$$

Where $I \in \mathbb{C}^N$ is a vector with the complex current injected at each node $n \in \mathcal{N}$, and where the size of the set $\mathcal{N}$ is N; whereas, $V \in \mathbb{C}^N$ is the complex voltage applied at each node $n \in \mathcal{N}$; $Y \in \mathbb{R}^{N \times N}$ is a complex square matrix that models the distribution network.

Another usual choice in power distribution systems is to use cartesian components for the KCL, so equation (1.2.1) can be partitioned as:

$$\begin{bmatrix} I^r \\ I^i \end{bmatrix} = \begin{bmatrix} G & -B \\ B & G \end{bmatrix} \begin{bmatrix} V^r \\ V^i \end{bmatrix} \tag{1.2.2}$$

Where, $I = I^r + jI^i$, $V = V^r + jV^i$, and $Y = G + jB$. For a constant power injection $P + jQ$ at node n, the real and imaginary components are:

$$\begin{aligned} I^r &= \frac{PV^r + QV^i}{(V^r)^2 + (V^i)^2} \\ I^i &= \frac{PV^i - QV^r}{(V^r)^2 + (V^i)^2} \end{aligned} \tag{1.2.3}$$

Combining equations (1.2.2) and (1.2.3) give the problem residuals for the current balance equations.

1.3 Convex and non-convex quadratic formulations

In (Robbins and Dominguez-Garcia, 2015), *Robbins et al.* present a Quadratic Programming formulation for the 3ϕ-ACOPF that also gives a lower bound for the problem. There, the authors claim that branch-flow Second Order Cone Programming (SOCP) approaches (like the presented in (Huang et al., 2016), see Frame (5) for an example of most SOCP formulations) are unable to cope with system unbalance, and even if the presented linearizations are applied to the SOCP formulation, there is no guarantee on the lower bound for such problem. Moreover, *Christakou et al.* (Christakou et al., 2017b) show that branch-flow formulations also may introduce errors in branch currents for congested networks.

Frame 5. Distribution flow equations for second order cone formulations

Most Second Order Cone Programming (SOCP) formulations use the following equations to model the power flow through a distribution line (also called the *Distribution flow* equations):

$$S_{ds} = S_{us} - S_{loss} + S_n \tag{1.3.1}$$

$$V_n = V_m - Z_{mn} I_{us} \tag{1.3.2}$$

Figure 9: *Distribution flow* model for power distribution analysis.

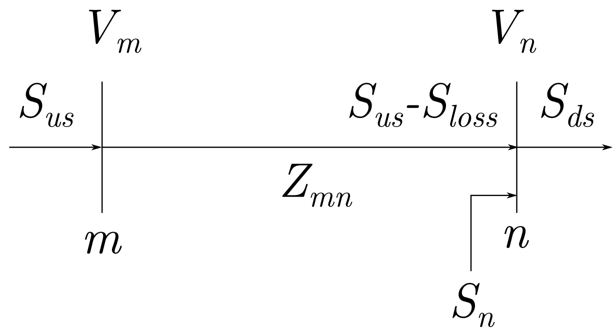

There, all variables take complex values. Equation (1.3.1) is the power balance equation, and it states that the apparent power flowing down stream (S_{ds}) must be equal to the sum between the apparent power flowing upstream (S_{us}) minus the line losses (S_{loss}) and the total apparent power being injected at the node n (S_n). Equation (1.3.2) states that voltage at node n (V_n) can be computed as the difference between the voltage at node m (V_m) and the voltage drop due to the distribution line impedance. The voltage drop is calculated as the product between the line impedance (Z_{mn}) and the current flowing upstream (I_{us}), which is the current flowing through the line.

Two decisions are taken in order to embed these two equations into a second order cone:

1. Remove the angle dependency from equation (1.3.2) by multiplying each equality side with the corresponding complex conjugate. So, the voltage drop equation becomes:

$$|V_n|^2 = |V_m|^2 - 2\Re\{Z_{mn}S_{us}\} + |Z_{mn}|^2 |I_{us}|^2 \tag{1.3.3}$$

2. Make a change of variables: $w_n = |V_n|^2$ and $l_{us} = |I_{us}|^2$

Where $|\cdot|$ operator takes the magnitude of the complex number and the $\Re\{\cdot\}$ operator takes the real value of the complex number. Since line losses can be written as $Z_{mn}|I_{us}|^2$, the balance and voltage drop equations can be written as:

$$S_{ds} = S_{us} - Z_{mn}l_{us} + S_n \tag{1.3.4}$$

$$w_n = w_m - 2\Re\{Z_{mn}S_{us}\} + |Z_{mn}|^2 l_{us} \tag{1.3.5}$$

$$l_{us} = \frac{|S_{us}|^2}{w_m} \tag{1.3.6}$$

Now, assuming that: (1) the objective function increases with l_{us}; (2) The loads have not upper bound on their values; the following relaxation is exact:

$$l_{us} \geqslant \frac{|S_{us}|^2}{w_m} \tag{1.3.7}$$

Furthermore, this equation defines a rotated second order cone:

$$\mathcal{Q} = \left\{ (S_{us}, l_{us}, w_m) : l_{us} w_m \geqslant \|S_{us}\|_2^2 \,, l_{us} \geqslant 0, w_m \geqslant 0 \right\}$$

Therefore, it can be rewritten as (Zheng et al., 2016):

$$\left\| \begin{array}{c} 2\mathfrak{R}\left(S_{us}\right) \\ 2\mathfrak{I}\left(S_{us}\right) \\ l_{us} - w_m \end{array} \right\|_2 \leqslant l_{us} + w_m$$

Since $l_{us} + w_m \geqslant 0$, this constraint also can be written as:

$$\begin{bmatrix} l_{us} + w_m \\ 2\mathfrak{R}\left(S_{us}\right) \\ 2\mathfrak{I}\left(S_{us}\right) \\ l_{us} - w_m \end{bmatrix} \succeq_{\mathcal{Q}} 0 \tag{1.3.8}$$

Note that in $\mathbb{R}^2$, if the cone defined by $\mathcal{Q}$ is the positive quadrant, the $\succeq_{\mathcal{Q}}$ is equal to a component wise $\geqslant$. Thus, equation (1.3.8) indicates that the vector in the left side of the general inequality ($\succeq_{\mathcal{Q}}$) must be inside the cone $\mathcal{Q}$.

Such problems have led researches to new approximations. For example, in (Ahmadi et al., 2016), *Ahmadi et al.* study how the linear approximation over a bounded feasible region can be useful for the solution of three-phase power flow equations. This formulation seems to be superior to standard first order Taylor approximations, moreover, it can be used to warm-start CIM algorithms. The formulation drawbacks are mainly small errors induced in constant current and constant power load models, and the constant maximum mismatch error in voltage magnitudes across iterations.

In general, Quadratic Programming (QP) and Quadratically Constrained Quadratic Programming (QCP) are the most common formulations used for solving the 3ϕ-ACOPF. For example, in (Su et al., 2014) a 3ϕ-ACOPF including network neutral is solved with a sequential quadratic programming algorithm with multiple starting points. They show how to manage the power injections of Photovoltaic (PV) system inverters with reactive compensation in a distribution network. One interesting characteristic of their proposal is that voltage magnitude and unbalance factor limits are treated with a dead band function: The objective function has two terms (one for voltage magnitude limits and other for voltage unbalance factor limits) that are equal to zero if the voltage is within the required limits, otherwise they are equal to some positive value, namely, the square of the difference between the computed voltage/unbalance and the required limit.

In (Watson et al., 2017), there is a non-iterative convex QCP formulation to solve a 3ϕ-ACOPF to analyze the effects of the neutral conductor and system storage in a distribution network. Besides, the proposed formulation can be extended to cope with storage system scheduling without losing the convexity nor computational efficiency.

On the other hand, in (Zamzam et al., 2017), *Zamzam et al.* present a non-convex QCP formulation that also helps to find "problematic" constraints thanks to their Feasible Point Pursuit (FPP) Successive Convex Approximation (SCA) algorithm. Their algorithm has two main parts, the first one (FPP) is designed to minimize the unfeasibility of the initial point used by the second part (SCA), and in fact, for the tested networks, it always succeeds to find a feasible startig point. Furthermore, with very slightly modifications this algorithm can identify problematic constraints. The second part (SCA) is also a modification of the FPP, only that it is designed to minimize a given objective function. This algorithm is tested for transmission and distribution systems, the latter also for one and three phase system models.

Therefore, recent advances show that QP and QCP are promising alternatives to solve the energy resource allocation problem in ADNs, moreover, it seems to be a viable solution for analyzing the optimal operation of transmission and distribution network systems as well (Guggilam et al., 2016; Coffrin et al., 2016).

Additionally, Semidefinite Programming (SDP) also has been used for power distribution ACOPF, however, its application has been very limited due to two main reasons: 1) A key characteristic in SDP solutions is to find a *rank 1* solution to the problem, since it is the only solution with physical meaning. Now, because such rank constraint is non-convex, usually it is dropped. However, this rank relaxation might lead to answers without physical meaning for some networks. 2) SDP optimum computation is a resource intensive task.

The time performance problem is being solved by *Li et al.* in (Li et al., 2017) by using an SDP equivalent of the SOCP branch-flow formulation for the unbalanced problem. *Li et al.* points that, although all studied cases have a *rank 1* solution, there is no formal proof of the existence of *rank 1* solutions. Another approach to solve the SDP performance limitations is based on finding a network partition that exploits chordal sparsity of the SDP formulation (Wang and Yu, 2017; Liu et al., 2018). Such solutions have shown simulation times comparable to those achieved by the IP algorithms –a common reference for testing new ACOPF algorithms. Additionally, the rank relaxation problem is addressed in (Wang and Yu, 2017) by solving the 3ϕ-ACOPF as a sequence of SDP problems that converge to a *rank 1* solution.

1.4 Decentralized formulations

A key idea for problem decomposition comes from Leon Walras (1834-1910), one of the founders of marginal analysis and one of the most influential economists due to his work on general equilibrium (Landreth and Colander, 2002): He created a formal framework to compute the general equilibrium of a competitive market as a tâtonnement process. This process shows that, under very specific conditions, the general equilibrium can be computed as a sequence of partial equilibria. This kind of tâtonnement process is nowadays called Walrasian Auction (although is not an actual auction), and it can be described by solving the dual problem of an optimal allocation problem with a separable objective function (see (Conejo et al., 2006) and section 1.1.2).

In general, given a convex problem with a separable objective function, the global optimum can be computed from the dual problem as a sequence of local optima. This is possible because convex problems have zero duality gap, thus, primal and dual problem solutions are equal. Furthermore, advances in convex programming have shown that some non-linear problems can be reformulated as convex ones, then extending the scope and pertinence of this kind of results.

When applied to optimal DER scheduling, dual decomposition strategies not only take advantage of the separability of the objective function, but also exploits network structure to come with efficient answers. In general, this kind of solutions are often computed by reformulating the primal problem so the augmented Lagrangian can be solved concurrently, i.e., applying what is called the Alternating Direction Method of Multipliers (see section 1.1.2 for more details). Because of its convergence requirements and speed, the ADMM is nowadays a common choice to derive decentralized solutions to convex and non-convex problems (Boyd et al., 2010).

One of the first applications of the ADMM to ACOPF can be found in (Sun et al., 2013). There, *Sun et al.* use an indicator function of the feasible set to decouple the ACOPF for each node. The resulting optimization steps have a very close resemblance with a Walrasian Auction:

1. Each node find the optimal local power injections and voltages given some known values of the voltages on adjacent nodes.

2. Local voltages and power injections are recomputed given the new voltages in adjacent nodes.

3. Differences between the answers of the two previous steps are used to update the Lagrange multipliers.

4. Steps 1) to 3) are repeated until answers from steps 1) and 2) are close enough.

Although valid, decomposing the problem to the node level is not a common practice, instead, usually the network is partitioned in independent operation areas. So, in the second step instead of updating each node voltage in the system, the new answer is computed by sharing information between network areas, i.e., between the voltages at the boundaries of each of the adjacent network partitions. On this characteristic, in (Loukarakis et al., 2015a) there is a study on how decentralized approaches based on ADMM behave to several partition levels given three operation scenarios: one scenario to explore the effects of different levels of network partitioning (*network-wise scalability*); and two scenarios to explore the impact of changing the number of users in the network (*user-wise scalability*).

To test the *network-wise scalability*, *Loukarakis et al* use a *k-means* clustering after a spectral analysis of the normalized Laplacian of the network to define each network partition. They claim that optimal network partitioning is a problem complex enough by its own, and that the *k-means* spectral clustering is not necessarily optimal.

To test the *user-wise scalability*, three agents are taken into account: 1) A transmission system operator (TSO), 2) a distribution system operator (DSO), and 3) a microgrid operator (MO). The TSO has information only regarding the transmission system, while the DSO is implemented as a system aggregator, i.e., it is in charge of the coordination of the power injections and in charge of the Lagrange multipliers update for several MO. In turn, each MO controls a set of nearby users, all users in a node or a single user. As a system aggregator, the DSO is in charge of communicating the resulting power injections of each MO under its command to the TSO. Without a system aggregator, each MO has to directly communicate the power injections to the TSO agent.

Two important conclusions are presented in (Loukarakis et al., 2015a): 1) *As the network partition increases, the number of iterations increases on average*. Interesting enough, the full-ACOPF and a non-linear DCOPF (node voltages set to unity, without reactive power flows, but with line losses) have a similar performance, thus, the increase on iterations is not determined by the problem complexity but by the network characteristics. 2) *As the number of users increases, the number of iterations increases rapidly if there is not a system aggregator*. So, the main idea is to use few system aggregators as a proxy between users and the transmission system operator.

In general, (Loukarakis et al., 2015a) and (Sun et al., 2013) implicitly present two reasons that makes ADMM the preferred decomposition technique based on mathematical programming:

1. In spite of the non-linearity of the ACOPF models, the ADMM seems to be able to converge to the answer obtained by Interior Point Algorithms. Of course, still there is no a formal proof of convergence and under some very specific assumptions ADMM seems to diverge (Christakou et al., 2017b), however, tests done in (Mhanna et al., 2018) have shown the broad spectrum of networks for which it works.

2. Due to the resulting problem structure, the ADMM offers a decentralization framework with which new decomposition schemes can be derived, often based in some kind of "proximal algorithm" (Loukarakis et al., 2015b) (see section 1.1.2).

As an example of the second point, in (Erseghe, 2014) a compact formulation for ADMM-based ACOPF is presented. There, by applying a specific set of assumptions, and unlike all methods above, a "memory" term is used to account for the error between the local solution answer (see step one in the list above) and the recomputed answer (see step two in the list above), which in turn, transforms the local problem in a much simpler and clearer form. A closer look reveals that the assumptions done and the memory term coincides with the indicator function pattern and the scaled Lagrangian multiplier of the scaled ADMM (see section 1.1.2). Another difference in (Erseghe, 2014) is that the calculation of one "memory" term includes a constant scaling of the difference between the local solution and recomputed solutions –this is done to improve the convergence of the algorithm.

Up to here, all ADMM algorithms have been applied to non-convex formulations of the ACOPF, however, some approximations can be made to improve other useful OPF formulations. For example, in (Zheng et al., 2015) a linearized version of the active power loss in each line is included to formulate a better DCOPF. For this problem the network structure is exploited to reduce to two steps the distributed calculation of the optimal power flow: 1) The local solution is solved. 2) Local copies of auxiliary parameters on the boundary with adjacent areas are updated.

Lagrange multipliers are a function of the selected auxiliary parameter, which in turn can be seen as a surrogate for the power flowing between areas. Furthermore, the elimination of the Lagrangian multiplier update through the inclusion of this auxiliary parameter, transform the ADMM into a completely asynchronous algorithm.

Because this algorithm is just an improvement over the DCOPF, still the answer is not good enough when compared against a full ACOPF solution. To cope with this, in (Zheng et al., 2016) the same principle is applied using an exact convex approximation based upon Second Order Cone Programming (SOCP).

From these two works of *Zheng et al.* it seems to be a problem when a global variable need to be computed locally and the algorithm has to run asynchronously. However, the need to update a global variable can also be done asynchronously without the need of auxiliary parameters. In (Binetti et al., 2014) an estimation of the total losses mismatch of the network is needed to achieve the consensus among the incremental costs of generators. Since line agents can only pass messages to adjacent line agents, each time a message is broadcast, a copy of the current state of the line losses mismatch is also shared. So, after the first broadcasting, each line agent will have a copy of the loss mismatches of the adjacent lines; on the second broadcasting, each line will update the copy of his neighbors loss mismatches and will have a copy of the loss mismatch of the lines adjacent to his neighbors; and so forth. At one point, each line will have a copy of the loss mismatches for all the network, with which an estimation of the total loss mismatch can be computed.

Additionally to the non-linear and convex formulations so far described, (Guggilam et al., 2016) present a Quadratically Contrained Quadratic Programming (QCQP) formulation for scheduling PV inverters. This formulation assumes that the nominal voltage in each node is 1 p.u. and that deviations from this voltage due to power injections from a line without shunt elements can be approximated as $\Delta V = (RP + XQ) + j\,(XP - RQ)$, where $P + jQ$ is the power being injected from the line and $R + jX$ is the line impedance; the only quadratic term is the one limiting the reactive power injection of each PV inverter. Again, the ADMM is used as a way to decompose the problem, this time in “utility” and “user” agents. As a first step the utility problem is solved, afterwards, the local PV (user) problem, to lastly, update the Lagrange multipliers given the differences between the power injections resulting from the “utility” and “user” steps.

On the other hand, (Christakou et al., 2017a) propose a primal decomposition approach to solve the ACOPF. This primal approach use the Method of Multipliers to formulate the master problem, and instead of reformulating the primal problem to find a problem decomposition, it directly exploits the problem structure to come with a distributed solution. Namely, the problem is decomposed to the node level and into two stages by letting voltages at the end of a line to be constant when solving the local problem. In the first stage, a gradient descent update is applied to compute the next set of constant voltage ends; the algorithm stops when the gradient is small enough. After this first stage, the update of the Lagrange multipliers is done by projecting the dual ascent update to the set $\left[-\hat{\lambda}, \hat{\lambda}\right]$, where $\hat{\lambda}$ is such that the optimal Lagrange multiplier λ^* satisfies $\lambda^* \in \left[-\hat{\lambda}, \hat{\lambda}\right]$. The algorithm stops when the maximum number of iterations are reached, or when the change in the Lagrange multipliers between two consecutive iterations is less than a given tolerance. *Christakou et al.* propose this new algorithm to solve a convergence problem that appears in non-convex ADMM formulations when shunt elements are included. However, the wide range of problems solved with ADMM in (Mhanna et al., 2018) shows that this problem might not appear if shunt elements are properly included in the optimization problem formulation.

From all reviewed literature so far, only (Robbins and Dominguez-Garcia, 2015) present a three-phase formulation of the ADMM. To make the extension possible, voltage magnitude between nodes is considered very close, furthermore, node voltages are considered nearly balanced. The problem does not seem to have problems to converge, mainly because the almost balanced conditions are enforced by the objective function, which is to minimize the voltage variations with respect to a given reference point.

1.5 Remarks and research questions

The former review gives some hints for 3ϕ-ACOPF modeling:

- Polar and cartesian formulations lead to similar results and time performances (Zhang et al., 2005; Meng et al., 2017; Torres, 1998), although, as pointed out in (Meng et al., 2017), the cartesian formulations are the preferred way to solve large and complex 3ϕ-ACOPF because of their robustness. Furthermore, cartesian formulations include constant impedance and constant current models as linear equations, which in turn, can bring some computational benefits (Jiang et al., 2009).

- Linear and convex approximations are important because they allow the inclusion of integer variables to 3ϕ-ACOPF (Franco et al., 2015) and it can be used to derive distribution network locational marginal prices (Yuan et al., 2018). The same can be said about the use of legacy three-phase power flow solvers for optimal DER scheduling (Bruno et al., 2011; Borghetti et al., 2010).

- There is a tendency on ACOPF solutions to be stated as a sequence of optimization problems (Wang and Yu, 2017; Zamzam et al., 2017; Castillo et al., 2016b; Su et al., 2014).

Also, this review shows six problems still open:

1. In (Li et al., 2017) the effects of the optimal DER dispatch (including PV and storage systems) on the network are explored, however, they only use one objective function.

2. In (Zamzam et al., 2017) there is a comparison between a one-phase and three-phase OPF, but given a single scenario and without considering system storage.

3. Formulations like (Robbins and Dominguez-Garcia, 2015) require almost balanced conditions to solve the 3ϕ-ACOPF, however, it is unclear how realistic this assumption might be.

4. In (Watson et al., 2017) and (Su et al., 2014), the network unbalance in optimal DER scheduling for unbalanced distribution networks is explicitly handled, however, it is not clear if this modeling decision may be avoided.

5. Only analyses on three-phase power flow algorithms, as (Ahmadi et al., 2016), seem to explicitly employ delta load models.

6. The ZIP loads are often treated with the polynomial model (Ahmadi et al., 2016; Wang et al., 2017b), or not treated at all; on the latter case, constant power load model is preferred (Zamzam et al., 2017; Li et al., 2017; Robbins and Dominguez-Garcia, 2015; Wang and Yu, 2017; Liu et al., 2018). In contrast, (Watson et al., 2017) use cartesian components in the problem formulation, and as a consequence, load constant power components are replaced by an equivalent constant current components.

In general, 3ϕ-ACOPF analyses are more focused on the algorithms itself than on the consequences of the optimum to the network. Also, in spite of the importance of network unbalance and power generation in the network, most formulations are unclear on how optimal DER scheduling might affect the distribution network. Additionally, relevant load models for distribution network modeling are often ignored or implicitly handled. Therefore, a look at the technical literature shows that (Q-I)[1] is partially answered.

On one hand, all presented formulations take advantage of two key characteristics of 3ϕ-ACOPF for distribution networks: problem sparsity and small voltage angle differences between nodes. However, some other characteristics are often ignored. Interesting enough, R/X ratio does not appear to be a major problem, i.e., present formulations do not depend on high sensitivities between active/reactive power and voltage angle/magnitude.

On the other hand, still there is no a comprehensive study that shed some light on 3ϕ-ACOPF limits and impacts of optimal DER scheduling on the network. From all the possible questions that could be stated about 3ϕ-ACOPF limits, here are tackled two that aim to solve problems 1 to 4:

[1]What are the limits and characteristics of the 3ϕ-ACOPF?

(Q-Ia) Are the solutions obtained by a 3ϕ-ACOPF different enough from those given by a single-phase ACOPF?

(Q-Ib) Is the optimal DER scheduling increasing or decreasing the voltage unbalance in the network?

In contrast, the literature review gives a wide spectrum on (Q-II)[2] answers (Robbins and Dominguez-Garcia, 2015; Watson et al., 2017; Li et al., 2017; Wang and Yu, 2017; Liu et al., 2018). However, such answers still lack some key modeling elements.

About goal (G-I)[3], each research on distributed ACOPF derives its own interpretation of the ADMM, method of multipliers or primal decomposition scheme, and so, the fundamental ideas get easily lost. On goal (G-II)[4], researches like (Loukarakis et al., 2015a; Mhanna et al., 2018; Christakou et al., 2017b,a) explore in a very detailed way the limits, performance problems and tuning of state-of-the-art techniques for decentralized ACOPF computation, however, always limited to one-line models of the distribution network. Although in this book a fully asynchronous 3ϕ-ACOPF is out of scope, a simpler problem structure is used to analyze the performance of the decentralized optimization solutions.

The rest of this document shows how optimal DER scheduling affects the electrical variables in a distribution network (chapter 3); how such impacts could be handled with a convex formulation that takes into account the distribution network characteristics presented in page (section 5.1); and how from there, a decentralized operation strategy for active management of DERs in distribution networks can be designed (section 5.2).

[2] Is it possible to have an exact convex relaxation of a 3ϕ-ACOPF?

[3] To characterize the decentralized decision taking for distributed energy resource allocation in a power distribution network.

[4] To propose a comparative analysis of decentralized strategies for distributed energy resource allocation in a power distribution network.

I Non-convex 3ϕ-ACOPF Evaluation

CHAPTER 2

NON-CONVEX MODELS

This chapter describes the mathematical programming model to solve a 3ϕ-ACOPF suitable for Active Distribution Network optimal operation. In section (2.1) the nomenclature is presented to describe the non-convex formulation of the 3ϕ-ACOPF. The rest of the chapter is organized as follows: Generation, demand and network models are described in sections 2.2, 2.3 and 2.4, respectively. All equations are presented in terms of complex numbers, but actually they are handled to the solver in cartesian form, similarly to the non-linear formulation in (Castillo et al., 2016b); and without using discrete variables for the storage model, as in (Gill et al., 2014). Finally, these models are used to formulate the optimization problem in section 2.5.

2.1 NOMENCLATURE

The three-phase Alternating Current Optimal Power Flow (3ϕ-ACOPF) model presented below uses the following basic nomenclature:

- For an electric distribution network, let $\mathcal{N} = \{1, 2, 3, \dots N\}$ be the set of nodes and $\mathcal{R}$=$\{1, 2, 3, \dots R\}$ be the set of branches –each branch $r \in \mathcal{R}$ is defined by a pair of nodes $n, m \in \mathcal{N}$. Now, let $\mathcal{G}$, $\mathcal{D}$, and Φ be the set of elements that are able to inject power into the network, the set of loads and the set of phases, respectively. A subindex in any set indicates that a specific partition is being made, e.g., for a node $n \in \mathcal{N}$ and a generator $g \in \mathcal{G}$, $\mathcal{G}_n$ is the set of generators connected to node n, $\mathcal{N}_g$ is the set of nodes to which generator g is connected, and Φ_g is the set of phases that generator g has.

- Voltages are represented with the letter V, currents with I, apparent power with S (active power with P and reactive power with Q), impedance with Z ($\textsc{r}$ for the resistance and $\textsc{x}$ for the reactance) and admittance with Y ($\textsc{g}$ for the conductance and $\textsc{b}$ for the susceptance). A superscript ϕ is used to denote that the electrical variable is measured at phase ϕ.

- All electrical variables and parameters are presented as complex values when required, so for a complex number C, its complex conjugate is denoted by C^*; $\Re\{C\} = C^r$ and $\Im\{C\} = C^i$ are their real and imaginary parts, respectively; and $|C|$ and $\angle\delta_C$ denote its magnitude and angle δ_C.

- To keep notation simple, all variables and constants are intended to be column vectors of complex numbers. Each component of the vector is the value of the variable in the corresponding time period, e.g. $C = [C_1, C_2 \dots C_\tau]^T$, for a time window $\mathcal{T} = \{1, 2, \dots \tau\}$ and where $C_t \in \mathbb{C}$ is the value variable $C \in \mathbb{C}^\tau$ has at time t, and τ is the total number of time periods. With this in mind, all operations and equations are supposed to be time-component wise, e.g., for two complex vectors A and B, and $\tau = 2$, $A/B = C$, mean $A_1/B_1 = C_1$ and $A_2/B_2 = C_2$.

Note that this is not an exhaustive list of all the symbols used to describe the 3ϕ-ACOPF, but a basic set of rules and conventions that are used to describe the power system element models. Thus, all elements are properly introduced and defined as they are required according to the basic nomenclature here presented. Please refer to Frame 6 for an example on the use of this nomenclature.

Frame 6. NOMENCLATURE EXAMPLE

The apparent power injected by each generator g connected to node n is:

$$S_g^{\phi} = P_g^{\phi} + jQ_g^{\phi} = V_n^{\phi} I_g^{\phi *} \quad g \in \mathcal{G}_n,\ \phi \in \Phi_g \tag{2.1.1}$$

Now, let us expand equation (2.1.1) for generators at node 2 of the network in Figure 10. The resulting set of equations are:

$$S_{g1}^{a} = P_{g1}^{a} + jQ_{g1}^{a} = V_{n2}^{a} I_{g1}^{a*} \tag{2.1.2}$$

$$S_{g2}^{a} = P_{g2}^{a} + jQ_{g2}^{a} = V_{n2}^{a} I_{g2}^{a*} \tag{2.1.3}$$

$$S_{g2}^{b} = P_{g2}^{b} + jQ_{g2}^{b} = V_{n2}^{b} I_{g2}^{b*} \tag{2.1.4}$$

$$S_{g2}^{c} = P_{g2}^{c} + jQ_{g2}^{c} = V_{n2}^{c} I_{g2}^{c*} \tag{2.1.5}$$

Figure 10: Example network. System header is at node 1.

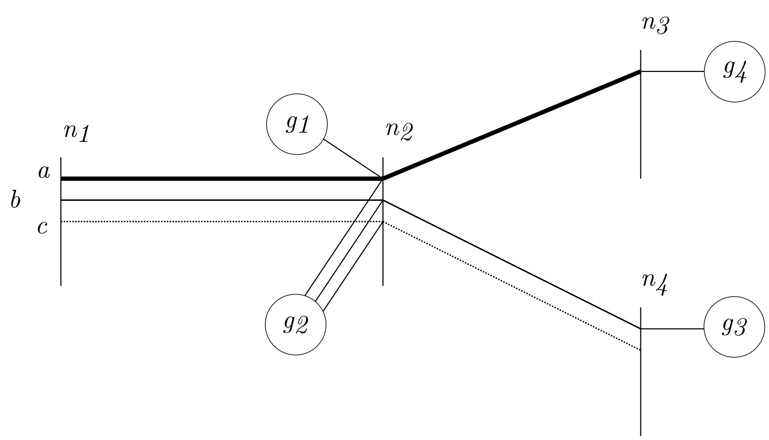

Note that $\mathcal{G}_{n2} = \{g1, g2\}$ and that $\Phi_{g1} = \{a\}$, i.e., g1 is a single phase generator; whereas $\Phi_{g2} = \{a, b, c\}$, i.e., g2 is a three-phase generator. Now, if cartesian components were to be used, equation (2.1.2) can be written as:

$$S_{g1}^{a} = P_{g1}^{a} + jQ_{g1}^{a} = V_{n2}^{ra} I_{g1}^{ra} + V_{n2}^{ia} I_{g1}^{ia} + j\left(V_{n2}^{ia} I_{g1}^{ra} - V_{n2}^{ra} I_{g1}^{ia}\right)$$

Therefore, for each complex equation there are two equations, one for the real component and the other for the imaginary component:

$$P_{g1}^{a} = V_{n2}^{ra} I_{g1}^{ra} + V_{n2}^{ia} I_{g1}^{ia}$$
$$Q_{g1}^{a} = V_{n2}^{ia} I_{g1}^{ra} - V_{n2}^{ra} I_{g1}^{ia}$$

Assuming that $\tau = 2$, equation (2.1.2) can be expanded to:

$$P^{a}_{g1,t1} = V^{ra}_{n2,t1} I^{ra}_{g1,t1} + V^{ia}_{n2,t1} I^{ia}_{g1,t1}$$
$$Q^{a}_{g1,t1} = V^{ia}_{n2,t1} I^{ra}_{g1,t1} - V^{ra}_{n2,t1} I^{ia}_{g1,t1}$$

$$P^{a}_{g1,t2} = V^{ra}_{n2,t2} I^{ra}_{g1,t2} + V^{ia}_{n2,t2} I^{ia}_{g1,t2}$$
$$Q^{a}_{g1,t2} = V^{ia}_{n2,t2} I^{ra}_{g1,t2} - V^{ra}_{n2,t2} I^{ia}_{g1,t2}$$

Note that, since all variables are column vectors the following notation can be used:

$$\iota^{T} P^{a}_{g1} = \sum_{t \in \mathcal{T}} P^{a}_{g1,t} = P^{a}_{g1,t1} + P^{a}_{g1,t2}$$

Where $\iota \in \mathbb{R}^{\tau}$ is a column vector with every component equal to one.

2.2 Generation

In Active Distribution Networks (ADNs), there are two basic kinds of power generation: from the bulk transmission system and from Distributed Energy Resources (DERs). Transmission system power injections are done at the network header node, while DER power injections can be done at any node $n \in \mathcal{N}$ of the network. Then, the injected apparent power from the transmission system at phase ϕ is defined as:

$$S^{\phi}_{g} = V^{\phi}_{h} \left(I^{\phi}_{g}\right)^{*} \quad g \in \mathcal{G}_{h},\ \phi \in \Phi_{g} \tag{2.2.1}$$

Where h is used to denote that the power from the transmission system is injected at the network header node, therefore, V^{ϕ}_{h} is the voltage at phase ϕ of the network header node. Besides, the injected apparent power at phase ϕ of node $n \in \mathcal{N}$ is defined as:

$$S^{\phi}_{g} = V^{\phi}_{n} \left(I^{\phi}_{g}\right)^{*} \quad g \in \mathcal{G}_{n},\ \phi \in \Phi_{g} \tag{2.2.2}$$

Unlike transmission system power injections, to define DER power injections it is required a complementary set of equations that depend on the kind of DER to be modeled. A simple schematic of a typical DER system is depicted in Figure 11.

A key component of DER systems is the Power Electronics Interface (PEI) since this is the equipment that allows power injections to be flexible enough so they could change in a matter

Figure 11: DER system. The Point of Common Coupling is the electrical point of connection with the distribution network.

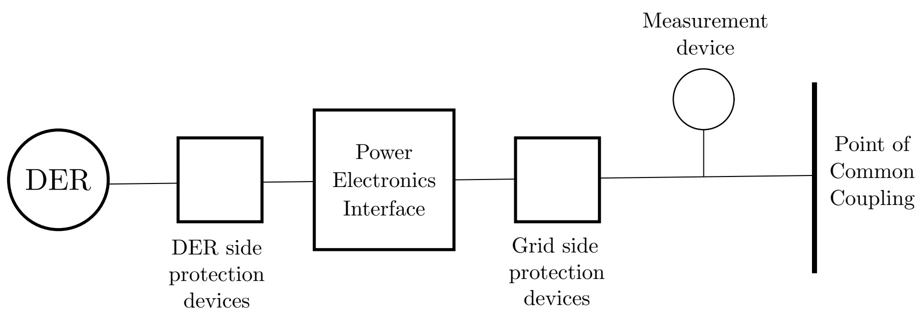

of few minutes (or even seconds). The PEIs are very complex electrical systems that change depending on the kind of DER to be controlled, hence, a deeper insight on its behavior is out of the scope of the present document.

As a consequence, equations presented below model only the power injections as seen by a bidirectional measurement device connected before the Point of Common Coupling (i.e., the electrical point of connection with the distribution network). Furthermore, only two kinds of DER systems are described: Photovoltaic (PV) and Electrical Storage (ES).

2.2.1 Photovoltaic systems.

Photovoltaic system active power injections are defined as the difference between the total available power and the curtailed power (see Figure 12):

Figure 12: Power injection by a PV system g at phase ϕ of node n.

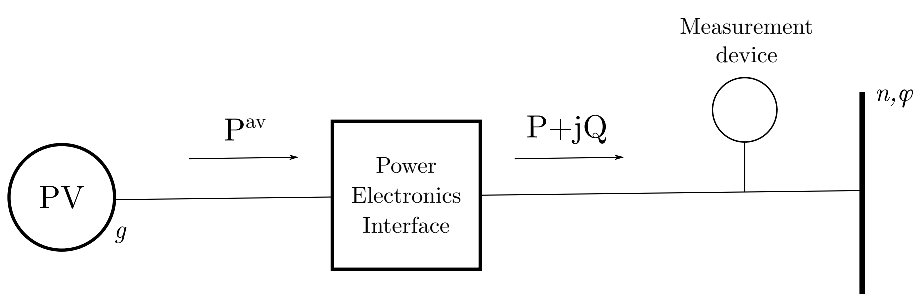

A portion of the total power available can be curtailed in order to mantain voltages within operational limits, i.e., $P^{av} \geqslant P$. PV systems can also inject reactive power to control the node voltage. For the present model, only constant power factor mode is implemented, i.e., $|Q| = P \tan \Theta$, for a given minimum power factor equal to $\cos \Theta$ (Standars Coordinating Committee, 2018).

$$P_g^{\phi} = P_g^{av.,\phi} - p_g^{\phi}, \quad \forall g \in \mathcal{G}_{pv}, \forall \phi \in \Phi_g \tag{2.2.3}$$

Where P_g^{ϕ} is the power being injected to the network, $P_g^{av.}$ is the total available power from a given irradiance, p_g is the total power being curtailed and $P_g^{\phi}, p_g^{\phi} \geqslant 0$. Power curtailment is mainly used to avoid voltage limit violations, however, standards like (Standars Coordinating Committee, 2018) propose reactive compensation as another way to keep voltages within operational limits. Namely, reactive power injected by the PV system is limited:

$$|Q_g^\phi| \leqslant P_g^\phi \tan \Theta_g^{max.}, \quad \forall g \in \mathcal{G}_{pv}, \forall \phi \in \Phi_g \tag{2.2.4}$$

So, it always injects apparent power with at least a power factor equal to $\cos \Theta_g^{max}$. This is what is called *constant power factor mode* for DER reactive power compensation (Standars Coordinating Committee, 2018). Note that $\Theta_g^{max} = 0$ enforce the system to only inject active power, i.e., equation (2.2.4) becomes $Q_g^\phi = 0$, $\forall g \in \mathcal{G}_{pv}$, $\forall \phi \in \Phi_g$.

2.2.2 Electric storage systems. In contrast to all other system elements, Electric Storage (ES) has two *exclusive disjunctive* states, i.e., an ES can be charging or discharging, but not both. Therefore, its behavior can be modeled with auxiliary time-dependent boolean (integer) variables. This drastically increases the problem complexity, hence, since an efficient mixed-integer formulation of the ES system is beyond the scope of the present model description, this behavior is modeled by choosing a specific objective function (see section 2.5.2) and by using the equations below.

Figure 13: Electrical storage model.

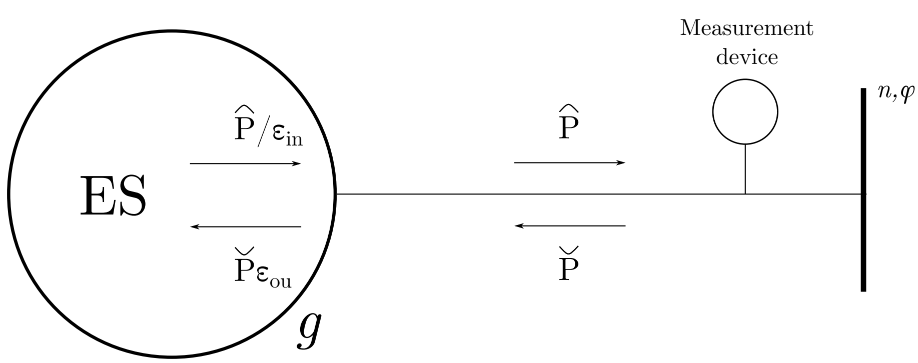

$\hat{P}$ and $\check{P}$ are the power being injected (discharged) to and withdrawn (charged) from the network by the battery; and ϵ_{in} and ϵ_{ou} are the efficiencies when injecting and withdrawing such energy, respectively. Note that a portion of the discharged energy (from the battery) is actually injected to the network, and a portion of the withdrawn energy (from the network) is used to charge the battery.

At first place, the power that being injected into or withdrawn from the network can be expressed as:

$$P_g^\phi = \hat{P}_g^\phi - \check{P}_g^\phi, \quad \forall g \in \mathcal{G}_{ES}, \forall \phi \in \Phi_g \tag{2.2.5}$$

Where $\hat{P}_g$ and $\check{P}_g$ are the power being injected to and withdrawn from the network (respectively); P_g^ϕ is the power being injected to or withdrawn from the network, since $\hat{P}_g = 0$

if $\check{P}_g \neq 0$ and *vice versa*, and $\hat{P}_g, \check{P}_g \geqslant 0$. Therefore, since $\hat{P}_g$ and $\check{P}_g$ represent *exclusive disjunctive* states, when the battery is discharging energy $P_g^\phi = \hat{P}_g$ and when the battery is charging $P_g^\phi = -\check{P}_g$. Note that in this formulation storage systems are not allowed to inject or withdraw reactive power, so $Q_g^\phi = 0$, $\forall g \in \mathcal{G}_{\text{ES}}$, $\forall \phi \in \Phi_g$. As presented in section 2.5.2, the complementary nature of $\hat{P}_g$ and $\check{P}_g$ is enforced using a specific objective function.

At second place, here it is considered that if some amount of energy would be withdrawn from the network, only a portion of this energy would be used to charge the battery; similarly, if some amount of energy would be discharged, only a portion of this energy would be injected to the network (See Figure 13). That is, the electrical storage charging and discharging efficiencies are less than one. Therefore, the power that is being injected to or withdrawn from the battery g is:

$$\tilde{P}_g^\phi = \hat{P}_g^\phi / \epsilon_{in} - \check{P}_g^\phi \times \epsilon_{ou} \tag{2.2.6}$$

Where $\tilde{P}_g^\phi$ is the actual energy being charged to or discharged from the ES system, and ϵ_{in} and ϵ_{ou} are their respective efficiencies.

At third place, ES systems connect two points in time. So, for any time period t, this property is defined by:

$$\tilde{P}_{g,t}^\phi = \left(SOC_{g,t-1}^\phi - SOC_{g,t}^\phi\right) E_g/\Delta t, \quad \forall g \in \mathcal{G}_{\text{ES}}, \forall \phi \in \Phi_g, \forall t \in \mathcal{T} \tag{2.2.7}$$

Where $SOC_g \in \mathbb{R}^\tau$ is the state of charge of the ES system, and $SOC_{g,0}^\phi = SOC_{g,\tau}^\phi = SOC_g^{\text{min.}}$; $E_g \in \mathbb{R}$ is the maximum energy that can be stored; and $\Delta t = 1$ hour. From equation (2.2.7) one can see that the scaled change in the SOC defines the power being charged or discharged from the electrical storage. Finally, each storage system has the following constraints for all $g \in \mathcal{G}_{ss}$ and for all $\phi \in \Phi_g$:

$$SOC_g^{\text{min.}} \leqslant SOC_g^\phi \leqslant 1 \tag{2.2.8}$$

$$\hat{P}_g^\phi \leqslant P_g^{\text{max.}} \times \epsilon_{in} \tag{2.2.9}$$

$$\check{P}_g^\phi \leqslant P_g^{\text{max.}} / \epsilon_{ou} \tag{2.2.10}$$

2.3 Demand

Power distribution network demand depends heavily on the type of connection and on the changes in power consumed due to changes in the steady state voltage applied. The two basic types of load connection are the *wye* and *delta* connection (see Figure 14). Note that if a branch is removed from a wye load, a two-phase-to-ground load is left, and if an additional phase is removed, a single-phase load is left. On the other hand, if two branches are removed from a delta load, a phase-to-phase load is left.

Figure 14: Wye (left) and delta (right) load connections. Branch voltage for the wye load is equal to the phase-to-neutral voltage, while for the delta load is equal to the phase-to-phase voltage.

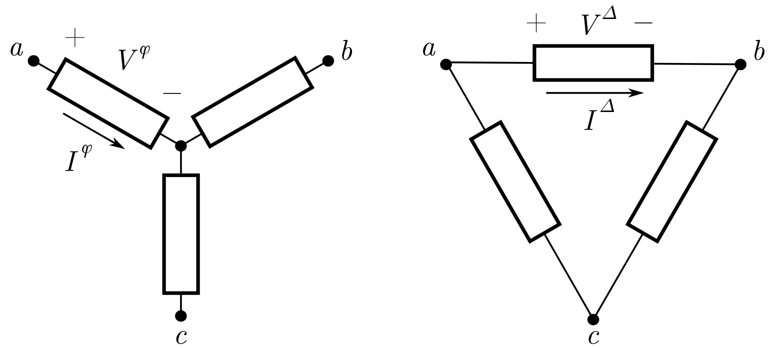

The three basic types of load behavior considered here are the constant power, constant current and constant impedance behavior (see Figure 15), and they may be characterized as:

Constant power loads are those that in spite of changes in the steady state voltage, they always consume the same amount of power; therefore, a voltage dip linearly rises the load current, while a voltage rise linearly diminishes the load current.

Constant current loads are those that in spite of changes in steady state voltage, they always withdraw the same current; therefore, a voltage dip linearly diminishes the power consumed and a voltage rise linearly increases the power consumed.

Constant impedance loads are those that in spite in changes in steady state voltage, they always have the same equivalent impedance; therefore, a voltage dip quadratically diminishes the power consumed and a voltage rise quadratically increases the power consumed.

So, in first place, for any wye connected load, and $\mathcal{N}_{S_Y}$ being the set of all nodes with constant (apparent) power injections; $\mathcal{N}_{I_Y}$ being the set of all nodes with constant current injections; and $\mathcal{N}_{Z_Y}$ being the set of all nodes with constant impedance current injections; the load current is defined by:

$$\tilde{S}_d^\phi = V_n^\phi \bar{I}_{S_Y d}^\phi, \quad \forall n \in \mathcal{N}_{S_Y}, \forall d \in \mathcal{D}_{Y n}, \forall \phi \in \Phi_d \tag{2.3.1}$$

$$\tilde{I}_d^\phi = I_{I_Y d}^\phi, \quad \forall n \in \mathcal{N}_{I_Y}, \forall d \in \mathcal{D}_{Y n}, \forall \phi \in \Phi_d \tag{2.3.2}$$

$$I_{Z_Y d}^\phi = \tilde{Y}_d^\phi V_n^\phi, \quad \forall n \in \mathcal{N}_{Z_Y}, \forall d \in \mathcal{D}_{Y n}, \forall \phi \in \Phi_d \tag{2.3.3}$$

Where $\mathcal{D}_{\curlyvee n}$ is the set of wye loads connected to node n, and $\tilde{S}_d$, $\tilde{I}_d$ and $\tilde{Y}_d$ are the known wye load parameters that remain constant in spite of steady state voltage variations. Thus, the total current injected at phase ϕ of node n from a wye load d is defined as:

$$I^{\phi}_{\curlyvee d} = I^{\phi}_{S\curlyvee d} + I^{\phi}_{I\curlyvee d} + I^{\phi}_{Z\curlyvee d}, \quad d \in \mathcal{D}_{\curlyvee n},\ \phi \in \Phi_d \tag{2.3.4}$$

Figure 15: ZIP load model independent of the connection type. Note that the load has a constant impedance component, a constant current component and a constant power component.

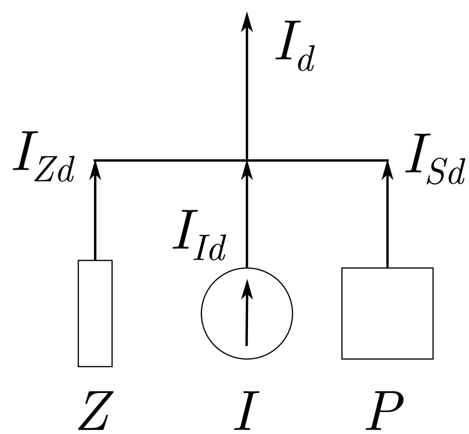

In second place, for any delta connected load, and $\mathcal{N}_{S\Delta}$ being the set of all nodes with constant (apparent) power injections; $\mathcal{N}_{I\Delta}$ being the set of all nodes with constant current injections; and $\mathcal{N}_{Z\Delta}$ being the set of all nodes with constant impedance current injections; the load current is defined by:

$$\tilde{S}^{\Delta}_{d} = V^{\Delta}_{n}\bar{I}^{\Delta}_{Sd}, \quad \forall\Delta \in \mathcal{F},\ \forall n \in \mathcal{N}_{S\Delta},\ \forall d \in \mathcal{D}_{\Delta n} \tag{2.3.5}$$

$$\tilde{I}^{\Delta}_{d} = I^{\Delta}_{Id}, \quad \forall\Delta \in \mathcal{F},\ \forall n \in \mathcal{N}_{I\Delta},\ \forall d \in \mathcal{D}_{\Delta n} \tag{2.3.6}$$

$$I^{\Delta}_{Zd} = \tilde{Y}^{\Delta}_{d}V^{\Delta}_{n}, \quad \forall\Delta \in \mathcal{F},\ \forall n \in \mathcal{N}_{Z\Delta},\ \forall d \in \mathcal{D}_{\Delta n} \tag{2.3.7}$$

Where $\mathcal{D}_{\Delta n}$ is the set of delta loads connected to node n, $\Delta = \{\phi, \varphi\}$ is a delta branch between phases ϕ and φ, and $\mathcal{F} = \{(a,b),(b,c),(c,a)\}$; $\tilde{S}^{\Delta}_{d}$, $\tilde{I}^{\Delta}_{d}$ and $\tilde{Y}^{\Delta}_{d}$ are the known Δ branch load parameters that remain constant in spite of steady state voltage variations; and V^{Δ}_{n} is the applied voltage to the Δ branch, i.e., $V^{\Delta}_{n} = V^{\phi}_{n} - V^{\varphi}_{n}$. Thus, the total current injected at phase ϕ of node n from a delta load d is defined as:

$$I^{\phi}_{\Delta d} = \sum_{\Delta\in\mathcal{F}_{\phi}} I^{\Delta}_{Sd} + \sum_{\Delta\in\mathcal{F}_{\phi}} I^{\Delta}_{Id} + \sum_{\Delta\in\mathcal{F}_{\phi}} I^{\Delta}_{Zd},\ d \in \mathcal{D}_{\Delta n},\ \phi \in \Phi_d \tag{2.3.8}$$

Where, $\mathcal{F}_{\phi}$ is the set of delta branches connected to phase ϕ, e.g., for $\phi = a$, $\mathcal{F}_{\phi} =$

$\{(a,b),(a,c)\}$. Adding up everything, the total current demanded by a load d at phase ϕ of node n is:

$$I_d^{\phi} = I_{Yd}^{\phi} + I_{\Delta d}^{\phi}, \quad d \in \mathcal{D}_n,\ \phi \in \Phi_d \tag{2.3.9}$$

2.4 Network

Two network components are treated: Lines and nodes. In contrast with previous elements, line equations involve variables from two nodes. Let us apply KCL to the line model depicted in Figure 16:

$$I_{(n,m)} = I_{r(n)} + I_{r(n,m)} \tag{2.4.1}$$

$$I_{(n,m)} = jb_{r(n)}V_n + y_{r(n,m)}\left(V_n - V_m\right) \tag{2.4.2}$$

$$I_{(n,m)} = \left(y_{r(n,m)} + jb_{r(n)}\right)V_n - y_{r(n,m)}V_m \tag{2.4.3}$$

Figure 16: General current balance at node n.

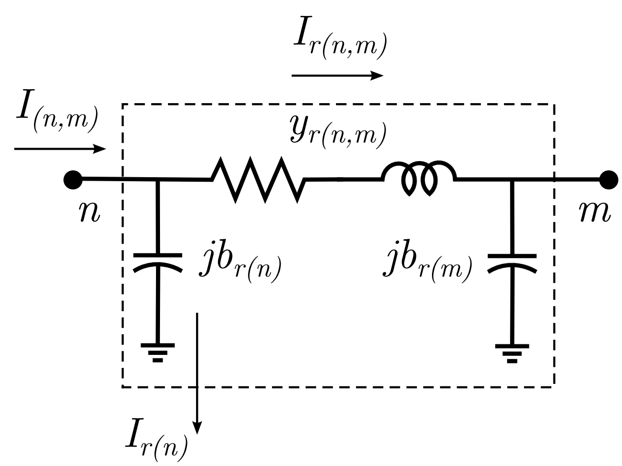

Where $jb_{r(n)} = y_{r(n)}$ is the shunt susceptance of branch r at node n, $y_{r(n,m)}$ is the serial admittance of branch r, $I_{r(n)}$ is the current flowing through $y_{r(n)}$, $I_{r(n,m)}$ is the current flowing from node n to node m through $y_{r(n,m)}$, V_n is the voltage at node n and V_m is the voltage at node m –Note that $y_{r(n,m)} = y_{r(m,n)}$ and $y_{r(n)} = y_{r(m)}$. From equation (2.4.3) and defining $y_{r(n,m)}^{\text{from}} = y_{r(n,m)} + y_{r(n)}$ and $y_{r(n,m)}^{\text{to}} = -y_{r(n,m)}$, the current injected from the network at node n is defined by:

$$I_{(n,m)} = y_{r(n,m)}^{\text{from}}V_n + y_{r(n,m)}^{\text{to}}V_m \tag{2.4.4}$$

Similar calculations can be done to deduce the three-phase line model, being the main difference the fact that each line shunt and series admittances are matrices for lines with more than one phase, hence, there are as much equations per branch as phases:

$$I^{\phi}_{(n,m)} = \sum_{\varphi \in \Phi_n} \left(y^{\phi,\varphi,\text{from}}_{r(n,m)} V^{\varphi}_{n} + y^{\phi,\varphi,\text{to}}_{r(n,m)} V^{\varphi}_{m} \right), \; \forall \phi \in \Phi_r, \, \forall r \in \mathcal{R} \tag{2.4.5}$$

Where $y^{\phi,\varphi,\text{from}}_{r(n,m)} = y^{\phi,\varphi}_{r(n,m)} + y^{\phi,\varphi}_{r(n)}$, with $y^{\phi\varphi}_{r(n)} = 0$ if $\phi \neq \varphi$; and $y^{\phi,\varphi,\text{to}}_{r(n,m)} = -y^{\phi,\varphi}_{r(n,m)}$.

In order to include a voltage regulator in any branch r, equation (2.4.5) must be modified in the following way (with tap on node n):

$$y^{\phi,\varphi,\text{from}}_{r(n,m)} = \bar{t}^{\phi} \left(y^{\phi\varphi}_{r(n,m)} + y^{\phi\varphi}_{r(n)} \right) t^{\varphi} \tag{2.4.6}$$

$$y^{\phi,\varphi,\text{to}}_{r(n,m)} = \bar{t}^{\phi} \left(-y^{\phi\varphi}_{r(n,m)} \right) \tag{2.4.7}$$

Where t^{ϕ} is the selected tap on phase ϕ. Furthermore, since $I^{\phi}_{(n,m)} \neq I^{\phi}_{(m,n)}$:

$$y^{\phi,\varphi,\text{to}}_{r(m,n)} = \left(-y^{\phi\varphi}_{r(m,n)} \right) t^{\varphi} \tag{2.4.8}$$

With the generation, demand and line current injections defined at node n, the current balance must satisfy (see Figure 17):

$$I_g - I_d = I_n \tag{2.4.9}$$

Figure 17: Current balance at node n.

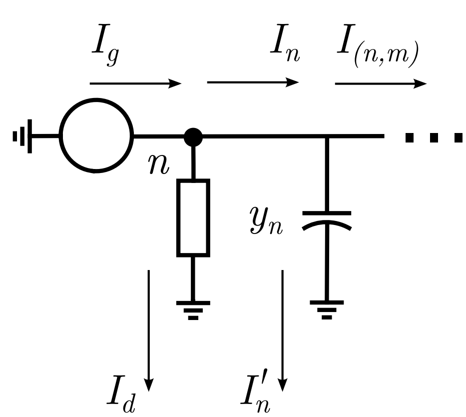

Where $I_n = I'_n + I_{(n,m)}$ is the total current injected from the network and $I'_n = y_n V_n$ is the current flowing through the equivalent shunt admittance connected to node n. Therefore, equation (2.4.9) can be generalized as:

$$\sum_{g \in \mathcal{G}_n} I_g^{\phi} - \sum_{d \in \mathcal{D}_n} I_d^{\phi} = I_n^{\phi}, \quad \forall \phi \in \Phi_n, \forall n \in \mathcal{N} \tag{2.4.10}$$

Where $I_n^{\phi} = y_n^{\phi} V_n^{\phi} + \sum_{r \in \mathcal{R}_n} I_{(n,m)}^{\phi}$. Note that $I_n^{\phi} = 0$ at nodes without generation nor demand.

2.5 Problem definition

Given the models presented above, an optimization problem can be formulated to find the optimal power injections set-points for each DER. For all cases and for each time period, decision variables are the real and imaginary components of voltages, injected currents and branch currents for each connected phase. On the DER side, the decision variables are the active power curtailed for each PV system and the storage system active power injected to and withdrew from the network. When including PV reactive compensation, reactive power injected by each PV system for each connected phase is also a decision variable. With this in mind, the non-convex 3ϕ-ACOPF formulation is presented in Frame 7 .

Frame 7. 3ϕ Alternating Current Optimal Power Flow

The 3ϕ-ACOPF can be formulated as follows:

$$\max\{F\}$$

s.t.

Power Flow Equations: (2.2.1), (2.3.1–2.3.9), (2.4.5), (2.4.10)

See Frame 8

$$\tag{2.5.1}$$

PV System Equations: (2.2.2-2.2.4) (2.5.2)

$$S_g^\phi = V_n^\phi \left(I_g^\phi\right)^* \; \forall g \in \mathcal{G}_{pv}, \forall n \in \mathcal{N}_g, \forall \phi \in \Phi_g$$

$$P_g^\phi = P_g^{av.,\phi} - p_g^\phi \; \forall g \in \mathcal{G}_{pv}, \forall \phi \in \Phi_g$$

$$|Q_g^\phi| \leqslant P_g^\phi \tan \Theta_g^{max.} \; \forall g \in \mathcal{G}_{pv}, \forall \phi \in \Phi_g$$

ES System Equations: (2.2.2),(2.2.5-2.2.10)

$$S_g^\phi = V_n^\phi \left(I_g^\phi\right)^* \; \forall g \in \mathcal{G}_{ES}, \forall n \in \mathcal{N}_g, \forall \phi \in \Phi_g$$

$$P_g^\phi = \hat{P}_g^\phi - \check{P}_g^\phi \; \forall g \in \mathcal{G}_{ES}, \forall \phi \in \Phi_g$$

$$\tilde{P}_g^\phi = \hat{P}_g^\phi / \epsilon_{in} - \check{P}_g^\phi \times \epsilon_{ou} \; \forall g \in \mathcal{G}_{ES}, \forall \phi \in \Phi_g$$

$$\tilde{P}_{g,t}^\phi = \left(SOC_{g,t-1}^\phi - SOC_{g,t}^\phi\right) E_g / \Delta t \; \forall g \in \mathcal{G}_{ES}, \forall \phi \in \Phi_g, \forall t \in \mathcal{T}$$

$$SOC_g^{min.} \leqslant SOC_g^\phi \leqslant 1 \; \forall g \in \mathcal{G}_{ES}, \forall \phi \in \Phi_g$$

$$SOC_{g,0}^\phi = SOC_{g,\tau}^\phi = SOC_g^{min.}, \; \forall g \in \mathcal{G}_{ES}, \forall \phi \in \Phi_g$$

$$\hat{P}_g^\phi \leqslant P_g^{max.} \times \epsilon_{in} \; \forall g \in \mathcal{G}_{ES}, \forall \phi \in \Phi_g$$

$$\check{P}_g^\phi \leqslant P_g^{max.} / \epsilon_{ou} \; \forall g \in \mathcal{G}_{ES}, \forall \phi \in \Phi_g$$

Voltage magnitude limit equations:

$$|V_n^{min}|^2 \leqslant |V_n^\phi|^2 \leqslant |V_n^{max}|^2 \quad \forall \phi \in \Phi_n, \forall n \in \mathcal{N} \tag{2.5.3}$$

Voltage angle reference equations:

$$\Im\{V_h^a\} = 0 \tag{2.5.4}$$

$$\Re\{V_h^b\} \tan(-2\pi/3) = \Im\{V_h^b\} \tag{2.5.5}$$

$$\Re\{V_h^c\} \tan(-4\pi/3) = \Im\{V_h^c\} \tag{2.5.6}$$

Where the Power Flow Equations are the set of equations that, when solved simultaneously, give the solution of a three-phase power flow (see section 2.5.1); F depends on the case being analyzed (see section 3.1.3); equation (2.5.3) is used to enforce a solution within acceptable voltage magnitude limits; and equations (2.5.4–2.5.6) establish the voltage angle reference at the network header node h.

2.5.1 Power flow equations. Equations (2.2.1), (2.3.1–2.3.9), (2.4.5), (2.4.10) define the Power Flow Equations (PFE), i.e., the set of equations that, when solved simultaneously, give the solution of a three-phase power flow. They are summarized in Frame 8 for the sake of reference, although not in the order they were presented.

Frame 8. POWER FLOW EQUATIONS

The Power Flow Equations (PFE) can be classified in two groups, (1) Current balance equations and (2) Electrical element definitions:

Current balance equations:

$$\begin{aligned}
\textit{Node:}\quad & I_n^\phi = \sum_{g\in\mathcal{G}_n} I_g^\phi - \sum_{d\in\mathcal{D}_n} I_d^\phi \quad \phi\in\Phi_n,\ \forall n\in\mathcal{N}\\
\textit{Total Demand:}\quad & I_d^\phi = I_{\curlyvee d}^\phi + I_{\Delta d}^\phi,\quad d\in\mathcal{D}_n,\ \phi\in\Phi_d\\
\textit{Network:}\quad & I_n^\phi = y_n^\phi V_n^\phi + \sum_{r\in\mathcal{R}_n} I_{(n,m)}^\phi \ \phi\in\Phi_n,\ \forall n\in\mathcal{N}\\
\textit{Line:}\quad & I_{(n,m)}^\phi = \sum_{\varphi\in\Phi_n}\left(y_{r(n,m)}^{\phi,\varphi,\mathrm{from}} V_n^\varphi + y_{r(n,m)}^{\phi,\varphi,\mathrm{to}} V_m^\varphi\right)\ \forall\phi\in\Phi_r,\ \forall r\in\mathcal{R}\\
\textit{Wye Demand:}\quad & I_{\curlyvee d}^\phi = I_{S\curlyvee d}^\phi + I_{I\curlyvee d}^\phi + I_{Z\curlyvee d}^\phi\ d\in\mathcal{D}_{\curlyvee n},\ \phi\in\Phi_d\\
\textit{Delta Demand:}\quad & I_{\Delta d}^\phi = \sum_{\Delta\in\mathcal{F}_\phi} I_{Sd}^\Delta + \sum_{\Delta\in\mathcal{F}_\phi} I_{Id}^\Delta + \sum_{\Delta\in\mathcal{F}_\phi} I_{Zd}^\Delta,\ d\in\mathcal{D}_{\Delta n},\ \phi\in\Phi_d
\end{aligned}$$

Electrical element definitions:

$$\begin{aligned}
&\textit{Header power injection:} && S_g^{\phi} = V_h^{\phi}\left(I_g^{\phi}\right)^{*} && g \in \mathcal{G}_h,\ \phi \in \Phi_g \\
&\textit{Constant power wye load:} && \tilde{S}_d^{\phi} = V_n^{\phi}\left(I_{S_Y d}^{\phi}\right)^{*} && n \in \mathcal{N}_{S_Y},\ d \in \mathcal{D}_{Yn},\ \phi \in \Phi_d \\
&\textit{Constant current wye load:} && \tilde{I}_d^{\phi} = I_{I_Y d}^{\phi} && n \in \mathcal{N}_{I_Y},\ d \in \mathcal{D}_{Yn},\ \phi \in \Phi_d \\
&\textit{Constant impedance wye load:} && I_{Z_Y d}^{\phi} = \tilde{Y}_d^{\phi} V_n^{\phi} && n \in \mathcal{N}_{Z_Y},\ d \in \mathcal{D}_{Yn},\ \phi \in \Phi_d \\
&\textit{Constant power delta load:} && \tilde{S}_d^{\Delta} = V_n^{\Delta}\left(I_{Sd}^{\Delta}\right)^{*} && \Delta \in \mathcal{F},\ n \in \mathcal{N}_{S\Delta},\ d \in \mathcal{D}_{\Delta n} \\
&\textit{Constant current delta load:} && \tilde{I}_d^{\Delta} = I_{Id}^{\Delta} && \Delta \in \mathcal{F},\ n \in \mathcal{N}_{I\Delta},\ d \in \mathcal{D}_{\Delta n} \\
&\textit{Constant impedance load:} && I_{Zd}^{\Delta} = \tilde{Y}_d^{\Delta} V_n^{\Delta} && \Delta \in \mathcal{F},\ n \in \mathcal{N}_{Z\Delta},\ d \in \mathcal{D}_{\Delta n}
\end{aligned}$$

The solution of the three-phase power flow without DERs can be calculated by solving the Power Flow Equations for a given network topology and the following problem parameters:

- The voltage angle references of the header node ($\angle\delta_{V_h^a} = 0^{\underline{o}}$, $\angle\delta_{V_h^b} = -120^{\underline{o}}$, $\angle\delta_{V_h^c} = 120^{\underline{o}}$)
- The voltage time profile at the header (V_h^{ϕ})
- The line admittances ($y_{r(n,m)}^{\phi,\varphi,\text{from}}$, $y_{r(n,m)}^{\phi,\varphi,\text{to}}$)
- The ZIP load parameters ($\tilde{S}_d^{\phi}$, $\tilde{I}_d^{\phi}$, $\tilde{Y}_d^{\phi}$, $\tilde{S}_d^{\Delta}$, $\tilde{I}_d^{\Delta}$, $\tilde{Y}_d^{\Delta}$)

In annex (C) is found the results of applying these equations to the well known 13, 34 and 123 node IEEE test feeders.

2.5.2 Objective functions. Four types of objectives functions are considered: active power costs, weighted apparent power costs, costs of active power losses and storage arbitrage benefits. Please note that the forthcoming analyses (see chapter 3) are not meant to deduce or give insights on proper active and reactive power pricing in Active Distribution Networks, instead, these kinds of analyses are left for future researches.

Active power costs Suppose that energy is bought at the system header for a given price at each time t given by $\pi_t \in \mathbb{R}_+$, so $\pi \in \mathbb{R}_+^{\tau}$. Also suppose that the DNO wants to minimize the total energy consumption costs at the system header. The active power costs at the system header (f^P) are:

$$f^P = \sum_{\phi\in\Phi}\sum_{t\in\mathcal{T}} \pi_t P_{h,t}^{\phi} \tag{2.5.7}$$

Weighted apparent power costs Suppose that the DNO wants to minimize active and reactive power imports (Madani et al., 2015) using the energy price at the header as a weight for all power transfers and time periods. Therefore, the weighted apparent power costs (f^S) are:

$$f^S = \sum_{\phi \in \Phi} \sum_{t \in \mathcal{T}} \pi_t \left[\left(P^{\phi}_{h,t} \right)^2 + \left(Q^{\phi}_{h,t} \right)^2 \right] \tag{2.5.8}$$

Costs of active power losses Total losses for each time period in a three-phase power distribution system (P^{LOSS}) can be calculated as:

$$P^{LOSS} = \sum_{r \in \mathcal{R}} \sum_{\phi \in \Phi_r} P^{LOSS,\phi}_r = \sum_{r \in \mathcal{R}} \sum_{\phi \in \Phi_r} \Re \left\{ V^{\phi}_n \bar{I}^{\phi}_{(n,m)} + V^{\phi}_m \bar{I}^{\phi}_{(m,n)} \right\} \tag{2.5.9}$$

Assuming $I_{(m,n)} \approx -I_{(n,m)}$:

$$P^{LOSS} = \sum_{r \in \mathcal{R}} \sum_{\phi \in \Phi_r} \Re \left\{ \bar{I}^{\phi}_{(n,m)} \left(V^{\phi}_n - V^{\phi}_m \right) \right\} \tag{2.5.10}$$

Then, if $I_{r(n,m)} \approx I_{(n,m)}$, and since $z^{\phi\varphi}_{r(n,m)} = z^{\varphi\phi}_{r(n,m)}$ and with $\Re \left\{ z^{\phi\varphi}_{r(n,m)} \right\} = R^{\phi\varphi}_{r(n,m)}$ for all connected phases, equation (2.5.10) can be written as:

$$P^{LOSS} = \sum_{r \in \mathcal{R}} \left\{ \sum_{\phi,\varphi \in \Phi_r} R^{\phi\phi}_{r(n,m)} \left| I_{(n,m)} \right|^2 + \sum_{\phi,\varphi \in \{\mathcal{F} \cap \Phi_r\}} R^{\phi\varphi}_{r(n,m)} \left[\Re \left(I^{\phi}_{(n,m)} \bar{I}^{\varphi}_{(n,m)} \right) \right] \right\} \tag{2.5.11}$$

So, ignoring the coupling effects:

$$P^{LOSS} = \sum_{r \in \mathcal{R}} \sum_{\phi \in \Phi_r} \left\{ R^{\phi\phi}_{r(n,m)} \left| I_{(m,n)} \right|^2 \right\} \tag{2.5.12}$$

Equation (2.5.9) gives the exact value for losses, while equation (2.5.11) gives a good estimation for the network losses. On the other hand, equation (2.5.12) have been reported in the literature (Watson et al., 2017; Li et al., 2017; Su et al., 2014) as a surrogate of the total losses equation. In general, total losses are defined as $L_T = \sum_{t \in \mathcal{T}} P^{LOSS}_t$. Thus, total costs of active power losses (f^{LOSS}) can be defined as:

$$f^{LOSS} = \sum_{t \in \mathcal{T}} \pi_t P^{LOSS}_t \tag{2.5.13}$$

Storage arbitrage benefits As reported in (Gill et al., 2014), by assuring that the round-trip efficiency of the storage system is less than one (i.e., $\epsilon_{in}\epsilon_{ou} < 1$) and if power injections are meant to be maximized, and power withdrawals are meant to be minimized, one can model the storage device behavior without discrete variables if the following objective function is used:

$$f^{\mathrm{ES}} = \frac{1}{\rho} \sum_{g \in \mathcal{G}_{ss}} \sum_{\phi \in \Phi_g} \sum_{t \in \mathcal{T}} \pi_t \left[\hat{P}^{\phi}_{g,t} - \check{P}^{\phi}_{g,t} \right] \tag{2.5.14}$$

Where f^{ES} are the total arbitrage benefits that are captured by the electrical storage systems in the network and ρ is a scaling factor used to diminish the impact of the time arbitrage over the other objectives. The choice of ρ when combining objective functions is very important: If ρ is too large, f^{ES} will lose importance in the optimization, and so the storage injections. As a consequence, $\hat{P}^{\phi}_{g}$ and $\check{P}^{\phi}_{g}$ might have values different to zero on the same time period, i.e., the ES will be charging and discharging power at the same time, which is physically impossible (Gill et al., 2014). Furthermore, the ρ parameter can be used to adjust what it would be considered as "zero" when charging or discharging energy. Hence, depending on the value of ρ a zero $\hat{P}^{\phi}_{g}$ or $\check{P}^{\phi}_{g}$ can vary from 1×10^{-1} to 1×10^{-7}.

CHAPTER 3

Centralized DER Scheduling

This chapter shows a comprehensive study on the impact of optimal DER scheduling in distribution networks for a centralized operation strategy. This study is based on the models presented in section 2.5 (non-convex 3ϕ-ACOPF formulation) and its main goal is to answer the questions stated at the end of chapter 1: (Q-Ia) Are the answers obtained by a 3ϕ-ACOPF different enough from those given by a single-phase ACOPF? (Q-Ib) Is the optimal DER scheduling increasing or decreasing the voltage unbalance in the network? This chapter is organized as follows: In section 3.1 are described the simulated cases; later, section 3.2 presents an analysis of the obtained results. This chapter closes in section 3.3 with a discussion and some concluding remarks.

3.1 Test cases

A total of 144 study cases were constructed to evaluate the performance of the non-convex model presented in section 2.5. Four factors are tested: (1) Type of circuit, (2) Type of DER, (3) Type of objective, and (4) Type of irradiance. In section 3.1.1, circuit types are described. This factor helps to see how useful a balanced model is (thus, one-line equivalents) when analyzing unbalanced systems. In section 3.1.3, the objective functions used are described. By testing for several objective functions and analyzing their effects on the network, it is expected to find some criteria to help choosing a suitable objective depending on the desired outcome. In section 3.1.2, DER configuration types are described. Changing the DER type helps to see if PV reactive compensation and storage are complementary measures for reactive and active power control in the network. All these factors are also tested for three levels of irradiance, which are described in section 3.1.4. For each case, the system parameters presented in section 3.1.5 are calculated after having the problem solution. All cases were implemented using GAMS 24.5.4 and the IPOPT 3.12 solver (with MUMPS as linear solver). Simulations were carried out on a laptop computer with an Intel(R) Core(TM) i7-4700MQ processor (2.4GHz) with 6GB of RAM.

3.1.1 Circuits. Three test systems are studied, all of them based on the IEEE 34 node test feeder (Kersting, 2001), which is depicted in Figure 18, and with the following modifications:

Complete: This is the *complete* circuit. For this case, the regulator taps were modified as presented in Table 5. No other modification took place in the construction of the network model.

Unbalanced: This is the circuit with *unbalanced* loads and only three-phase lines. For this case, regulator taps are the same than those for the *complete* circuit. Besides, all non-three-phase branches were removed; all loads that were on such branches are moved to the nearest three-phase node. This circuit helps to differentiate the error induced by ignoring system unbalance, and the error induced by ignoring non-three-phase laterals.

Balanced: This is the equivalent *balanced* circuit, and thus, the answers with this circuit are the same to those obtained with a one-line equivalent. Regulator taps are the same for each phase and were set to 7 and 10 for regulators at branches 814-850 and 852-832, respectively. Also, all non-three-phase branches are treated as in the *unbalanced* circuit. Besides, all lines are transposed and non-balanced loads/DERs were transformed into a balanced three-phase equivalent. Three load/DER transformations are treated: (1) One-phase loads/DERs are replaced by three-phase loads/DERs with 1/3 of the total power on each phase, e.g. a 3 MW load in one phase becomes three one-phase loads of 1 MW; (2) Two-phase loads/DERs are replaced by three-phase loads/DERs with 2/3 of the total power on each phase, e.g., a biphasic load of 1.5 MW per phase becomes three one-phase loads of 1 MW; (3) Unbalanced three-phase loads/DERs are replaced by balanced version with 1/3 of the total three-phase power on each phase, e.g. a total three-phase load of 3 MW (irrespective of the unbalance) will result in three one-phase loads of 1 MW.

Figure 18: One line of the 34 node IEEE test feeder. Nodes with DERs are marked with an outer circunference.

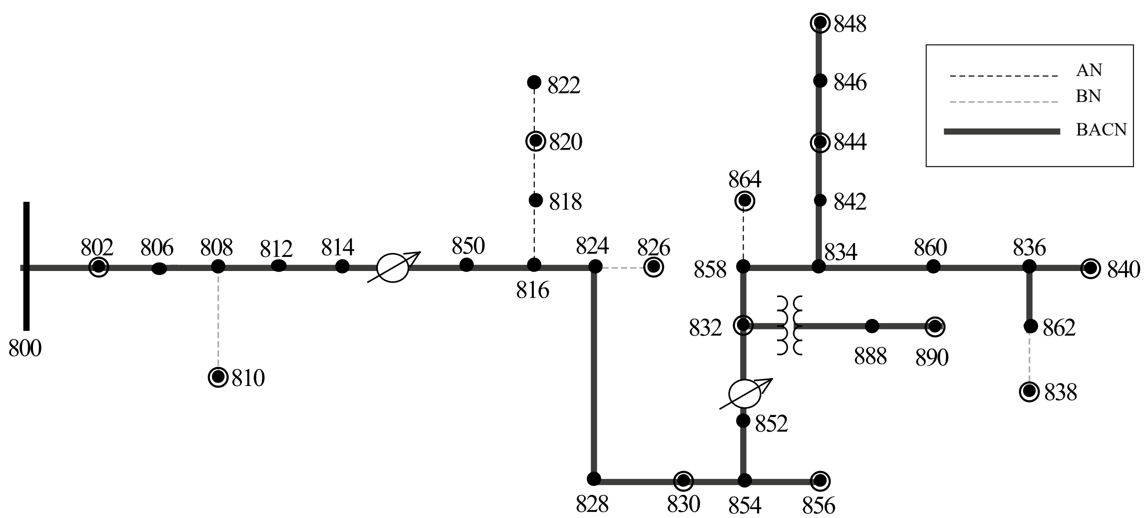

3.1.2 DER models.

Four DER models are studied, all including PV generation with curtailment at nodes presented in Table 5. The PV power curtailment is implemented to maintaining the voltage magnitude within the required operational limits; however, note that PV curtailment must be considered as an undesired action. With this in mind, the DER models to test are:

Base is the base case, i.e., only PV systems with curtailment ;

Q is the same as case (1), but with reactive compensation on each PV system –minimum power factor equal to 0.9;

Table 5: Test feeder parameters for the *complete* circuit

DER nodes	*Voltage limits* $[\mathrm{V_{p.u.}}]$	*Regulators (from-to nodes)*		
		a	*b*	*c*
810-b, 820-a, 826-b, 864-a, 890, 848, 840, 838-b, 856-b, 844, 830, 802, 832	0.90 to 1.05	814-850		
		14	7	7
		852-832		
		12	10	11
Electrical storage system parameters				
$\varepsilon_{\mathrm{in}} = 0.9$, $\varepsilon_{\mathrm{ou}} = 0.8$, $\mathrm{SOC_{min}} = 0.1$, $\mathrm{SOC_{max}} = 1$				
100 kWh per phase, 2.7 MWh of installed capacity				

DERs with unspecified phases are connected to all phases, i.e., they are connected to phase a, b and c.

ES is the same as case (1), but with electrical storage; and

ES-Q is the same as case (2), but with electrical storage.

Electrical storage is placed at nodes with PV generation. The placement of DERs was done arbitrarily, therefore, the study on the impact of DER location is left for future research.

3.1.3 Objectives.

The 3ϕ-ACOPF to be solved is defined in Frame 7, and all objectives studied here can be constructed from the objectives described in section 2.5.2. The idea is the following: In case of having electrical storage (i.e., for DER cases "ES" and "ES-Q"), the arbitrage benefits must be included. With this in mind, the four objectives studied when including electrical storage are:

Active power costs The objective *active power costs* consists in minimizing total active power costs at the header, i.e., $F = f^{\mathrm{ES}} - f^{\mathrm{P}}$;

Apparent power costs The objective *apparent power costs* consists on minimizing total weighted apparent power at the header, i.e., $F = f^{\mathrm{ES}} - f^{\mathrm{S}}$;

Costs of losses The objective *cost of losses* consists on minimizing the active power losses considering line coupling effects, i.e., $F = f^{\mathrm{ES}} - f^{\mathrm{LOSS}}$ using equation (2.5.11);

Costs of self losses The objective *costs of self losses* consists in minimizing the active power losses without line coupling effects, i.e., $F = f^{\mathrm{ES}} - f^{\mathrm{LOSS}}$ using equation (2.5.12).

In all cases f^{ES} is at least three orders of magnitude lower than the other objective and ρ is further adjusted so $\hat{P}_g^{\phi}$ and $\check{P}_g^{\phi}$ are at least 1×10^{-4} when charging and discharging, respectively. Of course $f^{\text{ES}} = 0$ if there is no electrical storage (i.e., for DER cases "Base" and "Q").

3.1.4 PV penetrations. Penetration is here defined as the ratio between the total available irradiance and the total active power injections at the system header without DERs (see Table 7). This is similar to the ratio between PV installed capacity and rated capacity of the header substation presented in (Su et al., 2014). Three PV penetration levels are studied:

max. Full irradiance, which corresponds to 129% of PV penetration, so the total energy given by all PV systems is about 30% more than the total demanded energy;

med. 3/5 of the total irradiance, which corresponds to 77% of PV penetration, so the total energy given by all the PV systems is 77% of the total demanded energy; and

min. 1/5 of the total irradiance, which corresponds to 26% of PV penetration, so the total energy given by all the PV systems is 26% of the total demanded energy.

The last two penetrations levels are usual values (Su et al., 2014; Li et al., 2017; Meng et al., 2017; Zamzam et al., 2017), while the former is used to test the impacts of very high penetrations on the distribution network, a needed feature of future distribution networks given the rapid increase of installed solar capacity (Meng et al., 2017; Su et al., 2014; Zamzam et al., 2017). For all cases that include electrical storage, the total installed capacity is always the same.

3.1.5 System parameter calculations. For each case, apart from the objective function value, apparent power injected by all PV systems is calculated as:

$$S_T^{pv} = \sum_{g \in \mathcal{G}_{pv}} \sum_{\phi \in \Phi_g} \sum_{t \in \mathcal{T}} S_{g,t}^{\phi}$$

Similarly, the following parameters are as well calculated:

➤ Total PV energy curtailed:

$$p_T = \sum_{g \in \mathcal{G}_{pv}} \sum_{\phi \in \Phi_g} \sum_{t \in \mathcal{T}} p_{g,t}$$

➤ Total ES energy injected :

$$P_T^{\wedge} = \sum_{g \in \mathcal{G}_{\text{ES}}} \sum_{\phi \in \Phi_g} \sum_{t \in \mathcal{T}} \hat{P}_{g,t}^{\phi}$$

➤ Total storage energy withdrawn :

$$P_T^{\vee} = \sum_{g \in \mathcal{G}_{ES}} \sum_{\phi \in \Phi_g} \sum_{t \in \mathcal{T}} \check{P}_{g,t}^{\phi}$$

➤ Total apparent power at the system header

$$S_T^h = P_T^h + jQ_T^h = \sum_{\phi \in \Phi_g} \sum_{t \in \mathcal{T}} S_{h,t}^{\phi}$$

Additionally, it is computed the negative and zero sequence Voltage Unbalance Factor (VUF) for all three-phase nodes. For example, the negative sequence VUF for the node n is defined as:

$$\mathrm{VUF}_n^{(-)} = \frac{|V_n^{(-)}|}{|V_n^{(+)}|} = \frac{|V_n^a + aV_n^b + a^2V_n^c|}{|V_n^a + a^2V_n^b + aV_n^c|}$$

Where $a = 1\angle -120°$. So the average negative sequence VUF is:

$$\mathrm{VUF}_{\mathrm{avg.}}^{(-)} = \frac{\iota^T}{|\mathcal{N}_{3\phi}| \times \tau} \sum_{n \in \mathcal{N}_{3\phi}} \mathrm{VUF}_n^{(-)}$$

Where $\mathcal{N}_{3\phi}$ is the set of all nodes that have phases a, b and c connected to it; and $|\mathcal{N}_{3\phi}|$ is the number of 3-phase nodes. Similar definitions can be constructed for the average zero sequence VUF, given that $V_n^{(0)} = 1/3 \sum_{\phi \in \Phi_n} V_n^{\phi}$.

3.2 Results

3.2.1 Changing circuit type. By changing the circuit type, it is expected to quantify the differences between an optimal DER scheduling in unbalanced and balanced distribution networks. Two circuits, the *complete* and *balanced* types were designed for this purpose. However, in the case of the *balanced* circuit, all non-three phase laterals were removed, so, to quantify the error induced by ignoring this kind of laterals a third kind of circuit was created: the *unbalanced* type, which consists in a completely unbalanced network without non-three phase laterals. Table 6 presents the percentage change in each of the calculated parameters (labeled at the table top) with respect a given circuit type (labeled at the table bottom), for

Table 6: Circuit type variations in percentage.

(a) Minimizing *active power costs*.

		f^P			L_T			P_T^h			Q_T^h			p_T		
		$\Delta_{C,U}$	$\Delta_{U,B}$	$\Delta_{C,B}$	$\Delta_{C,U}$	$\Delta_{U,B}$	$\Delta_{C,B}$	$\Delta_{C,U}$	$\Delta_{U,B}$	$\Delta_{C,B}$	$\Delta_{C,U}$	$\Delta_{U,B}$	$\Delta_{C,B}$	$\Delta_{C,U}$	$\Delta_{U,B}$	$\Delta_{C,B}$
max	DER Base	0.7	34.9	35.4	1.1	-13.6	-12.4	0.7	38.0	38.4	-2.0	-4.7	-6.8	-0.1	16.1	16.0
max	DER Q	0.8	65.6	65.9	0.6	-15.6	-14.9	0.8	72.3	72.5	-1.0	2.7	1.8	-0.3	29.8	29.5
max	DER ES	-1.0	-85.6	-87.5	1.0	-19.9	-18.7	1.1	60.9	61.4	-2.0	-5.6	-7.7	-0.1	20.5	20.4
max	DER ES-Q	-0.3	-46.9	-47.4	0.7	-16.5	-15.7	3.7	279.8	273.2	-0.9	3.0	2.1	-0.5	41.8	41.5
med	DER Base	0.4	15.8	16.1	1.2	-9.0	-7.7	0.4	16.5	16.9	-2.0	-3.6	-5.7	-0.3	36.1	35.9
med	DER Q	0.4	16.3	16.7	0.9	-7.3	-6.4	0.4	16.7	17.0	-1.2	9.0	7.8	-1.1	78.2	78.0
med	DER ES	3.6	249.5	244.1	1.1	-14.8	-13.5	0.5	18.8	19.2	-2.0	-4.2	-6.3	-0.6	80.1	80.0
med	DER ES-Q	-8.4	-350.0	-387.6	0.3	20.1	20.4	0.6	7.9	8.4	-1.7	30.8	29.6			
min	DER Base	0.3	-0.2	0.2	1.4	1.1	2.5	0.3	0.1	0.4	-2.1	-1.0	-3.1			
min	DER Q	0.3	-0.1	0.2	1.7	1.8	3.6	0.3	0.2	0.5	-2.3	0.6	-1.7			
min	DER ES	0.4	3.1	3.5	1.1	2.4	3.5	0.3	0.3	0.6	-2.0	-0.3	-2.2			
min	DER ES-Q	0.5	3.4	3.8	1.4	3.7	5.0	0.3	0.5	0.8	-2.1	5.2	3.2			

		Q_T^{pv}			f^{ES}			$P_T^{\wedge}$			$P_T^{\vee}$		
		$\Delta_{C,U}$	$\Delta_{U,B}$	$\Delta_{C,B}$	$\Delta_{C,U}$	$\Delta_{U,B}$	$\Delta_{C,B}$	$\Delta_{C,U}$	$\Delta_{U,B}$	$\Delta_{C,B}$	$\Delta_{C,U}$	$\Delta_{U,B}$	$\Delta_{C,B}$
max	DER Base												
max	DER Q	0.8	32.2	32.8									
max	DER ES				-0.1	-28.2	-28.3	0.0	1.3	1.3	0.0	1.4	1.4
max	DER ES-Q	1.0	33.8	34.4	0.4	-27.8	-27.2	-0.3	3.7	3.4	-0.3	3.9	3.6
med	DER Base												
med	DER Q	1.7	83.0	83.3									
med	DER ES				-0.0	-23.1	-23.1	-0.2	4.7	4.5	-0.2	4.9	4.8
med	DER ES-Q	-0.4	176.8	177.1	0.0	-24.0	-24.0	-0.0	-0.4	-0.4	-0.0	-0.4	-0.4
min	DER Base												
min	DER Q	-1.3	-4.7	-6.0									
min	DER ES				0.1	-8.4	-8.2	-0.2	1.3	1.1	-0.2	1.4	1.2
min	DER ES-Q	-1.4	-16.0	-17.7	0.1	-7.8	-7.7	-0.1	0.1	0.1	-0.1	0.2	0.1

(b) Minimizing *costs of losses*.

		f^P			L_T			P_T^h			Q_T^h			p_T		
		$\Delta_{C,U}$	$\Delta_{U,B}$	$\Delta_{C,B}$	$\Delta_{C,U}$	$\Delta_{U,B}$	$\Delta_{C,B}$	$\Delta_{C,U}$	$\Delta_{U,B}$	$\Delta_{C,B}$	$\Delta_{C,U}$	$\Delta_{U,B}$	$\Delta_{C,B}$	$\Delta_{C,U}$	$\Delta_{U,B}$	$\Delta_{C,B}$
max	DER Base	0.2	0.9	1.1	1.2	1.1	2.2	0.2	0.8	1.0	-2.2	-2.7	-5.0	-0.1	1.9	1.9
max	DER Q	0.3	1.3	1.6	1.9	1.8	3.7	0.3	1.4	1.6	-4.2	0.9	-3.3	-0.0	-0.4	-0.5
max	DER ES	0.4	0.6	1.0	1.2	1.9	3.0	0.3	0.1	0.4	-2.3	-2.6	-4.9	-0.1	2.3	2.2
max	DER ES-Q	0.5	2.1	2.6	2.2	3.2	5.4	0.3	1.1	1.4	-4.0	0.4	-3.6	-0.4	-0.1	-0.5
med	DER Base	0.3	0.8	1.1	1.3	1.1	2.4	0.2	0.8	1.0	-2.2	-2.5	-4.8	-0.2	4.3	4.1
med	DER Q	0.3	2.1	2.4	2.0	2.0	4.0	0.3	2.2	2.5	-4.2	2.2	-1.9	-0.1	1.0	0.9
med	DER ES	0.4	1.3	1.7	1.5	1.9	3.3	0.3	0.4	0.7	-2.2	-2.4	-4.7	-0.3	7.1	6.8
med	DER ES-Q	0.4	4.9	5.3	2.4	3.6	5.9	0.3	3.0	3.3	-4.0	2.0	-1.9	-0.3	3.1	2.7
min	DER Base	0.3	0.9	1.2	1.4	1.1	2.5	0.3	0.9	1.2	-2.1	-1.1	-3.2			
min	DER Q	0.3	1.0	1.3	1.7	1.5	3.2	0.3	1.0	1.2	-3.1	1.3	-1.8			
min	DER ES	0.3	1.1	1.4	1.4	1.1	2.5	0.3	0.6	0.9	-2.1	-1.0	-3.2			
min	DER ES-Q	0.3	1.5	1.8	1.7	1.5	3.2	0.3	0.9	1.2	-3.1	-0.1	-3.2			

		Q_T^{pv}			f^{ES}			$P_T^{\wedge}$			$P_T^{\vee}$		
		$\Delta_{C,U}$	$\Delta_{U,B}$	$\Delta_{C,B}$	$\Delta_{C,U}$	$\Delta_{U,B}$	$\Delta_{C,B}$	$\Delta_{C,U}$	$\Delta_{U,B}$	$\Delta_{C,B}$	$\Delta_{C,U}$	$\Delta_{U,B}$	$\Delta_{C,B}$
max	DER Base												
max	DER Q	-0.9	-2.0	-2.9									
max	DER ES				0.6	-1.0	-0.3	0.0	0.3	0.4	0.0	0.4	0.4
max	DER ES-Q	-1.0	-1.6	-2.6	0.7	-6.4	-5.7	0.0	0.5	0.5	0.0	0.5	0.6
med	DER Base												
med	DER Q	-0.6	-3.5	-4.2									
med	DER ES				0.3	-7.1	-6.7	0.1	0.6	0.6	0.1	0.6	0.7
med	DER ES-Q	-0.9	-2.9	-3.9	0.4	-14.5	-14.0	0.1	0.4	0.5	0.1	0.5	0.6
min	DER Base												
min	DER Q	-0.4	-4.9	-5.3									
min	DER ES				0.3	-2.4	-2.1	0.1	-1.0	-0.8	0.1	-1.1	-0.9
min	DER ES-Q	-0.4	-1.9	-2.3	0.3	0.3	0.5	0.1	-5.4	-5.4	0.1	-6.0	-5.9

$\Delta_{X,Y}$ are differences between the X and Y circuits, with $X, Y \in \{C, U, B\}$ and C being the *complete* circuit, U being the *unbalanced* circutit and B being the *balanced* circuit. For each sub-table, a cell with four rows –one for each DER type– and three columns –one for each possible comparison between circuits– is depicted. The parameter being compared in each cell is marked in the table top, while the irradiance level is marked in the right side of the table. Percentage changes are computed as $100\times(\sigma_X - \sigma_Y)/\sigma_X$, where σ is the parameter being compared.

each DER type (labeled at the table left side) and each PV penetration (labeled at the table right side).

When minimizing the *active power costs*, the differences between the *complete* and *balanced* circuits become larger as PV penetration increases. This is due to differences in the moments where active power injections take place. For a low difference in the total energy injected by storage systems, there is a large difference in the total time arbitrage benefits (up to 28% more benefits are captured for maximum irradiance, see Table 6.a , max irradiance rows of f^{ES}columns).

Besides, from Table 6.a can be observed the following: the *balanced* circuit has lower curtailed active power (up to 80.1% less for medium irradiance, see medium irradiance rows of p_T columns) and lower PV reactive consumption (up to 176% less for medium irradiance, see medium irradiance rows of Q_T^{PV} columns), causing a lower total active power injections at system header (up to 279% less for maximum irradiance, see maximum irradiance rows of P_T^h columns). So, when using power injections from the *balanced* circuit in the *complete* circuit, one might expect voltage violations to occur.

The *complete* circuit and the *balanced* circuit have a negative objective function value ($f^P < 0$) for maximum irradiance, i.e., the total energy purchase costs are lower than the total energy sales. Therefore, according to Table 6.a, the balanced circuit has 47% more profits than the complete circuit (see maximum irradiance rows of f^P columns); and for the case with medium irradiance, the difference rises to 480%. As a consequence, an analysis of the expected benefits of ADNs can be misleading when using the *balanced* circuit and while minimizing the active power costs.

In general, differences between *complete* and *balanced* circuits when minimizing *active power costs* objective are due to the higher availability of active power in the *balanced* circuit, which in turn increases reverse active power flows, i.e., power flows going from the network to the header. So, if the reverse power flow is small, the differences between the *complete* and *balanced* circuits, and between *complete* and *unbalanced* circuits must be comparable. This is actually what is observed for the minimum PV penetration case, where the power curtailment is zero for all cases and the available irradiance is not enough to cause significant reverse power flows. Furthermore, the results are very similar to those obtained when minimizing *apparent power costs* and both, the *costs of losses* and the *self losses*.

When the objective function causes a reduction in active power losses (e.g. when minimizing *apparent power costs* and both types of *costs of losses*) the curtailed power differences with respect the *balanced* circuit are the smaller among all cases. Hence, because losses may increase due to the higher availability of active power in the *balanced* circuit, the PV system

Figure 19: Comparison between storage active power injections (up, price p.u. as reference), PV system active power injections (middle, total PV available as reference) and voltage profile in time at node 848 (left) and 830 (right), for maximum PV penetration and when minimizing *apparent power costs.*

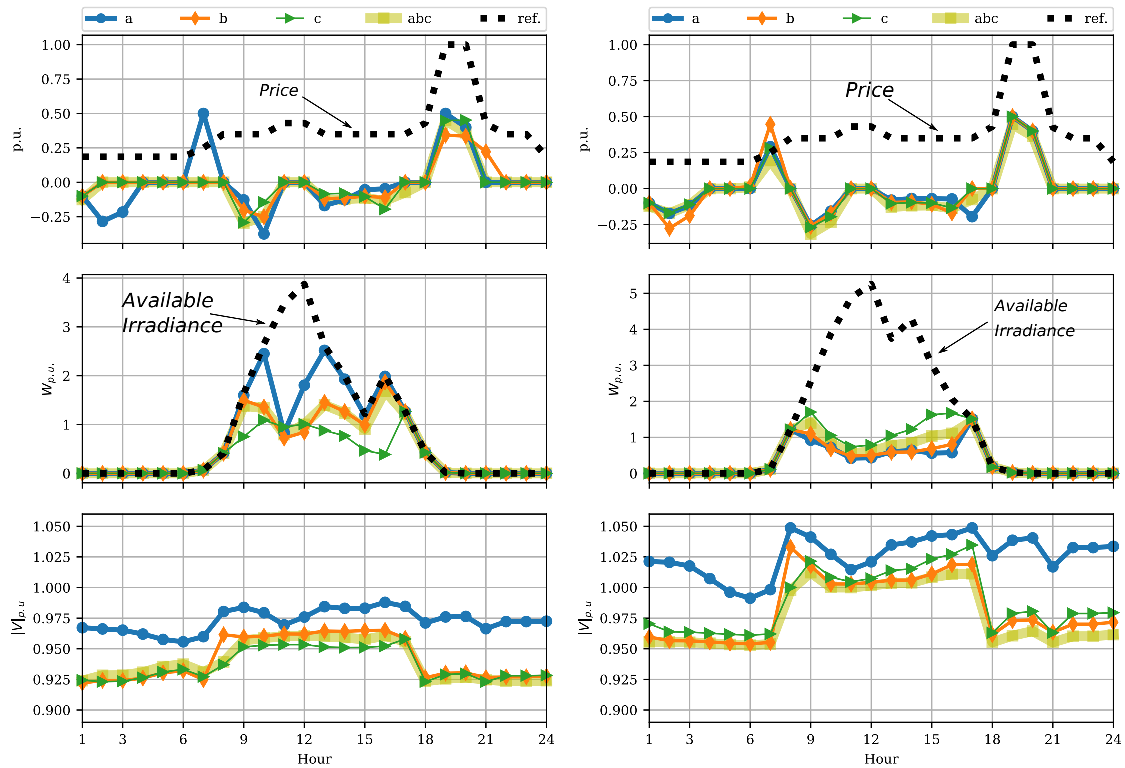

available power is curtailed to reduce reverse flows, if needed. This can be seen in Table 6.b and in Figure 19. In the latter, it is presented the power injections from the ES system and PV system for each of the three phases for the *complete* and *balanced* circuit types (top and medium), and the voltage time-profile for the *complete* and *balanced* circuit types.

Since the lowest network losses are those appearing with the *balanced* circuit, it makes sense that the solution is as balanced as possible when trying to minimize the *cost of losses* in an unbalanced system. In contrast, although the *balanced* circuit has the lowest values of active power costs at system header, the more unbalance the *complete* circuit has, the lower the active power costs are. This is mainly because it is more effective to improve the *active power costs* by maximizing the negative entries of P_h than by reducing system unbalance.

Table 11 summarizes the DER impacts for each circuit, and for selected objectives and parameters, given a maximum irradiance; while Table 12 presents the same information for medium irradiance. There, one can observe that the impact due to changes in DER power injections is poorly reflected on the *balanced* circuit when minimizing *active power costs*. In contrast, for all other objectives, changes in DER power injections seem to be well estimated.

3.2.2 Changing objective functions.

By changing the objective function, it is expected to gain a deeper insight into the effects of each objective in the network parameters. Four types of objectives are minimized: *active* and *apparent power cost*; and *cost of losses* considering line coupling effects and considering only the line self impedance. For all cases, the energy price time-profile is known and equal in all the network, so, the renewable energy pricing or the reactive power pricing is left for future research.

Table 7 presents the three-phase power flow results together with the 3ϕ-ACOPF without and with DERs, the latter being for maximum PV penetration and "ES-Q" DER case. There, *active power costs* give the lower costs and the highest system losses among the studied cases; on the other hand, the *costs of losses* give the lowest network losses.

Table 7: Results between solutions.

	Power flow	OPF cases				
		No DERs	*Active power costs*	*Apparent power costs*	*Cost of losses*	*Cost of self losses*
f^P	3711.01	3619.58	-735.47	718.801	724.111	723.695
L_T	7.3105	7.2826	10.1539	2.1057	1.8526	1.8543
P_T^h	49.2442	48.2509	1.2196	15.3536	15.6884	15.6593
Q_T^h	17.3669	17.2517	29.6541	5.9153	5.9183	5.9052

f^P in millions of the monetary unit, L_T and P_T^h in [MWh] and Q_T^h in [MVArh].

Note that minimizing *active power costs*, lower costs are achieved by increasing reactive power consumption. This is because higher active power injections tend to increase the system voltage magnitude; therefore, consumption of reactive power must increase to maintain voltages within operational limits. Overall, for high and medium PV penetration, PV reactive power injections have a lagging power factor when minimizing *active power costs*, whereas, for the other objectives, PV reactive power injections have a leading power factor. For minimum PV penetration, all cases have a leading power factor.

Differences between *cost of losses* and *self losses* are usually less than or equal to 1% in each of the system parameters computed (see section 3.1.5), so the mutual line impedance has little impact in the optimal objective value. Similarly, minimizing the *apparent power costs* and *costs of losses* are also very similar; however, this time the difference ranges from 2% to 6%. Besides, since the current magnitude depends on the active and reactive power, minimizing the *costs of losses* results in the lowest reactive power flows among all cases.

Therefore, both minimization of *apparent power costs* and *cost of losses* can be used to reactive power control in the network. However, reactive power control through *apparent power cost* minimization has one drawback: for the non-linear formulation, it is very hard to find a solution when including PV reactive compensation. For example, with maximum PV penetration, inclusion of reactive compensation increases simulation time by 22 times (from 11.1s to 222.1 without storage, and from 20.9s to 462.9s with storage); For medium PV penetration, the solver is not able to find a solution for the "Q" DER case within 20 minutes, while the "Base" case is solved in 11.4s; The medium PV penetration with "ES" case took almost 2/3 of the "ES-Q" DER case simulation time (130.6s and 209.7s, respectively). For minimum PV penetration with storage, including PV reactive compensation almost doubles the simulation time (from 37.2s to 69.5s). Additionally, for the *unbalanced* circuit, minimizing *apparent power costs* exceeds the simulation time limits when including reactive compensation for the maximum and medium irradiances.

Figure 20 presents the VUF for all nodes, time periods, PV penetrations and objective functions. From there is clear that when minimizing the *cost of losses* for very high irradiances the maximum 2% of VUF for voltage unbalance (IEC, 2015) is not compromised. Of course, this comes at the cost of curtailing large amounts of PV energy if necessary: With maximum irradiance and "ES-Q" DER case, minimizing *active power costs* objective curtails 1/6 of the available energy, while minimizing *apparent power costs*, *costs of losses* and *self losses* half of the available energy is curtailed.

With minimum irradiance all objectives have zero curtailment, the minimization of *active power costs* results in lower costs and higher losses, while the minimization of *cost of losses* results in higher costs and lower losses. However, for minimum irradiance, the *cost of losses* also have VUF above 2%, and actually, the less irradiance the more unbalance in the network. In contrast, for the *active power costs* objective, the less irradiance the less unbalance in the network.

Table 8 presents the average VUF (column A) and the maximum VUF (column B) for each PV penetration and DER case for the objective functions *active power costs* and *cost of losses*. There it is revealed that although reactive compensation is always helping to reduce PV curtailment (see Table 11 and 12), the effect on the network depends on the objective function: In the case of minimizing *active power costs*, reactive compensation comes with an increase in system unbalance; whereas, for the *cost of losses* it comes with a reduction in system unbalance.

Figure 20: Negative sequence VUF, for "ES-Q" DER case, for each objective, from top to bottom: *active power costs*, *apparent power costs*, *cost of self losses* and *cost of losses*; and for each PV penetration: maximum (left column), medium (center column) and minimum (right column).

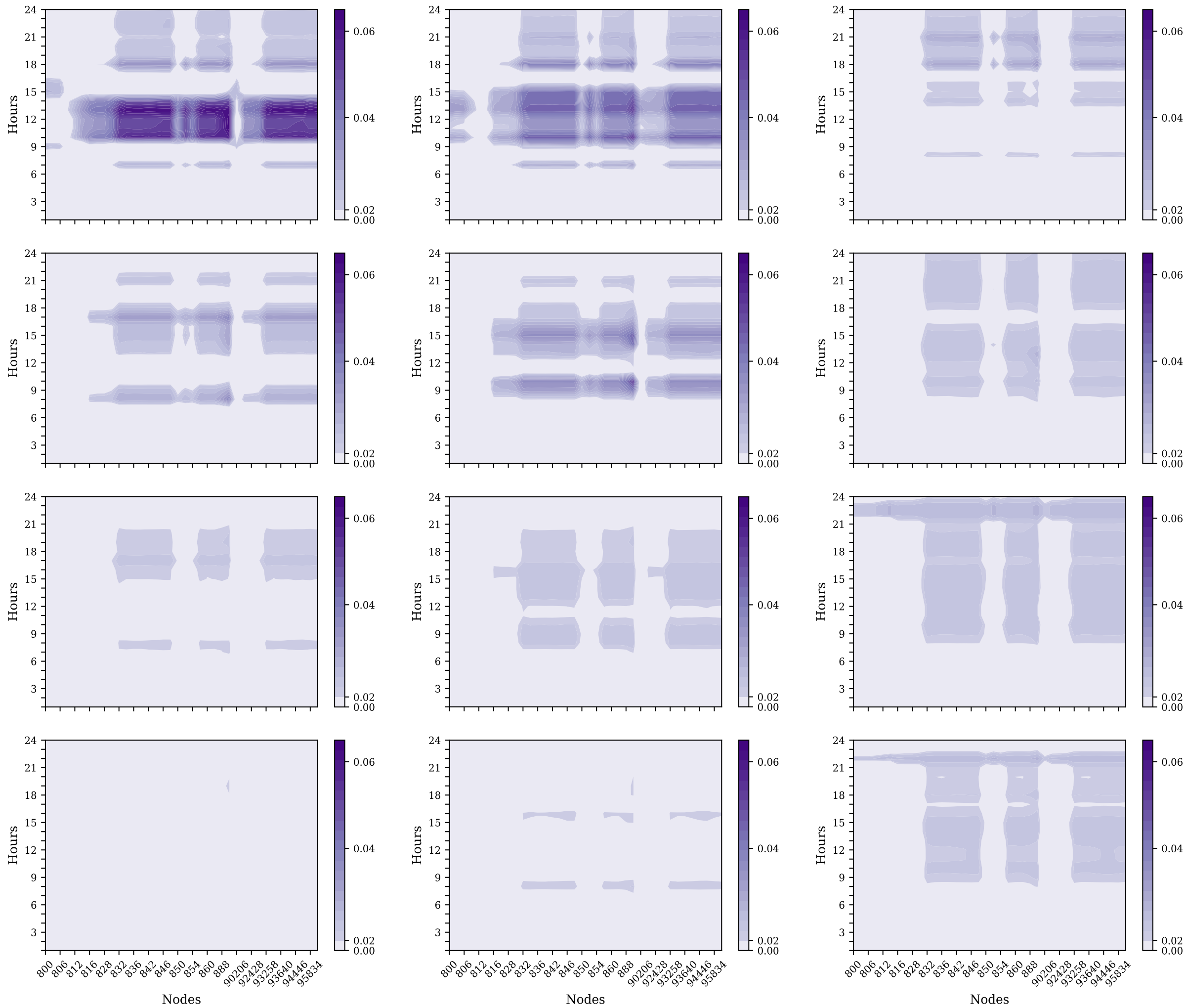

Table 8: Negative sequence Voltage Unbalance Factor for the *active power costs* and *cost of losses* objectives. For each cell, the left value corresponds to the average VUF, while the right value is the maximum VUF.

Active power costs

DER	PV penetration		
	max.	med.	min.
Base	1.538 | 2.857	1.573 | 2.879	1.467 | 2.144
Q	2.210 | 7.390	1.982 | 5.517	1.502 | 2.408
ES	1.600 | 2.989	1.658 | 3.907	1.514 | 3.338
ES-Q	2.068 | 6.483	2.008 | 5.531	1.512 | 3.403

Cost of losses

DER	PV penetration		
	max	med	min
Base	2.139 | 3.121	2.057 | 3.115	1.614 | 2.975
Q	1.625 | 2.975	1.689 | 2.975	1.653 | 2.975
ES	1.884 | 3.103	1.820 | 3.112	1.523 | 2.667
ES-Q	1.384 | 2.019	1.465 | 2.116	1.574 | 2.667

Also, it is observed that an increase in voltage unbalance lead to a decrease in voltage profile. This relation appears in low irradiance scenarios, where the active and reactive power injections of the *active power costs* and *cost of losses* objectives are very similar. To test further this relationship, let us define the following indexes:

$$K_{V^+} = \sum_{t \in \mathcal{T}} \sum_{n \in \mathcal{N}} \sum_{\phi \in \Phi_n} \left\| V_{n,t}^{\phi} \right\|_2^2 \tag{3.2.1}$$

$$K_{V^-} = \sum_{t \in \mathcal{T}} \sum_{n \in \mathcal{N}_{3\phi}} \left\| V_{n,t}^{(-)} \right\|_2^2 \tag{3.2.2}$$

Where K_{V^+} is an index used to measure how large the voltage profile is in the system, while K_{V^-} is an index to measure how much negative sequence the system has. Being a sum of positive values, these indices can be used to determine between two scenarios, which one has higher voltage profile/unbalance.

Table 9 presents the results for minimum irradiance, with (column B) and without (column A) constraints in voltage unbalance. Note that the voltage profile index in column B is always higher than in column A, i.e., it is higher for lower unbalance cases. This is by no means a formal proof of this relationship, however, results in Table 9 indicate that it might be typical of power distribution networks with a high number of three-phase branches.

Table 9: Three-phase optimal power flow for minimum PV penetration. Column A has no restriction on the maximum unbalance index per node, while in column B maximum unbalance index per node is limited as presented in each table bottom.

	Active power costs		*Apparent power costs*		*Cost of losses*	
	A	B	A	B	A	B
L_T	**55.049**	**53.087**	38.605	39.063	40.856	41.249
P_T	350.22	352.37	332.54	337.66	339.81	343.74
Q_T	128.99	143.21	98.717	100.35	100.11	102.67
K_{V-}	2.110	0.936	2.287	1.021	2.225	1.003
K_{V+}	2909	2964.6	2867	2929	2953	2990.1

DER case: SS-Q, $\left\|V_{n,t}^{(-)}\right\|_2^2 \leqslant 0.0015$, $\left\|V_{n,t}^{(0)}\right\|_2^2 \leqslant 0.0015$

	Active power costs		*Apparent power costs*		*Cost of losses*	
	A	B	A	B	A	B
L_T	**58.267**	**56.413**	43.229	43.683	45.470	45.735
P_T	351.88	354.86	334.39	338.93	341.07	344.55
Q_T	**171.01**	**170.07**	160.20	160.65	161.54	162.22
K_{V-}	2.130	0.975	2.073	1.006	2.066	0.971
K_{V+}	2908.8	2970.5	2870.2	2930.0	2953.9	2987.7

DER case: SS, $\left\|V_{n,t}^{(-)}\right\|_2^2 \leqslant 0.0015$, $\left\|V_{n,t}^{(0)}\right\|_2^2 \leqslant 0.0015$

	Active power costs		*Apparent power costs*		*Cost of losses*	
	A	B	A	B	A	B
L_T	41.687	41.899	40.260	40.414	40.124	40.364
P_T	328.59	332.18	329.58	333.607	332	334.23
Q_T	118.95	133.38	100.5	101.10	100.32	101.88
K_{V-}	1.943	0.965	2.148	0.986	2.399	0.976
K_{V+}	2882.0	2929.3	2888.8	2936.5	2931.2	2946.552

DER case: Q, $\left\|V_{n,t}^{(-)}\right\|_2^2 \leqslant 0.0015$, $\left\|V_{n,t}^{(0)}\right\|_2^2 \leqslant 0.002$

	Active power costs		*Apparent power costs*		*Cost of losses*	
	A	B	A	B	A	B
L_T	45.056	45.331	45.070	45.3324	45.038	45.289
P_T	330.38	335.09	330.68	335.09	332.83	335.68
Q_T	161.70	162.19	161.68	162.21	161.51	162.27
K_{V-}	1.855	0.960	1.883	0.955	2.298	0.926
K_{V+}	2882	2934.7	2881.8	2935.5	2928	2950.4

DER case: Base, $\left\|V_{n,t}^{(-)}\right\|_2^2 \leqslant 0.0015$, $\left\|V_{n,t}^{(0)}\right\|_2^2 \leqslant 0.002$

Table 10: Comparison of the solution for maximum irradiance when minimizing active power costs for the "ES-Q" DER case.

	O	A [%]	B [%]
Objective	735.53	-3.28	-6.316
Sol. time [s]	69.328	32.433	115.44
Network			
f^{P}[M$]	-735.46	-3.28	-6.316
L_T [MWh]	10.154	-9.618	-8.994
P^{h}_{T} [MWh]	1.2196	10.774	19.793
Q^{h}_{T} [MVArh]	29.654	-4.481	-3.585
$V^{(+)}_{avg}$	0.983	0.102	0.305
$K_{V^{+}}$	2991.9	0.187	0.678
$VUF^{(-)}_{avg.}$	2.067	-33.43	-35.123
$VUF^{(-)}_{max.}$	6.485	-69.761	-69.761
$VUF^{(0)}_{max.}$	7.489	-32.968	-73.815
PV			
P^{PV}_{T} [MWh]	51.345	-1.896	-1.862
Q^{PV}_{T} [MVArh]	-6.9444	-7.242	-3.766
p_T [MWh]	12.197	7.98	7.838
SS			
f^{ES} [M$]	414.76	-2.606	-4.942
$P^{\vee}_{T}$ [MWh]	150.02	-3.929	-2.942
$P^{\wedge}_{T}$ [MWh]	10.180	-4.169	-3.122

Column "O" is the original case, column "A" are the results of restricting the negative sequence VUF to at most 2%, while column "B" are the results of restricting the negative and zero sequence VUF to at most 2%. Column "A" and "B" are given in percentage with respect column "O".

From the latter results, it seems that active power injections have a low sensitivity to change in VUF. This is corroborated in Table 10, which presents the change in percentage for each calculated parameter between a case without limiting the VUF against a case where the VUF is enforced to be within recommended limits (given maximum PV penetration and for the "ES-Q" DER case). There it is observed that optimal DER power injections have a low sensitivity to variations on voltage VUF, since, for example, a change as large as 70% in the VUF causes a change of only a 20% in the total imported active power. Interesting enough, while network losses are diminished by 9% when constraining the system unbalance, active power costs increase by 3% if only negative sequence constrained and by 6% if both negative and zero sequence are constrained.

3.2.3 Changing DER type. By changing the DER type, it is expected to see if PV reactive compensation and ES complement each other, or if on the contrary, they are interchangeable technologies. To this extent, four changes in DER type are analyzed (see Table 11): Adding storage to the "Base" case, which is denoted as Δ(ES); adding storage to the "Q" case, which is denoted as Δ(ES-Q); adding PV reactive compensation to the "Base" case, which is denoted as Δ(Q); and adding PV reactive compensation to the "ES" case, which is denoted as Δ(Q-ES). Table 11 presents the percentage change occurring for each of these cases for maximum PV penetration, while Table 12 presents the same information for medium PV penetration. Both tables present the results for the *active* and *apparent power costs* (labeled as PCOSTS and SCOSTS, respectively) and the *cost of losses* (labeled as CLOSSES) objective functions, for each of the parameters presented in the right hand side of each table.

For the objective functions *apparent power costs* and *cost of losses*, ES systems have more impact on total costs and total curtailed power. For example, in Table 11 (see f^Prows on the SCOSTS columns) it can be seen that with or without reactive compensation, including system storage reduces up to 56% of the active power costs at the header (total costs around \$700 millions); while with or without storage, including reactive compensation only reduces it up to 2.3% (total costs around \$1600 millions).

Table 11: Percentage variations due to DER changes for maximum PV penetration, for a given objective (shown at the table top) and a given parameter (shown at the table right-hand side).

Parameter	DER change	PCOSTS C	PCOSTS U	PCOSTS B	SCOSTS C	SCOSTS U	SCOSTS B	CLOSSES C	CLOSSES U	CLOSSES B
f^P	Δ(ES)	156.0	156.9	262.4	55.4	55.4	56.2	55.6	55.7	55.6
f^P	Δ(ES-Q)	277.2	279.1	865.6	56.0		56.8	56.4	56.5	56.8
f^P	Δ(Q)	42.7	42.7	69.7	0.9		1.0	1.8	1.9	2.3
f^P	Δ(Q-ES)	-81.5	-80.2	-42.6	2.3	2.3	2.2	3.5	3.5	5.0
L_T	Δ(ES)	-4.1	-4.1	-9.9	19.7	19.8	19.7	20.7	20.8	21.4
L_T	Δ(ES-Q)	-6.1	-6.0	-6.9	26.1		27.7	27.1	27.4	28.4
L_T	Δ(Q)	-129.2	-130.2	-134.3	20.8		23.7	23.0	23.6	24.2
L_T	Δ(Q-ES)	-133.6	-134.3	-127.7	27.1	27.7	31.3	29.2	29.9	30.9
P_T^h	Δ(ES)	40.0	40.3	62.4	27.8	27.9	28.4	27.2	27.3	26.8
P_T^h	Δ(ES-Q)	76.5	77.2	247.7	28.2		28.7	27.5	27.6	27.4
P_T^h	Δ(Q)	44.3	44.4	75.1	1.0		1.0	1.7	1.8	2.3
P_T^h	Δ(Q-ES)	78.2	78.8	197.7	1.5	1.5	1.5	2.2	2.2	3.1
Q_T^h	Δ(ES)	-2.5	-2.5	-3.4	1.5	1.5	1.5	1.5	1.4	1.5
Q_T^h	Δ(ES-Q)	-4.5	-4.4	-4.1	4.3		4.0	4.3	4.5	4.0
Q_T^h	Δ(Q)	-61.1	-59.5	-48.2	61.0		60.8	61.9	61.1	62.5
Q_T^h	Δ(Q-ES)	-64.2	-62.5	-49.3	62.1	61.6	61.8	63.0	62.4	63.4
p_T	Δ(ES)	18.7	18.6	22.9	15.3	15.3	15.3	15.6	15.6	15.9
p_T	Δ(ES-Q)	31.0	30.9	42.8	15.6		15.6	15.6	15.3	15.6
p_T	Δ(Q)	33.1	32.9	43.9	1.4		1.8	0.3	0.4	-2.0
p_T	Δ(Q-ES)	43.3	43.0	58.3	1.8	1.7	2.1	0.3	0.0	-2.4

Each circuit type is given one label at the bottom of the table:C being the *complete* circuit, U being the *unbalanced* circuit and B being the *balanced* circuit. Each objective is given a label at the top of the table: PCOSTS being the *active power costs*, SCOSTS being the *apparent power costs*, and CLOSSES being the *cost of losses* objective. Each DER change is given a label at the left of the table: Adding storage to the "Base" case, which is denoted as Δ(ES); adding storage to the "Q" case, which is denoted as Δ(ES-Q); adding PV reactive compensation to the "B" case, which is denoted as Δ(Q); and adding PV reactive compensation to the "ES" case, which is denoted as Δ(Q-ES). Thus, each cell has four rows –one for each variation on the DER type– and three columns –one column for each type of circuit.

On the other hand, for the objective functions *apparent power costs* and *cost of losses* including reactive power compensation has a major impact on total imported reactive power, e.g., with or without storage, reactive power injections at the header are reduced by around 60% if PV reactive compensation is enabled (see Table 11 Q_T^h rows on the SCOSTS columns). Looking at Table 11 (L_T rows on SCOSTS and CLOSSES columns), one also can see that storage and reactive compensation have a similar impact on total system losses, by themselves and when combined.

When minimizing *active power costs*, total system losses are 133% higher: Losses change from approximately 4 MWh to 10 MWh, with or without storage, when using reactive compensation. This is due to an increase in reactive power consumption of the PV reactive power compensation (see Table 11 and 12, L_T rows, PCOSTS column).

The PV reactive power compensation and ES system have the same effect on power injections at the header (see Table 11, P_T^h rows, PCOSTS columns). Active power injections at the header go from 9 MWh to 5 MWh when including reactive compensation or storage; and they go from 5 MWh to 1MWh when both, reactive compensation and storage are available. It is interesting to note that the impact on the total imported active power of having both, PV reactive compensation and storage, it is almost the sum of the individual impacts.

On the other hand, curtailed PV energy is mainly affected by PV reactive compensation, but it can be reduced further by having an ES system available (see Table 11, p_T rows, PCOSTS columns).

When comparing Table 11 and 12, it is observed that *apparent power costs* and *cost of losses* minimization lead to similar behavior for maximum and medium irradiance (i.e., changing DER type causes a similar effect). In contrast, the reduction in PV penetration yields a different pattern when minimizing *active power costs*. Namely, including storage, while having reactive compensation, results in the bigger change in costs of power injections at system header; on the other hand, reactive compensation and storage have a similar impact on curtailed PV energy. Furthermore, curtailed energy is zero when both, reactive compensation and storage are available.

Table 12: Percentage variations due to DER changes for medium PV penetration, for a given objective (shown at the table top) and a given parameter (shown at the table right-hand side).

Parameter	DER change	PCOSTS C	PCOSTS U	PCOSTS B	SCOSTS C	SCOSTS U	SCOSTS B	CLOSSES C	CLOSSES U	CLOSSES B
f^P	Δ(ES)	90.6	90.9	116.1	50.9	50.9	51.4	51.5	51.5	51.8
f^P	Δ(ES-Q)	104.2	104.6	124.7			52.6	51.5	51.5	52.9
f^P	Δ(Q)	16.1	16.1	16.6			1.4	0.6	0.6	1.9
f^P	Δ(Q-ES)	137.7	142.4	-27.7	4.5	2.5	3.8	0.5	0.5	4.2
L_T	Δ(ES)	-9.8	-9.9	-15.7	21.4	21.5	22.2	20.7	20.9	21.5
L_T	Δ(ES-Q)	4.0	3.4	28.1			27.9	25.9	26.2	27.4
L_T	Δ(Q)	-72.5	-73.0	-70.3			22.2	20.1	20.7	21.4
L_T	Δ(Q-ES)	-50.9	-52.1	-5.8	23.6	26.3	27.9	25.3	26.1	27.3
P_T^h	Δ(ES)	20.3	20.4	22.5	25.3	25.3	25.6	24.9	24.9	24.6
P_T^h	Δ(ES-Q)	20.1	20.2	11.8			26.4	24.6	24.6	25.2
P_T^h	Δ(Q)	16.0	16.0	16.1			1.5	0.5	0.6	2.0
P_T^h	Δ(Q-ES)	15.8	15.9	4.5	1.3	1.7	2.6	0.2	0.2	2.8
Q_T^h	Δ(ES)	-3.5	-3.4	-4.1	1.5	1.4	1.5	1.6	1.5	1.7
Q_T^h	Δ(ES-Q)	-1.6	-2.1	22.4			3.9	3.9	4.1	3.9
Q_T^h	Δ(Q)	-32.7	-31.7	-15.7			57.2	57.5	56.6	58.6
Q_T^h	Δ(Q-ES)	-30.3	-29.9	13.7	58.0	57.8	58.2	58.5	57.8	59.6
p_T	Δ(ES)	55.5	55.3	86.1	36.4	36.3	35.8	37.3	37.2	39.1
p_T	Δ(ES-Q)	100.0	100.0	100.0			37.2	36.6	36.4	37.7
p_T	Δ(Q)	58.2	57.9	85.7			4.5	-1.0	-1.0	-4.4
p_T	Δ(Q-ES)	100.0	100.0	100.0	5.7	6.4	6.5	-2.3	-2.3	-6.8

Each circuit type is given one label at the bottom of the table:C being the *complete* circuit, U being the *unbalanced* circuit and B being the *balanced* circuit. Each objective is given a label at the top of the table: PCOSTS being the *active power costs*, SCOSTS being the *apparent power costs*, and CLOSSES being the *cost of losses* objective. Each DER change is given a label at the left of the table: Adding storage to the "Base" case, which is denoted as Δ(ES); adding storage to the "Q" case, which is denoted as Δ(ES-Q); adding PV reactive compensation to the "B" case, which is denoted as Δ(Q); and adding PV reactive compensation to the "ES" case, which is denoted as Δ(Q-ES). Thus, each cell has four rows –one for each variation on the DER type– and three columns –one column for each type of circuit.

3.3 Remarks and research questions

3.3.1 Result summary. From the previous study, one can see that it is indeed necessary to solve a 3ϕ-ACOPF, not only to properly schedule DERs in an unbalanced distribution system but also to be able to understand its solution. For example, when the objective function caused a reduction on the system unbalance (e.g., when minimizing the *costs of losses*), differences between unbalanced and balanced circuits are low enough to consider the balanced answer as a way to improve the performance of 3ϕ-ACOPF, e.g., for a warm start. Moreover, for this kind of objective changes in available DERs in the system can be predicted using the *balanced* circuit; therefore, balanced answers (thus, one-line equivalents) could be useful when analyzing unbalanced power networks.

For maximum irradiance and when minimizing *active power costs*, reactive compensation has more impact on power curtailment; while for medium irradiance both, reactive compensation and storage have the same impact. Whatever the case may be, having both yields to the lower curtailment among all cases.

It is also observed that when minimizing the *apparent power costs* and the *cost of losses* storage has a major impact on active power costs and curtailed energy. In contrast, reactive power compensation and storage have the same impact on system losses. The latter is also true for all objectives when considering minimum PV penetration, although the impact of storage is slightly more relevant when minimizing *active power costs*.

Note also that as long as the energy available from DERs is such that there are little reverse power flows, minimizing *active power costs* and the *cost of losses* yield to similar results. As the available energy in the ADN increases, minimizing the *cost of losses* causes a decrease in reverse power flows if the higher availability tends to increase system losses –thus PV curtailment also might be increased. On the other hand, minimizing the *active power costs* causes an increase in the exported energy (i.e., there is an increase in reverse power flows), thus increasing system losses.

When obtaining the results presented in Table 9, it was found that is not possible to reduce system unbalance arbitrarily with DERs; instead, it seems to be a minimum feasible unbalance, which in turn seems to be higher than the unbalance achieved without DERs. Besides, although for objective functions that reduce reverse power flow the VUF may have values within acceptable limits, this cannot always be assured since it also depends on the DER type and PV penetration level. Thus, a constraint in VUF is needed to assure a safe network operation.

In general, although minimizing *active power costs* lead to very high unbalances, adding a constraint on the voltage unbalance fix this problem very easily for low unbalances. Also, note that it is recommended to use the *cost of losses* objective over the *costs of self losses* objective because the former yields to lower voltage unbalance.

From this tests also was found that it is better to limit voltage unbalance with inequality constraints: Trying to minimize voltage unbalance often exceeded the maximum simulation time criteria, which make this approach unreliable for real applications. However, constraining both, negative and zero sequence also yield to long computation times (see Table 10).

Results suggest that minimization of active power injection costs at system header can work as a surrogate for curtailment minimization. Since the former objective not only accounts for the actual power being curtailed but also accounts for the resulting system losses, it can also be useful for pricing scheme assessment.

For high PV penetration, losses minimization are better handled by the objectives *apparent power costs* and *costs of losses*. The former is the best option when treating only with PV curtailment, because of its good reactive power control, low computation time and low active power costs; while the latter is the best option when including storage and reactive compensation. However, note that under this kind of objectives there is a clear limit on the amount of PV energy that can be injected.

In Table 13 are the total losses and the total PV injections for the three irradiance levels described in section 3.1 plus one with even more irradiance than the maximum scenario (9/5 of the total irradiance, i.e., three times the medium irradiance). There one can see that the maximum PV energy that can be injected into the ADN when minimizing the *cost of losses* is around the 30 MWh, and that the losses can be reduced to around 2 MWh. This is the law of diminishing returns in action: even if there is more irradiance, losses cannot be improved further, and instead, all the additional radiation is just being curtailed. Assuming that curtailment is an undesired action in an ADN, data in Table 13 is telling us that the maximum capacity of PV energy that the ADN can handle while minimizing the *cost of losses* is somewhere between 13 MWh and 28 MWh.

Table 13: Curtailment and losses while minimizing *cost of losses* for several irradiance levels. The column with irradiance "max.+" corresponds to three times the irradiance in the medium scenario.

	Irradiance			
	min.	med.	max.	max.+
L_T [MWh]	4.0856	2.0762	1.8526	1.7030
P_T^{PV} [MWh]	12.710	27.563	30.011	31.309
Q_T^{PV} [MVArh]	5.5619	8.4122	9.0988	9.5623
p_T [MWh]	0	10.564	33.531	83.066

Finally, Table 14 presents the result of running the case where PV penetration is three times the medium PV penetration case for the *active power costs*, *cost of losses* and a combination of these two objective functions. This is done to highlight two points:

1. When minimizing the *active power costs*, although for very high irradiance there is also curtailment, the ratio being curtailed is almost halved. Of course, as a consequence,

large unbalances appear in the network. This can be solved by constraining the unbalance in each three-phase node, however, such action increases the computation time if the original unbalance is too large. Although reducing curtailment by half sounds like a positive outcomes, when comparing the power being curtailed against the power being injected, it can be observed that still most of the energy is wasted under this scenario.

2. Therefore, for low PV penetration, the *active power costs* minimization is the best at balancing losses and costs; on the other hand, for high PV penetration, a combination of *active power costs* and *cost of losses* objectives give a better balance between losses, energy consumption costs at the header and computation time. Finally, the large amounts of curtailed energy indicate that the circuit is not well designed to handle such high DER penetration.

Table 14: Comparison between minimizing *active power costs*, *cost of losses* and a combination of both objectives.

	Active power costs	*Cost of losses*	Combined objective
Sol. time [s]	364.03	26.093	40.078
Network			
f^{P} [M$]	-1503.9	628.99	-1297.6
L_T [MWh]	12.394	1.7030	5.5679
P_T^h [MWh]	-9.9335	14.353	-7.5665
Q_T^h [MVArh]	34.055	5.396	19.950
$V_{avg}^{(+)}$	0.988	0.987	0.987
K_{V^+}	3020.9	3019.0	3019.3
$VUF_{avg.}^{(-)}$	1.378	1.366	1.281
$VUF_{max.}^{(-)}$	1.961	2.33	1.944
$VUF_{max.}^{(0)}$	1.971	2.168	1.974
PV			
P_T^{PV} [MWh]	64.555	31.309	56.413
Q_T^{PV} [MVArh]	-9.5321	9.5623	-0.8616
p_T [MWh]	49.819	83.066	57.961
SS			
f^{ES}[M$]	336.25	171.99	361.67
$P_T^{\vee}$ [MWh]	15.324	10.050	13.165
$P_T^{\wedge}$ [MWh]	10.412	6.6151	8.8576

No scaling was introduced for any of these two objectives, moreover, the presented results are for a irradiance level three times the medium irradiance scenario and for the "ES-Q" DER case. The negative sequence and zero sequence VUF were constrained when minimizing *active power cost* objective and the combined objective.

3.3.2 Research questions. By analyzing the results, answers to (Q-Ia)[1] and (Q-Ib)[2] are now clearer:

(Q-Ia) An unbalanced system with DERs can be modeled with a balanced equivalent if there is little or no reversed flows in the network. Under such circumstances, the impact of DERs can also be predicted with a balanced equivalent. Both cases induce errors in the final answer, so always it should be analyzed if the errors are small enough for the required application. Also, note that the "almost balanced" conditions do not require balanced power injections since the network unbalance can be easily controlled by constraining the VUF in the network. However, note that if the unbalance is large under unconstrained conditions, the computation time might be significantly increased when the constraints are included.

(Q-Ib) Optimal DER scheduling increases or decreases network unbalance depending on the nature of the objective function to be considered. Results show that minimizing the *cost of losses* reduces network unbalance while minimizing the *active power costs* at the header increase network unbalance. The common factor in both cases is the reverse power flows: since DER power injections are unbalanced, reducing them to avoid further losses decrease network unbalance while increasing them to allow larger savings at the header increase network unbalance. Also, it seems to be a relationship between voltage unbalance and voltage profile, namely, the higher the voltage unbalance the lower the resulting voltage profile. This characteristic appears only when the amount of available energy from DERs is the same between cases and it shows that it seems viable to reduce network unbalance without large changes in optimal power injections.

Thus, three out of the six open problems presented at the end of chapter 1 have been covered, in summary:

1. The effects of the optimal DER dispatch (including PV and storage systems) have been studied for more than one objective function.

2. The differences between one-phase and three-phase OPF have been studied, with and without system storage.

3. The "almost balanced" conditions that several formulations require have been characterized.

[1] Are the answers obtained by a 3ϕ-ACOPF different enough from those given by a single-phase ACOPF?
[2] Is the optimal DER scheduling increasing or decreasing the voltage unbalance in the network?

Problems 5 and 6 (about the use of delta and ZIP load models) are not on equal ground with the non-linear formulation, since the ZIP models are not being approximated. Additionally, problem 4 (about the need to include explicitly a control for voltage unbalance) has been only partially answered, since it seems to be necessary to limit voltage unbalance in order to avoid unsafe operation.

Of course, from this point forward another question might appear, like if there is an objective function or circuit for which these conclusions are not valid (which will require a formal proof of convergence for the solution algorithm), however, this kind of question is left for future researches.

II Convex 3ϕ-ACOPF Evaluation

CHAPTER 4

CONVEX MODELS

This chapter describes a novel convex formulation to solve the 3ϕ-ACOPF as a Sequence of Convex Quadratically Constrained Quadratic Programs. The model is based on the non-convex formulation introduced in section 2.5 and it can converge to a primal feasible point of the non-convex formulation. Section 4.1 explains the applied approximations, while in section 4.2 are presented the solution steps to solve the 3ϕ-ACOPF as a Sequence of Convex Quadratically Constrained Quadratic Programs.

4.1 Linearizations

The model introduced in section 2.5 has two non-convexities: 1) The active/reactive power relationship with node voltages and currents (see equations 2.2.1, 2.3.1 and 2.3.5); and 2) The lower limit for the voltage magnitude (see equation 2.5.3) . These set of equations will be treated as described bellow.

4.1.1 Power equations. If e denote a circuit element that can be a generator or a constant apparent power component of a demand. For an operation point defined by the tuple $\left(v_e^{0r}, v_e^{0i}, i_e^{0r}, i_e^{0i}, P_e^0, Q_e^0\right)$, equations 2.2.1, 2.3.1 and 2.3.5 are linearized using the First-Order Taylor approximation:

$$P_e = i_e^{0r} V_e^r + i_e^{0i} V_e^i + v_e^{0r} I_e^r + v_e^{0i} I_e^i - P_e^0 \tag{4.1.1}$$

$$Q_e = i_e^{0r} V_e^i - i_e^{0i} V_e^r + v_e^{0i} I_e^r - v_e^{0r} I_e^i - Q_e^0 \tag{4.1.2}$$

With $e \in \{\mathcal{G} \cup \mathcal{D}_{S\curlyvee} \cup \mathcal{D}_{S\Delta}\}$ and $\mathcal{D}_{S\curlyvee}$ and $\mathcal{D}_{S\Delta}$ being the sets of wye and delta constant power loads, and $P_e^0 + jQ_e^0 = v_e^0 \left(i_e^0\right)^*$. Variables V_e, v_e^0, I_e and i_e^0 are associated to the element, e.g., for a wye load d connected at phase ϕ of n, $V_e = V_n^\phi$ and $I_e = I_{S\curlyvee d}^\phi$; whereas, for a delta branch $\Delta \in \mathcal{F}$ of load d connected at n,$V_e = V_n^\Delta$ and $I_e = I_{Sd}^\Delta$. In Frame 9 there are some examples of this linearization.

Frame 9. Power injection linearization

In Figure 21 is depicted the voltage and current for a wye load branch and for a delta load branch. Assuming that the loads are connected to node n, power injections for the wye branch are then:

$$\tilde{P}_d^a = i_{S\curlyvee d}^{0ar} V_n^{ar} + i_{S\curlyvee d}^{0ai} V_n^{ai} \tag{4.1.3}$$

$$+ v_n^{0ar} I_{S\curlyvee d}^{ar} + v_n^{0ai} I_{S\curlyvee d}^{ai} - P_n^{0a} \quad d \in \mathcal{D}_{S\curlyvee} \tag{4.1.4}$$

$$\tilde{Q}_d^a = i_{S\curlyvee d}^{0ar} V_n^{ai} - i_{S\curlyvee d}^{0ai} V_n^{ar} \tag{4.1.5}$$

$$+ v_n^{0ai} I_{S\curlyvee d}^{ar} - v_n^{0ar} I_{S\curlyvee d}^{ai} - Q_n^{0a} \quad d \in \mathcal{D}_{S\curlyvee} \tag{4.1.6}$$

While the behavior of the delta branch would be:

Figure 21: Voltage across the element "e" of a wye load and a delta load.

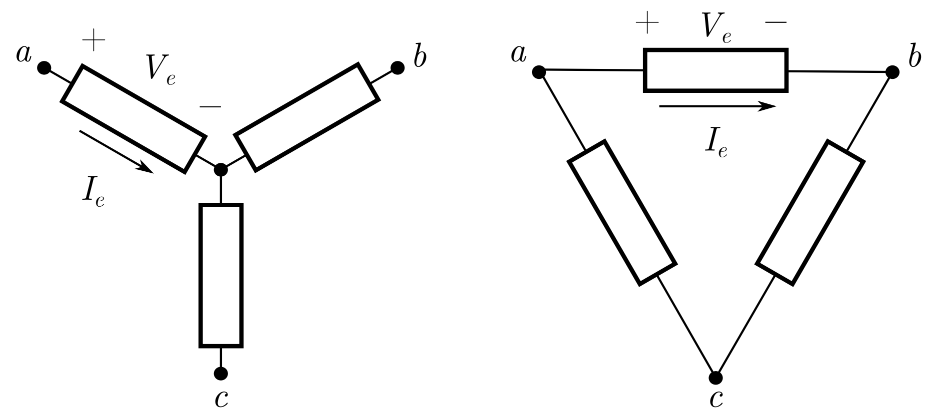

$$\tilde{P}_d^{\{a,b\}} = i_{Sd}^{0\{a,b\}r}\left(V_n^{ar} - V_n^{br}\right) + i_{Sd}^{0\{a,b\}i}\left(V_n^{ai} - V_n^{bi}\right) \tag{4.1.7}$$

$$+ \left(v_n^{0ar} - v_n^{0br}\right) I_{Sd}^{\{a,b\}r} + \left(v_n^{0ai} - v_n^{0bi}\right) I_{Sd}^{\{a,b\}i} - P_n^{0\{a,b\}} \quad d \in \mathcal{D}_{S\Delta} \tag{4.1.8}$$

$$\tilde{Q}_d^{\{a,b\}} = i_{Sd}^{0\{a,b\}r}\left(V_n^{ai} - V_n^{bi}\right) - i_{Sd}^{0\{a,b\}i}\left(V_n^{ar} - V_n^{br}\right) \tag{4.1.9}$$

$$+ \left(v_n^{0ai} - v_n^{0bi}\right) I_{Sd}^{\{a,b\}r} - \left(v_n^{0ar} - v_n^{0br}\right) I_{Sd}^{\{a,b\}i} - Q_n^{0\{a,b\}} \quad d \in \mathcal{D}_{S\Delta} \tag{4.1.10}$$

4.1.2 Voltage lower limit.

Preliminary testing with the linearized power equations resulted in good estimations for the active power injections and very poor approximations for the reactive power injections. Moreover, voltage angles were very close to those obtained by the non-linear model. This motivated the following approximation: Instead of the non-convex lower limit on equation (2.5.3), the lower limit is modeled as a semiplane tangent to the non-convex lower limit constraint. So, the upper and lower limits are:

$$(V^{max.})^2 \geqslant |V_n^{\phi}|^2, \ \phi \in \Phi_n, \ n \in \mathcal{N} \tag{4.1.11}$$

$$\left(V^{min.}\right)^2 \leqslant V^{min.} \cos\left(\delta_{V_n}^{\phi}\right) V_n^{\phi r} + V^{min.} \sin\left(\delta_{V_n}^{\phi}\right) V_n^{\phi i}, \ \forall \phi \in \Phi_n, \ \forall n \in \mathcal{N} \tag{4.1.12}$$

Where $\delta_{V_n}^{\phi}$ is the phase ϕ angle of the voltage at node n. In Figure (22) there is an example of the new feasible region for a voltage that is on the fourth quadrant in the complex plane.

Figure 22: Rotating tangent line for a voltage at node n which is in the fourth quadrant and with $\delta_n \approx -30°$. The light gray area is the new feasible region, while the whole area between both circumferences is the old feasible region.

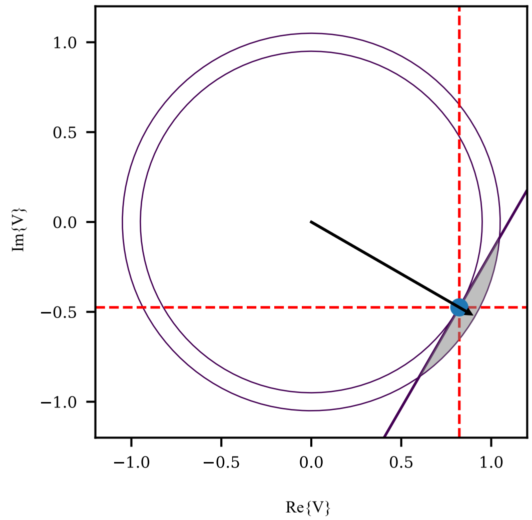

All other equations remain unaltered from the non-linear case since they are linear or convex functions that can be handled by a Quadratically Constrained Programming (QCP) solver.

4.2 Solution steps

In addition to objectives described in equations (2.5.11) and (2.5.14), and to improve the quality and speed of the linearized power solution, the following objective function is included:

$$f^{TR} = \alpha \left\{ \sum_{g \in \mathcal{G}_{pv}} \sum_{\phi \in \Phi_g} \sum_{t \in \mathcal{T}} \left[\left(P^{\phi}_{g,t} - P^{\phi 0}_{g,t} \right)^2 + \left(Q^{\phi}_{g,t} - Q^{\phi 0}_{g,t} \right)^2 \right] \right. \\ \left. + \sum_{g \in \mathcal{G}_{ss}} \sum_{\phi \in \Phi_g} \sum_{t \in \mathcal{T}} \left(P^{\phi}_{g,t} - P^{\phi 0}_{g,t} \right) \right\} \tag{4.2.1}$$

This *trust-region objective* function assures that the next operation point does not fall too far from the current operation point. This is often useful near an NLP feasible operation point and, in most cases, it helps to find a better answer in terms of NLP primal feasibility.

The resulting Sequential Quadratically Constrained Quadratic Programming (S-QCP) formulation consists on 4 steps: 1) Initialize, 2) Solve the current QCP model, 3) Check stopping criteria, if it fails, continue, otherwise return the answer, 4) Update and continue to step 2. Each time the algorithm falls on step 3, it is said an *outer iteration* has been completed.

4.2.1 Initialize. All voltages initiate as a set of balanced phasors with the nominal voltage magnitude. Storage injections are set to zero, PV injections are equal to the available irradiance and for the trust-region objective function $\alpha = 0$. Only initial values near the answer have a significant impact on the method performance, otherwise, the problem final answer seems to be insensitive to initial values.

4.2.2 Solve. The QCP problem including PV reactive power compensation can be stated as follows:

$$\max\{f^{ES} - f^{LOSS} - f^{TR}\}$$
$$\text{s.t. equations}$$
$$\widehat{\mathrm{PFE}},\ (2.2.4),\ (2.2.5\text{-}2.2.10),\ (4.1.11),\ (4.1.12)$$

Where $\widehat{\mathrm{PFE}}$ are the power flow equations with the non-linear power injections replaced by their equivalent linearized power injections, i.e., with equations (4.1.1) and (4.1.2) instead of equations (2.2.1), (2.2.2), (2.3.1) and (2.3.5). Again, for the case without reactive compensation, equation 2.2.4 is evaluated for $\Theta^{\max.} = 0$, i.e., it is replaced by $Q_g^{\phi} = 0$, $\forall g \in \mathcal{G}_{pv}$, $\forall \phi \in \Phi_g$. For a detailed list of the problem equations, please refer to Frames 7 and 8.

In order to know when the trust-region objective must be included, the last optimal solution for the active and reactive power is compared against the respective product between the optimal voltage and current, so the following index is calculated for all linearized power equations:

$$m_{P,e} = P_e^{\star} - \left(V_e^r I_e^r + V_e^i I_e^i\right)^{\star}$$
$$m_{Q,e} = Q_e^{\star} - \left(V_e^i I_e^r - V_e^r I_e^i\right)^{\star}$$

Where $P_e^{\star}$ and $Q_e^{\star}$ are the last optimal solution of the linearized model for element e. So, if $\max\{|m_P|, |m_Q|\} \leqslant \hat{\epsilon}$, for a given tolerance $\hat{\epsilon}$, $\alpha = 1$, on the contrary $\alpha = 0$.

4.2.3 Stop. The algorithm will stop if $\max\{|m_P|, |m_Q|\} \leqslant \epsilon$, given a tolerance level ϵ. Note that if all mismatch indices are zero, then the S-QCP solution is a primal feasible point for the NLP problem. Additionally, NLP model simulation time is also used as stopping criteria.

4.2.4 Update. If the tuple $\left(V_e^r, V_e^i, P_e, Q_e\right)^{\star}$ is the more recent QCP solution, then the next operation point is computed as follows:

$$\left(v_e^{0r}, v_e^{0i}, p_e^0, q_e^0\right)^{\text{new}} \leftarrow \left(V_e^r, V_e^i, P_e, Q_e\right)^\star \tag{4.2.2}$$

$$i_e^{0r} = \left(p_e^0 v_e^{0r} + q_e^0 v_e^{0i}\right) / \left|v_e^0\right|^2 \tag{4.2.3}$$

$$i_e^{0i} = \left(p_e^0 v_e^{0i} - q_e^0 v_e^{0r}\right) / \left|v_e^0\right|^2 \tag{4.2.4}$$

After this, the rotating tangent lines are updated with the last solution for δ_{V_n}.

CHAPTER 5

DECENTRALIZED DER SCHEDULING

Part one of this document is dedicated to analyzing the solutions of a 3ϕ-ACOPF for an Active Distribution Network with high DER penetration. Then, beginning part two, a novel convex formulation for the 3ϕ-ACOPF is presented in chapter 4. With all this ready, the path towards a decentralized operation strategy for DER scheduling is almost finished. However, before continuing the characteristics of the centralized convex operation strategy must be analyzed, since it constitutes the base of the decentralized problem formulation. Therefore, section 5.1 presents a comprehensive performance evaluation for the convex formulation presented in chapter 4. There it is shown that the linear approximations of power injections converge to the optimal non-linear values, making the solution primal feasible for the non-convex formulation. After testing the centralized operation strategy, in section 5.2 it is presented how can be designed a decentralized operation strategy from this convex formulation by applying the Alternating Direction Method of Multipliers, furthermore, the resulting control proposes a new way to understand decentralized controls and black-box solutions presented in chapter 1. This characterization helps to improve the understanding in decentralized operation strategies presented in section 1.4, thus achieving goal (G-I)[1]. Only then a performance evaluation of the decentralized formulation is shown, thus achieving (G-II)[2]. At the end of the chapter, in section 5.3, there are presented a discussion and the chapter concluding remarks.

[1]To characterize the decentralized decision taking for distributed energy resource allocation in a power distribution network.

[2]To propose a comparative analysis of decentralized strategies for distributed energy resource allocation in a power distribution network.

5.1 Centralized operation strategy

This chapter section is devoted to show the limits on the convex approximation presented in chapter 4 and to give some light on the problems four to six (see section 1.5)[3]. To this end, the twelve cases simulated are described in section 5.1.1, while the results are summarized in section 5.1.2.

5.1.1 Test cases.

Models are tested for modified versions of the 13, 34 and 123 node IEEE test feeders (Kersting, 2001), which are depicted in Figure 23 to 25. Table 15 presents each circuit general parameters, e.g., DER nodes, voltage limits and tap position of regulators.

Table 15: Case general characteristics

Circuit (nodes)	*DER nodes*	*Voltage limits* $[V_{p.u.}]$	*Regulators (from-to nodes)*		
			a	*b*	*c*
13	645, 684, 671, 632, 633, 675	0.97 to 1.07	650-632		
			0	0	0
34	810, 820, 826, 864, 890, 848, 840, 838, 856, 844, 830, 802, 832	0.90 to 1.05	814-850		
			14	7	7
			852-832		
			12	10	11
123	30, 22, 50, 45, 36, 68, 59, 113, 110, 105, 100, 70, 78, 89, 96, 16, 31, 73, 92, 103	0.95 to 1.05	150-149		
			0	0	0
			25-26		
			0	–	-1
			60-67		
			8	1	5
			9-14		
			-1	–	–
Storage system parameters					
$\varepsilon_{in} = 0.9$, $\varepsilon_{ou} = 0.8$, $SOC_{min} = 0.1$, $SOC_{max} = 1$					

Additionally, two scenarios were simulated for each circuit: a minimum scenario and a maximum scenario, having the latter twice the load and DER levels than the former; and

[3] On one hand, problems five and six are about how to include delta load models and about approximations for ZIP load models, respectively; On the other hand, problem four is about the need for including specific limits on voltage unbalance.

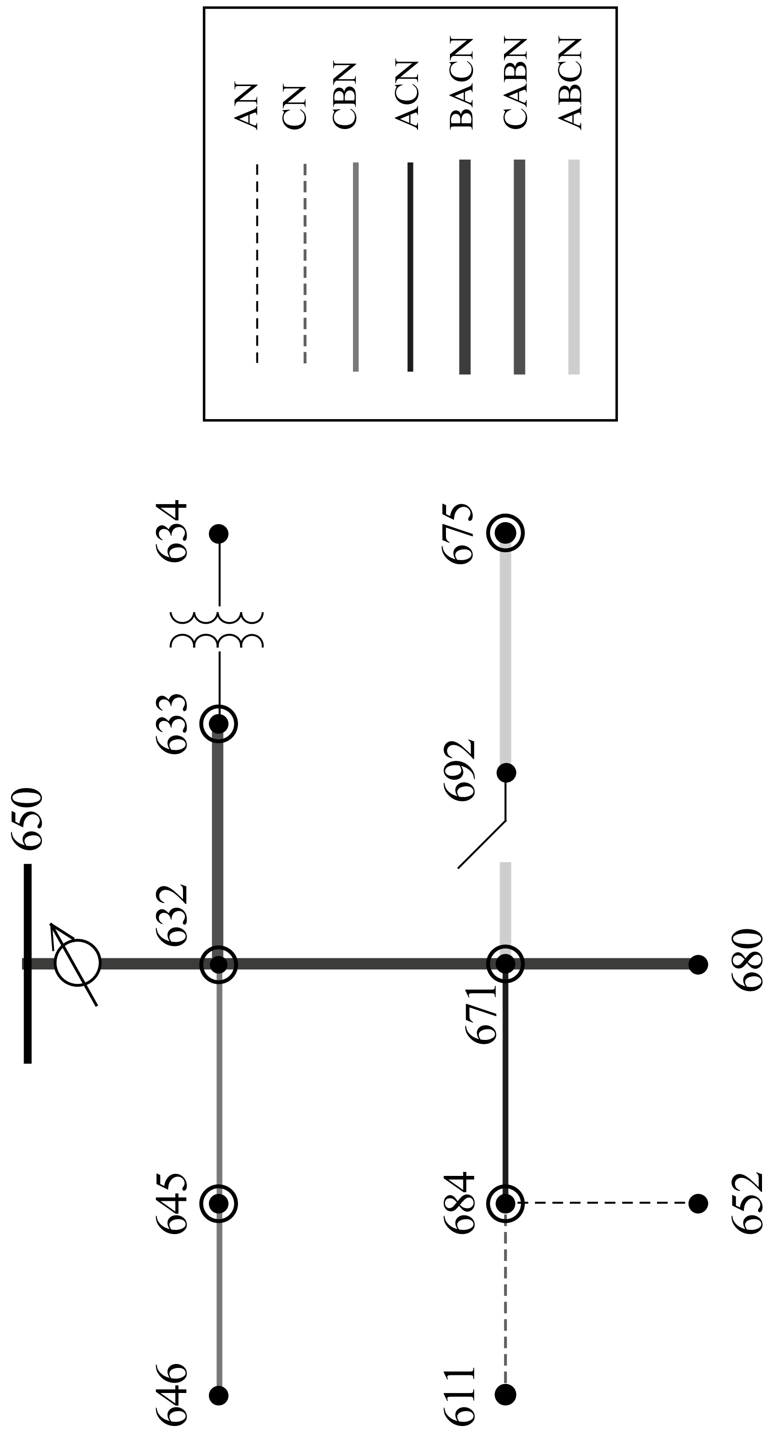

Figure 23: One line of the 13 node IEEE test feeder. Nodes with DERs are marked with an outer circumference.

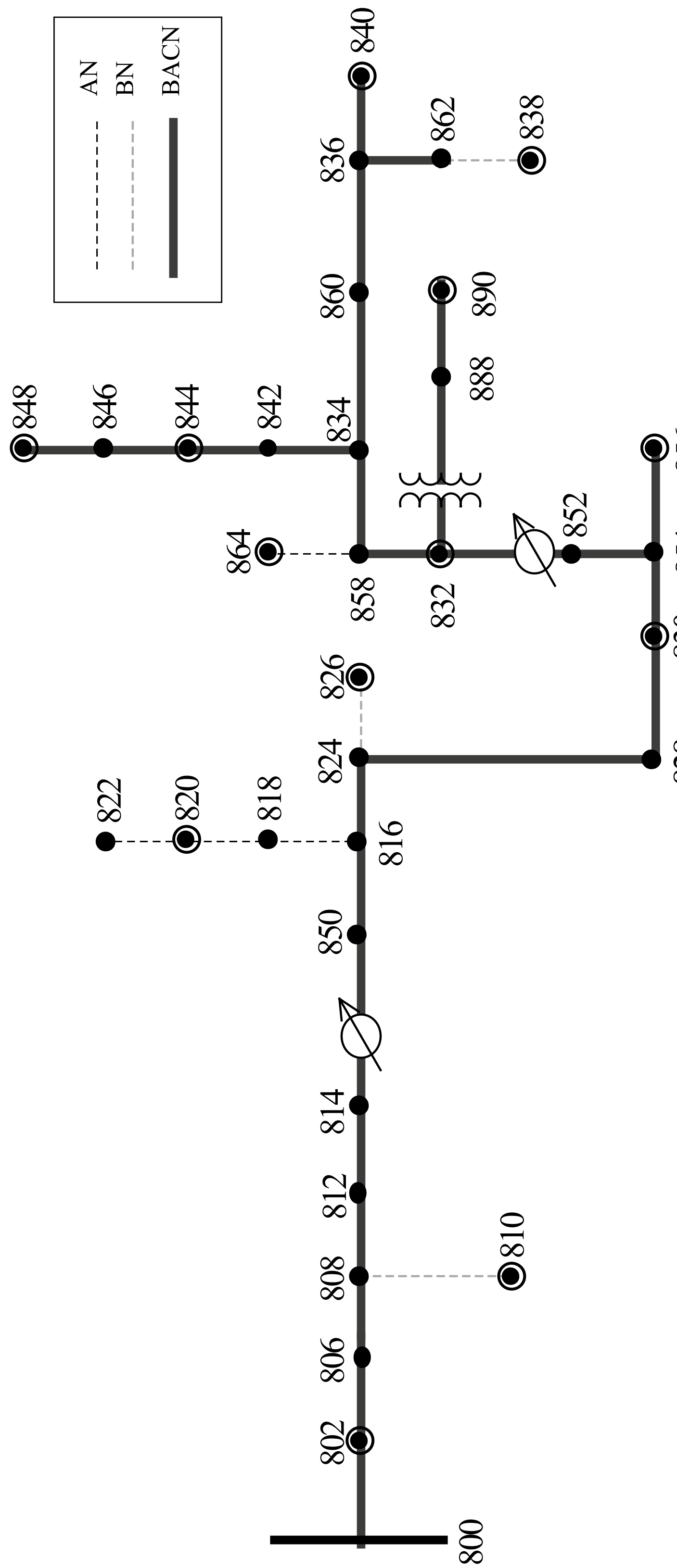

Figure 24: One line of the 34 node IEEE test feeder. Nodes with DERs are marked with an outer circumference.

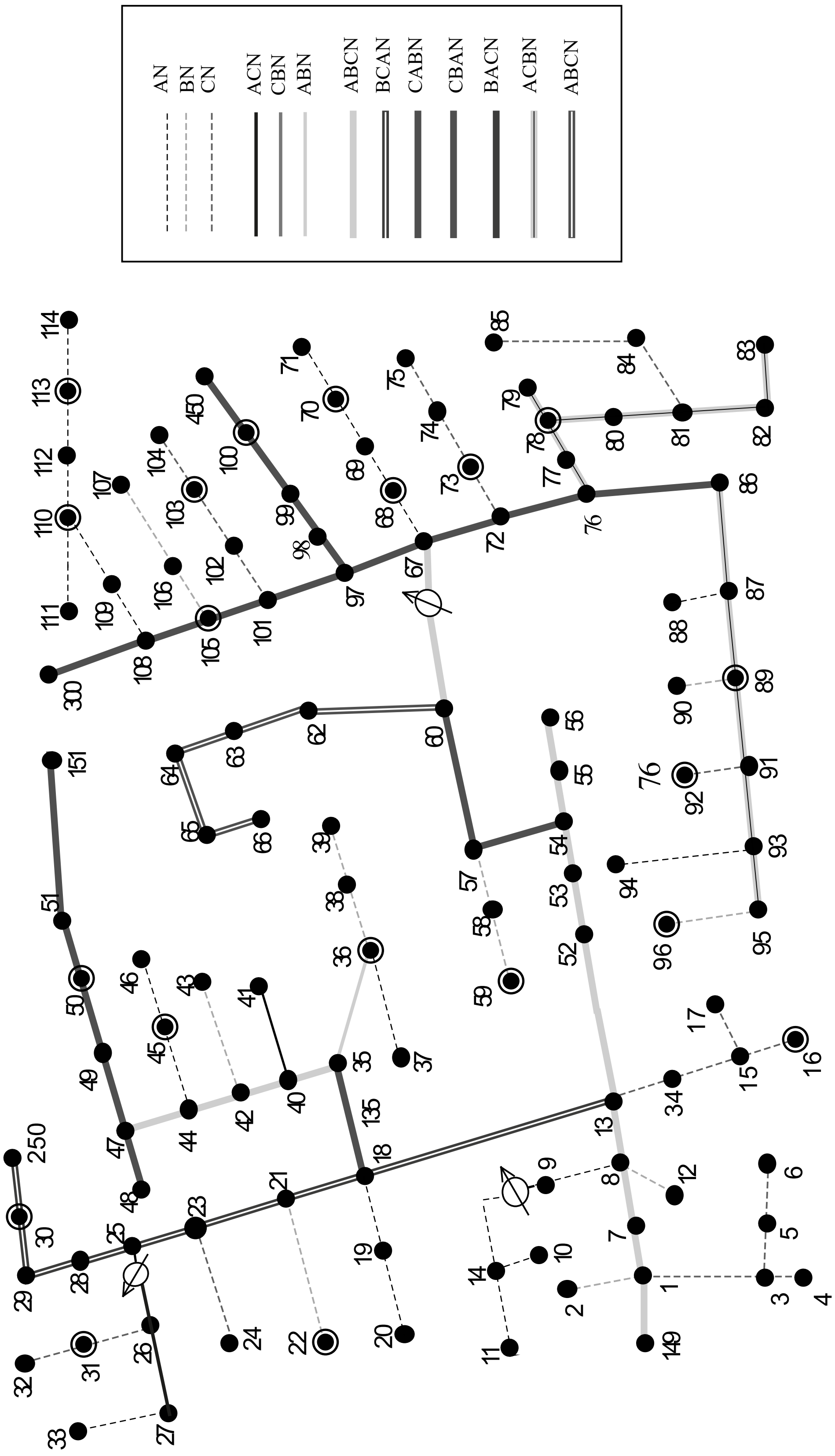

Figure 25: One line of the 34 node IEEE test feeder. Nodes with DERs are marked with an outer circumference.

both having 60% of PV penetration, i.e., total available irradiance accounts for 60% of the total active power energy consumption at the header. Also, there were simulated cases with and without PV reactive power compensation for each circuit and scenario, resulting in a total of twelve cases. Simulations were done for a 24 hour time lapse with a Δt equal to one hour. Solver tolerance parameters were set at 1×10^{-6}. The S-QCP tolerances where set to $\hat{\epsilon} = 1 \times 10^{-2}$ and $\epsilon = 1 \times 10^{-3}$.

Test feeders differ from the reference parameters only on tap setting values, moreover, maximum and minimum voltage magnitude values are adjusted to those observed in the test feeder reference. On the other hand, load and available PV power are known parameters. Also, at each DER node, there are connected a PV system and an electrical storage system (see Table (15)). Load profiles were constructed from three basic types while the PV profile is taken from available measures. All calculations are done under a *per unit system*, with a power base of 100 kVA and proper voltage bases. All cases were implemented using GAMS 24.5.4, using IPOPT 3.12 solver (with MUMPS as linear solver) for the NLP model; and using CPLEX 12.6.2.0 solver for the S-QCP model. Simulations were done on a laptop computer with an Intel(R) Core(TM) i7-4700MQ processor (2.4GHz) with 6GB of RAM. For each case, apart from f^{LOSS} and f^{SS}, the same parameters described in section 3.1.5 are calculated.

5.1.2 Results.

Table 16 presents the percentage difference between the solution of the NLP formulation and the S-QCP formulation for the twelve test cases defined in section 5.1. There, one can see that objective function of the S-QCP formulation differs by less than 0.25% than its NLP counterpart in every tested case. Objective function and storage benefit differences are very alike because the latter are two to three orders of magnitude bigger than network active losses. On the other hand, Figure 26 presents the DER power injections by the NLP and S-QCP formulations; note that such power injections are very close between models.

Also note that the S-QCP formulation finds a solution in less time than the NLP formulation. This is achieved within 4 outer iterations, and in general, after the first outer iteration active power injections are very close to the NLP optimal value. So, remaining outer iterations are mainly for answer refining. As a consequence, trust region objective function is usually included in the third outer iteration.

For S_h the mismatch indices have a maximum value of 4.27×10^{-4}, while the maximum value for all the remaining non-linear variables is always lower than 1×10^{-4}. Mismatch indices for each variable are between 1×10^{-5} and 1×10^{-13}, and in fact, such maximum values are uncommon.

Table 16: Sequential QCP model percentage differences with respect to NLP model for each case. Time reference correspond to the NLP model.

	Feeder – $Q_{pv} \neq 0$							*Feeder* – $Q_{pv} = 0$					
	13 nodes		34 nodes		123 nodes			13 nodes		34 nodes		123 nodes	
Case	max.	min.	max.	min.	max.	min.	*Case*	max.	min.	max.	min.	max.	min.
Objective	-0.043	0.002	0.012	0.101	0.233	0.002	*Objective*	-0.056	0.002	0.024	0.095	0.183	0.005
Time %	**-22.89**	**-45.19**	**-72.12**	**-59.22**	**-5.052**	**-30.22**	*Time %*	**-2.862**	**-33.94**	**-65.22**	**-87.07**	**-22.87**	**-51.16**
Time Ref. [s]	4.656	4.625	87.58	112.7	62.45	38.31	*Time Ref.* [s]	3.250	3.656	150.6	260.8	94.56	61.09
Network							*Network*						
f^{P}	-0.565	-0.613	**-1.826**	**-1.742**	-0.782	0.399	f^{P}	**-1.098**	-0.413	**-1.089**	0.390	-0.121	0.516
L_T	-0.067	-0.246	-0.641	-0.579	-0.160	0.297	L_T	0.093	-0.205	**-1.237**	-0.423	-0.171	0.367
P_T^h	-0.535	-0.496	**-1.576**	**-1.455**	-0.636	0.241	P_T^h	-0.877	-0.334	-0.771	0.127	-0.176	0.214
Q_T^h	**3.014**	**15.34**	**8.416**	**68.30**	**3.571**	**8.841**	Q_T^h	**1.464**	**7.530**	0.075	**6.763**	**1.312**	0.331
$V_{avg}^{(+)}$	-0.191	-0.380	-0.306	-0.407	-0.100	0.510	$V_{avg}^{(+)}$	-0.096	-0.473	-0.407	-0.711	-0.690	0.510
$VUF_{avg.}^{(-)}$	**-9.048**	**-18.02**	**-11.27**	**-9.101**	**-10.25**	**-17.98**	$VUF_{avg.}^{(-)}$	**-1.371**	**-4.194**	**-13.20**	**-4.664**	**-10.82**	**-17.71**
PV							*PV*						
P_T^{PV}	-0.086	0.106	0.705	0.443	0.275	0.103	P_T^{PV}	0.944	-0.477	0.134	**-3.551**	**-1.307**	0.174
Q_T^{PV}	**-1.155**	**-1.439**	**-5.423**	**-9.660**	**-1.897**	**-9.747**	Q_T^{PV}	–	–	–	–	–	–
p_T	0.215	-0.255	-2.494	-1.397	-0.295	-0.112	p_T	**-2.154**	**1.105**	-0.438	**11.60**	**1.410**	-0.184
SS							*SS*						
f^{ES}	-0.043	0.002	0.002	0.097	0.232	0.002	f^{ES}	-0.056	0.002	0.003	0.091	0.183	0.005
$P_T^{\vee}$	0.310	0.000	0.008	0.085	-0.075	0.000	$P_T^{\vee}$	0.404	0.000	0.010	0.085	-0.068	0.004
$P_T^{\wedge}$	0.329	0.000	0.013	0.095	-0.077	0.003	$P_T^{\wedge}$	0.429	0.000	0.015	0.090	-0.071	0.005

Figure 26: DERs active power injections of the 123 node test feeder for the maximum load and DER level scenario.

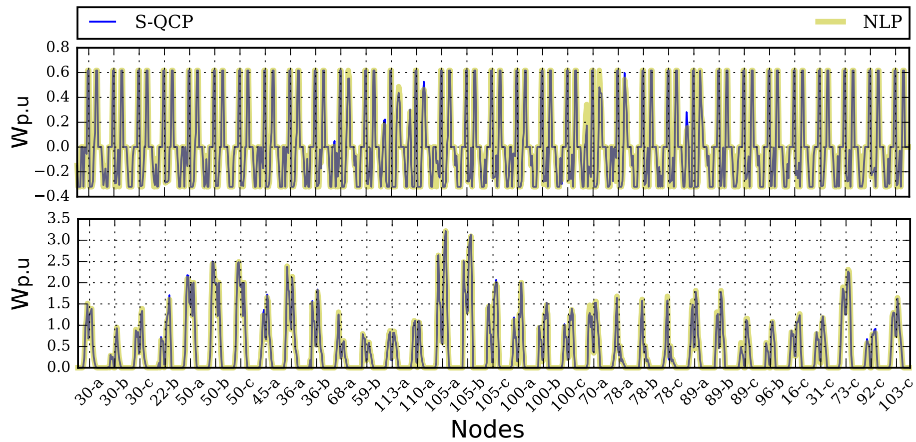

Figure 27 presents the voltage differences for both, the NLP and S-QCP formulations for the IEEE 123 node test feeder. There, a darker color indicates that the NLP formulation results in a lower voltage, while a lighter color indicates that the NLP formulation has a higher voltage. One can observe that voltage profile differences between formulations range from 0.1 to -0.1 $V_{\text{p.u.}}$, on the other hand, running some calculations reveal that the NLP formulation has a higher average voltage magnitude than the S-QCP formulation, except for the min. scenario. Also, it is remarkable that for the same storage power injections, the voltage for each model is different, specifically: (1) a darker zone around the 19:00 hours, indicate that the NLP formulation drops as much as possible the node voltage to withstand the active power injection. (2) A lighter zone around before the 6:00 hours, indicate that the NLP formulation increases as much as possible the node voltage in order to withstand the active power withdraw.

Figures 28 and 29 present the voltage magnitudes for all test cases involving the IEEE 123 node test feeder. There one can see that the voltage differences between formulations are due to the approximation itself. For a given power injection in the NLP formulation, the relationship between node voltage and injected current is hyperbolic, thus, voltage profile presents sharp changes because it is sensitive to changes in current injections. In contrast, for the S-QCP formulation the relationship between node voltage and injected current is linear, and so, voltage profile is flatter because it is less sensitive than the NLP formulation to current injections.

Figure 27: Voltage differences between S-QCP model and NLP formulations, for each phase (a –up, b –middle, c –down) and each scenario (minimum –left– and maximum –right– load and DER levels, of the 123 node test feeder.

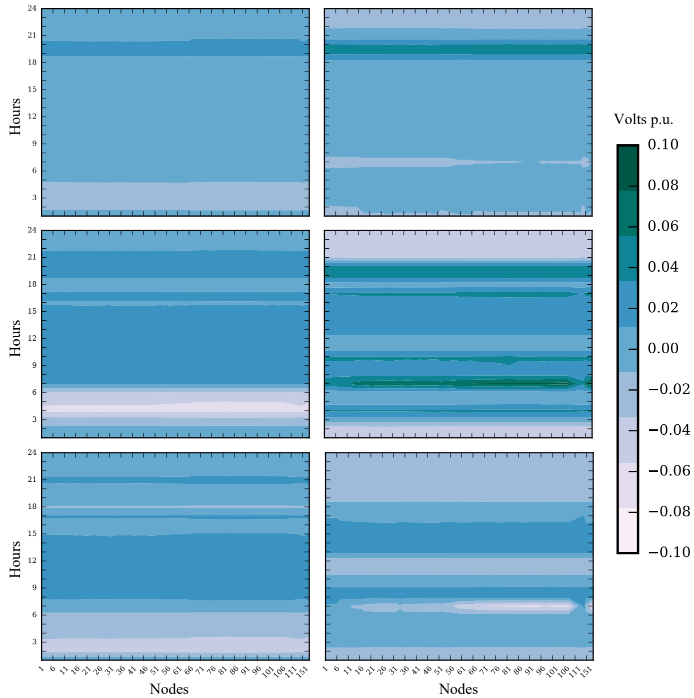

As can be seen in Table 16, these flatter voltage profile in the S-QCP model causes higher differences on PV active power injections for the case without PV reactive compensation as well as higher differences in PV reactive compensation. For example, for a given active power injection, the NLP formulation might have a very low voltage, therefore, since the S-QCP formulation voltage is not so low, to maintain this optimal voltage profile some of the injected power must be curtailed. Similarly, in cases with reactive compensation, the best solution to maintain the optimal node voltage magnitude is to reduce the reactive power injection or even consume reactive power.

Also note that voltage differences for all tested cases (e.g., see Figure (27)) are lacking vertical lighter or darker areas. This means that voltage differences between nodes for the NLP and the S-QCP formulations are very similar. This reinforces the fact that power injections are very similar since, for different voltage differences between nodes, there are different power flows. Voltage differences are then more sensitive to changes between time periods, namely, because of the differences between the active/reactive power needed to maintain the optimal voltage magnitude.

Therefore, in spite of the differences listed above, resulting reactive power, voltage magnitude and voltage unbalance differences are not large enough to change the active power flows in the system. Tested cases suggest that those differences depend mainly on the system topology and the required operation parameters (e.g. PV curtailment and voltages limits). Also note that as a consequence of having a lower average voltage magnitude and unbalance factor, losses, and costs for the S-QCP model are slightly lower in most of the cases. Additionally, lower unbalance is mainly due to the reduced voltage feasible region of the S-QCP formulation, since after constraining voltage unbalance in the NLP formulation the active power schedule is barely changed. Like in chapter 3, balanced power injections are not needed to obtain a solution within the admissible VUF, since in case of having a VUF out of the allowed limits a voltage unbalance constraint can be included to enforce a safe operation. Furthermore, the lower unbalance in the S-QCP solution sometimes give an answer already within the required VUF limits, mainly in the minimum DER scenario. This can be seen in Table 17 where a comparison between the average and maximum negative sequence VUF for the NLP formulation and the S-QCP formulation is presented. The lower unbalance in the S-QCP is an important characteristic, since if the base circuit has the VUFs far from the required limit, to find a solution within the VUF limits require a considerable amount of additional computation time (see Table 14).

Table 17: Average (right) and maximum (left) negative sequence VUF for each tested case.

	Feeder – $Q_{pv} \neq 0$					
	13 nodes		34 nodes		123 nodes	
Case	max.	min.	max.	min.	max.	min.
NLP	1.050 | 2.683	0.749 | 3.078	1.686 | 3.349	1.725 | 3.019	1.297 | 3.522	0.940 | 2.425
S-QCP	0.955 | 2.330	0.614 | 1.785	1.496 | 2.415	1.568 | 2.054	1.164 | 3.243	0.771 | 1.891
	Feeder – $Q_{pv} = 0$					
	13 nodes		34 nodes		123 nodes	
Case	max.	min.	max.	min.	max.	min.
NLP	0.948 | 2.212	0.763 | 2.625	1.856 | 3.349	1.608 | 3.018	1.386 | 4.434	0.898 | 2.428
S-QCP	0.935 | 2.140	0.731 | 1.779	1.611 | 2.763	1.533 | 2.106	1.236 | 3.240	0.739 | 1.837

Figure 28: Voltage magnitudes for the max. scenario, with PV reactive compensation (first two rows) and without PV reactive compensation (last two rows), each model (NLP-up, S-QCP-down), and for each phase (a-left, b-center and c-right).

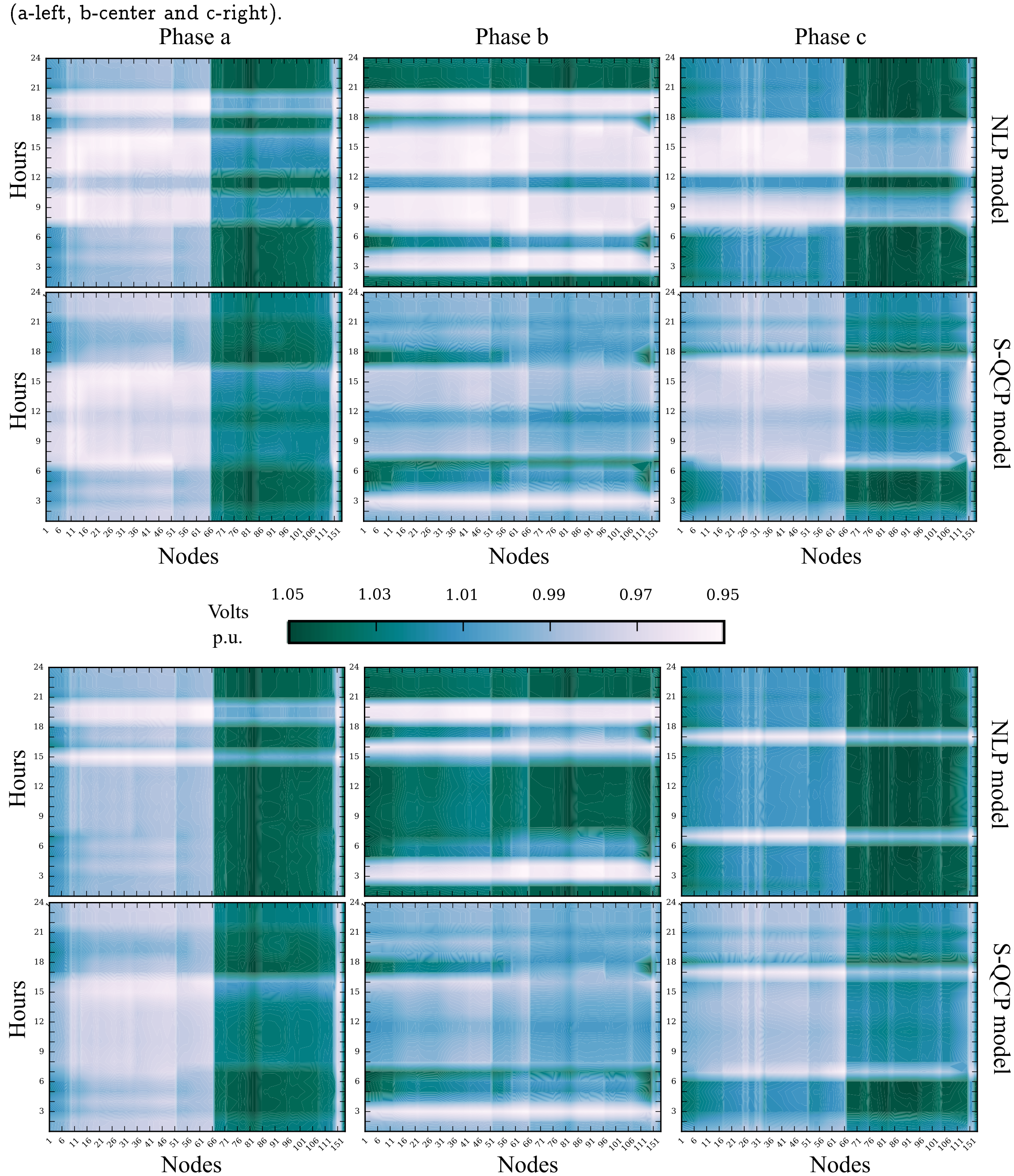

Figure 29: Voltage magnitudes for the min. scenario, with PV reactive compensation (first two rows) and without PV reactive compensation (last two rows), each model (NLP up, S-QCP down), and for each phase (a-left, b-center and c-right).

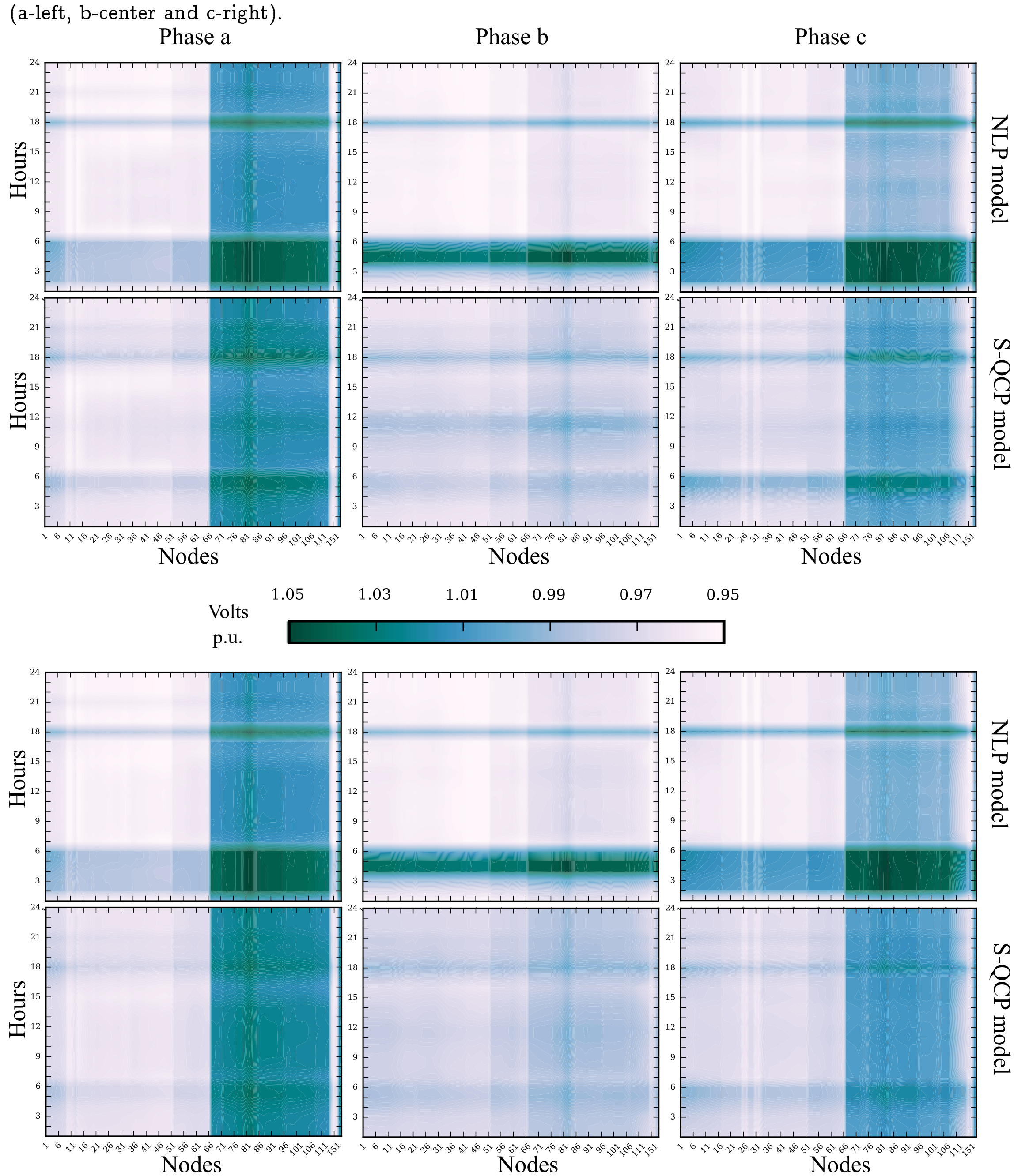

5.2 Decentralized operation strategy

This chapter section presents how from the convex approximation in chapter 4 a distributed operation strategy for Active Distribution Systems can be derived. First in section 5.2.1 is presented a characterization of the methods reviewed in section 1.4. Then, in section 5.2.2 it is explained and applied such framework to the 13, 34 and 123 node IEEE feeders to give a glimpse of its performance.

5.2.1 Decentralized control characterization. From section 1.4, two common elements are present in every reviewed decentralized control technique:

1. All of them use dual ascent steps applied to the Method of Multipliers to find a solution. Most of them decentralize the solution computation by reformulating the primal problem to apply the Alternating Direction Method of Multipliers (ADMM). In the case of (Christakou et al., 2017a) the dual ascent steps are divided into a primal decomposition and a price update step. In all cases, network topology is used to fully decouple DER power injections from network and load power injections. In general, the solution computation must have at least two stages: One for finding the optimal for each DER; and other for adjusting the DER optimal solution to a feasible point. Only (Loukarakis et al., 2015a) and (Guggilam et al., 2016) make this difference explicit, while the other methods reviewed only clarify that the decomposition can be done up to the node level. Note that in the latter case all nodes without DERs can form one or several network partitions, each one defining a subproblem; and that the solution of these subproblems leads to a feasible solution.

2. All of them include local constraints (like DER constraints or current balance at the node where DER are connected) in the solution computation of each of the subproblems. This is done to reduce the information burden and assure data privacy. However, there is another reason: A look to equation 1.1.12, shows that in order to apply the indicator function pattern the unconstrained optimization must lie in the feasible region. All methods then assure the local feasibility by including the constraints in the subproblems; nevertheless, with a feasible starting point will be enough.

Now, let us look to equations (1.1.12) to (1.1.14), here repeated for the sake of reference:

$$
\begin{aligned}
x^{k+1} &:= \mathrm{prox}_{f,\rho}\left(\varkappa^{k} - \mu^{k}\right),\ \varkappa^{k} \in \mathcal{R} \\
\varkappa^{k+1} &:= \mathrm{proj}_{\mathcal{R}}\left(x^{k+1} + \mu^{k}\right) \\
\mu^{k+1} &:= \mu^{k} + r^{k}
\end{aligned}
$$

Where x is the vector of primal variables, $\varkappa$ is the vector with the copies of the primal variables, and μ is the vector of the scaled dual variables, $\mathcal{R}$ is the feasible region of the problem, ρ is a constant factor to adjust the proximal operator behavior, and k is the iteration counter. For a more detailed description please refer to 1.1.2. Note that these steps encapsulate the basic steps to decentralize the solution computation of a 3ϕ-ACOPF. Let us analyze them in order to check this claim.

In the first step, *the proximal optimization step*, an unconstrained optimization takes place given a feasible starting point. Note that the objective function must be separable in order to run this step in a parallel or concurrent fashion. This is the case for the energy resource allocation problem in ADNs; furthermore, each subproblem is related to one DER schedule. As a rule of thumb, proximal optimizations must have a very low computation time, or even a closed form to increase the method performance. Having the form of a proximal operator means that the unconstrained optimization is not totally free, instead, it considers a possible near solution (in form of the constant value $\varkappa^k - \mu^k$). In this sense, the proximal optimization is solving a trust region problem. Actually, the trust region problem and the proximal optimization are equivalent, as presented in (Parikh and Boyd, 2013).

Network constraints (e.g., current balance in each node and maximum and minimum voltage magnitude limits) are enforced in the second step: *the projection step*. This step is used to find the nearest point to the proximal optimization solution in the feasible set. Note that the projection step may also be decomposed, thus adding one decomposition layer to the problem. Also note that the interaction between the proximal optimization step and the projection step is similar to the interaction between local optimization and legacy power flow solvers used in (Bruno et al., 2011). There, in order to compute a search direction, it is introduced a small perturbation into the latest set of power injections. To assure feasibility, a three-phase power flow must be run for each objective function term. Instead, with the ADMM a 3ϕ-ACOPF is run once for adjusting the feasibility of all power injections.

Up to this point, the projection step goes strictly after solving the proximal optimization for each DER, i.e., the solution computation is running in a decentralized way, but synchronously. To run asynchronously the ADMM the proximal optimization layer must be able to run independently from the projection layer, and *vice versa*. This is achieved by running the third step, *the residual update step*, according to two Poisson clocks, one for the proximal optimization layer and other for the projection layer. As a rule of thumb, the Poisson clock of the proximal optimization layer must have a higher rate than the clock of the projection layer. This way the projection step can be done with the most up-to-date information (Christakou et al., 2017a; Wei and Ozdaglar, 2013). As a way to reduce the communication burden, the update could be done only after an actual change occurs in the network, as presented in (Wan and Lemmon, 2010, 2009).

Note that in the third step, the scaled Lagrange multiplier can be written as:

$$\mu^k = \sum_{\kappa=1}^{k-1} r^\kappa$$

Hence, μ^k is the sum of the running errors up to iteration k. Now, let us turn the attention to the proximal operator argument, which in this case is $\varkappa^k - \mu^k$. The value of μ^k will be very small if x and $\varkappa$ are already similar, i.e., if the objective function minimum is already near to the problem optimum. Otherwise, errors will start to sum up in order to make x and $\varkappa$ as similar as possible. Thus, the goal of μ^k is to shift the optimal value so it also minimizes the error between x and $\varkappa$. Note that in this sense, the ADMM steps are a generalization of the Walrasian auction.

As a conclusion, the scaled form of the ADMM not only helps to solve in a decentralized way but also, it helps to look from a very general way to the steps in doing so. Next chapter applies these three basic steps to solve the 3ϕ-ACOPF in a decentralized and synchronous way.

5.2.2 Distributed control design.

Bellow is described how a decentralized operation strategy can be derived for optimal DER scheduling in an unbalance distribution network from the application of equations (1.1.12), (1.1.13) and (1.1.14) to the problem described in section 4.2.

Optimization problem

The four steps on section 4.2 remain unchanged. However, the QCP problem to be solved is now (see section (4.2.2)):

$$\max \left\{ \sum_{g \in \mathcal{G}_{\text{ES}}} \sum_{\phi \in \Phi_g} \sum_{t \in \mathcal{T}} \pi_t \left[\hat{P}^{\phi}_{g,t} - \check{P}^{\phi}_{g,t} \right] + \sum_{g \in \mathcal{G}_{\text{PV}}} \sum_{\phi \in \Phi_g} \sum_{t \in \mathcal{T}} \pi_t P^{\phi}_{g,t} \right\}$$

s.t. equations

$$\widehat{\text{PFE}}, (2.2.4), (2.2.5\text{-}2.2.10), (4.1.11), (4.1.12)$$

Hence, the first term of the objective function still is to maximize the benefits from time arbitrage of electrical storage; while the second term maximizes the benefits from selling PV energy. Before running the proximal optimization for the first time, one outer iteration of the S-QCP is completed to find a feasible starting operation point.

Proximal optimization Since for the current formulation the unconstrained proximal step may lead to values of $\hat{P}_g^\phi \neq 0$ when $\check{P}_g^\phi \neq 0$ and *vice versa*, $P_g^\phi \forall g \in \mathcal{G}_{\text{ES}}$, $\forall \phi \in \Phi_g$ is used as a decision variable for the proximal optimization. Note that $\hat{P}_g^\phi$ is recovered from positive values of P_g^ϕ, whereas, $\check{P}_g^\phi$ is recovered from negative values of P_g^ϕ. With this in mind, let us define:

$$\gamma_T^{\text{ES}}(P_g^\phi) = \sum_{g \in \mathcal{G}_{\text{ES}}} \sum_{\phi \in \Phi_g} \sum_{t \in \mathcal{T}} \pi_t P_{g,t}^\phi$$
$$\gamma_T^{\text{PV}}\left(P_g^\phi\right) = \sum_{g \in \mathcal{G}_{\text{PV}}} \sum_{\phi \in \Phi_g} \sum_{t \in \mathcal{T}} \pi_t P_{g,t}^\phi$$

Since these objective functions are separable, the proximal iterations (see equation (1.1.12)) are:

$$\dot{P}_g^\phi = \text{prox}_{\gamma_T^{\text{ES}}, \rho_{\text{ES}}}\left(\mathring{P}_g^\phi - \mu_g^\phi\right), \; g \in \mathcal{G}_{\text{ES}}, \forall \phi \in \Phi_g \tag{5.2.1}$$
$$\dot{P}_g^\phi = \text{prox}_{\gamma_T^{\text{PV}}, \rho_{\text{PV}}}\left(\mathring{P}_g^\phi - \mu_g^\phi\right), \; g \in \mathcal{G}_{\text{PV}}, \forall \phi \in \Phi_g \tag{5.2.2}$$

Where μ_g^ϕ is the most up-to-date value for the scaled prices. Now, depending on the iteration number k, $\mathring{P}_g^\phi$ is the feasible optimal value obtained after one outer iteration of the S-QCP (if $k = 1$) or from the projection step problem (if $k > 1$).

Projection The projection on the feasible set is computed by solving the following optimization problem:

$$\begin{aligned}\mathring{P}_g^\phi = \arg\min \Bigg\{ & \sum_{g \in \mathcal{G}_{\text{ES}}} \sum_{\phi \in \Phi_g} \sum_{t \in \mathcal{T}} \rho_{\text{ES}} \left\| P_{g,t}^\phi - \dot{P}_{g,t}^\phi - \mu_{g,t}^\phi \right\|_2^2 + \\ & \sum_{g \in \mathcal{G}_{\text{PV}}} \sum_{\phi \in \Phi_g} \sum_{t \in \mathcal{T}} \rho_{\text{PV}} \left\| P_{g,t}^\phi - \dot{P}_{g,t}^\phi - \mu_{g,t}^\phi \right\|_2^2 : \\ & P_g^\phi \in \mathcal{S}_{\text{CVX}}, \forall g \in \{\mathcal{G}_{\text{ES}} \cup \mathcal{G}_{\text{PV}}\}, \forall \phi \in \Phi_g \Bigg\}\end{aligned} \tag{5.2.3}$$

Where the set $\mathcal{S}_{\text{CVX}}$ is defined by equations $\widehat{\text{PFE}}$, (2.2.4), (2.2.5-2.2.10), (4.1.11), and (4.1.12).

Update After the projection step is done, a new operation point is computed, of course, this time based on the solution of the projection. Additionally, the problem prices are updated as follows:

$$\mu_g^\phi \leftarrow \mu_g^\phi + \dot{P}_g^\phi - \mathring{P}_g^\phi, \; \forall g \in \{\mathcal{G}_{\text{ES}} \cup \mathcal{G}_{\text{PV}}\}, \forall \phi \in \Phi_g$$

The algorithm stops when the following two conditions are met: 1) Conditions stated in section (4.2.3); and 2) Primal residual condition, i.e., $\left\|\dot{P}_g^{\phi} - \mathring{P}_g^{\phi}\right\|_2 \leqslant \epsilon_p$, for a given tolerance ϵ_p.

5.2.3 Test cases and results.

This section presents the results of applying the distributed control described in section 5.2.2 to the 13, 34 and 123 node IEEE test feeders for the maximum DER scenario described in section (5.1.1). Such results are summarized in Table 18 to 20. All calculations are done under a *per unit system*, with a power base of 100 kVA and proper voltage bases. All projection steps were implemented in GAMS 24.5.4, using IPOPT 3.12 solver (with MUMPS as linear solver) for the NLP formulations; CPLEX 12.6.2.0 solver for the QCP formulations; and using GAMS/Python API and Scipy library to implement the proximal optimization and the virtual framework for data exchange between GAMS and Python applications. Simulations were done on a laptop computer with an Inter(R) Core(TM) i7-4700MQ processor (2.4GHz) with 6GB of RAM.

From Table 18 to 20, note that solutions from the centralized and decentralized operation strategies vary slightly. Even after removing the trust region objective in the S-QCP centralized problem, the differences persist, meaning that the S-QCP formulation and the decentralized solution here presented are not equivalents. The exact dual for the S-QCP formulation can be derived only for one outer iteration, which would imply to leave unchanged the initial guess of the reference operating point. What is more interesting, it is that the decentralized answer is actually slightly better than the other for the 123 test node feeder, while it is more similar to the S-QCP formulation answer for the IEEE 34 node test feeder case, and it is also similar to the NLP formulation for the IEEE 13 node test feeder case.

Note that since the VUF is not constrained, the answers for the IEEE 34 and 123 node test feeders are impractical; however, they show that the three formulations can handle large unbalances in the network. Of course, by constraining the VUF a useful answer can be obtained without major changes in DER power injections or computation time. Furthermore, for some cases, the lower unbalance causes a higher voltage profile, which in turn cause a slight increase in losses.

Another remarkable characteristic of the decentralized solution is that DER prices can be recovered from the scaled prices μ_g^{ϕ}. Of course, for this special case DER prices are equal to the price vector π, but note that being the centralized solution based on a QCP, not always the dual variables are directly available.

Table 18: Decentralized and centralized solution comparison for the 13 nodes IEEE test feeder and for the maximum DER scenario as described in section (5.1.1).

Case	Centralized (NLP)	Centralized (S-QCP)	Decentralized (QCP)
Objective [M$]	3128.4	3128.1	3127.9
Mismatch (max.)	–	4.6×10^{-4}	3.7×10^{-4}
Time [s]	2.375	1.815	1.783
Network			
f^{P} [M$]	2780.4	2745.8	2753.4
L_T [MWh]	1.4668	1.4912	1.4827
P_T^h [MWh]	45.047	44.562	44.662
Q_T^h [MVArh]	27.728	27.773	27.939
$V_{avg}^{(+)}$	1.021	1.005	1.010
$VUF_{avg.}^{(-)}$	0.824	0.903	0.851
$VUF_{max.}^{(-)}$	1.549	2.353	1.687
PV			
P_T^{PV} [MWh]	30.657	30.568	30.657
Q_T^{PV} [MVArh]	2.089	2.8086	2.5053
p_T [MWh]	0	0	0
SS			
f^{ES}[M$]	517.12	516.81	516.66
$P_T^{\vee}$ [MWh]	8.6	8.6394	8.6574
$P_T^{\wedge}$ [MWh]	5.76	5.7884	5.8014

Table 19: Decentralized and centralized solution comparison for the 34 nodes IEEE test feeder and for the maximum DER scenario as described in section (5.1.1).

Case	Centralized (NLP)	Centralized (S-QCP)	Decentralized (QCP)
Objective [M$]	2073.1	2072.9	2059.5
Mismatch (max.)	–	2.1×10^{-4}	1.8×10^{-4}
Time [s]	190.92	29.512	19.568
Network			
f^{P} [M$]	1998.1	1997.9	2012.1
L_T [MWh]	5.9257	6.6413	6.7462
P_T^h [MWh]	32.952	32.775	32.660
Q_T^h [MVArh]	16.802	23.497	24.560
$V_{avg}^{(+)}$	0.990	0.974	0.974
$VUF_{avg.}^{(-)}$	1.349	1.681	1.670
$VUF_{max.}^{(-)}$	5.419	4.484	4.308
PV			
P_T^{PV} [MWh]	21.810	21.181	21.181
Q_T^{PV} [MVArh]	3.0471	-3.196	-4.2214
p_T [MWh]	0	0	0
SS			
f^{ES}[M$]	289.48	289.21	275.89
$P_T^{\vee}$ [MWh]	4.7602	4.7439	4.2643
$P_T^{\wedge}$ [MWh]	3.1844	3.1729	2.8273

Table 20: Decentralized and centralized solution comparison for the 123 nodes IEEE test feeder and for the maximum DER scenario as described in section (5.1.1).

Case	Centralized (NLP)	Centralized (S-QCP)	Decentralized (QCP)
Objective [M$]	5210.4	5211.3	5218.2
Mismatch (max.)	-	1×10^{-3}	2.2×10^{-4}
Time [s]	100.12	32.325	37.659
Network			
f^{P} [M$]	1200.9	1175.8	11683.3
L_T [MWh]	1.9255	1.8793	1.9002
P_T^{h} [MWh]	24.643	24.371	24.211
Q_T^{h} [MVArh]	23.565	21.450	22.963
$V_{avg}^{(+)}$	1.007	1.003	1.001
$VUF_{avg.}^{(-)}$	1.283	1.285	1.313
$VUF_{max.}^{(-)}$	3.545	3.272	3.326
PV			
P_T^{PV} [MWh]	58.627	58.622	58.736
Q_T^{PV} [MVArh]	4.6312	6.7413	5.3038
p_T [MWh]	2.7765	2.7811	2.6672
SS			
f^{ES}[M$]	366.61	367.60	360.75
$P_T^{\vee}$ [MWh]	7.5922	7.5750	7.6151
$P_T^{\wedge}$ [MWh]	5.0209	5.0085	5.0374

A crucial step when designing this kind of controls is to find an appropriate value for the ρ parameters. After some tuning, it was found that $\rho_{PV} = \rho_{SS} = 1000$ allow the algorithm to find a primal feasible answer for the IEEE 13 and 34 node test feeders, while a $\rho_{PV} = \rho_{SS} = 10000$ worked for the IEEE 123 node test feeder. The number of iterations, primal residual and total time (i.e., including pre and post-processing routines) are also presented in Table 21. It was observed that a ρ too small or too large lead to more iterations and to solutions that are not primal feasible for the non-linear problem.

Table 21: Decentralized algorithm parameters, primal residual, number of iterations and total time for each test feeder.

Feeder	ρ_{PV}	ρ_{ES}	r_{primal}	Iter.	Total time [s]
13 nodes	1000	1000	3.81×10^{-5}	2	5.13
34 nodes	1000	1000	4.1×10^{-6}	3	28.6
123 nodes	10000	10000	8.14×10^{-5}	5	84.4

Finally, the decentralized solution was implemented using Python "Futures" data type and Scipy library for the proximal optimization, along with the GAMS/Python API for the projection steps and to exchange information between problems. Although effective, the processing burden not related to the actual solution of the optimization problems is still high. From the last column in Table 21, one can see that for the IEEE 13 node test feeder, the difference between solution computation time and total time is large because the time spent preparing the data is greater than the time spent solving the problem. On the other side, for the IEEE 123 node test feeder, the time spent preparing the data is also comparable. Therefore, by using more specialized programming languages for concurrent computations, like Earlang or Akka module for Java or Scala, the data transfer between applications can be improved, thus removing some boilerplate code, adding resiliency to the software application and diminishing total execution times.

5.3 Remarks and research questions

5.3.1 Result summary. A novel solution for the full 3ϕ-ACOPF based on a Sequential Quadratically Constraint Quadratic Programming formulation (S-QCP) was presented. Each QCP is convex, and the proposed solution steps can find a primal feasible point for the Non-Linear Programming formulation. Besides, this formulation is computationally more efficient than the tested Interior Point algorithm, it leads to flatter voltage time-profiles and to more balanced answers for some objective functions. Elements such as ZIP loads, voltage regulators and delta loads are easily included, making it ideal for active distribution network analysis.

Furthermore, it was introduced a design framework for distributed controls based on the scaled form of the Alternating Direction Method of Multipliers (ADMM). The resulting framework can be condensed in three steps: 1) Run a local –proximal– optimization, 2) Project the answer onto the feasible set, and 3) Keep track of the differences of both previous answers to adjust the optimization path. This framework not only helps to understand the current decentralized approaches to optimal DER scheduling, but also can be seen as a generalization of the black-box approaches based on legacy power flow solvers, since these kinds of problems can be though as optimization problems with a constant objective function and a feasible region without voltage limits nor unknown power injections; while in the presented design framework the objective function is used to come with the closest feasible operating point with respect to a reference. This parallel gives a hint on why the S-QCP and the decentralized formulation works: For a power flow problem, the solution is usually computed with a fixed point algorithm, i.e., the solution is computed by evaluating a given function with the previous evaluation results. Since at the core of the OPF are the power flow equations, it is natural that a fixed point iteration works with the convex approximation presented; finding the kind of problems for which this is not valid can be an interesting research topic.

Unlike other 3ϕ-ACOPF approximations, the proposed formulations do not need any special network conditions: they work for high DER penetrations, given a considerable unbalance in the network, and also can manage electrical storage without using discrete variables. Furthermore, the solutions tend to have lower VUFs, which make unnecessary the addition of voltage unbalance constraints for some cases. Note that when voltage unbalance violations occur, adding these kinds of constraints do not lead to significant higher computation times.

5.3.2 Research questions and goals. By analyzing the results, the dependency of voltage unbalance to the objective function has been corroborated. Furthermore, it seems that the relationship between voltage unbalance and voltage profile might be more general, thus reinforcing the answer given for question research question (Q-Ib)[4] in the previous chapter. For the tested feeders, if the S-QCP solution has the same DER energy available than the NLP solution, the lower voltage profile of S-QCP model induces a voltage unbalance that is higher than the observed in the NLP case. This is very similar to what is presented at the end of section 3.2. By limiting the unbalance for the tested feeder with the decentralized strategy similar conclusions can be drawn.

Therefore, as an answer to problem 4 (about the need to include explicitly a control for voltage unbalance), voltage unbalance must be correctly assessed in the system given the optimal DER injections to know if it should be limited or not within the optimization problem.

In contrast to problem 4, answers to problems 5 and 6 (about the use of delta and ZIP load models) are sound. First, there is no need to avoid delta loads or to model them with wye

[4]Is the optimal DER scheduling increasing or decreasing the voltage unbalance in the network?

equivalents, since using cartesian components of the electric variables allow to model delta loads without much more effort. Second, cartesian components allow a clear and flexible load modeling, thus it must be avoided to exclude any of the ZIP load components. Specifically, for the S-QCP and the decentralized formulation, all load components are included as linear equations, thus reducing the computation burden. Furthermore, this is done without scarifying precision in the final answer, since all power injections are primal feasible for the NLP model.

As a consequence of achieving goal (G-I), a novel distributed control for Active Distribution Networks was devised. Moreover, the implementation of the distributed control allowed a side by side comparison with respect to the centralized formulations presented in previous chapters, thus achieving goal (G-II). For the implementation and comparison there could be highlighted three points: 1) The decentralized strategy successfully solved the 3ϕ-ACOPF, so the S-QCP formulation and the NLP formulation. Then, as a consequence of having three different voltage profiles for almost the same power injections, it is clear that there still is so much to know about the nature of the solutions in three-phase networks. In this search, the decentralized formulation presented here could be used as a starting point to characterize or find a global solution for the 3ϕ-ACOPF (if exists); the key element to achieving this, is without a doubt the projection step; 2) The tuning of the decentralized formulation is easy, meaning that with few problem instances one can find the correct parameters. 3) The efficiency of the decentralized formulation can be increased by constructing a custom algorithm for solving the projection step. Of course, taking advantage of the network topology is very relevant to this end, but also the mathematical properties that can be observed in the vicinity of the solution.

III CONCLUSIONS, BIBLIOGRAPHY AND APPENDICES

CHAPTER 6

CONCLUSIONS AND FURTHER RESEARCH

With the increasing adoption of Distributed Energy Resources (DERs), power distribution system participants can capture a whole new kind of benefits. However, the distribution system operator must change the current passive practices for more active measures to capturing such benefits while preserving the safety and reliability of the network. That is, legacy power distribution networks must make a transition to become Active Distribution Networks (ADN). At the core of every ADN there is a decision making unit in charge of allocating the DER energy efficiently for any penetration level; moreover, the combination of power electronics and communication technology could increase the network resiliency if instead of a centralized operation strategy, a decentralized operation strategy is implemented. The current state-of-the-art in convex programming has lead to many advances in this topic, however, they are often limited to one-line equivalent models, thus ignoring some key characteristics of power distribution networks. This lack of application creates some uncertainty about the potential of these advances for solving the energy allocation problem in ADNs.

As a consequence, to evaluate the performance of decentralized operation strategies for ADNs, first, a non-linear formulation and a convex formulation were presented. The former formulation not only helps to understand why it is necessary to model all three phases in distribution networks but also, it shows when a single-phase formulation could be useful. The latter formulation prove that it is possible to come with a convex formulation that considers all the key characteristics of a distribution network; moreover, unlike other convex formulations found in the technical literature the solution has lower computation time than the non-linear counterpart, lead to a primal feasible point for the non-linear formulation, and it can find an optimal solution even if the network has a high DER penetration or (and) the resulting solution is highly unbalanced. Interesting enough, the convex formulation solutions tend to have a lower voltage unbalance with respect to the non-linear formulation solutions; nevertheless, when voltage unbalance constraints are needed, they can be included without major impact in computation time. In general, the non-linear and convex formulations are able to handle any type of DER type and combination, i.e., unlike most proposals it can handle power conversion DERs and power storage DERs at the same time.

Given a convex formulation, a decentralized control strategy was designed. The decision to derive the distributed control from a mathematical programming perspective is twofold:

1. Due to the fact that convex optimization solution algorithms have been proven to be applicable to some non-linear problems after some relaxations. Note that having access to convex optimization algorithms ultimately translate to highly efficient solution computation.

2. Because from the solution of the dual problem of a convex programming formulation the coordination scheme of the decentralized system can be defined. This is thanks to the fact that convex programming formulations often have zero duality gap (i.e., the primal and dual problem solutions are the same), thus, the solution can be computed using dual decomposition techniques. Therefore, convex programming can be used to define one of the most difficult and important components in a decentralized system: the coordination scheme.

A novel decentralized formulation for the solution of the three-phase Alternating Current Optimal Power Flow (3ϕ-ACOPF) that works even in presence of voltage unbalance is one of the major contributions presented (see section 5.2.2), since it is common that decentralized 3ϕ-ACOPF require (or enforce) "almost balanced" conditions to find a solution; furthermore, they are mainly tested for one-line equivalent models, i.e., for perfectly balanced conditions. This novel decentralized formulation comes from an analysis of the technical literature that resulted in a design framework for decentralized operation strategies for ADNs (see section 5.2.1), thus achieving goal (G-I)[1].

The dual decomposition technique chosen is based on the Alternating Direction Method of Multipliers (ADMM), a technique that has been widely used because of its convergence properties. Namely, unlike the other applications in reviewed literature (excepting (Erseghe, 2014), where it is presented an equivalent approach implicitly), here it is applied the scaled ADMM to solve the 3ϕ-ACOPF. Being the convex formulation actually a sequence of Quadratically

[1] To characterize the decentralized decision taking for distributed energy resource allocation in a power distribution network

Constrained Quadratic Programs (QCPs), there was some concern about the equivalence of the convex formulation solution and the results obtained by applying the ADMM to such convex formulation. It was found that the resulting decentralized operation strategy is not equivalent to the convex formulation because of the "sequential" nature of the proposed convex solution. However, knowing the convex formulation made easy to solve all the implementation details of the decentralized solution; furthermore, the solutions are very close to those obtained with the convex and non-linear formulations. Note that, because the decentralized formulation is based on the convex approximation, all the characteristics of the convex formulation are inherited (e.g., primal feasibility and lower computation time).

Overall, the non-linear, the convex and decentralized formulations presented were tested for three IEEE test feeders (13, 34 and 123 nodes), allowing a comparison not only among the decentralized strategy against the other two centralized formulations (see section 5.2.2), but also between the centralized formulations themselves (see section 5.1.2), thus, achieving more than what was expected with objective (G-II)[2]. Note also that although there is no formal proof of convergence for the formulations proposed, it is expected that any power distribution network could be handled by them.

Other contributions

In addition to the novel decentralized formulation for the solution of the 3ϕ-ACOPF, the present document has extended the knowledge about this kind of problems by giving a concrete answer to the six open problems identified in the technical literature (see section 1.5):

1. The effects of optimal DER scheduling were presented for the *active power cost minimization*, *apparent power cost minimization*, *cost of losses* and the *cost of self losses* (see section 3.2.2); unlike (Li et al., 2017), where some consequences are explored but given only one objective function. As a conclusion, the minimization of active power costs presents the highest losses, highest unbalances and lowest active power costs; while the cost of losses presents the lowest losses, lowest unbalances and highest active power costs. Cost of self losses and apparent power costs are very similar to the cost of losses; however, cost of losses lead to lower unbalances for high DER penetrations. The minimization of apparent power costs has a good performance if there is no PV reactive compensation. Additionally, when analyzing the DER capacity of an ADN, and for low DER penetrations, the objective with the better performance is the active power cost

[2] To propose a comparative analysis of decentralized strategies for distributed energy resource allocation in a power distribution network

minimization at the network header. As the DER penetration increases, combining the cost minimization with the loss minimization results in the best performance.

2. An extensive analysis of the solutions of the three-phase and the perfectly balanced OPF was carried out for different PV penetration, DER types (including electrical storage) and test feeders (see sections 3.2.1, 3.2.2 and 3.2.3); unlike (Zamzam et al., 2017), where a solution for the 3ϕ-ACOPF only is there to show the capabilities of the algorithm described and no to be compared with the rest of single-phase ACOPF tests presented. Moreover, most solutions are only focused on one single type of DER. Then, solving this problem also lead to an answer to the research question (Q-Ia): Are the solutions obtained by a 3ϕ-ACOPF different enough from those given by a single-phase ACOPF? As a conclusion, the result of minimizing the cost of losses is very similar for unbalanced and balanced conditions. That is because for this kind of objective in both cases the solution has lower unbalance and lower reverse flows. In contrast, when minimizing the active power costs, the solution for unbalanced conditions differs greatly from the balanced condition solution for high DER penetrations. That is because for this kind of objective, the better the solution the more the unbalance in the network. It is then observed that for an unbalanced circuit, minimizing the active power costs is improved by increasing the exported energy, and not by reducing network unbalance. Therefore, for a DER penetration low enough, unbalanced and balanced circuits lead to similar answers as long as there are no reverse power flows in the network. As another conclusion, for high penetrations, PV reactive compensation appears as an effective way to diminishing PV curtailment when minimizing the active power costs; on the other hand, for this objective function and for low penetrations, PV reactive compensation and electrical storage have a similar effect. Finally, storage appears as an effective way to diminishing PV curtailment when minimizing the cost of losses, irrespective of the DER penetration.

3. A novel convex approximation of the 3ϕ-ACOPF that finds a solution in less time than its non-linear counterpart, and that converge to a primal feasible point of the non-linear formulation is presented (see chapter 4 and section 5.1); unlike the solution given by (Robbins and Dominguez-Garcia, 2015), the presented convex formulation does not require special conditions on the voltage unbalance. Then, solving this problem also lead to a novel answer to the research question (Q-II): Is it possible to have an exact convex relaxation of a 3ϕ-ACOPF?

4. The results obtained for the non-linear, convex and decentralized formulations of the

3ϕ-ACOPF problem clarify the decision taken by (Watson et al., 2017) and (Su et al., 2014) of constraining the voltage unbalance in the network. As a conclusion, depending on the DER penetration level and the objective function, the voltage unbalance might be over the recommended minimum (see chapter 3.2.2). Additionally, it was observed that, for a given DER capacity, if the unbalance is beyond the recommended limits, finding a balanced answer by constraining the Voltage Unbalance Factor on each node does not cause major changes in active power injections. From these tests, another pattern emerged: Given the same DER capacity, a decrease in voltage unbalance yields an increase in the voltage profile. Depending on the network topology, this can cause an increase in the system losses. Then, solving this problem also lead to an answer to the research question (Q-1b): Is the optimal DER scheduling increasing or decreasing the voltage unbalance in the network?

5. The load model explicitly included the delta connection type for every 3ϕ-ACOPF formulation, i.e., without wye connection equivalents (see equations (2.3.5) to (2.3.8)), a feature only present in three-phase power flow algorithms like (Ahmadi et al., 2016).

6. A ZIP load model not based in the polynomial model was presented (see equation (2.3.4) and (2.3.8)), departing thus from the models described in (Ahmadi et al., 2016; Wang et al., 2017b). Moreover, the constant power component is approximated exactly using only linear equations, thus avoiding crude assumptions on the load behavior like those in (Zamzam et al., 2017; Li et al., 2017; Robbins and Dominguez-Garcia, 2015; Wang and Yu, 2017; Liu et al., 2018), where all loads have only the constant power component; and avoiding approximations based on the other components like the one presented in (Watson et al., 2017), where the constant power component is replaced by an equivalent constant current component.

Additionally, it was presented that the amount of energy from DERs an ADN can allocate depends also on the objective function (see section 3.2.2). An objective function that encourages reverse power flows may allocate energy up to the network limits; while an objective function which discourages reverse power flows would allocate only a fraction of the energy beyond one point. Such point has two characteristics: 1) Reverse power flows are low, and 2) Almost all the increase in available energy is curtailed.

Applications and further research

All the formulations and tests done are to show that current technology can handle the complexity of present and future power distribution systems. Direct applications are DER planning and DER capacity assessment in power distribution networks, and after few adjustments, the following topics also may be treated:

- Computing network partitions in distribution systems, not only taking into account network topology but also network observability and measurement uncertainty. This is actually a key step to accelerate the transition from passive to active distribution networks since both observability and measurement uncertainty help to determine the minimum number of measurements needed to operate the network.
- Computing the distribution system locational marginal prices to derive an active and reactive power pricing scheme in Active Distribution Networks.
- Quantifying impacts of network congestion in power distribution systems to estimate benefits of investment deferral.
- Quantifying impacts of Plug-in Electrical Vehicles in power distribution systems.
- Computing the optimal schedules for shorter time windows with a rolling-horizon (Palma-Behnke et al., 2013).

Finally, the following topics are left for future research:

- Including upper voltage magnitude limits as a dead-band penalty in the objective function would transform the present formulation in a Quadratic Programming problem, which can be solved with simplex methods. Unlike interior point methods, the simplex method is very sensitive to initial conditions. This is a problem when initializing the problem, but clearly an advantage after the first iteration since given that the answer is close enough, it is likely that the problem answer could be computed even faster, although maybe with more outer iterations. The problem here is to come with a proper penalty term and a proper variable updating step. A warm start using one outer iteration of the convex formulation here presented may be used to solve the initial condition problem for the quadratic problem.
- Presented results opened a question about the uniqueness of 3ϕ-ACOPF solutions in a vicinity. This problem can be tackled by deriving a formal proof for the decentralized formulation convergence and an analysis of the quality of the resulting optimum. These

kinds of problems are in a very early stage, being the studies on three-phase power flow in (Sur and Sarkar, 2017; Wang et al., 2017a) the only researches closest to the topic. Another interesting starting point would be to come with algorithms that improve the computation efficiency of the projection step.

- Described formulation applies a pure form of the scaled ADMM to solve the 3ϕ-ACOPF, i.e., all the problem constraints are included in the projection step. This is done to have a clear way to compare the convex centralized and decentralized formulations. However, most researches include system constraints in each step. Departing from the pure form and including DER constraints in the proximal optimization step would lead to a more realistic approach for implementing decentralized DER controls in ADNs. Now, observe that local computation power may be limited, therefore, to avoid negative impacts in the computation times, closed forms of the proximal optimization problems should be derived.

- Decomposing the projection step up to the node level is impractical, instead, a few network partitions must be defined in order to operate the distribution network. However, even with few partitions, the information exchange when implementing an asynchronous DER control strategy could represent an important burden if done carelessly. One possible solution is to limit the information exchange only when there is a change in the network state. Of course, this implies to define such states, what it is considered as a change and to adjust the system parameter to assure that even with this low information exchange the problem converges fast enough to the desired answer (Wan and Lemmon, 2010, 2009).

- Including other energy carriers in the distribution network open the possibility to optimize not only the electricity use but also the thermal energy use. Under this scenario, integer variables may be needed, and although current software can solve mixed-integer QCP, to derive a mixed-integer model that is computationally efficient is not a trivial task. The goal here would be to find the convex hull for the mixed-integer problem, and although it would be useful for network optimal operation, it also would open the path for stochastic and robust planning and operation.

Bibliografic references

A

Frank Ackerman and Lisa Heinzerling. Pricing the priceless: Cost-benefit analysis of environmental protection. *University of Pennsylvania Law Review*, 150(5):1553–1584, 2002. ISSN 00419907. URL http://www.jstor.org/stable/3312947.

H. Ahmadi, J. R. MartíÂ, and A. von Meier. A linear power flow formulation for three-phase distribution systems. *IEEE Transactions on Power Systems*, 31(6):5012–5021, Nov 2016. ISSN 0885-8950. doi: 10.1109/TPWRS.2016.2533540.

Ayed A. S. Algarni. *Operational and Planning Aspects of Distribution Systems in Deregulated Electricity Markets*. PhD thesis, Electrical and Computer Engineering, 2009.

R.N. Anderson, A. Boulanger, W.B. Powell, and W. Scott. Adaptive stochastic control for the smart grid. *Proceedings of the IEEE*, 99(6):1098–1115, 6 2011. ISSN 0018-9219. doi: 10.1109/JPROC.2011.2109671.

L. R. Araujo, D. R. R. Penido, S. Carneiro, and J. L. R. Pereira. A three-phase optimal power-flow algorithm to mitigate voltage unbalance. *IEEE Transactions on Power Delivery*, 28(4):2394–2402, Oct 2013. ISSN 0885-8977. doi: 10.1109/TPWRD.2013.2261095.

B

S. Bahramirad, A. Khodaei, and R. Masiello. Distribution markets. *IEEE Power and Energy Magazine*, 14(2):102–106, March 2016. ISSN 1540-7977. doi: 10.1109/MPE.2016.2543121.

Ambarnath Banerji, Debasmita Sen, Ayan K. Bera, Debtanu Ray, Debjyoti Paul, Anurag Bhakat, and Sujit K. Biswas. Microgrid: A review. In *Global Humanitarian Technology Conference: South Asia Satellite (GHTC-SAS), 2013 IEEE*, pages 27–35, 2013. doi: 10.1109/GHTC-SAS.2013.6629883.

A.K. Basu, S. Chowdhury, and S. P. Chowdhury. Operational management of chp-based microgrid. In *Power System Technology (POWERCON), 2010 International Conference on*, pages 1–5, 2010. doi: 10.1109/POWERCON.2010.5666084.

Ashoke Kumar Basu, S.P. Chowdhury, S. Chowdhury, and S. Paul. Microgrids: Energy management by strategic deployment of der – a comprehensive survey. *Renewable and Sustainable Energy Reviews*, 15(9):4348 – 4356, 2011. ISSN 1364-0321. doi: http://dx.doi.org/10.1016/j.rser.2011.07.116. URL http://www.sciencedirect.com/science/article/pii/S1364032111003637.

N. Bazmohammadi, A. Karimpour, and S. Bazmohammadi. Optimal operation management of a microgrid based on mopso and differential evolution algorithms. In *Smart Grids (ICSG), 2012 2nd Iranian Conference on*, pages 1–6, 2012.

M. Bazrafshan and N. Gatsis. Decentralized Stochastic Optimal Power Flow in Radial Networks with Distributed Generation. *ArXiv e-prints*, January 2016.

S.N. Bhaskara and B.H. Chowdhury. Microgrids a review of modeling, control, protection, simulation and future potential. In *Power and Energy Society General Meeting, 2012 IEEE*, pages 1–7, 2012. doi: 10.1109/PESGM.2012.6345694.

G. Binetti, A. Davoudi, F. L. Lewis, D. Naso, and B. Turchiano. Distributed consensus-based economic dispatch with transmission losses. *IEEE Transactions on Power Systems*, 29 (4):1711–1720, July 2014. ISSN 0885-8950. doi: 10.1109/TPWRS.2014.2299436.

Steven W. Blume. *Electric Power System Basics*. IEEE Press, 2007.

R.H. Bordini, J.F. Hubner, and M. Wooldridge. *Programming Multi-Agent Systems in AgentSpeak using Jason*. Wiley Series in Agent Technology. Wiley, 2007. ISBN 9780470061831. URL http://books.google.com.co/books?id=AJHD4GkIQs0C.

A. Borghetti, M. Bosetti, S. Grillo, S. Massucco, C. A. Nucci, M. Paolone, and F. Silvestro. Short-term scheduling and control of active distribution systems with high penetration of renewable resources. *IEEE Systems Journal*, 4(3):313–322, Sept 2010. ISSN 1932-8184. doi: 10.1109/JSYST.2010.2059171.

Stephen Boyd and Lieven Vandenberghe. *Convex Optimization*. Cambridge University Press, 2009. URL https://www.stanford.edu/~boyd/cvxbook/bv_cvxbook.pdf.

Stephen Boyd, Neal Parikh, Eric Chu, Borja Peleato, and Jonathan Eckstein. Distributed optimization and statistical learning via the alternating direction method of multipliers. *Foundations and Trends in Optimization*, 3(1):1–122, 2010.

Richard E. Brown. *Electric Power Distribution Reliability*. CRC Press, 2009.

S. Bruno, S. Lamonaca, G. Rotondo, U. Stecchi, and M. La Scala. Unbalanced three-phase optimal power flow for smart grids. *Industrial Electronics, IEEE Transactions on*, 58 (10):4504–4513, Oct 2011. ISSN 0278-0046. doi: 10.1109/TIE.2011.2106099.

C

Working Group C6.11. Development and operation of active distribution networks. Technical report, CIGRE, 2011.

Working Group C6.19. Planning and optimization methods for active distribution systems. Technical report, CIGRE, 2014.

Working Group C6.24. Capacity of distribution feeders for hosting der. Technical report, CIGRE, 2014.

Florin Capitanescu. Critical review of recent advances and further developments needed in ac optimal power flow. *Electric Power Systems Research*, 136:57 – 68, 2016. ISSN 0378-7796. doi: http://dx.doi.org/10.1016/j.epsr.2016.02.008. URL http://www.sciencedirect.com/science/article/pii/S0378779616300141.

A. Castillo, C. Laird, C. A. Silva-Monroy, J. P. Watson, and R. P. O'Neill. The unit commitment problem with ac optimal power flow constraints. *IEEE Transactions on Power Systems*, PP(99):1–14, 2016a. ISSN 0885-8950. doi: 10.1109/TPWRS.2015.2511010.

A. Castillo, P. Lipka, J. P. Watson, S. S. Oren, and R. P. O'Neill. A successive linear programming approach to solving the iv-acopf. *IEEE Transactions on Power Systems*, 31(4):2752–2763, July 2016b. ISSN 0885-8950. doi: 10.1109/TPWRS.2015.2487042.

S. Chakraborty and M.G. Simoes. Pv-microgrid operational cost minimization by neural forecasting and heuristic optimization. In *Industry Applications Society Annual Meeting, 2008. IAS '08. IEEE*, pages 1–8, 2008. doi: 10.1109/08IAS.2008.147.

Chen Changsong, Duan Shanxu, Cai Tao, Liu Bangyin, and Yin Jinjun. Energy trading model for optimal microgrid scheduling based on genetic algorithm. In *Power Electronics and Motion Control Conference, 2009. IPEMC '09. IEEE 6th International*, pages 2136–2139, 2009. doi: 10.1109/IPEMC.2009.5157753.

A. Chaouachi, R.M. Kamel, R. Andoulsi, and K. Nagasaka. Multiobjective intelligent energy management for a microgrid. *Industrial Electronics, IEEE Transactions on*, 60(4):1688–1699, 2013. ISSN 0278-0046. doi: 10.1109/TIE.2012.2188873.

Liang Che, M. E. Khodayar, and M. Shahidehpour. Adaptive protection system for microgrids: Protection practices of a functional microgrid system. *IEEE Electrification Magazine*, 2 (1):66–80, March 2014. ISSN 2325-5897. doi: 10.1109/MELE.2013.2297031.

C. Chen, S. Duan, T. Cai, B. Liu, and G. Hu. Smart energy management system for optimal microgrid economic operation. *Renewable Power Generation, IET*, 5(3):258–267, 2011. ISSN 1752-1416. doi: 10.1049/iet-rpg.2010.0052.

S. Chowdhury, S.P. Chowdhury, and P. Crossley. *Microgrids and Active Distribution Networks*. The Institution of Engineering and Technology, 2009.

Konstantina Christakou, Dan-Cristian Tomozei, Jean-Yves Le Boudec, and Mario Paolone. Ac opf in radial distribution networks. part ii: An augmented lagrangian-based opf algorithm, distributable via primal decomposition. *Electric Power Systems Research*, 150:24–35, 2017a. ISSN 0378-7796. doi: https://doi.org/10.1016/j.epsr.2017.04.028. URL http://www.sciencedirect.com/science/article/pii/S0378779617301827.

Konstantina Christakou, Dan-Cristian Tomozei, Jean-Yves Le Boudec, and Mario Paolone. Ac opf in radial distribution networks - part i: On the limits of the branch flow convexification and the alternating direction method of multipliers. *Electric Power Systems Research*, 143:438–450, 2017b. ISSN 0378-7796. doi: https://doi.org/10.1016/j.epsr.2016.07.030. URL http://www.sciencedirect.com/science/article/pii/S0378779616304758.

C. Coffrin, H. L. Hijazi, and P. Van Hentenryck. The qc relaxation: A theoretical and computational study on optimal power flow. *IEEE Transactions on Power Systems*, 31 (4):3008–3018, July 2016. ISSN 0885-8950. doi: 10.1109/TPWRS.2015.2463111.

C.M. Colson and M.H. Nehrir. A review of challenges to real-time power management of microgrids. In *Power Energy Society General Meeting, 2009. PES '09. IEEE*, pages 1–8, 2009. doi: 10.1109/PES.2009.5275343.

C.M. Colson and M.H. Nehrir. Comprehensive real-time microgrid power management and control with distributed agents. *Smart Grid, IEEE Transactions on*, 4(1):617–627, 2013. ISSN 1949-3053. doi: 10.1109/TSG.2012.2236368.

C.M. Colson, M.H. Nehrir, R.K. Sharma, and B. Asghari. Improving sustainability of hybrid energy systems part ii: Managing multiple objectives with a multiagent system, 2013a. ISSN 1949-3029.

C.M. Colson, M.H. Nehrir, R.K. Sharma, and B. Asghari. Improving sustainability of hybrid energy systems part i: Incorporating battery round-trip efficiency and operational cost factors. *Sustainable Energy, IEEE Transactions on*, PP(99):1–9, 2013b. ISSN 1949-3029. doi: 10.1109/TSTE.2013.2269318.

A.J. Conejo, E. Castillo, R. Minguez, and R. Garcia-Bertrand. *Decomposition Techniques in Mathematical Programming: Engineering and Science Applications*. Springer, 2006. ISBN 9783540276852.

Paulo Moises Costa, Manuel A. Matos, and J.A. Pecas Lopes. Regulation of microgeneration and microgrids. *Energy Policy*, 36(10):3893 – 3904, 2008. ISSN 0301-4215. doi: http://dx.doi.org/10.1016/j.enpol.2008.07.013. URL http://www.sciencedirect.com/science/article/pii/S0301421508003601.

P.M. Costa and M.A. Matos. Economic analysis of microgrids including reliability aspects. In *Probabilistic Methods Applied to Power Systems, 2006. PMAPS 2006. International Conference on*, pages 1–8, 2006. doi: 10.1109/PMAPS.2006.360236.

D

E. Dall'Anese and A. Simonetto. Optimal power flow pursuit. *IEEE Transactions on Smart Grid*, 9(2):942–952, March 2018. ISSN 1949-3053. doi: 10.1109/TSG.2016.2571982.

E. Dall'Anese, Hao Zhu, and G.B. Giannakis. Distributed optimal power flow for smart microgrids. *Smart Grid, IEEE Transactions on*, 4(3):1464–1475, Sept 2013. ISSN 1949-3053. doi: 10.1109/TSG.2013.2248175.

Francisco Diaz-Gonzalez, Andreas Sumper, Oriol Gomis-Bellmunt, and Roberto Villafafila-Robles. A review of energy storage technologies for wind power applications. *Renewable and Sustainable Energy Reviews*, 16(4):2154 – 2171, 2012. ISSN 1364-0321. doi: https://doi.org/10.1016/j.rser.2012.01.029. URL http://www.sciencedirect.com/science/article/pii/S1364032112000305.

M.J. Dolan, E.M. Davidson, G.W. Ault, K.R.W. Bell, and S.D.J. McArthur. Distribution power flow management utilizing an online constraint programming method. *Smart Grid, IEEE Transactions on*, 4(2):798–805, June 2013. ISSN 1949-3053. doi: 10.1109/TSG.2012.2234148.

E

F.Y.S. Eddy and H. B. Gooi. Multi-agent system for optimization of microgrids. In *Power Electronics and ECCE Asia (ICPE ECCE), 2011 IEEE 8th International Conference on*, pages 2374–2381, 2011. doi: 10.1109/ICPE.2011.5944510.

T. Erseghe. Distributed optimal power flow using admm. *Power Systems, IEEE Transactions on*, 29(5):2370–2380, Sept 2014. ISSN 0885-8950. doi: 10.1109/TPWRS.2014.2306495.

F

F. Farahmand, T. Khandelwal, J. J. Dai, and F. Shokooh. An enterprise approach to the interactive objectives and constraints of smart grids. In *Innovative Smart Grid Technologies - Middle East (ISGT Middle East), 2011 IEEE PES Conference on*, pages 1–6, 2011. doi: 10.1109/ISGT-MidEast.2011.6220790.

M. Fathi and H. Bevrani. Adaptive energy consumption scheduling for connected microgrids under demand uncertainty. *Power Delivery, IEEE Transactions on*, 28(3):1576–1583, 2013. ISSN 0885-8977. doi: 10.1109/TPWRD.2013.2257877.

P. D. F. Ferreira, P. M. S. Carvalho, L. A. F. M. Ferreira, and M. D. Ilic. Distributed energy resources integration challenges in low-voltage networks: Voltage control limitations and risk of cascading. *IEEE Transactions on Sustainable Energy*, 4(1):82–88, Jan 2013. ISSN 1949-3029. doi: 10.1109/TSTE.2012.2201512.

J. F. Franco, M. J. Rider, and R. Romero. A mixed-integer linear programming model for the electric vehicle charging coordination problem in unbalanced electrical distribution systems. *IEEE Transactions on Smart Grid*, 6(5):2200–2210, Sept 2015. ISSN 1949-3053. doi: 10.1109/TSG.2015.2394489.

G

S.A. Gabriel, A.J. Conejo, J.D. Fuller, B.F. Hobbs, and C Ruiz. *Complementarity Modeling in Energy Markets*. Springer, 2012.

Elvis Eduardo Gaona, Tatiana Morales, César Leaonardo Trujillo, and Francisco Santamaría. Esquemas de transmisión de datos en una microrred a través de una infraestructura de medición avanzada. *Revista UIS ingenierías*, 15(2), 2016.

P. A. N. Garcia, J. L. R. Pereira, S. Carneiro, V. M. da Costa, and N. Martins. Three-phase power flow calculations using the current injection method. *IEEE Transactions on Power Systems*, 15(2):508–514, May 2000. ISSN 0885-8950. doi: 10.1109/59.867133.

D.L. Gazzoni, I. Azurdia, G. Blanco, C.A. Estrada, and I. de C. Macedo. Sustainable energy in latin america and the caribbean: Potential for the future. Technical report, International Council for Science, Regional Office for Latin America and the Caribbean, 2010.

H. Gharavi, H. H. Chen, and C. Wietfeld. Guest editorial special section on cyber-physical systems and security for smart grid. *IEEE Transactions on Smart Grid*, 6(5):2405–2408, Sept 2015. ISSN 1949-3053. doi: 10.1109/TSG.2015.2464911.

H. A. Gil and G. Joos. Models for quantifying the economic benefits of distributed generation. *IEEE Transactions on Power Systems*, 23(2):327–335, May 2008. ISSN 0885-8950. doi: 10.1109/TPWRS.2008.920718.

S. Gill, I. Kockar, and G.W. Ault. Dynamic optimal power flow for active distribution networks. *Power Systems, IEEE Transactions on*, 29(1):121–131, Jan 2014. ISSN 0885-8950. doi: 10.1109/TPWRS.2013.2279263.

Antonio Gomez-Exposito, Antonio J. Conejo, and Claudio A. Canizares. *Electric Energy Systems Analysis and Operation*. CRC Press, 2018.

Michael Grant, Stephen Boyd, and Yinyu Ye. *Global Optimization: From Theory to Implementation*, chapter Disciplined Convex Programming, pages 155–210. Springer, 2006.

S. S. Guggilam, E. Dall'Anese, Y. C. Chen, S. V. Dhople, and G. B. Giannakis. Scalable optimization methods for distribution networks with high pv integration. *IEEE Transactions on Smart Grid*, 7(4):2061–2070, July 2016. ISSN 1949-3053. doi: 10.1109/TSG.2016.2543264.

H

A. Hooshmand, B. Asghari, and R. Sharma. A novel cost-aware multi-objective energy management method for microgrids. In *Innovative Smart Grid Technologies (ISGT), 2013 IEEE PES*, pages 1–6, 2013. doi: 10.1109/ISGT.2013.6497882.

M. I. Hossain, R. Yan, and T. K. Saha. Investigation of the interaction between step voltage regulators and large-scale photovoltaic systems regarding voltage regulation and unbalance. *IET Renewable Power Generation*, 10(3):299–309, 2016. ISSN 1752-1416. doi: 10.1049/iet-rpg.2015.0086.

Zechun Hu and Furong Li. Cost-benefit analyses of active distribution network management, part i: Annual benefit analysis. *Smart Grid, IEEE Transactions on*, 3(3):1067–1074, 2012a. ISSN 1949-3053. doi: 10.1109/TSG.2012.2205412.

Zechun Hu and Furong Li. Cost-benefit analyses of active distribution network management, part ii: Investment reduction analysis. *Smart Grid, IEEE Transactions on*, 3(3):1075–1081, 2012b. ISSN 1949-3053. doi: 10.1109/TSG.2011.2177869.

S. Huang, Q. Wu, J. Wang, and H. Zhao. A sufficient condition on convex relaxation of ac optimal power flow in distribution networks. *IEEE Transactions on Power Systems*, PP (99):1–1, 2016. ISSN 0885-8950. doi: 10.1109/TPWRS.2016.2574805.

I

IEC. Testing and measurement techniques – Power quality measurement methods. 61000.4.30: Electromagnetic compatibility (EMC), February 2015. URL https://webstore.iec.ch/publication/22270.

J

Q. Y. Jiang, H. D. Chiang, C. X. Guo, and Y. J. Cao. Power-current hybrid rectangular formulation for interior-point optimal power flow. *IET Generation, Transmission Distribution*, 3(8):748–756, August 2009. ISSN 1751-8687. doi: 10.1049/iet-gtd.2008.0509.

K

H. Kanchev, D. Lu, B. Francois, and V. Lazarov. Smart monitoring of a microgrid including gas turbines and a dispatched pv-based active generator for energy management and emissions reduction. In *Innovative Smart Grid Technologies Conference Europe (ISGT Europe), 2010 IEEE PES*, pages 1–8, 2010. doi: 10.1109/ISGTEUROPE.2010.5638875.

Hyun-Koo Kang, Il-Yop Chung, and Seung-Il Moon. Coordination strategy for harmonic compensation using multiple distributed resources. In *Power and Energy Society General Meeting, 2012 IEEE*, pages 1–7, 2012. doi: 10.1109/PESGM.2012.6344671.

R. Karki, S. Thapa, and R. Billinton. A simplified risk-based method for short-term wind power commitment. *Sustainable Energy, IEEE Transactions on*, 3(3):498–505, 2012. ISSN 1949-3029. doi: 10.1109/TSTE.2012.2190999.

F. Katiraei, R. Iravani, N. Hatziargyriou, and A. Dimeas. Microgrids management. *Power and Energy Magazine, IEEE*, 6(3):54–65, May 2008. ISSN 1540-7977. doi: 10.1109/MPE.2008.918702.

W. H. Kersting. Radial distribution test feeders. In *2001 IEEE Power Engineering Society Winter Meeting. Conference Proceedings (Cat. No.01CH37194)*, volume 2, pages 908–912 vol.2, 2001. doi: 10.1109/PESW.2001.916993.

H. Kirkham, D. Nightingale, and T. Koerner. Energy management system design with dispersed storage and generation. *Power Apparatus and Systems, IEEE Transactions on*, PAS-100(7):3432–3441, 1981. ISSN 0018-9510. doi: 10.1109/TPAS.1981.316686.

D.S. Kirschen and G. Strbac. *Power System Economics*. Jhon Wiley & Sons, 2004.

A. L. Kulasekera, R. A. R. C. Gopura, K. T. M. U. Hemapala, and N. Perera. A review on multi-agent systems in microgrid applications. In *ISGT2011-India*, pages 173–177, Dec 2011. doi: 10.1109/ISET-India.2011.6145377.

L

H. J. Laaksonen. Protection principles for future microgrids. *IEEE Transactions on Power Electronics*, 25(12):2910–2918, Dec 2010. ISSN 0885-8993. doi: 10.1109/TPEL.2010.2066990.

H. Landreth and D.C. Colander. *History of Economic Thought*. Houghton Mifflin, 2002. ISBN 9780618133949.

R.H. Lasseter. Microgrids. In *Power Engineering Society Winter Meeting, 2002. IEEE*, volume 1, pages 305–308 vol.1, 2002. doi: 10.1109/PESW.2002.985003.

J. Lavaei, D. Tse, and Baosen Zhang. Geometry of power flows and optimization in distribution networks. *Power Systems, IEEE Transactions on*, 29(2):572–583, March 2014. ISSN 0885-8950. doi: 10.1109/TPWRS.2013.2282086.

B.C. Lesieutre, D.K. Molzahn, A.R. Borden, and C.L. DeMarco. Examining the limits of the application of semidefinite programming to power flow problems. In *Communication, Control, and Computing (Allerton), 2011 49th Annual Allerton Conference on*, pages 1492–1499, Sept 2011. doi: 10.1109/Allerton.2011.6120344.

P. Li, H. Ji, C. Wang, J. Zhao, G. Song, F. Ding, and J. Wu. Optimal operation of soft open points in active distribution networks under three-phase unbalanced conditions. *IEEE Transactions on Smart Grid*, PP(99):1–1, 2017. ISSN 1949-3053. doi: 10.1109/TSG.2017.2739999.

H. Z. Liang and H.B. Gooi. Unit commitment in microgrids by improved genetic algorithm. In *IPEC, 2010 Conference Proceedings*, pages 842–847, 2010. doi: 10.1109/IPECON.2010.5697083.

H. Liao and J. V. Milanovic. Methodology for the analysis of voltage unbalance in networks with single-phase distributed generation. *IET Generation, Transmission Distribution*, 11(2):550–559, 2017. ISSN 1751-8687. doi: 10.1049/iet-gtd.2016.1155.

Y. Liu, J. Li, L. Wu, and T. Ortmeyer. Chordal relaxation based acopf for unbalanced distribution systems with ders and voltage regulation devices. *IEEE Transactions on Power Systems*, 33(1):970–984, Jan 2018. ISSN 0885-8950. doi: 10.1109/TPWRS.2017.2707564.

T. Logenthiran, D. Srinivasan, A.M. Khambadkone, and Htay Nwe Aung. Multiagent system for real-time operation of a microgrid in real-time digital simulator. *Smart Grid, IEEE Transactions on*, 3(2):925–933, 2012. ISSN 1949-3053. doi: 10.1109/TSG.2012.2189028.

J.A. Pecas Lopes, N. Hatziargyriou, J. Mutale, P. Djapic, and N. Jenkins. Integrating distributed generation into electric power systems: A review of drivers, challenges and opportunities. *Electric Power Systems Research*, 77(9):1189 – 1203, 2007. ISSN 0378-7796. doi: http://dx.doi.org/10.1016/j.epsr.2006.08.016. URL http://www.sciencedirect.com/science/article/pii/S0378779606001908. Distributed Generation.

E. Loukarakis, J. Bialek, and C. Dent. Investigation of maximum possible opf problem decomposition degree for decentralized energy markets. In *Power Energy Society General Meeting, 2015 IEEE*, pages 1–1, July 2015a. doi: 10.1109/PESGM.2015.7285815.

E. Loukarakis, C.J. Dent, and J.W. Bialek. Decentralized multi-period economic dispatch for real-time flexible demand management. *Power Systems, IEEE Transactions on*, PP(99): 1–13, 2015b. ISSN 0885-8950. doi: 10.1109/TPWRS.2015.2402518.

S. Low, D. Gayme, and U. Topcu. Convexifying optimal power flow: Recent advances in opf solution methods. In *American Control Conference (ACC), 2013*, pages 5245–5245, June 2013.

M

R. Madani, S. Sojoudi, and J. Lavaei. Convex relaxation for optimal power flow problem: Mesh networks. *IEEE Transactions on Power Systems*, 30(1):199–211, Jan 2015. ISSN 0885-8950. doi: 10.1109/TPWRS.2014.2322051.

R. Madani, M. Ashraphijuo, and J. Lavaei. Promises of conic relaxation for contingency-constrained optimal power flow problem. *IEEE Transactions on Power Systems*, 31(2): 1297–1307, March 2016. ISSN 0885-8950. doi: 10.1109/TPWRS.2015.2411391.

T.S. Mahmoud, D. Habibi, and O. Bass. Fuzzy logic for smart utilisation of storage devices in a typical microgrid. In *Renewable Energy Research and Applications (ICRERA), 2012 International Conference on*, pages 1–6, 2012. doi: 10.1109/ICRERA.2012.6477333.

Arthur Mazer. *Electric Power Planning for Regulated and Deregulated Markets*. IEEE Press, 2007.

S.D.J. McArthur, E.M. Davidson, V.M. Catterson, A.L. Dimeas, N.D. Hatziargyriou, F. Ponci, and T. Funabashi. Multi-agent systems for power engineering applications; part i: Concepts, approaches, and technical challenges. *Power Systems, IEEE Transactions on*, 22(4):1743 –1752, nov. 2007a. ISSN 0885-8950. doi: 10.1109/TPWRS.2007.908471.

S.D.J. McArthur, E.M. Davidson, V.M. Catterson, A.L. Dimeas, N.D. Hatziargyriou, F. Ponci, and T. Funabashi. Multi-agent systems for power engineering applications; part ii: Technologies, standards, and tools for building multi-agent systems. *Power Systems, IEEE Transactions on*, 22(4):1753 –1759, nov. 2007b. ISSN 0885-8950. doi: 10.1109/TPWRS.2007.908472.

Mao Meiqin, Ji Meihong, Dong Wei, and Liuchen Chang. Multi-objective economic dispatch model for a microgrid considering reliability. In *Power Electronics for Distributed Generation Systems (PEDG), 2010 2nd IEEE International Symposium on*, pages 993–998, 2010. doi: 10.1109/PEDG.2010.5545765.

V.H. Méndez, J. Rivier, J.I. de la Fuente, T. Gómez, J. Arceluz, J. Marín, and A. Madurga. Impact of distributed generation on distribution investment deferral. *International Journal of Electrical Power & Energy Systems*, 28(4):244 – 252, 2006. ISSN 0142-0615. doi: http://dx.doi.org/10.1016/j.ijepes.2005.11.016. URL http://www.sciencedirect.com/science/article/pii/S0142061505001511.

F. Meng, B. Chowdhury, and M. Chamana. Three-phase optimal power flow for market-based control and optimization of distributed generations. *IEEE Transactions on Smart Grid*, PP(99):1–1, 2017. ISSN 1949-3053. doi: 10.1109/TSG.2016.2638963.

Sleiman Mhanna, Archie C. Chapman, and Gregor Verbic. Component-based dual decomposition methods for the opf problem. *Sustainable Energy, Grids and Networks*, 16: 91 – 110, 2018. ISSN 2352-4677. doi: https://doi.org/10.1016/j.segan.2018.04.003. URL http://www.sciencedirect.com/science/article/pii/S2352467718300389.

Kaisa Miettinen. *Nonlinear Multiobjective Optimization.* Kluwer Academic Publishers, Operations Research and Management Science, 1999.

J. Mitra, S.B. Patra, and S.J. Ranade. Reliability stipulated microgrid architecture using particle swarm optimization. In *Probabilistic Methods Applied to Power Systems, 2006. PMAPS 2006. International Conference on*, pages 1–7, 2006. doi: 10.1109/PMAPS.2006.360256.

G.Y. Morris, C. Abbey, S. Wong, and G. Joos. Evaluation of the costs and benefits of microgrids with consideration of services beyond energy supply. In *Power and Energy Society General Meeting, 2012 IEEE*, pages 1–9, 2012. doi: 10.1109/PESGM.2012.6345380.

H. Mortazavi, H. Mehrjerdi, M. Saad, S. Lefebvre, D. Asber, and L. Lenoir. A monitoring technique for reversed power flow detection with high pv penetration level. *IEEE Transactions on Smart Grid*, 6(5):2221–2232, Sept 2015. ISSN 1949-3053. doi: 10.1109/TSG.2015.2397887.

O

P. Oliveira, T. Pinto, I. Praca, Z. Vale, and H. Morais. Intelligent micro grid management using a multi-agent approach. In *PowerTech (POWERTECH), 2013 IEEE Grenoble*, pages 1–6, 2013. doi: 10.1109/PTC.2013.6652263.

P

R. Palma-Behnke, C. Benavides, F. Lanas, B. Severino, L. Reyes, J. Llanos, and D. Saez. A microgrid energy management system based on the rolling horizon strategy. *Smart Grid, IEEE Transactions on*, 4(2):996–1006, 2013. ISSN 1949-3053. doi: 10.1109/TSG.2012.2231440.

Neal Parikh and Stephen Boyd. Proximal Algorithms. *Foundations and Trends in Optimization*, 1(3):123–231, 2013.

A. Parisio and L. Glielmo. Multi-objective optimization for environmental/economic microgrid scheduling. In *Cyber Technology in Automation, Control, and Intelligent Systems (CYBER), 2012 IEEE International Conference on*, pages 17–22, 2012. doi: 10.1109/CYBER.2012.6392519.

Yong Peng, Shun Tao, Qun Xu, and Xiangning Xiao. Harmonic pricing model based on harmonic costs and harmonic current excessive penalty. In *Artificial Intelligence, Management Science and Electronic Commerce (AIMSEC), 2011 2nd International Conference on*, pages 4011–4014, 2011. doi: 10.1109/AIMSEC.2011.6009892.

D. R. R. Penido, L. R. de Araujo, S. Carneiro, J. L. R. Pereira, and P. A. N. Garcia. Three-phase power flow based on four-conductor current injection method for unbalanced distribution networks. *IEEE Transactions on Power Systems*, 23(2):494–503, May 2008. ISSN 0885-8950. doi: 10.1109/TPWRS.2008.919423.

Ignacio Perez-Arriaga, Christopher Knittel, Raanan Miller, and Richard Tabors. Utility of the Future. Technical report, MIT energy institute and IIT-Comillas, 2016.

R. Perman. *Natural Resource and Environmental Economics*. Pearson Education, 2003. ISBN 9780273655596. URL http://books.google.com.co/books?id=BtFEUHZMGDwC.

M. Pipattanasomporn, H. Feroze, and S. Rahman. Multi-agent systems in a distributed smart grid: Design and implementation. In *Power Systems Conference and Exposition, 2009. PSCE '09. IEEE/PES*, pages 1 –8, march 2009. doi: 10.1109/PSCE.2009.4840087.

J.F. Prada. The value of reliability in power systems: Pricing operating reserves. Technical report, Energy Laboratory, Massachusetts Institute of Technology, june 1999.

Danny Pudjianto, Elias Zafiropoulos, and L. Daoutis. Methodology for quantifying economic and environmental benefits of microgrids. Technical report, Large scale integration of microgrids to low voltage grids, deliverable DG4, 2005.

Q

V. H. M. Quezada, J. R. Abbad, and T. G. S. Roman. Assessment of energy distribution losses for increasing penetration of distributed generation. *IEEE Transactions on Power Systems*, 21(2):533–540, May 2006. ISSN 0885-8950. doi: 10.1109/TPWRS.2006.873115.

R

Fenghui Ren, Minjie Zhang, and D. Sutanto. A multi-agent solution to distribution system management by considering distributed generators. *Power Systems, IEEE Transactions on*, 28(2):1442–1451, 2013. ISSN 0885-8950. doi: 10.1109/TPWRS.2012.2223490.

B.A. Robbins and A.D. Dominguez-Garcia. Optimal reactive power dispatch for voltage regulation in unbalanced distribution systems. *Power Systems, IEEE Transactions on*, PP(99):1–11, 2015. ISSN 0885-8950. doi: 10.1109/TPWRS.2015.2451519.

R. Roche, B. Blunier, A. Miraoui, V. Hilaire, and A. Koukam. Multi-agent systems for grid energy management: A short review. In *IECON 2010 - 36th Annual Conference on IEEE Industrial Electronics Society*, pages 3341 –3346, nov. 2010. doi: 10.1109/IECON.2010.5675295.

A.C. Rueda-Medina and A. Padilha-Feltrin. Pricing of reactive power support provided by distributed generators in transmission systems. In *PowerTech, 2011 IEEE Trondheim*, pages 1–7, 2011. doi: 10.1109/PTC.2011.6019300.

S

W. Saad, Zhu Han, H.V. Poor, and T. Basar. Game-theoretic methods for the smart grid: An overview of microgrid systems, demand-side management, and smart grid communications. *Signal Processing Magazine, IEEE*, 29(5):86–105, Sept 2012. ISSN 1053-5888. doi: 10.1109/MSP.2012.2186410.

H. Saboori, M. Mohammadi, and R. Taghe. Virtual power plant (vpp), definition, concept, components and types. In *2011 Asia-Pacific Power and Energy Engineering Conference*, pages 1–4, March 2011. doi: 10.1109/APPEEC.2011.5749026.

M. Salani, A. Giusti, Gianni Di Caro, A.-E. Rizzoli, and L.M. Gambardella. Lexicographic multi-objective optimization for the unit commitment problem and economic dispatch in a microgrid. In *Innovative Smart Grid Technologies (ISGT Europe), 2011 2nd IEEE PES International Conference and Exhibition on*, pages 1–8, 2011. doi: 10.1109/ISGTEurope.2011.6162806.

B.R. Sathyanarayana and G.T. Heydt. Sensitivity-based pricing and optimal storage utilization in distribution systems. *Power Delivery, IEEE Transactions on*, 28(2):1073–1082, 2013. ISSN 0885-8977. doi: 10.1109/TPWRD.2012.2230192.

Yoshikazu Sawaragi, Hirotaka Nakayama, and Tetsuzo Tanino. *Theory of Multiobjective Optimization*. Academic Press, Inc., 1985.

Christine Schwaegerl, Ling Tao, Joao Pecas-Lopes, Andre Madureira, Pierluigi Mancarella, Anestis Anastasiadis, Nikos Hatziargyriou, and Aleksandra Krkoleva. Report on the technical, social, economic, and environmental benefits provided by microgrids on power system operation. Technical report, Advanced Architectures and Control Concepts for More Microgrids, 2009.

Hossein Seifi and Mohammad Sadegh Sepasian. *Electric Power System Planning*. Springer, 2011.

P. Siano, P. Chen, Z. Chen, and A. Piccolo. Evaluating maximum wind energy exploitation in active distribution networks. *Generation, Transmission Distribution, IET*, 4(5):598–608, May 2010. ISSN 1751-8687. doi: 10.1049/iet-gtd.2009.0548.

H. M. Soliman and A. Leon-Garcia. Game-theoretic demand-side management with storage devices for the future smart grid. *IEEE Transactions on Smart Grid*, 5(3):1475–1485, May 2014. ISSN 1949-3053. doi: 10.1109/TSG.2014.2302245.

E. Sortomme and M.A. El-Sharkawi. Optimal power flow for a system of microgrids with controllable loads and battery storage. In *Power Systems Conference and Exposition, 2009. PSCE '09. IEEE/PES*, pages 1–5, 2009. doi: 10.1109/PSCE.2009.4840050.

Standars Coordinating Committee. Interconection and Interoperability of Distributed Energy Resources with Associated Electric Power Systems Interfaces, 2018.

M. Strrelec and J. Berka. Microgrid energy management based on approximate dynamic programming. In *Innovative Smart Grid Technologies Europe (ISGT EUROPE)*, pages 1–5, Oct 2013. doi: 10.1109/ISGTEurope.2013.6695439.

X. Su, M. A. S. Masoum, and P. J. Wolfs. Optimal pv inverter reactive power control and real power curtailment to improve performance of unbalanced four-wire lv distribution networks. *IEEE Transactions on Sustainable Energy*, 5(3):967–977, July 2014. ISSN 1949-3029. doi: 10.1109/TSTE.2014.2313862.

M.J. Sullivan and D.M. Keane. Outage cost estimation guidebook. Technical report, Electric power research institute, 1995.

M.J. Sullivan, M.G. Mercurio, J.A. Schellenberg, and J.H. Eto. How to estimate the value of service reliability improvements. In *Power and Energy Society General Meeting, 2010 IEEE*, pages 1–5, 2010. doi: 10.1109/PES.2010.5589316.

A.X. Sun, D.T. Phan, and S. Ghosh. Fully decentralized ac optimal power flow algorithms. In *Power and Energy Society General Meeting (PES), 2013 IEEE*, pages 1–5, July 2013. doi: 10.1109/PESMG.2013.6672864.

U. Sur and G. Sarkar. A sufficient condition for multiple load flow solutions existence in three phase unbalanced active distribution networks. *IEEE Transactions on Circuits and Systems II: Express Briefs*, 65(6):784–788, June 2017. ISSN 1549-7747. doi: 10.1109/TCSII.2017.2751542.

T

P. J. Talacek and N. R. Watson. Marginal pricing of harmonic injections. *Power Engineering Review, IEEE*, 22(1):68–68, 2002a. ISSN 0272-1724. doi: 10.1109/MPER.2002.4311676.

P.J. Talacek and N.R. Watson. Marginal pricing of harmonic injections. *Power Systems, IEEE Transactions on*, 17(1):50–56, 2002b. ISSN 0885-8950. doi: 10.1109/59.982192.

Geraldo Leite Torres. *Nonlinear Optimal Power Flow by Interior and Non-Interior Point Methods*. PhD thesis, Electrical and Computer Engineering, 1998.

V

H. Vahedi, R. Noroozian, and S.H. Hosseini. Optimal management of microgrid using differential evolution approach. In *Energy Market (EEM), 2010 7th International Conference on the European*, pages 1–6, 2010. doi: 10.1109/EEM.2010.5558708.

H.R. Varian. *Intermediate Microeconomics: A Modern Approach*. W W Norton & Company Incorporated, 2010. ISBN 9780393934243.

J. Vasiljevska and J. Lopes. On the microgrid and multi microgrid impact assessment: Cost and benefits evaluation. In *Cigre Bologna Symposium*, 2011.

Walter Vergara, Paul Isbell, Ana Rios, José Ramon Gómez, and Leandro Alves. Beneficios para la sociedad de la adopción de fuentes renovables de energía en américa latina y el caribe. Technical report, Banco Interamericano de Desarrollo, División de Cambio Climático y Sostenibilidad, División de Energía, 4 2014.

W

Pu Wan and M.D. Lemmon. Optimal power flow in microgrids using event-triggered optimization. In *American Control Conference (ACC), 2010*, pages 2521–2526, 2010.

Pu Wan and M.D. Lemmon. Distributed network utility maximization using event-triggered augmented lagrangian methods. In *American Control Conference, 2009. ACC '09.*, pages 3298–3303, 2009. doi: 10.1109/ACC.2009.5160088.

C. Wang, A. Bernstein, J. Y. Le Boudec, and M. Paolone. Existence and uniqueness of load-flow solutions in three-phase distribution networks. *IEEE Transactions on Power Systems*, 32(4):3319–3320, July 2017a. ISSN 0885-8950. doi: 10.1109/TPWRS.2016.2623979.

Cheng-Shan Wang, Bo Yu, Jun Xiao, and Li Guo. Multi-scenario, multi-objective optimization of grid-parallel microgrid. In *Electric Utility Deregulation and Restructuring and Power Technologies (DRPT), 2011 4th International Conference on*, pages 1638–1646, 2011. doi: 10.1109/DRPT.2011.5994160.

M. Q. Wang and H.B. Gooi. Effect of uncertainty on optimization of microgrids. In *IPEC, 2010 Conference Proceedings*, pages 711–716, 2010. doi: 10.1109/IPECON.2010.5697018.

W. Wang and N. Yu. Chordal conversion based convex iteration algorithm for three-phase optimal power flow problems. *IEEE Transactions on Power Systems*, PP(99):1–1, 2017. ISSN 0885-8950. doi: 10.1109/TPWRS.2017.2735942.

Y. Wang, N. Zhang, H. Li, J. Yang, and C. Kang. Linear three-phase power flow for unbalanced active distribution networks with pv nodes. *CSEE Journal of Power and Energy Systems*, 3(3):321–324, Sept 2017b. doi: 10.17775/CSEEJPES.2017.00240.

J. D. Watson, N. R. Watson, and I. Lestas. Optimized dispatch of energy storage systems in unbalanced distribution networks. *IEEE Transactions on Sustainable Energy*, PP(99): 1–1, 2017. ISSN 1949-3029. doi: 10.1109/TSTE.2017.2752964.

E. Wei and A. Ozdaglar. On the o(1/k) convergence of asynchronous distributed alternating direction method of multipliers. *Mathematical Programming*, page preprint, 2013. URL http://arxiv.org/abs/1307.8254.

H. Lee Willis. *Power Distribution Planning Reference Book*. Marcel Dekker, 2004.

Michael Wooldridge. *An Introduction to Multiagent Systems*. Jhon Wiley & Sons, 2009.

X

Chun xia Dou, Xing bei Jia, Zhi qian Bo, Fang Zhao, and Dong le Liu. Optimal management of microgrid based on a modified particle swarm optimization algorithm. In *Power and Energy Engineering Conference (APPEEC), 2011 Asia-Pacific*, pages 1–8, 2011. doi: 10.1109/APPEEC.2011.5747690.

Jianxin Xu, Sicong Tan, and S.K. Panda. Optimization of economic load dispatch for a microgrid using evolutionary computation. In *IECON 2011 - 37th Annual Conference on IEEE Industrial Electronics Society*, pages 3192–3197, 2011. doi: 10.1109/IECON.2011.6119821.

Y

H. Yuan, F. Li, Y. Wei, and J. Zhu. Novel linearized power flow and linearized opf models for active distribution networks with application in distribution lmp. *IEEE Transactions on Smart Grid*, 9(1):438–448, Jan 2018. ISSN 1949-3053. doi: 10.1109/TSG.2016.2594814.

Z

A. S. Zamzam, N. D. Sidiropoulos, and E. Dall'Anese. Beyond relaxation and newton-raphson: Solving ac opf for multi-phase systems with renewables. *IEEE Transactions on Smart Grid*, PP(99):1–1, 2017. ISSN 1949-3053. doi: 10.1109/TSG.2016.2645220.

X. P. Zhang, S. G. Petoussis, and K. R. Godfrey. Nonlinear interior-point optimal power flow method based on a current mismatch formulation. *IEE Proceedings - Generation, Transmission and Distribution*, 152(6):795–805, Nov 2005. ISSN 1350-2360. doi: 10.1049/ip-gtd:20050076.

Y. Zhang and G.B. Giannakis. Distributed Stochastic Market Clearing with High-Penetration Wind Power. *ArXiv e-prints*, April 2015.

Yu Zhang, N. Gatsis, and G.B. Giannakis. Robust energy management for microgrids with high-penetration renewables. *Sustainable Energy, IEEE Transactions on*, 4(4):944–953, 2013. ISSN 1949-3029. doi: 10.1109/TSTE.2013.2255135.

Z.J. Zhang and N.-C.C. Nair. Economic and pricing signals in electricity distribution systems: A bibliographic survey. In *Power System Technology (POWERCON), 2012 IEEE International Conference on*, pages 1–6, 2012. doi: 10.1109/PowerCon.2012.6401470.

B. Zhao, X. Zhang, J. Chen, C. Wang, and L. Guo. Operation optimization of standalone microgrids considering lifetime characteristics of battery energy storage system. *Sustainable Energy, IEEE Transactions on*, PP(99):1–10, 2013. ISSN 1949-3029. doi: 10.1109/TSTE.2013.2248400.

Binyan Zhao, Yi Shi, Xiaodai Dong, Wenpeng Luan, and J. Bornemann. Short-term operation scheduling in renewable-powered microgrids: A duality-based approach. *Sustainable Energy, IEEE Transactions on*, 5(1):209–217, Jan 2014. ISSN 1949-3029. doi: 10.1109/TSTE.2013.2279837.

W. Zheng, W. Wu, B. Zhang, H. Sun, and Y. Liu. A fully distributed reactive power optimization and control method for active distribution networks. *Smart Grid, IEEE Transactions on*, 7(2):1021–1033, March 2016. ISSN 1949-3053. doi: 10.1109/TSG.2015.2396493.

Weiye Zheng, Wenchuan Wu, Boming Zhang, Zhigang Li, and Yibing Liu. Fully distributed multi-area economic dispatch method for active distribution networks. *Generation, Transmission Distribution, IET*, 9(12):1341–1351, 2015. ISSN 1751-8687. doi: 10.1049/iet-gtd.2014.0904.

APPENDICES

APPENDIX A

ACTIVE DISTRIBUTION NETWORK BENEFITS

As presented in (Vergara et al., 2014), in this very moment social benefits of local renewable generation compensates any cost disadvantage. Furthermore, Active Distribution Networks (ADNs) can translate economic and energetic efficiency to short/medium term benefits, hence increasing renewable penetration in power distribution systems.

This will solve some of the main problems that prevents local renewable generation to take a bigger share in local energy consumption. Namely there are four main problems (Vergara et al., 2014): generation cost is still too high for some technologies, there is not a common methodology to evaluate benefits, intangible benefits are usually reduced to emission mitigation (thus ignoring social or other kind of environmental benefit), and benefits are analyzed only in local scenarios. To those problems one should add the lack of an "adaptation process of the state-of-the-art technologies to local and regional scenarios" (Gazzoni et al., 2010) which inhibit massification of needed technologies –this is why Gazoni *et al.* recognize this element as a relevant goal for researches on non-conventional renewable energy sources.

This annex presents the benefits that can be captured by introducing an Active Distribution Network operation scheme into a power distribution network, including applicable material from microgrid and distributed generation experiences. First the types of benefits depending on the system participant are described (section A.1), later, some tangible benefits are described (section A.2) –mainly based on (Gil and Joos, 2008; Morris et al., 2012; Costa et al., 2008). This annex closes with a brief discussion on some of the characteristics of the described benefits (section A.3).

Note that benefits here presented are a general overview and not a exhaustive list of all possible price or economic signals that might support Active Distribution System deployment.

Further readings on the topic include: A survey on economic signals for power distribution system in (Zhang and Nair, 2012); A survey on microgrid benefits that may serve as an introduction in (Basu et al., 2011); And the studies in (Schwaegerl et al., 2009; Pudjianto et al., 2005) which offers an extended insight on DERs social-economic benefits.

A.1 Types

Direct benefits of Active Distribution Networks are usually associated with bill reduction and system loss reduction. Consumers benefit from bill reduction and distribution system operator benefits from loss reduction, but by taking advantage of those benefits, they can indirectly capture benefits such as enhanced reliability (for the consumer) and congestion mitigation (for the system operator). With the adequate incentives and property rights, these benefits can yield other benefits by allowing investment deferral, peak shaving and demand bids. Note that a rigorous analysis must be done to avoid speculators overvalue these benefits and to avoid risk adverse stakeholders undervalue them, thus it is important an objective characterization of such benefits. Here, benefits types are described according to the agents involved. Like (Morris et al., 2012) propose, there are four kinds of agents:

The customer is an agent that consumes energy from the system. Its benefits are associated to reduction in energy cost and constant supply of energy.

The independent power producer is an agent that generates energy in the system. Its benefits are associated to selling energy or services based on energy supply through contractual agreements.

The distribution network operator is an agent that assures the energy delivery service in the distribution network. Its benefits are associated to low cost and efficient operation over time.

The external agent is an agent who is outside or partially inside the system. It can be concrete entities like adjacent distribution systems and the power system operator; or it can be abstract entities like society and economy. Its benefits are associated to positive externalities[1] due to efficient operation of the power distribution system.

In (Vasiljevska and Lopes, 2011) is suggested that profit optimization for the independent power producer may lead to an overall optimization. To explore that concept, the independent

[1] From (Perman, 2003, sec. 5.10): «An external effect, or an externality, is said to occur when the production or consumption decisions of one agent have an impact on the utility or profit of another agent in an unintended way [...]».

power producer benefits will be described in the first place, to then explain how they may affect other agent benefits. This also helps to show the complexity of the benefits available in an Active Distribution Network (Morris et al., 2012, p.1). For an easy reference, the Table 22 summarizes the benefits to be presented (Morris et al., 2012; Gil and Joos, 2008; Costa et al., 2008).

A.1.1 Independent power producer benefits. There are two ways an independent power producer (IPP) could benefit in a network: energy sales and service provision. The energy sales can provide some benefits by local production to a price higher than wholesale/spot market and lower than distribution system tariff; this is called the *local benefit* (Morris et al., 2012). On the other hand, the IPP could set its strategy to sell when energy price is high and buy from the main grid to satisfy its demand when energy price is low; this is called the *selectivity benefit* (Morris et al., 2012). Service provision consists on three services:

Balancing services, which consist on selling active power support to keep system frequency under required limits. This kind of service also includes the reserve provision, which consists on an instant support of active power anytime the distribution system or the power system operator needs it (Kirschen and Strbac, 2004). In the latter case, the IPP sells its service through the reserve market (Wang et al., 2011; Gil and Joos, 2008).

Power quality services, which consist on selling reactive and distortion power support to keep system voltage and harmonic distortion under required limits (Rueda-Medina and Padilha-Feltrin, 2011; Kang et al., 2012; Morris et al., 2012).

Service quality services, which consist on energy sales during an outage. This kind of service includes blackstart support, system restoration support and reliability support (Costa and Matos, 2006; Wang et al., 2011). Both kinds can be transacted inside or outside the power distribution network.

A.1.2 Customer benefits. The customers can benefit from an energy cost reduction due to the local benefit or due to a downward pressure on electricity prices caused by an increase in the penetration of low cost local generation (Gil and Joos, 2008; Morris et al., 2012). Therefore, this benefit can be captured if customer plays also as IPP or if the energy consumed is from an IPP.

Note that if the customer and the IPP are the same players, the IPP profit maximization yields to energy cost minimization, because the greater the difference between local and

Table 22: Benefits for the independent power producers, customers, distribution network operator and some positive impacts for external agents like adjacent power distribution systems or power system operators, or like society and economy (Morris et al., 2012; Gil and Joos, 2008; Costa et al., 2008).

Independent Power Producer		*Customers*	*Distribution Network Operator*	*External agents*
Energy sales	Service provision			
1. Local benefit 2. Selectivity benefit	Balancing 1. Active power support 2. Reserve support Power quality 1. Reactive power support 2. Harmonic power mitigation Service quality 1. Black start or system restoration 2. Reliability support	1. Energy cost reduction 2. Power and service quality improvement	1. Reduced operation and maintenance costs 2. Deferred investments and upgrade costs 3. Reduction in contractual compensations for poor power and service quality 4. Reduced or avoided energy or service purchases	1. Adjacent network power and service quality improvement 2. Pollutant reduction 3. Downward pressure on electricity prices 4. Reduced nonrenewable resource use 5. Infrastructure footprint reduction 6. Increase in employment

central energy costs, the greater the benefits captured.

The same can be expected with the selectivity benefit, although it may have different minimum energy cost: In the local benefit case, the minimum energy cost is constrained to the operation cost of the local generator; in the selectivity benefit case, the minimum energy cost is constrained to the minimum price between central and local generation.

Additionally, if continuity of energy service has value to the customer, the reliability service from an IPP could be used to increase the IPP benefits. However, in a de-regulated environment, efficient operation of this conti-nuity energy service is possible only if the customer and the IPP are the same players and the IPP is allowed only to supply the load associated to its customer. Otherwise, there is a need to regulate the maximum outage energy price, since in a contingency the few local generators constitute an oligopoly inside the microgrid (Chowdhury et al., 2009, sec.1.8, (5)). As a conclusion, unless the perfect competition conditions are met, not in all cases profit optimization of the IPP leads to an global optimum for the network.

A.1.3 Distribution network operator benefits. This kind of benefits can be summarized as actions that lead to a lower operational cost. Operation cost could be diminished by technical loss and congestion mitigation, thanks to in-site generation and consumption. This rises automatically the overall system efficiency. Also, the maintenance cost of equipment could be reduced by implementing controls with smoother transitions between operational states (Gil and Joos, 2008).

The Distribution Network Operator (DNO) could also reduce the reliability compensations associated to service quality problems (Costa and Matos, 2006). If reactive and harmonic active filtering is implemented within power electronic interfaces, also a better power quality could be achieved (Rueda-Medina and Padilha-Feltrin, 2011; Kang et al., 2012; Morris et al., 2012).

The DNO can encourage Independent Power Producer (IPP) to prefer a selectivity benefit strategy (see IPP benefits on page 167), by observing that price reactivity from the IPP could alleviate distribution system congestion, thus reducing the amount of energy purchased in the wholesale market and/or deferring infrastructure updates (Wang et al., 2011; Morris et al., 2012; Costa et al., 2008). System congestion reduction can also be translated to the power system operator to reduce the transmission costs due to constraints.

A.1.4 External benefits. So far the benefits of the main participants were reviewed. Customers care about low cost and reliable energy service, IPPs care about big sales at high prices and DNO cares about low cost and efficient operation. None of the agents presented attempts to affect other participants, but actually, because of the complexity of Active Distribution Networks and power transmission and delivery systems, they cannot avoid external impacts (Morris et al., 2012, p.1). Here the focus is towards the positive impacts, for a full review of the pros and cons please see (Chowdhury et al., 2009).

Until this moment, two positive external consequences have been presented: downward pressure due to high local generation penetration and power system congestion reduction by selling local energy at strategic time slots. Because local generation can take advantage of the natural resources, also a general reduction in pollutants can be achieved. State policies like pollutant vouchers (See (Ackerman and Heinzerling, 2002, p.1582) and (Varian, 2010, p.654) for a technical description) or pollution penalties can translate that pollution decrease to a benefit increase.

Intangible positive consequences are lower infrastructure footprint, overall consumption reduction of nonrenewable sources and even increase in employment (Morris et al., 2012).

A.2 Tangible benefits accounting

As a matter of scope, this subsection presents the most promising tangible benefits because of their low regulation requirements, short-term/medium-term nature, ease of implementation and ease of gross benefit calculation. With this in mind, the following benefits were left out of this review:

Balance services, which includes active power support and reserve support for the power system operator. Please refer to (Prada, 1999) for an overview; and (Gil and Joos, 2008, sec.C(3), p. 332) and (Morris et al., 2012, sec. 8, p. 7) for an introduction to possible applications.

System restoration support, which implies system reconfiguration and coordination rules (not related with the steady state operation) that have to take into account adjacent systems (other power distribution systems or power transmission systems).

Harmonic power mitigation, which consist in controlling total harmonic distortion within the system. An approach that do not require additional active filters to compensate the harmonic power is presented in (Kang et al., 2012); there, Kang *et al.* attempts to solve the physical compensation problem from a technical point of view, but their approach has a clear impact on total harmonic compensation costs. A harmonic pricing based on a pollution market mechanism (see section A.1.4) is presented in (Talacek and Watson, 2002a,b) and a harmonic pricing based on harmonic losses is presented in (Peng et al., 2011).

Reduced maintenance, which bases its results on analysis of equipment failure times. Although without formal analysis of the failures times, in (Chaouachi et al., 2013; Colson et al., 2013a) the authors present an initial approach focused in an expected longer battery life due to the smooth operation strategy.

Lower electricity prices, which can be seen as a long-term effect of high penetration of microgeneration with competitive price. An introductory analysis is presented in (Gil and Joos, 2008, sec.C(1)).

Adjacent system benefits, which can be counted as indirect/unintended benefits because of the existence of the Active Distribution Network (a positive externality). This topic was left out of the present review because it is the following step once the power distribution network with local renewable generation is efficiently operated. Hence, there exists a methodological gap that has to be filled before moving forward.

Tangible benefits described bellow are those related to price selectivity, reactive support, system reliability, loss reduction and investment deferral.

A.2.1 Selectivity benefit. Energy purchases are made by utilities mostly through long-term bilateral contracts, however a portion of them is through the short-term spot market. Covering those short-term purchases for the Distribution Network Operator in critical hours is a way to increase the benefits from a local microgeneration installation. Those kind of benefits are constrained to the following conditions (Gil and Joos, 2008):

1. The price per energy delivered has to be lower than the spot market price.
2. The price per energy delivered has to be higher than the final customer price, if the Independent Power Producer and final customer are different agents.
3. Local generation has to be flexible and dispatchable.

The dispatchable condition could be granted with reliable and strategic storage management. Like in the unit commitment problem, the optimization process might charge (or do not use) storage units in low profit hours to sell greater amounts of energy at high profit hours.

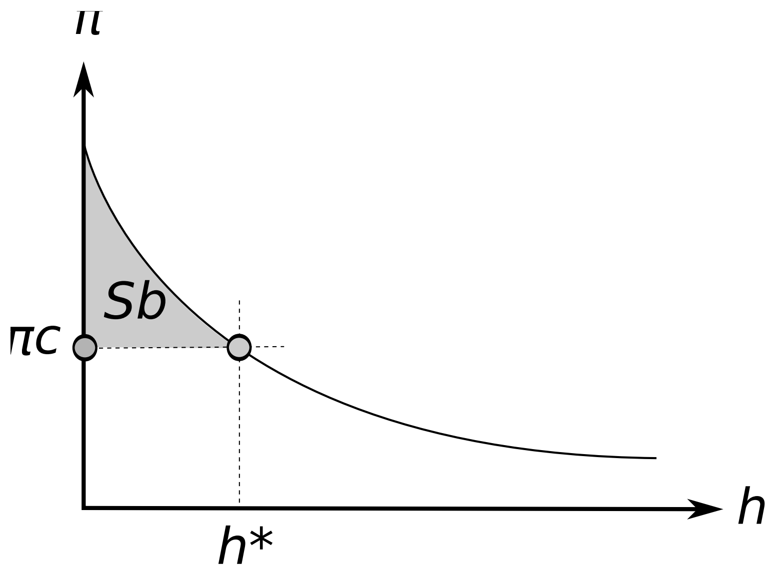

Figure 30: Price duration curve and the selectivity benefit potential (gray area). Adapted from (Gil and Joos, 2008).

One may use the market price-duration curve[2] to calculate the selectivity benefit potential as follows (Gil and Joos, 2008):

$$Sb = \int_0^{h^*} \left[\pi\left(h\right) - \pi_c\right] dh \qquad [\$/kW]$$

Where, $\pi\left(h\right)$ is the price-duration curve and h^* are the hours that the local generation ought to sell energy at π_c to maximize the profit (Gil and Joos, 2008). Graphically (see Figure 30) Sb results from the difference between all possible prices above the local generation price times the number of hours they appear, and the optimal local generation price times the number of hours it appear ($\pi_c \times h^*$).

If the Independent Power Producer (IPP) and the customer are different agents, the benefits might be reduced when there is no interest from the Distribution Network Operator (DNO) to avoid wholesale market purchases. If the DNO is interested, it could reduce the cost of spot market purchases by contracting the IPP.

Gil *et. al* in (Gil and Joos, 2008) present a selectivity benefit study with «four-year historic of the Ontario electricity market price» where the Independent Power Producer and the customer were the same agent. The price-duration curves was approximated by a power function ($f\left(x\right) = ax^b$) for the top 1000 hours of the year. The benefit calculated with this price-duration curves range between 3.52¢/kWh and 7.05¢/kWh for the data analyzed. The average (over the 11 most important cities) of residential electricity price in 2008 was

[2]That curve shows the time that lasted a specific spot price over the observation time period.

10.44¢/kWh [3].

A.2.2 Reactive power support. An adaptation of harmonic compensation pricing presented in (Peng et al., 2011) could be implemented to reactive power pricing into Active Distribution Networks. Also, reactive power could be valued for minimum power losses by calculating how active flow changes affect the reactive flow within the network. In (Rueda-Medina and Padilha-Feltrin, 2011) this change ratios are measured with an index called *Lost of Opportunity Cost*. Albeit in that work only the methodology is established, future studies may try to evaluate its pros and cons as a real-time or market-based pricing mechanism.

Rueda-Medina *et al.* defines Lost of Opportunity Cost (LOC) for a local generator at node i as:

$$LOC_i = C_i \left| \frac{\Delta P}{\Delta Q} \right|$$

Where C_i is the generation cost, ΔP_i is a change in active power from a base case and ΔQ_i is a change in reactive power due to a change in the active power. The idea behind this index is that if a decrease in active power increases the reactive power flow, then less active power could be transacted into the microgrid. Hence, the reactive power is priced by how much active power is no longer transacted into the network.

Because the uncertainties in the renewable local generations the following methodology was implemented (Rueda-Medina and Padilha-Feltrin, 2011): first a forecast process is run to fix the outputs of renewable local generators, next the program solves a multiobjective optimization problem, which consider the local generation costs and the voltage stability of the system. The operation point for the multiobjective optimization is based on an optimal power flow that minimizes the power losses in the system. This is done $\aleph$ times, changing the forecasted time series through a Monte Carlo simulation in each iteration. With a Pareto Front for a specific time series an additional criterion is applied to choose the solution (max-min or intermediate criteria for the operation cost or voltage stability index). Finally, with the optimal solution the LOC is calculated.

In (Morris et al., 2012, sec.B) there are some other mechanisms to reactive power pricing that follows the idea behind the LOC and the idea of standard reactive power regulation. Finally, Morris *et al.* highlight the feasibility conditions of reactive support into a microgrid. This kind of service depends on the actual characteristics of the network and the absence of a mandatory reactive power support, so the Independent Power Producer has a margin of

[3] This information is available on line in Canadian Electricity Association website: http://www.electricity.ca/media/Electricity101/Electricity101.pdf, page 54.

active power increase by reactive compensation.

A.2.3 Reliability support. There are some benefits associated to service continuity (reliability); greater benefits come from power distribution systems with low reliability and high load density. However, today major applications lie on rural areas, where the service quality and load densities are low (Pudjianto et al., 2005, p.56). Thus before any real implementation the investor must carefully estimate interruption rates and local generation installation costs. Such studies cannot be generalized (except for the methodology) because the success highly depends on regulation and utility characteristics.

A simple accounting method of the reliability support benefit is presented in (Costa et al., 2008; Costa and Matos, 2006).[4] There, Costa *et al.* presents the benefit based on typical reliability indexes without concerning the value of reliability itself. For a guide to outage valuation see (Sullivan and Keane, 1995); moreover (Sullivan et al., 2010) analyzes problems of usual practices for reliability improvement valuation.

From a single customer point of view, the benefit from increased reliability in a time period is[5]:

$$Rb_k^{(c)} = \lambda^{(c)} \times pT_r \times \overline{P}_G \times \left(\nu^{(c)} - \pi_c\right)$$

Where $Rb_k^{(c)}$ is the reliability benefit of customer c for the time period k, λ is the expected failure rate for period k for customer c, p is the probability that the isolation from the fault fails, T_r is the average restoration time after a fault, $\overline{P}_G$ is the average power generated (and consumed) in period k, ν is the value that customer c assigns to the local energy generation in islanded mode and π_c is the price at which the Independent Power Producer sell the energy in islanded mode. This benefit is divided in time periods to capture intertemporal variations of the involved variables (Costa and Matos, 2006, p.3).

For a single Independent Power Producer (IPP) point of view, the benefit from increased reliability in a time period is[6]:

$$Rb_k^{(g)} = \lambda^{(g)} \times pT_r \times \overline{P}_G \times \pi_c - C_{\Delta P}$$

Where $Rb_k^{(g)}$ is the reliability benefit of IPP g for the time period k and $C_{\Delta P}$ are the additional costs for active power increments in islanded mode.

---

[4] For a deep analysis on reliability benefits of microgrids please go to (Pudjianto et al., 2005, chap.6) and annex 4 of (Schwaegerl et al., 2009) which is available online in http://www.microgrids.eu/documents/672.pdf.

[5] Adapted from (Morris et al., 2012, sec.5) reliability calculations, but originally found in (Costa et al., 2008, sec.2.2.1)

[6] Adapted from (Morris et al., 2012, sec.5) reliability calculations, but originally found in (Costa et al., 2008, sec.2.2.1)

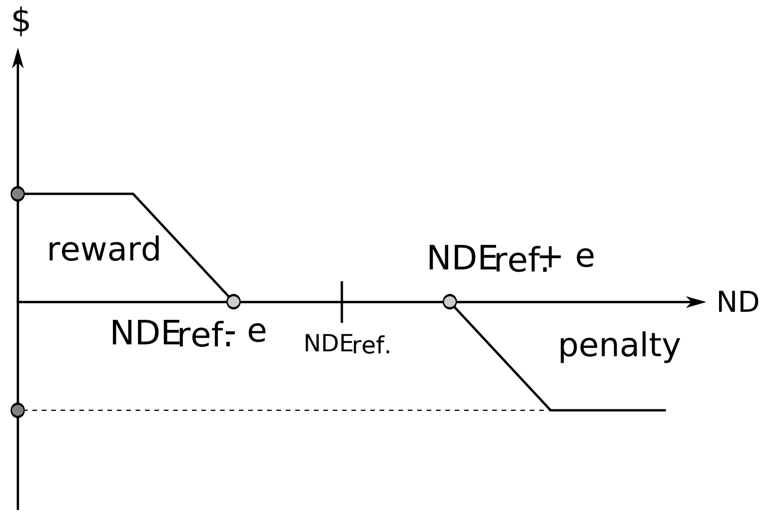

Figure 31: An incentive mechanism for service quality. NDE stands for Non Delivered Energy and ε is the minimum NDE difference to get a reward or a penalty. Adapted from (Costa et al., 2008).

For a Distribution Network Operator (DNO), the benefits come from compensation reduction, and thus depend on current regulation. For an incentive mechanism like the one depicted in Figure 31, based on Non Delivered Energy (NDE), a high improvement for a low reference not only decrease the compensation but actually turn them into a reward (Costa et al., 2008). Although the reward level is temporal for a moving reference, still this could be an important extra revenue stream.

A.2.4 Power loss reduction. Again, the price-duration curve (see Figure 30) could be used to calculate power loss benefits due to a local generation at bus i (Gil and Joos, 2008):

$$\mathrm{Lb} = \frac{\partial P_{loss}}{\partial S_{LGi}} \int_0^h \pi\,(h)\,dh \qquad [\$/kW]$$

Where S_{LGi} is the injected power in kVA of the local generation at node i, P_{loss} are the system losses, $\partial P_{loss}/\partial S_{LGi}$ is a sensitivity index that measures the marginal change in active power losses due to a power injection at node i, and h is the total *equivalent* time the local generation is up (Gil and Joos, 2008). If the Independent Power Producer is capturing the selectivity benefit, then $h = h^*$, the number of hours that market price get to the reference price π_c. The study in (Gil and Joos, 2008) reveals that the benefit is between 0.25¢/kWh and 8¢/kWh for a (reasonable) load reduction of 2%. The same 10.44¢/kWh for residential electricity customers can be applied as a comparison point.

One interesting result stated in (Pudjianto et al., 2005, p.55) is that, for the same installed capacity, the higher the density of local generation the lower the impact on system losses. This is reaffirmed in (Quezada et al., 2006), where also it is asserted that three local generation units strategically located has the same effect on losses that an ideal case with more than three microgenerators. Quezada *et al.* highlight the impact of microgeneration with reactive power control, since a better voltage profile will reduce reactive power flow and therefore system losses. They also clarify, that although this results can be reproduced qualitatively, numerical value of the system losses depends on power distribution topology and load pattern.

A.2.5 Investment deferral. It consists on in-site generation for strategic loads, specially in peak hours to shift in time a feeder improvement (Gil and Joos, 2008). In essence, this is the same approach of the selectivity benefit, but with a different set of rules, dictated this time directly by the Distribution Network Operator (in the selectivity benefit previously presented the rules were dictated by the power market prices and the customer). As a consequence, if the investment deferral benefit does not overlap with the selectivity benefit, there are two possible revenue streams to be exploited. If there exists overlapping, the state must develop regulations for fairly benefit allocation.

Summing up the investment deferral benefit for every possible feeder f in the network and subtracting the local generation installation cost, gives the total benefit at the i node (Gil and Joos, 2008):

$$Id_i = \sum_f C_f \left(1 - e^{-r \times t_{fi}}\right) - C_{LGi}$$

Where, C_f is the present value of the improvement, r is the discount rate, C_{LGi} is the installation cost of the local generation at node i and t_{fi} are the time periods for which the investment on feeder f has been shifted due to the added generation at node i. Note that the benefits for the investment deferral consist on the difference between the actual value of the investment and the present value of the future investment if the cost of the investment would not change (Gil and Joos, 2008). There, future value does not take into account changes in time, except those due to the money value.

In the study presented in (Gil and Joos, 2008), this benefit reveals a potential of 20¢/kWh (compare it with 10.44¢/kWh for residential customers) for covering near to six peak hours per week. However, that study assumes that the distribution utility does not incurs in costs for the local generation project ($C_{LGi} = 0$). Note that this benefit has a strong dependence on the utility's cost structure, planning projects and infrastructure. In (Méndez et al., 2006) it is shown that low density of microgeneration have a greater positive impact on this benefit. This is thanks to the complementarity between production patterns, which increase energy availability.

This benefit is akin to a short-term (low budget) planning, so for a more complete picture on network planning the reader could see (Mitra et al., 2006) and (Hu and Li, 2012b). Both of them treat reliability improvements as important criteria for benefit maximization: In Mitra *et al.* the reliability analysis is based on Expected Loss of Load and in Hu *et al.* the reliability analysis is based on the number of curtailments. Finally two expressions to investment deferral, one as a function of the load growth and other as a function of the installed capacity of the local generation can be found in (Costa et al., 2008, p.3897).

A.3 Discussion

Most promising indirect benefits are those related with system reliability, reactive support, loss reduction, investment deferral and price selectivity. They are suitable for investment funding and business case developing, because low regulation requirements, short-term/medium-term nature, ease of implementation into a Energy Management System (EMS) and ease of gross benefit calculation. Some of the benefits may overlap, like selectivity benefit and investment deferral benefit, whilst other benefits need a power or service quality deficiency to be feasible. On the latter case, even with tangible benefits at sight, nothing can be done if regulations demand high quality standards. Therefore, regulations must be created to increase the dynamism of the sector by letting new services appear. This way, market forces can be used to assure the quality of the service. Also, rigorous studies between the relation of Active Distribution Network efficiency and negative externalities are needed to better regulation designs. Such regulations must reward efficient operation to increase sector dynamism.

A close analysis of Active Distribution Networks benefits reveals that most benefits need reliable and flexible energy injection system at any time. The uncertainty around the energy injection time could be diminished by analyzing trends on energy consumption and generation. However, for any energy source installed in present distribution systems, that reliability and flexibility only is achieved by using some kind of energy storage. So, a key element to capture most of the presented benefits is the storage management system. Still is unknown the most efficient way to control this system in a power distribution network with renewable generation, yet some recent approaches (Colson et al., 2013a; Chaouachi et al., 2013; Mahmoud et al., 2012) suggest to treat it independently.

Except for some cases of the reliability support benefit and the investment deferral benefit, all benefits here explained can be implemented in real time control system with communications between any local generation and a central monitoring system.

APPENDIX B

ACTIVE DISTRIBUTION NETWORKS' ENERGY MANAGEMENT SYSTEM

Akin to Active Distribution Networks, microgrids appear as one of the enabling technologies for the inclusion of Distributed Energy Resources (DERs) into power distribution networks. In fact, the microgrid concept evolved from a convenient backup system for power distribution (Banerji et al., 2013) to a new paradigm for energy distribution systems in which generation (from a local energy source or storage device) is coordinated to supply local energy needs while behaving as a sole system (Lasseter, 2002).

For low DER penetration, microgrids can optimally schedule their local generation. However, as the DERs penetration or the number of microgrids in a distribution network increase, the problem complexity increases, since the independent local optimization of all DERs might lead to a suboptimal operation point from a system wide perspective. Therefore, to optimally coordinate multiple DERs in a power distribution system, there is a need to change the focus towards a more general approach: Active Distribution Networks (Gill et al., 2014; Hu and Li, 2012a,b; Chowdhury et al., 2009). Therefore, in the same way a microgrid can yield to higher efficiency and reliability for a distribution network with low DER penetration, an ADN can be used to increase reliability and assure the efficiency of the operation of a distribution network in presence of higher DER penetrations. Note that the ADN objectives are accomplished through the coordination of the microgrid(s) and DER(s) connected to the distribution network, akin to how microgrids coordinate all its local DERs given a suitable communication protocol (Gaona et al., 2016).

With this in mind, the following description of the characteristics of Energy Management Systems (EMSs) for ADNs includes applications designed for microgrids that can be easily adapted for cases with high DER penetration.

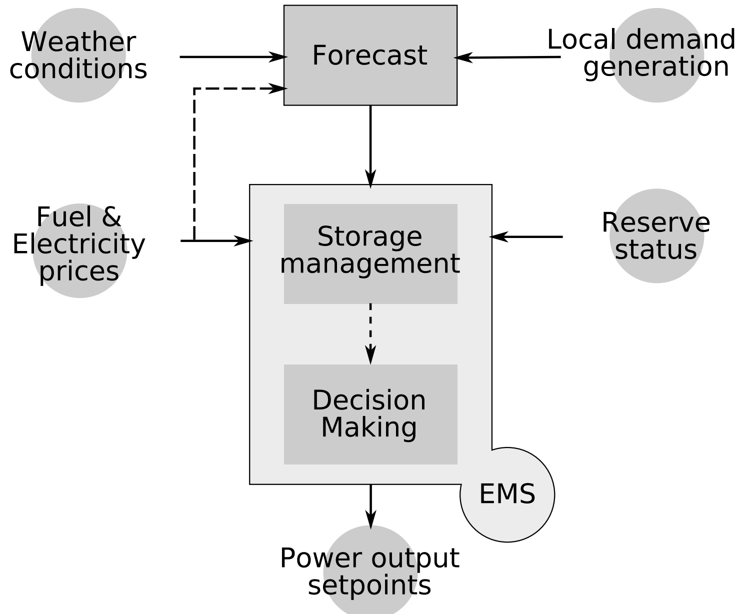

Figure 32: Typical Energy Management Systems (EMSs) architecture. Forecast is usually used to reduce uncertainty of input parameters. Adapted from (Chakraborty and Simoes, 2008, p.2) and (Chaouachi et al., 2013, p.1695).

The EMS architecture depicted in Figure 32 summarize the main components to be described in this annex. The main role of a EMS is then to find the power output settings of each DER in the system based in all the information available, e.g., price and load forecast and weather conditions. Dashed lines state an optional relation between blocks, thus, in case of fuel and/or electricity prices, depending on the study, this could be treated directly by the forecast module. In case of the storage management, this could be included directly into the decision making module. Following sections describe the characteristics of the forecasting module (section B.1), storage management systems (section B.2) and the decision making module (section B.3). This annex closes with a brief discussion about emergent ideas for implementing EMS in ADNs.

B.1 Forecast

A key feature in Energy Management Systems (EMSs) is the forecasting module, because better estimation of the decision making parameters improves the results (Changsong et al., 2009; Mahmoud et al., 2012). Most forecasting is done over 24 *time slots*, each corresponding to an hour of a day. This day-ahead forecasting is often applied to predict weather conditions, load levels and market prices, and depending on the application can be increased or reduced.

More time slots could seem to be a good option to improve the decision making results, however, as a consequence of the high variability of some local sources (e.g. wind), forecasts become less reliable (Meiqin et al., 2010, p.995). Now, by reducing the window size, e.g. from 24 hours to 1 hour, forecasts become more reliable (Palma-Behnke et al., 2013, Table 1), nevertheless storage management might be inefficient due to the lack of information. So there is a trade-off between forecast precision and EMS performance.

Overall reliability is improved when: the impact of less variable inputs (e.g. loads) is greater than the more variable input (e.g. wind), as shown in (Wang and Gooi, 2010); and the forecasting time window is moved after each period, i.e., if always is used the most up to date available (Palma-Behnke et al., 2013). Of course, if two-day-ahead forecasting error is close enough to the one-day-ahead forecast error, it will be wise to choose the longer scope (Palma-Behnke et al., 2013).

Once the variability is at the desired level, the next question lies on tool selection. In (Karki et al., 2012), the authors claim that auto regressive mean average (ARMA) models are well suited for predictions up to 10 hours in wind velocity estimation, surpassing numerical weather prediction methods in the range of 4 to 6 hours ahead. For a day ahead forecast, artificial neural networks seem to be a recurrent option (Changsong et al., 2009)(Chen et al., 2011)(Chaouachi et al., 2013)(Palma-Behnke et al., 2013).

Nonetheless, there are some other tools: In reference (Palma-Behnke et al., 2013) also is used an averaged index over the period of interest to forecast solar irradiance. Palma-Behnke *et al.* clarifies that this is possible because the latitude of the test system is above the 20°; In (Kanchev et al., 2010) a prediction of the load behavior with the total energy approach is done, therefore, total energy is predicted instead of predicting average power for each time slot. This is usually used when the average power profile is well known and when it has low variability. Finally, in reference (Meiqin et al., 2010) it is used a Markov process to incorporate the forecast problem into a reliability analysis.

B.2 Storage management

Depending on the available storage devices and local generation equipment the storage management could be composed by only a battery or several storage devices, both cases are treated bellow.

B.2.1 Battery management. Electrical storage is done typically with lead-acid batteries. Battery system is a sensible element in Energy Management Systems (EMSs) because «how

[it] performs over its lifetime is highly dependent upon how it is operated in real-time during each charge and discharge cycle.»(Colson et al., 2013b, p.2). Battery life cycle optimization needs to control battery state of charge and charge/discharge rates. Two main approaches have appeared to handle this: Rule-based methods and Fuzzy Logic methods.

Chen *et al.* in (Chen et al., 2011) shows a rule-based method which consists on changing the constraints (e.g. maximum charge/discharge rates) on the optimization problem depending on the actual state of the battery. A rule-based approach depending on actual and future (day-ahead) weather conditions is presented in (Chakraborty and Simoes, 2008).

The fuzzy logic approach in (Chaouachi et al., 2013) use the battery state of charge, electricity price, load demand, renewable energy generation, actual solar daily generation and next day solar availability to derive a charge or discharge signal. On the other side, in reference (Mahmoud et al., 2012) storage system depends mainly on the *charging price*: the difference between the maximum daily price and minimum daily price. There, storage charging/discharging rates are constraints in the optimization problem, while storage dispatch depends on comparing the charging price with local generation costs.

Colson *et al.* in (Colson et al., 2013b) developed a cost-efficient index for optimal operation of the storage system. This control system is implemented in an independent fashion and also offers a user interface to decide if battery health is more important than the system revenue stream.

B.2.2 Reserve management. Reserve management is usually included in the Energy Management System (EMS) as a constraint. For example, in reference (Meiqin et al., 2010) system reserve (including wind availability) is set to be greater than 5% of actual demand. Another way is to split reserve into both, operating and idle local generators, as proposed by (Liang and Gooi, 2010). Additionally, in (Wang and Gooi, 2010) is included the reserve into the objective function by establishing a reserve bid price, while calculating the expected energy not supplied.

B.3 Decision making

The decision making problem implicit in an Energy Management System (EMS) can be stated in several ways: as a control problem, as a rule-based system, as an expert system or as a mathematical optimization problem. Whatever is the case, these problems have two things in common:

1. They are designed to accomplish some goal related to the efficient management of the available energy resources in the Active Distribution Network (ADN).

2. They can be be solved in two ways:

   Centralized calculation Optimization is done with all the information available and without a coordination strategy between system participants. A central computation agent broadcast to each participant the respective optimal set point.

   Decentralized calculation Optimization is done with partial information and a coordination strategy between participants. A local computation process managed by each participant determines the respective optimal set point.

Next, it is discussed about some of the goals that can handle EMSs, followed by a description of some centralized and decentralized methods for solving the EMS energy allocation problem.

B.3.1 Goals. Let us define an *efficient solution point* as the solution of a problem when is computed with some formal decision making process, e.g., using an optimal control technique or in general when it is the solution of a mathematical optimization problem.

Most of the time EMS must handle several conflicting goals, e.g., looking for the lowest active system losses while trying to take the most of an abundant energy resource. This is why often the solution appears has a *Pareto front*, i.e., a set of the most efficient answers that met with all problem requirements. The resulting points are then processed by the so-called *decision maker*, an entity in charge of choosing one solution among the available solution points according to some subjective criteria. For a detailed and rigorous explanation of this topic in the mathematical optimization framework, please refer to (Miettinen, 1999; Sawaragi et al., 1985).

Whatever is the case, to find an *efficient point* a dominance structure is needed (Miettinen, 1999), i.e., a way to compare two solutions. Traditionally a scalar valued function (often called *objective function*) is used to measure how well a goal is achieved, since this way we can use the real line to compare two answers. When there are more than one goal, a vector valued objective function is used instead to state the problem, nevertheless, to solve the problem a surrogate scalar valued objective function must be used. A common practice is to replace the original vector valued objective function by a convex combination of each of its components. Therefore, if the vector valued objective function can be expressed as:

$$\mathcal{F}(x) = [f_1(x)\ f_2(x)\ \ldots\ f_n(x)]$$

Then, the surrogate scalar objective function is:

$$F(x) = a_1 f_1(x) + a_2 f_2(x) + \ldots a_n f_n(x) \qquad \left(\sum a_n = 1\right)$$

For each possible combination of coefficients, an efficient solution is found, and thus, a Pareto front point. This is not the only way to transform the original vector valued objective function (for a complete list refer again to (Miettinen, 1999)) but it seems to be the most common choice in the reviewed technical literature, even with decentralized calculation methods. Parisio *et al.* provide some support for this choice in (Parisio and Glielmo, 2012).

Although the usual objective functions are related to operational and environmental costs (Farahmand et al., 2011; Colson and Nehrir, 2009; Sortomme and El-Sharkawi, 2009, p.2), some authors add reliability-based objective functions (Wang and Gooi, 2010; Meiqin et al., 2010, sec. 2.2).

Additionally, in reference (Pudjianto et al., 2005, p. 26) it is concluded that for microgrids less outage costs are incurred after a short local generation interruption if continuous transitions to islanded mode are preferred over islanded operation. So a simple operational policy can also be important to the problem solution.

Because of the rich background in optimal operation of transmission systems, EMS problem is often stated as a mathematical optimization problem. Renewable energy fixed costs can be included in this problem as a penalty cost function that depends on each extra (unused) energy unit. The idea is to make fixed cost recovery time longer if the energy is not used. This philosophy is implemented in (Chakraborty and Simoes, 2008) as a penalty function based on the difference of the maximum generation available and actual generation. The extra power is multiplied by a constant that represents the fixed costs evenly distributed across the lifetime of the project. With a similar idea, (Xu et al., 2011) include a couple of penalty functions into the objective function of the EMS: the penalty cost function depends on the excess in local wind generation and the reserve cost function depends on the unavailability of local wind generation.

Optimization problem in (Salani et al., 2011) consist on minimizing energy bill price in first place and then a voltage variability index (based on steady state operation); the latter optimization flatten voltage fluctuations between time slots. Salani *et al.* show that cost minimization leaded by price signals affects negatively on the voltage variability index, then imposing a physical limit to the price reactiveness of participants.

B.3.2 Centralized solutions. In this subsection is presented a review of some heuristics applied to the decision making process of EMSs; after that, approaches that do not use heuristics are presented.

B.3.2.1 Heuristics Two main heuristics are usually employed to solve the optimization problem associated with the microgrid operation: *Genetic Algorithms* (Chen et al., 2011; Zhao et al., 2013; Vahedi et al., 2010; Liang and Gooi, 2010; Xu et al., 2011) and *Particle Swarm Optimization* (Basu et al., 2010; xia Dou et al., 2011; Bazmohammadi et al., 2012; Mahmoud et al., 2012). In particular, reference (Bazmohammadi et al., 2012) shows how Particle Swarm Optimization exploration capabilities can be improved with *Differential Evolution Algorithm*.

Two works from genetic algorithm implementations stands out: In (Liang and Gooi, 2010) the genetic algorithm is modified by incorporating a *Simulated Annealing* (SA) heuristic to discard poor solutions. With SA the genetic algorithm gets a velocity boost (from nearly an hour to a couple of minutes) without major precision lost (0,78% with respect the case without SA); In second place, Xu *et al.* in (Xu et al., 2011) compare the performance of the *Strength Pareto Evolutionary Algorithm 2* (SPEA2) and the *Non-dominated Sorting Genetic Algorithm* (NSGAII), and found that SPEA2 is a faster (needs fewer generations to find an optimal) but less precise method than NSGAII.

B.3.2.2 Other methods A control-theory like based on Adaptive Model-based Control is presented in (Hooshmand et al., 2013). The method was tested with a long-term forecast window of 12 hours and a 20 minutes update rate, which yield to a reduction of 21% of the cost with respect to a standard EMS strategy.

Sathyanarayana *et al.* develop in (Sathyanarayana and Heydt, 2013) a Locational Marginal Price (LMP) to energy pricing in a power distribution system. This LMP is calculated to minimize the peak power demand, the energy consumed, the total cost of energy and the total loss in the system. Because the objective functions can be expressed as a sum of simpler functions, the solution method is implemented for parallel processing.

Fathi *et al.* in (Fathi and Bevrani, 2013) minimize the cost function and the peak to average ratio of the load profile considering imperfect information over the actual loads of the system. Although the solution is suboptimal, Fathi *et al.* show that under load uncertainty the method outperforms game theory approaches.

B.3.3 Decentralized solutions. In this section, first there are presented solutions to the EMS optimization problem which involve multiagent systems. Then, some solutions based on the application of decomposition methods are presented.

B.3.3.1 Multiagent systems Active Distribution Networks (ADN) are decentralized systems, so applying Multiagent Systems (MAS) tools for ADN management seems natural –basic notions of agency, MAS implementations and its relation with ADNs can be found in (Bordini et al., 2007; McArthur et al., 2007a,b; Wooldridge, 2009).

Colson *et al.* in (Colson et al., 2013a) implement a MAS which manage a simulated network with two main objectives, cost minimization and storage performance maximization. Another implementation, this time specifying the system models implemented and the full MAS developing process is found in (Colson and Nehrir, 2013).

Logenthiran *et al.* in (Logenthiran et al., 2012) maximize local generation profit by minimizing the distance of the actual load profile and a reference load profile. Interesting enough, In (Logenthiran et al., 2012) is left to future works the decision process for optimal reference for the load profile.

Ren *et al.* in (Ren et al., 2013) present a (well documented) MAS tool based on JAVA for microgrid dynamic management based on InterPSS (MAS environment), JADE (MAS handling) and JUNG (Network visualization). The optimum is achieved through a well defined set of rules that determine agents' interaction for each possible scenario. The InterPSS integration offers not only a mean to compute power flow output but also a way to modeling and simulating connection and disconnection processes.

A set of two MAS tools are employed in (Oliveira et al., 2013) to analyze a market composed of microgrids. Namely, MASCEM and MASGriP: The first one offers a way to analyze market operation, while the latter allow the simulation of smart grid concepts, like the «Virtual Power Plant».

Not only simulation efforts are made in the field, there are some implementations of microgrids with MAS. A (mini)pilot with a Energy Management System based on MAS at Nanyang Technological University is presented in (Eddy and Gooi, 2011). Additional to the implementation results, the authors show an overview of the MAS JADE interfaces. In (Roche et al., 2010, sec. IV-C) are briefly presented the «GridAgents Framework» pilot ran in Australia and the MORE-Microgrids project MAS pilot in Kythnos island (Greece).

B.3.3.2 Methods As in (Sathyanarayana and Heydt, 2013), the objective functions in the work of (Zhang et al., 2013) are separable, nonetheless Zhang *et al.* take an interesting step forward into Energy Management System (EMS) solution: instead of parallel computation and because separability is translated to the dual problem, they use a subgradient algorithm to compute the optimum as a sequence of local optima. Here, dual decomposition solution is possible because power from microgenerators is taken from a time series, so it is a known value during the optimization steps.

However, as mentioned in (Wan and Lemmon, 2009, p.1), because dual decomposition message complexity is super-linear with the number of neighbors and the maximum length path, researchers must be careful when selecting the stabilizing step size of the messages, otherwise, the communication burden will be unacceptable. This is why in (Wan and Lemmon, 2010) the authors develop a decentralized optimization method to solve the DC optimal power flow problem that in addition does not require constant availability of the communication network. Instead, it converges to an optimum through an asynchronous sample of measures, using the communication network only when there is an immediate need.

Another problem with decentralized optimization methods is the rate of convergence. To solve this, Wei *et al.* in (Wei and Ozdaglar, 2013) have proposed an asynchronous Alternating Direction Method of Multipliers (ADMM) algorithm. Wei *et al.* probe that this method has a rate of convergence of $O(1/k)$ –where k is the number of iterations. Compare this with the $O(1/\sqrt{k})$ rate of convergence of dual decomposition solution with subgradient methods and the $O(1/k^2)$ rate of convergence of gradient methods with global information (Wei and Ozdaglar, 2013, p. 5). Although Wei *et al.* applies the method to a general network utility maximization problem, the results can be implemented to solve a DC optimal power flow problem.

Dual decomposition analysis also can be used to find an indicator function for the unit commitment problem, as shown in (Zhao et al., 2014), thus reducing the complexity of the optimal energy management problem.

Additionally, decentralized dispatch with losses is difficult because system losses are a function of all power system injections. In reference (Binetti et al., 2014), Binetti *et al.* solved this problem by calculating the power mismatch in each node in a distributed fashion in parallel with a consensus algorithm which updates the power cost for each generator. Results show that the method has a performance similar to the *lambda iteration method*. Furthermore, it increase optima reliability, a common characteristic of decentralized computations.

B.4 Discussion

Decentralized solutions based in optimization problem decomposition often requires a good insight in convex programming and modeling (Low et al., 2013; Lesieutre et al., 2011; Dall'Anese et al., 2013). In this direction efforts are beginning to extend the knowledge in power system analysis (Lavaei et al., 2014). Game-theoretic methods (Saad et al., 2012; Soliman and Leon-Garcia, 2014), constraint-programming (Dolan et al., 2013), adaptive stochastic control

(Anderson et al., 2011) (including pure approximate dynamical programming (Strrelec and Berka, 2013)) and complementary systems analysis (Gabriel et al., 2012) are in an early stage of development, so constitute an interesting research option.

There is little work on how must be handled multiple objectives in a EMS problem, so, new lines of research on this topic may include exploring the behavior of other objective functions transformations and exploiting and adapting the extra information of other methods, like the $\varepsilon-$constrained method.

APPENDIX C

POWER FLOW SOLUTIONS

This annex presents the results of applying equations in Frame (8) to solve the three-phase power flow problem for the three IEEE test feeders. First, it is presented the solution for the 13 node test feeder, then for the 34 node test feeder and finally for the 123 node test feeder. All network parameters can be consulted in (Kersting, 2001), moreover, all variables are presented in *per unit* with a 100 kVA base and proper voltage bases. Distributed loads were modeled as concentrated loads in the middle of the line (Kersting, 2001), therefore, a distributed load between node XYZ and XUW is connected to a ficticious node 9$YZUW$. All the three-phase power flow code is in GAMS 24.5.4, besides, the problem was solved using IPOPT 3.12 solver (with MUMPS as linear solver). Simulations were done on a laptop computer with an Inter(R) Core(TM) i7-4700MQ processor (2.4GHz) with 6GB of RAM.

C.1 IEEE 13 NODE TEST FEEDER

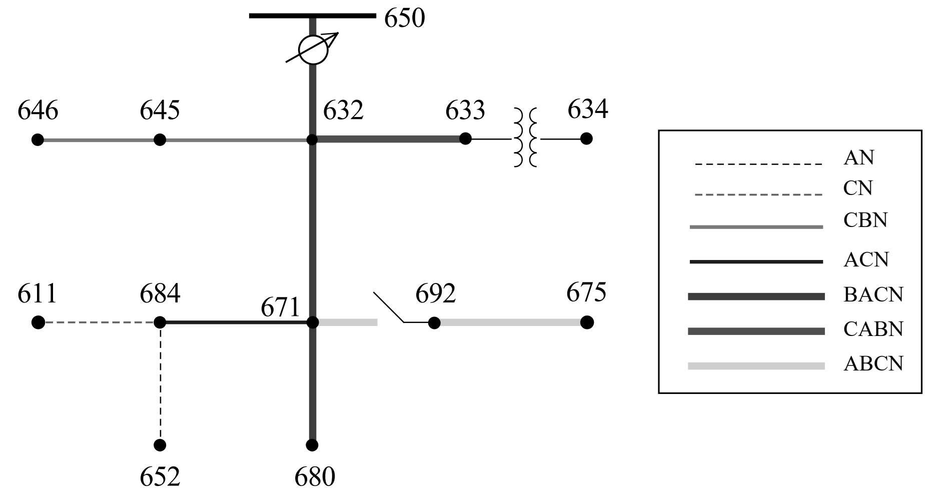

Node Voltage, Current and Power

		Mag. V	Ang. V	Mag. I	Ang. I	P	Q
611	a	0.0000	0.000	0.000	0.000	0.000	0.000
611	b	0.0000	0.000	0.000	0.000	0.000	0.000
611	c	1.0340	115.960	1.879	94.799	1.812	0.701
631	a	1.0668	-3.525	0.185	-33.991	0.170	0.100
631	b	1.1030	-121.881	0.690	-151.813	0.660	0.380
631	c	1.0539	117.009	1.284	86.844	1.170	0.680
632	a	1.0812	-2.273	0.000	0.000	0.000	0.000
632	b	1.0983	-121.593	0.000	0.000	0.000	0.000
632	c	1.0730	117.933	0.000	0.000	0.000	0.000
633	a	1.0784	-2.330	0.000	0.000	0.000	0.000
633	b	1.0966	-121.633	0.000	0.000	0.000	0.000
633	c	1.0705	117.928	0.000	0.000	0.000	0.000
634	a	1.0710	-2.527	1.813	-37.035	1.600	1.100
634	b	1.0908	-121.767	1.375	-158.637	1.200	0.900
634	c	1.0646	117.788	1.409	80.918	1.200	0.900
645	a	0.0000	0.000	0.000	0.000	0.000	0.000
645	b	1.0893	-121.767	1.937	-158.094	1.700	1.250
645	c	1.0707	117.966	0.000	0.000	0.000	0.000
646	a	0.0000	0.000	0.000	0.000	0.000	0.000
646	b	1.0875	-121.843	1.652	-122.058	1.796	0.007
646	c	1.0686	118.011	1.652	57.942	0.881	1.530
650	a	1.0500	0.000	13.664	152.764	-12.756	-6.566

650	b	1.0500	-120.000	10.012	40.976	-9.938	-3.427
650	c	1.0500	120.000	14.356	-84.233	-13.746	-6.187
652	a	1.0440	-4.761	1.610	-38.657	1.395	0.937
652	b	0.0000	0.000	0.000	0.000	0.000	0.000
652	c	0.0000	0.000	0.000	0.000	0.000	0.000
671	a	1.0520	-4.817	5.252	-42.230	4.388	3.357
671	b	1.1095	-122.164	4.158	-153.289	3.950	2.385
671	c	1.0376	116.224	5.402	91.849	5.106	2.313
675	a	1.0460	-5.050	4.980	-26.443	4.850	1.900
675	b	1.1119	-122.330	0.816	-163.754	0.680	0.600
675	c	1.0360	116.228	3.467	80.060	2.900	2.120
680	a	1.0520	-4.817	0.000	0.000	0.000	0.000
680	b	1.1095	-122.164	0.000	0.000	0.000	0.000
680	c	1.0376	116.224	0.000	0.000	0.000	0.000
684	a	1.0499	-4.835	0.000	0.000	0.000	0.000
684	b	0.0000	0.000	0.000	0.000	0.000	0.000
684	c	1.0358	116.114	0.000	0.000	0.000	0.000

Current and Power Flow

			Magnitude	Angle	Active	Reactive
632	645	a	0.000	0.000	0.00000	0.00000
632	645	b	3.414	-141.557	3.52433	1.28021
632	645	c	1.652	57.943	0.88637	1.53465
645	632	a	0.000	0.000	0.00000	0.00000
645	632	b	3.414	38.443	-3.49928	-1.25911
645	632	c	1.652	-122.058	-0.88366	-1.53197
671	680	a	0.000	81.524	0.00001	-0.00010
671	680	b	0.000	-36.268	0.00001	-0.00009
671	680	c	0.000	-145.658	-0.00001	-0.00009
680	671	a	0.000	-90.000	0.00000	0.00000
680	671	b	0.000	0.000	0.00000	0.00000
680	671	c	0.000	-90.000	0.00000	0.00000
671	675	a	4.645	-1.640	4.87876	-0.27077
671	675	b	1.792	-52.281	0.68395	-1.86729
671	675	c	2.799	116.765	2.90458	-0.02743
675	671	a	4.645	178.353	-4.85000	0.28840
675	671	b	1.792	127.713	-0.68000	1.87265
675	671	c	2.799	-63.246	-2.90000	0.02663
611	684	a	0.000	0.000	0.00000	0.00000

611	684	b	0.000	0.000	0.00000	0.00000
611	684	c	1.788	-52.563	-1.81167	0.36782
684	611	a	0.000	0.000	0.00000	0.00000
684	611	b	0.000	0.000	0.00000	0.00000
684	611	c	1.788	127.437	1.81585	-0.36359
632	633	a	1.813	-37.034	1.61031	1.11759
632	633	b	1.375	-158.636	1.20550	0.90982
632	633	c	1.409	80.919	1.20707	0.91007
633	632	a	1.813	142.965	-1.60728	-1.11312
633	632	b	1.375	21.363	-1.20419	-0.90755
633	632	c	1.409	-99.082	-1.20439	-0.90793
633	634	a	1.813	-37.035	1.60728	1.11312
633	634	b	1.375	-158.637	1.20419	0.90755
633	634	c	1.409	80.918	1.20439	0.90793
634	633	a	1.813	142.965	-1.60000	-1.10000
634	633	b	1.375	21.363	-1.20000	-0.90000
634	633	c	1.409	-99.082	-1.20000	-0.90000
645	646	a	0.000	0.000	0.00000	0.00000
645	646	b	1.652	-122.057	1.79928	0.00911
645	646	c	1.652	57.942	0.88366	1.53197
646	645	a	0.000	0.000	0.00000	0.00000
646	645	b	1.652	57.942	-1.79627	-0.00674
646	645	c	1.652	-122.058	-0.88066	-1.52958
632	650	a	12.810	152.763	-12.55614	-5.84545
632	650	b	9.511	40.975	-9.96666	-3.12952
632	650	c	13.459	-84.234	-13.37390	-5.44888
650	632	a	13.664	-27.236	12.75626	6.56594
650	632	b	10.012	-139.024	9.93809	3.42668
650	632	c	14.356	95.767	13.74597	6.18725
652	684	a	1.610	141.343	-1.39506	-0.93731
652	684	b	0.000	0.000	0.00000	0.00000
652	684	c	0.000	0.000	0.00000	0.00000
684	652	a	1.609	-38.633	1.40420	0.93994
684	652	b	0.000	0.000	0.00000	0.00000
684	652	c	0.000	0.000	0.00000	0.00000
631	632	a	11.028	154.366	-10.89974	-4.42789
631	632	b	4.844	48.235	-5.26386	-0.91712
631	632	c	10.880	-76.980	-11.12608	-2.77163

632	631	a	11.028	-25.634	10.94584	4.72786
632	631	b	4.844	-131.764	5.23683	0.93949
632	631	c	10.880	103.021	11.28045	3.00416
631	671	a	10.845	-25.492	10.72974	4.32789
631	671	b	4.202	-128.536	4.60386	0.53712
631	671	c	9.653	105.144	9.95608	2.09163
671	631	a	10.845	154.507	-10.67393	-4.02823
671	631	b	4.202	51.463	-4.63349	-0.51750
671	631	c	9.653	-74.856	-9.82994	-1.92505
671	684	a	1.609	-38.632	1.40670	0.94226
671	684	b	0.000	0.000	0.00000	0.00000
671	684	c	1.788	127.438	1.81978	-0.36077
684	671	a	1.609	141.367	-1.40420	-0.93994
684	671	b	0.000	0.000	0.00000	0.00000
684	671	c	1.788	-52.563	-1.81585	0.36359

C.2 IEEE 34 NODE TEST FEEDER

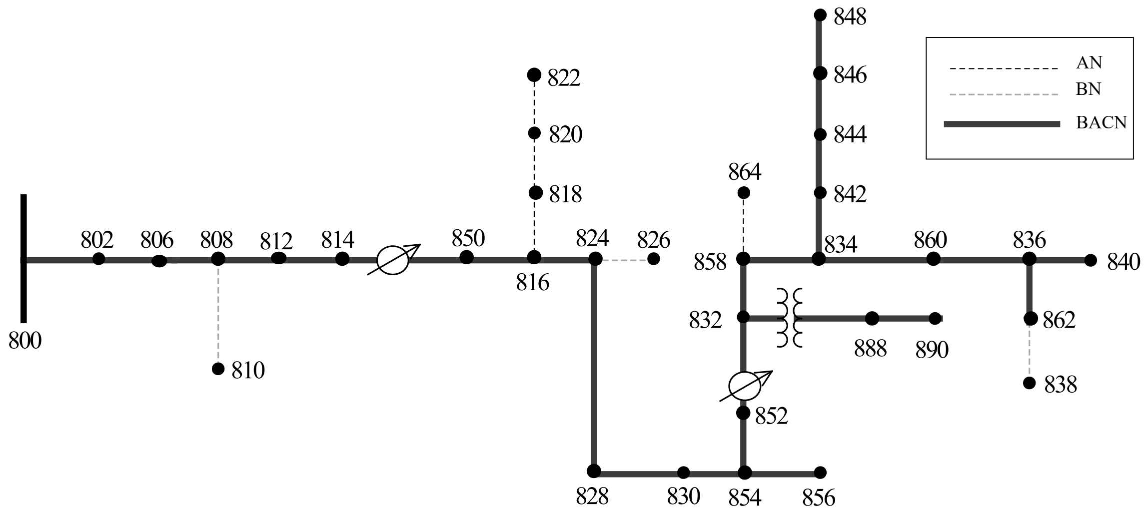

Node Voltage, Current and Power

		Mag. V	Ang. V	Mag. I	Ang. I	P	Q
800	a	1.0500	0.000	7.633	168.819	-7.862	-1.554
800	b	1.0500	-120.000	6.504	54.047	-6.792	-0.708
800	c	1.0500	120.000	6.017	-60.620	-6.317	-0.068
802	a	1.0474	-0.056	0.000	0.000	0.000	0.000
802	b	1.0485	-120.071	0.000	0.000	0.000	0.000
802	c	1.0484	119.945	0.000	0.000	0.000	0.000
806	a	1.0457	-0.094	0.000	0.000	0.000	0.000
806	b	1.0475	-120.119	0.000	0.000	0.000	0.000
806	c	1.0474	119.908	0.000	0.000	0.000	0.000
808	a	1.0130	-0.833	0.000	0.000	0.000	0.000
808	b	1.0300	-121.006	0.000	0.000	0.000	0.000
808	c	1.0288	119.244	0.000	0.000	0.000	0.000
810	a	0.0000	0.000	0.000	0.000	0.000	0.000
810	b	1.0298	-121.007	0.000	0.000	0.000	0.000
810	c	0.0000	0.000	0.000	0.000	0.000	0.000
812	a	0.9751	-1.752	0.000	0.000	0.000	0.000
812	b	1.0107	-122.035	0.000	0.000	0.000	0.000
812	c	1.0068	118.461	0.000	0.000	0.000	0.000
814	a	0.9451	-2.515	0.000	0.000	0.000	0.000
814	b	0.9956	-122.866	0.000	0.000	0.000	0.000
814	c	0.9892	117.829	0.000	0.000	0.000	0.000

816	a	1.0213	-2.521	0.000	0.000	0.000	0.000
816	b	1.0274	-122.874	0.000	0.000	0.000	0.000
816	c	1.0208	117.822	0.000	0.000	0.000	0.000
818	a	1.0204	-2.524	0.000	0.000	0.000	0.000
818	b	0.0000	0.000	0.000	0.000	0.000	0.000
818	c	0.0000	0.000	0.000	0.000	0.000	0.000
820	a	0.9967	-2.582	0.000	0.000	0.000	0.000
820	b	0.0000	0.000	0.000	0.000	0.000	0.000
820	c	0.0000	0.000	0.000	0.000	0.000	0.000
822	a	0.9937	-2.586	0.000	0.000	0.000	0.000
822	b	0.0000	0.000	0.000	0.000	0.000	0.000
822	c	0.0000	0.000	0.000	0.000	0.000	0.000
824	a	1.0121	-2.660	0.000	0.000	0.000	0.000
824	b	1.0180	-123.123	0.000	0.000	0.000	0.000
824	c	1.0123	117.549	0.000	0.000	0.000	0.000
826	a	0.0000	0.000	0.000	0.000	0.000	0.000
826	b	1.0178	-123.124	0.000	0.000	0.000	0.000
826	c	0.0000	0.000	0.000	0.000	0.000	0.000
828	a	1.0113	-2.673	0.000	0.000	0.000	0.000
828	b	1.0173	-123.142	0.000	0.000	0.000	0.000
828	c	1.0116	117.527	0.000	0.000	0.000	0.000
830	a	0.9931	-2.981	0.199	-39.367	0.159	0.117
830	b	1.0004	-123.621	0.112	-149.959	0.100	0.050
830	c	0.9944	116.980	0.191	107.375	0.187	0.032
832	a	1.0464	-3.559	0.000	0.000	0.000	0.000
832	b	1.0419	-124.496	0.000	0.000	0.000	0.000
832	c	1.0422	115.965	0.000	0.000	0.000	0.000
834	a	1.0414	-3.693	0.000	0.000	0.000	0.000
834	b	1.0369	-124.701	0.000	0.000	0.000	0.000
834	c	1.0375	115.724	0.000	0.000	0.000	0.000
836	a	1.0408	-3.684	0.000	0.000	0.000	0.000
836	b	1.0361	-124.704	0.000	0.000	0.000	0.000
836	c	1.0370	115.721	0.000	0.000	0.000	0.000
838	a	0.0000	0.000	0.000	0.000	0.000	0.000
838	b	1.0359	-124.706	0.000	0.000	0.000	0.000
838	c	0.0000	0.000	0.000	0.000	0.000	0.000
840	a	1.0407	-3.684	0.114	-37.875	0.098	0.067
840	b	1.0361	-124.704	0.114	-157.875	0.099	0.065
840	c	1.0369	115.721	0.114	82.125	0.098	0.065

842	a	1.0414	-3.698	0.000	0.000	0.000	0.000
842	b	1.0368	-124.706	0.000	0.000	0.000	0.000
842	c	1.0374	115.718	0.000	0.000	0.000	0.000
844	a	1.0411	-3.721	1.781	-41.596	1.463	1.138
844	b	1.0365	-124.731	1.773	-162.606	1.450	1.128
844	c	1.0372	115.692	1.774	77.817	1.452	1.130
846	a	1.0414	-3.765	0.000	0.000	0.000	0.000
846	b	1.0365	-124.777	0.000	0.000	0.000	0.000
846	c	1.0375	115.642	0.000	0.000	0.000	0.000
848	a	1.0414	-3.772	0.247	-42.964	0.199	0.162
848	b	1.0365	-124.784	0.247	-162.967	0.201	0.158
848	c	1.0375	115.634	0.247	77.034	0.200	0.160
850	a	1.0217	-2.515	0.000	0.000	0.000	0.000
850	b	1.0277	-122.866	0.000	0.000	0.000	0.000
850	c	1.0211	117.828	0.000	0.000	0.000	0.000
852	a	0.9614	-3.559	0.000	0.000	0.000	0.000
852	b	0.9703	-124.496	0.000	0.000	0.000	0.000
852	c	0.9640	115.965	0.000	0.000	0.000	0.000
854	a	0.9927	-2.989	0.000	0.000	0.000	0.000
854	b	1.0000	-123.633	0.000	0.000	0.000	0.000
854	c	0.9940	116.966	0.000	0.000	0.000	0.000
856	a	0.0000	0.000	0.000	0.000	0.000	0.000
856	b	0.9999	-123.640	0.000	0.000	0.000	0.000
856	c	0.0000	0.000	0.000	0.000	0.000	0.000
858	a	1.0441	-3.620	0.000	0.000	0.000	0.000
858	b	1.0396	-124.590	0.000	0.000	0.000	0.000
858	c	1.0400	115.855	0.000	0.000	0.000	0.000
860	a	1.0410	-3.686	0.246	-42.346	0.200	0.160
860	b	1.0365	-124.702	0.247	-163.361	0.200	0.160
860	c	1.0371	115.721	0.247	77.061	0.200	0.160
862	a	1.0408	-3.684	0.000	0.000	0.000	0.000
862	b	1.0361	-124.704	0.000	0.000	0.000	0.000
862	c	1.0370	115.720	0.000	0.000	0.000	0.000
864	a	1.0441	-3.620	0.000	0.000	0.000	0.000
864	b	0.0000	0.000	0.000	0.000	0.000	0.000
864	c	0.0000	0.000	0.000	0.000	0.000	0.000
888	a	1.0132	-5.277	0.000	0.000	0.000	0.000
888	b	1.0092	-126.252	0.000	0.000	0.000	0.000

888	c	1.0092	114.225	0.000	0.000	0.000	0.000
890	a	0.9319	-6.389	1.677	-26.565	1.467	0.539
890	b	0.9373	-127.810	1.677	-146.565	1.488	0.505
890	c	0.9288	112.806	1.677	93.435	1.469	0.517
90206	a	1.0465	-0.075	0.000	0.000	0.000	0.000
90206	b	1.0479	-120.095	0.320	-146.660	0.300	0.150
90206	c	1.0479	119.926	0.273	90.677	0.250	0.140
90810	a	0.0000	0.000	0.000	0.000	0.000	0.000
90810	b	1.0298	-121.007	0.179	-146.565	0.166	0.079
90810	c	0.0000	0.000	0.000	0.000	0.000	0.000
91624	a	1.0167	-2.591	0.000	0.000	0.000	0.000
91624	b	1.0227	-122.999	0.031	-111.801	0.031	-0.006
91624	c	1.0166	117.686	0.031	68.199	0.021	0.024
91820	a	1.0073	-2.562	0.383	-29.127	0.345	0.172
91820	b	0.0000	0.000	0.000	0.000	0.000	0.000
91820	c	0.0000	0.000	0.000	0.000	0.000	0.000
92022	a	0.9937	-2.586	1.530	-29.993	1.350	0.700
92022	b	0.0000	0.000	0.000	0.000	0.000	0.000
92022	c	0.0000	0.000	0.000	0.000	0.000	0.000
92426	a	0.0000	0.000	0.000	0.000	0.000	0.000
92426	b	1.0178	-123.124	0.447	-146.565	0.418	0.181
92426	c	0.0000	0.000	0.000	0.000	0.000	0.000
92428	a	1.0117	-2.667	0.000	0.000	0.000	0.000
92428	b	1.0177	-123.133	0.000	0.000	0.000	0.000
92428	c	1.0120	117.538	0.044	90.973	0.040	0.020
92830	a	1.0021	-2.828	0.076	-26.026	0.070	0.030
92830	b	1.0089	-123.381	0.000	0.000	0.000	0.000
92830	c	1.0030	117.256	0.000	0.000	0.000	0.000
93258	a	1.0452	-3.590	0.074	-26.489	0.071	0.030
93258	b	1.0407	-124.543	0.055	-165.534	0.043	0.037
93258	c	1.0411	115.910	0.048	105.683	0.050	0.009
93460	a	1.0411	-3.688	0.796	-53.768	0.532	0.635
93460	b	1.0367	-124.702	0.210	-147.430	0.201	0.084
93460	c	1.0372	115.721	0.810	111.254	0.837	0.065
93640	a	1.0407	-3.684	0.116	3.435	0.120	-0.015
93640	b	1.0361	-124.704	0.224	-143.261	0.220	0.074
93640	c	1.0369	115.721	0.142	63.435	0.090	0.116
94244	a	1.0412	-3.709	0.099	-32.764	0.090	0.050

94244	b	1.0367	-124.719	0.000	0.000	0.000	0.000
94244	c	1.0373	115.705	0.000	0.000	0.000	0.000
94446	a	1.0413	-3.742	0.000	0.000	0.000	0.000
94446	b	1.0364	-124.754	0.268	-150.395	0.250	0.120
94446	c	1.0373	115.666	0.220	86.855	0.200	0.110
94648	a	1.0414	-3.768	0.000	0.000	0.000	0.000
94648	b	1.0365	-124.781	0.246	-150.340	0.230	0.110
94648	c	1.0375	115.638	0.000	0.000	0.000	0.000
95456	a	0.0000	0.000	0.000	0.000	0.000	0.000
95456	b	0.9999	-123.639	0.045	-150.204	0.040	0.020
95456	c	0.0000	0.000	0.000	0.000	0.000	0.000
95834	a	1.0427	-3.656	0.096	-49.179	0.070	0.072
95834	b	1.0382	-124.646	0.110	-133.530	0.113	0.018
95834	c	1.0387	115.790	0.153	85.301	0.137	0.081
95864	a	1.0441	-3.620	0.021	-30.185	0.020	0.010
95864	b	0.0000	0.000	0.000	0.000	0.000	0.000
95864	c	0.0000	0.000	0.000	0.000	0.000	0.000
96036	a	1.0408	-3.685	0.390	-37.057	0.339	0.223
96036	b	1.0363	-124.702	0.229	-167.292	0.175	0.160
96036	c	1.0370	115.720	0.299	107.151	0.306	0.046
96238	a	0.0000	0.000	0.000	0.000	0.000	0.000
96238	b	1.0359	-124.706	0.302	-151.271	0.280	0.140
96238	c	0.0000	0.000	0.000	0.000	0.000	0.000

Current and Power Flow

			Magnitude	Angle	Active	Reactive
800	802	a	7.633	-11.181	7.86239	1.55414
800	802	b	6.504	-125.953	6.79227	0.70827
800	802	c	6.017	119.380	6.31743	0.06835
802	800	a	7.634	168.766	-7.84398	-1.54995
802	800	b	6.504	53.994	-6.78280	-0.70515
802	800	c	6.018	-60.682	-6.30895	-0.06901
816	818	a	1.867	-26.934	1.73644	0.78817
816	818	b	0.000	0.000	0.00000	0.00000
816	818	c	0.000	0.000	0.00000	0.00000
818	816	a	1.868	152.985	-1.73491	-0.79031
818	816	b	0.000	0.000	0.00000	0.00000
818	816	c	0.000	0.000	0.00000	0.00000
816	91624	a	5.295	-8.386	5.37983	0.55269

816	91624	b	5.856	-126.622	6.00334	0.39332
816	91624	c	5.626	118.150	5.74333	-0.03285
91624	816	a	5.296	171.474	-5.35533	-0.55677
91624	816	b	5.856	53.268	-5.97603	-0.38999
91624	816	c	5.628	-61.973	-5.72074	0.03399
824	91624	a	5.296	171.335	-5.33082	-0.56072
824	91624	b	5.826	53.079	-5.91781	-0.39287
824	91624	c	5.609	-61.853	-5.67777	0.05919
91624	824	a	5.296	-8.526	5.35533	0.55677
91624	824	b	5.826	-126.811	5.94484	0.39616
91624	824	c	5.608	118.269	5.70021	-0.05802
818	91820	a	1.868	-27.015	1.73491	0.79031
818	91820	b	0.000	0.000	0.00000	0.00000
818	91820	c	0.000	0.000	0.00000	0.00000
91820	818	a	1.885	151.869	-1.71315	-0.81969
91820	818	b	0.000	0.000	0.00000	0.00000
91820	818	c	0.000	0.000	0.00000	0.00000
820	91820	a	1.520	150.763	-1.35409	-0.67970
820	91820	b	0.000	0.000	0.00000	0.00000
820	91820	c	0.000	0.000	0.00000	0.00000
91820	820	a	1.503	-27.878	1.36819	0.64721
91820	820	b	0.000	0.000	0.00000	0.00000
91820	820	c	0.000	0.000	0.00000	0.00000
820	92022	a	1.520	-29.237	1.35409	0.67970
820	92022	b	0.000	0.000	0.00000	0.00000
820	92022	c	0.000	0.000	0.00000	0.00000
92022	820	a	1.525	150.383	-1.35000	-0.68878
92022	820	b	0.000	0.000	0.00000	0.00000
92022	820	c	0.000	0.000	0.00000	0.00000
822	92022	a	0.000	0.000	0.00000	0.00000
822	92022	b	0.000	0.000	0.00000	0.00000
822	92022	c	0.000	0.000	0.00000	0.00000
92022	822	a	0.011	87.414	0.00000	-0.01122
92022	822	b	0.000	0.000	0.00000	0.00000
92022	822	c	0.000	0.000	0.00000	0.00000
824	92426	a	0.000	0.000	0.00000	0.00000
824	92426	b	0.445	-145.963	0.41769	0.17592
824	92426	c	0.000	0.000	0.00000	0.00000

92426	824	a	0.000	0.000	0.00000	0.00000
92426	824	b	0.446	33.735	-0.41761	-0.17848
92426	824	c	0.000	0.000	0.00000	0.00000
826	92426	a	0.000	0.000	0.00000	0.00000
826	92426	b	0.000	0.000	0.00000	0.00000
826	92426	c	0.000	0.000	0.00000	0.00000
92426	826	a	0.000	0.000	0.00000	0.00000
92426	826	b	0.003	-33.124	0.00000	-0.00260
92426	826	c	0.000	0.000	0.00000	0.00000
824	92428	a	5.296	-8.665	5.33082	0.56072
824	92428	b	5.407	-125.382	5.50012	0.21695
824	92428	c	5.609	118.147	5.67777	-0.05919
92428	824	a	5.296	171.324	-5.32883	-0.56098
92428	824	b	5.407	54.608	-5.49824	-0.21688
92428	824	c	5.609	-61.863	-5.67587	0.05927
802	90206	a	7.634	-11.234	7.84398	1.54995
802	90206	b	6.504	-126.006	6.78280	0.70515
802	90206	c	6.018	119.318	6.30895	0.06901
90206	802	a	7.634	168.749	-7.83780	-1.54854
90206	802	b	6.504	53.976	-6.77963	-0.70409
90206	802	c	6.018	-60.703	-6.30610	-0.06923
828	92428	a	5.296	171.312	-5.32683	-0.56125
828	92428	b	5.407	54.599	-5.49635	-0.21680
828	92428	c	5.570	-61.666	-5.63401	0.07934
92428	828	a	5.296	-8.676	5.32883	0.56098
92428	828	b	5.407	-125.392	5.49824	0.21688
92428	828	c	5.570	118.344	5.63587	-0.07927
828	92830	a	5.296	-8.688	5.32683	0.56125
828	92830	b	5.407	-125.401	5.49635	0.21680
828	92830	c	5.570	118.334	5.63401	-0.07934
92830	828	a	5.297	171.037	-5.27823	-0.56740
92830	828	b	5.407	54.363	-5.45056	-0.21471
92830	828	c	5.572	-61.912	-5.58854	0.08118
830	92830	a	5.226	171.004	-5.16104	-0.54383
830	92830	b	5.406	54.129	-5.40454	-0.21230
830	92830	c	5.575	-62.155	-5.54304	0.08371
92830	830	a	5.225	-8.719	5.20823	0.53740
92830	830	b	5.407	-125.637	5.45056	0.21471
92830	830	c	5.572	118.088	5.58854	-0.08118

830	854	a	5.055	-7.858	5.00227	0.42684
830	854	b	5.305	-125.379	5.30447	0.16276
830	854	c	5.388	118.213	5.35623	-0.11532
854	830	a	5.055	172.127	-5.00002	-0.42722
854	830	b	5.305	54.609	-5.30221	-0.16267
854	830	c	5.388	-61.800	-5.35408	0.11537
832	93258	a	3.091	0.589	3.22557	-0.23392
832	93258	b	3.377	-116.634	3.48518	-0.48129
832	93258	c	3.524	128.406	3.58631	-0.79119
93258	832	a	3.090	-179.528	-3.22133	0.22876
93258	832	b	3.376	63.275	-3.48055	0.47788
93258	832	c	3.523	-51.690	-3.58250	0.78766
858	93258	a	3.023	-179.013	-3.14627	0.25353
858	93258	b	3.339	63.888	-3.43309	0.51173
858	93258	c	3.478	-51.481	-3.52930	0.79301
93258	858	a	3.024	1.105	3.15035	-0.25874
93258	858	b	3.340	-116.020	3.43763	-0.51518
93258	858	c	3.479	128.616	3.53299	-0.79659
832	888	a	1.677	-26.541	1.61541	0.68508
832	888	b	1.677	-146.544	1.61939	0.65585
832	888	c	1.677	93.456	1.61434	0.66899
888	832	a	1.677	153.459	-1.58331	-0.61615
888	832	b	1.677	33.456	-1.58729	-0.58692
888	832	c	1.677	-86.544	-1.58224	-0.60006
834	93460	a	1.601	-42.957	1.29055	1.05494
834	93460	b	1.301	-154.053	1.17540	0.66101
834	93460	c	1.535	99.715	1.53084	0.43922
93460	834	a	1.602	136.967	-1.28992	-1.05747
93460	834	b	1.302	25.858	-1.17503	-0.66320
93460	834	c	1.536	-80.369	-1.53080	-0.44155
860	93460	a	0.835	147.045	-0.75807	-0.42486
860	93460	b	1.095	24.469	-0.97422	-0.58143
860	93460	c	0.762	-92.902	-0.69374	-0.37860
93460	860	a	0.834	-32.793	0.75838	0.42220
93460	860	b	1.094	-155.426	0.97453	0.57920
93460	860	c	0.761	87.247	0.69351	0.37613
834	842	a	2.141	34.367	1.75588	-1.37481
834	842	b	2.353	-95.726	2.13462	-1.18201

834	842	c	2.184	150.864	1.85302	-1.30426
842	834	a	2.141	-145.647	-1.75563	1.37415
842	834	b	2.353	84.261	-2.13435	1.18148
842	834	c	2.184	-29.152	-1.85290	1.30368
806	90206	a	7.634	168.732	-7.83159	-1.54703
806	90206	b	6.206	54.999	-6.47683	-0.55329
806	90206	c	5.780	-59.426	-6.05350	0.07031
90206	806	a	7.634	-11.251	7.83780	1.54854
90206	806	b	6.206	-124.983	6.47963	0.55409
90206	806	c	5.780	120.596	6.05610	-0.07077
836	93640	a	0.215	-16.434	0.21831	0.04940
836	93640	b	0.335	-147.871	0.31898	0.13650
836	93640	c	0.251	72.047	0.18830	0.17977
93640	836	a	0.215	163.275	-0.21823	-0.05055
93640	836	b	0.335	31.975	-0.31893	-0.13749
93640	836	c	0.252	-108.102	-0.18843	-0.18084
840	93640	a	0.114	142.125	-0.09815	-0.06668
840	93640	b	0.114	22.125	-0.09888	-0.06463
840	93640	c	0.114	-97.875	-0.09848	-0.06542
93640	840	a	0.113	-37.392	0.09824	0.06553
93640	840	b	0.114	-157.456	0.09893	0.06364
93640	840	c	0.113	82.523	0.09835	0.06435
836	862	a	0.001	82.282	0.00005	-0.00075
836	862	b	0.298	-149.682	0.28008	0.13048
836	862	c	0.001	-147.150	-0.00009	-0.00070
862	836	a	0.000	0.000	0.00000	0.00000
862	836	b	0.298	30.206	-0.28004	-0.13112
862	836	c	0.000	0.000	0.00000	0.00000
842	94244	a	2.141	34.353	1.75563	-1.37415
842	94244	b	2.353	-95.739	2.13435	-1.18148
842	94244	c	2.184	150.848	1.85290	-1.30368
94244	842	a	2.140	-145.682	-1.75503	1.37254
94244	842	b	2.352	84.230	-2.13369	1.18020
94244	842	c	2.183	-29.190	-1.85261	1.30229
844	94244	a	2.102	-143.234	-1.66445	1.42093
844	94244	b	2.351	84.198	-2.13302	1.17892
844	94244	c	2.182	-29.228	-1.85231	1.30090
94244	844	a	2.103	36.800	1.66503	-1.42254

94244	844	b	2.352	-95.770	2.13369	-1.18020
94244	844	c	2.183	150.810	1.85261	-1.30229
844	94446	a	1.430	78.516	0.20110	-1.47513
844	94446	b	1.359	-63.710	0.68267	-1.23263
844	94446	c	1.362	-170.759	0.40000	-1.35469
94446	844	a	1.425	-101.496	-0.20024	1.47054
94446	844	b	1.356	116.215	-0.68191	1.22863
94446	844	c	1.358	9.167	-0.40000	1.35048
846	94446	a	1.421	-101.509	-0.19934	1.46592
846	94446	b	1.362	127.444	-0.43117	1.34466
846	94446	c	1.417	17.822	-0.19998	1.45628
94446	846	a	1.425	78.504	0.20024	-1.47054
94446	846	b	1.366	-52.512	0.43191	-1.34863
94446	846	c	1.421	-162.132	0.20000	-1.46048
846	94648	a	1.421	78.491	0.19934	-1.46592
846	94648	b	1.362	-52.556	0.43117	-1.34466
846	94648	c	1.417	-162.178	0.19998	-1.45628
94648	846	a	1.420	-101.510	-0.19921	1.46525
94648	846	b	1.362	127.438	-0.43106	1.34408
94648	846	c	1.416	17.816	-0.19998	1.45567
848	94648	a	1.419	-101.512	-0.19907	1.46458
848	94648	b	1.416	137.345	-0.20095	1.45351
848	94648	c	1.416	17.809	-0.19998	1.45505
94648	848	a	1.420	78.490	0.19921	-1.46525
94648	848	b	1.416	-42.653	0.20106	-1.45408
94648	848	c	1.416	-162.184	0.19998	-1.45567
816	850	a	7.090	166.809	-7.11627	-1.34086
816	850	b	5.856	53.378	-6.00334	-0.39332
816	850	c	5.626	-61.850	-5.74333	0.03285
850	816	a	7.090	-13.185	7.11901	1.34130
850	816	b	5.856	-126.616	6.00479	0.39355
850	816	c	5.626	118.157	5.74474	-0.03296
806	808	a	7.634	-11.268	7.83159	1.54703
806	808	b	6.206	-125.001	6.47683	0.55329
806	808	c	5.780	120.574	6.05350	-0.07031
808	806	a	7.645	168.091	-7.59998	-1.48779
808	806	b	6.208	54.310	-6.37262	-0.52215
808	806	c	5.789	-60.227	-5.95573	0.05502

832	852	a	4.646	171.116	-4.84098	-0.45116
832	852	b	4.902	53.545	-5.10457	-0.17456
832	852	c	4.992	-62.689	-5.20064	0.12220
852	832	a	5.057	-8.883	4.84102	0.45114
852	832	b	5.264	-126.455	5.10461	0.17456
852	832	c	5.396	117.312	5.20068	-0.12221
854	95456	a	0.000	0.000	0.00000	0.00000
854	95456	b	0.044	-98.729	0.04001	-0.01857
854	95456	c	0.000	0.000	0.00000	0.00000
95456	854	a	0.000	0.000	0.00000	0.00000
95456	854	b	0.040	55.341	-0.04000	-0.00071
95456	854	c	0.000	0.000	0.00000	0.00000
856	95456	a	0.000	0.000	0.00000	0.00000
856	95456	b	0.000	0.000	0.00000	0.00000
856	95456	c	0.000	0.000	0.00000	0.00000
95456	856	a	0.000	0.000	0.00000	0.00000
95456	856	b	0.019	-33.639	0.00000	-0.01929
95456	856	c	0.000	0.000	0.00000	0.00000
852	854	a	5.057	171.117	-4.84102	-0.45114
852	854	b	5.264	53.545	-5.10461	-0.17456
852	854	c	5.396	-62.688	-5.20068	0.12221
854	852	a	5.055	-7.873	5.00002	0.42722
854	852	b	5.265	-125.606	5.26220	0.18125
854	852	c	5.388	118.200	5.35408	-0.11537
858	95864	a	0.020	-23.113	0.02000	0.00708
858	95864	b	0.000	0.000	0.00000	0.00000
858	95864	c	0.000	0.000	0.00000	0.00000
95864	858	a	0.021	153.258	-0.02000	-0.00854
95864	858	b	0.000	0.000	0.00000	0.00000
95864	858	c	0.000	0.000	0.00000	0.00000
864	95864	a	0.000	0.000	0.00000	0.00000
864	95864	b	0.000	0.000	0.00000	0.00000
864	95864	c	0.000	0.000	0.00000	0.00000
95864	864	a	0.001	86.380	0.00000	-0.00146
95864	864	b	0.000	0.000	0.00000	0.00000
95864	864	c	0.000	0.000	0.00000	0.00000
858	95834	a	3.005	1.145	3.12627	-0.26061
858	95834	b	3.339	-116.112	3.43309	-0.51173
858	95834	c	3.478	128.519	3.52930	-0.79301

```
----------------------------------------------------------------------
95834  858    a      3.004  -178.997  -3.12148   0.25439
95834  858    b      3.338    63.778  -3.42768   0.50764
95834  858    c      3.478   -51.597  -3.52491   0.78878
----------------------------------------------------------------------
834    95834  a      2.941  -177.699  -3.04643   0.31987
834    95834  b      3.232    64.244  -3.31003   0.52100
834    95834  c      3.367   -49.936  -3.38386   0.86504
----------------------------------------------------------------------
95834  834    a      2.943     2.445   3.05103  -0.32614
95834  834    b      3.233  -115.643   3.31513  -0.52524
95834  834    c      3.367   130.183   3.38792  -0.86943
----------------------------------------------------------------------
860    96036  a      0.593   -29.076   0.55807   0.26486
860    96036  b      0.850  -153.262   0.77422   0.42143
860    96036  c      0.521    91.840   0.49374   0.21860
----------------------------------------------------------------------
96036  860    a      0.595   150.615  -0.55773  -0.26842
96036  860    b      0.852    26.556  -0.77390  -0.42443
96036  860    c      0.522   -88.465  -0.49411  -0.22191
----------------------------------------------------------------------
836    96036  a      0.215   163.756  -0.21836  -0.04865
836    96036  b      0.633    31.276  -0.59906  -0.26698
836    96036  c      0.251  -107.855  -0.18821  -0.17908
----------------------------------------------------------------------
96036  836    a      0.214   -15.332   0.21863   0.04507
96036  836    b      0.632  -148.471   0.59931   0.26394
96036  836    c      0.248    72.618   0.18780   0.17575
----------------------------------------------------------------------
808    90810  a      0.000     0.000   0.00000   0.00000
808    90810  b      0.175  -143.642   0.16622   0.06931
808    90810  c      0.000     0.000   0.00000   0.00000
----------------------------------------------------------------------
90810  808    a      0.000     0.000   0.00000   0.00000
90810  808    b      0.177    34.880  -0.16619  -0.07439
90810  808    c      0.000     0.000   0.00000   0.00000
----------------------------------------------------------------------
862    96238  a      0.000     0.000   0.00000   0.00000
862    96238  b      0.298  -149.794   0.28004   0.13112
862    96238  c      0.000     0.000   0.00000   0.00000
----------------------------------------------------------------------
96238  862    a      0.000     0.000   0.00000   0.00000
96238  862    b      0.300    29.463  -0.28000  -0.13555
96238  862    c      0.000     0.000   0.00000   0.00000
----------------------------------------------------------------------
838    96238  a      0.000     0.000   0.00000   0.00000
838    96238  b      0.000     0.000   0.00000   0.00000
838    96238  c      0.000     0.000   0.00000   0.00000
----------------------------------------------------------------------
96238  838    a      0.000     0.000   0.00000   0.00000
96238  838    b      0.004   -34.706   0.00000  -0.00445
```

```
96238  838    c      0.000     0.000   0.00000   0.00000
----------------------------------------------------------------------
888    890    a      1.677   -26.541   1.58331   0.61615
888    890    b      1.677  -146.544   1.58729   0.58692
888    890    c      1.677    93.456   1.58224   0.60006
----------------------------------------------------------------------
890    888    a      1.677   153.435  -1.46692  -0.53904
890    888    b      1.677    33.435  -1.48838  -0.50538
890    888    c      1.677   -86.565  -1.46942  -0.51664
----------------------------------------------------------------------
810    90810  a      0.000     0.000   0.00000   0.00000
810    90810  b      0.000     0.000   0.00000   0.00000
810    90810  c      0.000     0.000   0.00000   0.00000
----------------------------------------------------------------------
90810  810    a      0.000     0.000   0.00000   0.00000
90810  810    b      0.005   -31.007   0.00000  -0.00509
90810  810    c      0.000     0.000   0.00000   0.00000
----------------------------------------------------------------------
808    812    a      7.645   -11.909   7.59998   1.48779
808    812    b      6.042  -125.179   6.20640   0.45284
808    812    c      5.789   119.773   5.95573  -0.05502
----------------------------------------------------------------------
812    808    a      7.657   167.369  -7.33175  -1.40909
812    808    b      6.043    54.013  -6.09377  -0.42103
812    808    c      5.800   -61.137  -5.83873   0.04093
----------------------------------------------------------------------
812    814    a      7.657   -12.631   7.33175   1.40909
812    814    b      6.043  -125.987   6.09377   0.42103
812    814    c      5.800   118.863   5.83873  -0.04093
----------------------------------------------------------------------
814    812    a      7.665   166.815  -7.11910  -1.34131
814    812    b      6.045    53.384  -6.00483  -0.39356
814    812    c      5.808   -61.843  -5.74478   0.03296
----------------------------------------------------------------------
814    850    a      7.665   -13.185   7.11910   1.34131
814    850    b      6.045  -126.616   6.00483   0.39356
814    850    c      5.808   118.157   5.74478  -0.03296
----------------------------------------------------------------------
850    814    a      7.090   166.815  -7.11901  -1.34130
850    814    b      5.856    53.384  -6.00479  -0.39355
850    814    c      5.626   -61.843  -5.74474   0.03296
----------------------------------------------------------------------
```

C.3 IEEE 123 NODE TEST FEEDER

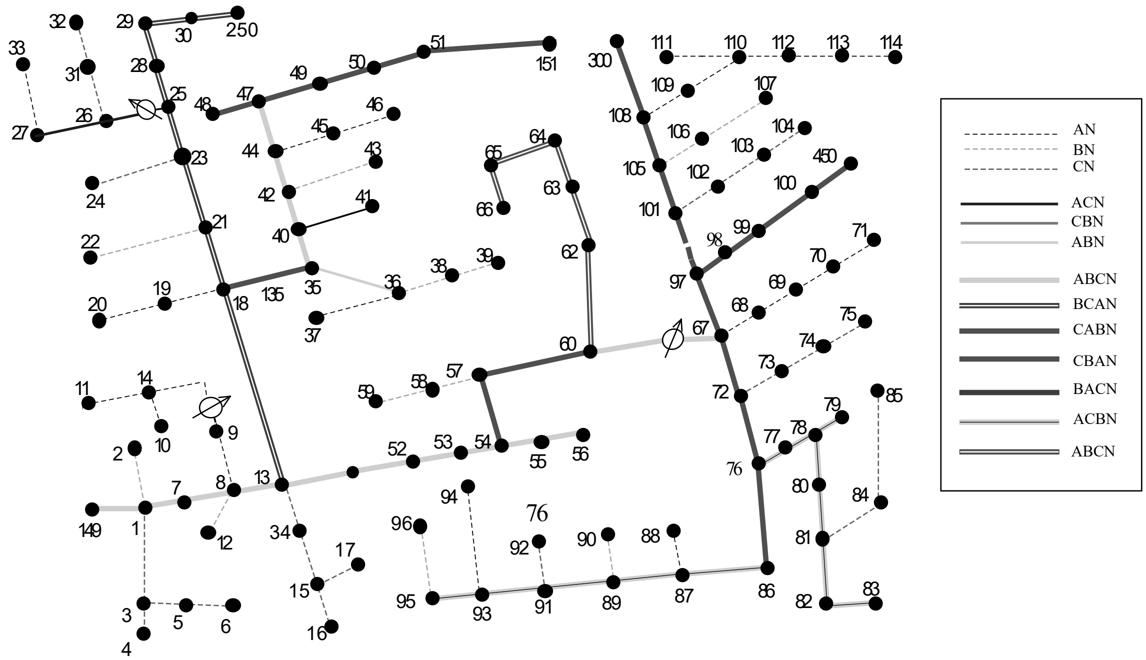

Node Voltage, Current and Power

		Mag. V	Ang. V	Mag. I	Ang. I	P	Q
1	a	1.0313	-0.644	0.434	-27.209	0.400	0.200
1	b	1.0411	-120.311	0.000	0.000	0.000	0.000
1	c	1.0347	119.615	0.000	0.000	0.000	0.000
2	a	0.0000	0.000	0.000	0.000	0.000	0.000
2	b	1.0409	-120.315	0.215	-146.880	0.200	0.100
2	c	0.0000	0.000	0.000	0.000	0.000	0.000
3	a	0.0000	0.000	0.000	0.000	0.000	0.000
3	b	0.0000	0.000	0.000	0.000	0.000	0.000
3	c	1.0331	119.584	0.000	0.000	0.000	0.000
4	a	0.0000	0.000	0.000	0.000	0.000	0.000
4	b	0.0000	0.000	0.000	0.000	0.000	0.000
4	c	1.0326	119.574	0.433	93.009	0.400	0.200
5	a	0.0000	0.000	0.000	0.000	0.000	0.000
5	b	0.0000	0.000	0.000	0.000	0.000	0.000
5	c	1.0318	119.559	0.224	93.435	0.207	0.102
6	a	0.0000	0.000	0.000	0.000	0.000	0.000
6	b	0.0000	0.000	0.000	0.000	0.000	0.000
6	c	1.0311	119.546	0.461	92.981	0.425	0.213

7	a	1.0222	-1.117	0.219	-27.683	0.200	0.100
7	b	1.0394	-120.560	0.000	0.000	0.000	0.000
7	c	1.0290	119.361	0.000	0.000	0.000	0.000
8	a	1.0162	-1.432	0.000	0.000	0.000	0.000
8	b	1.0382	-120.725	0.000	0.000	0.000	0.000
8	c	1.0252	119.186	0.000	0.000	0.000	0.000
9	a	1.0148	-1.460	0.441	-28.025	0.400	0.200
9	b	0.0000	0.000	0.000	0.000	0.000	0.000
9	c	0.0000	0.000	0.000	0.000	0.000	0.000
10	a	1.0065	-1.501	0.224	-26.565	0.204	0.095
10	b	0.0000	0.000	0.000	0.000	0.000	0.000
10	c	0.0000	0.000	0.000	0.000	0.000	0.000
11	a	1.0061	-1.507	0.450	-28.072	0.405	0.202
11	b	0.0000	0.000	0.000	0.000	0.000	0.000
11	c	0.0000	0.000	0.000	0.000	0.000	0.000
12	a	0.0000	0.000	0.000	0.000	0.000	0.000
12	b	1.0379	-120.731	0.215	-147.296	0.200	0.100
12	c	0.0000	0.000	0.000	0.000	0.000	0.000
13	a	1.0084	-1.868	0.000	0.000	0.000	0.000
13	b	1.0360	-120.958	0.000	0.000	0.000	0.000
13	c	1.0195	118.899	0.000	0.000	0.000	0.000
14	a	1.0068	-1.494	0.000	0.000	0.000	0.000
14	b	0.0000	0.000	0.000	0.000	0.000	0.000
14	c	0.0000	0.000	0.000	0.000	0.000	0.000
15	a	0.0000	0.000	0.000	0.000	0.000	0.000
15	b	0.0000	0.000	0.000	0.000	0.000	0.000
15	c	1.0182	118.872	0.000	0.000	0.000	0.000
16	a	0.0000	0.000	0.000	0.000	0.000	0.000
16	b	0.0000	0.000	0.000	0.000	0.000	0.000
16	c	1.0172	118.854	0.440	92.289	0.400	0.200
17	a	0.0000	0.000	0.000	0.000	0.000	0.000
17	b	0.0000	0.000	0.000	0.000	0.000	0.000
17	c	1.0177	118.864	0.220	92.299	0.200	0.100
18	a	0.9995	-2.299	0.000	0.000	0.000	0.000
18	b	1.0319	-121.208	0.000	0.000	0.000	0.000
18	c	1.0121	118.830	0.000	0.000	0.000	0.000
19	a	0.9982	-2.326	0.448	-28.891	0.400	0.200
19	b	0.0000	0.000	0.000	0.000	0.000	0.000

19	c	0.0000	0.000	0.000	0.000	0.000	0.000
20	a	0.9973	-2.345	0.447	-26.565	0.407	0.183
20	b	0.0000	0.000	0.000	0.000	0.000	0.000
20	c	0.0000	0.000	0.000	0.000	0.000	0.000
21	a	0.9990	-2.353	0.000	0.000	0.000	0.000
21	b	1.0320	-121.206	0.000	0.000	0.000	0.000
21	c	1.0109	118.808	0.000	0.000	0.000	0.000
22	a	0.0000	0.000	0.000	0.000	0.000	0.000
22	b	1.0305	-121.233	0.461	-147.798	0.425	0.212
22	c	0.0000	0.000	0.000	0.000	0.000	0.000
23	a	0.9986	-2.408	0.000	0.000	0.000	0.000
23	b	1.0324	-121.189	0.000	0.000	0.000	0.000
23	c	1.0098	118.792	0.000	0.000	0.000	0.000
24	a	0.0000	0.000	0.000	0.000	0.000	0.000
24	b	0.0000	0.000	0.000	0.000	0.000	0.000
24	c	1.0083	118.764	0.444	92.199	0.400	0.200
25	a	0.9979	-2.466	0.000	0.000	0.000	0.000
25	b	1.0328	-121.179	0.000	0.000	0.000	0.000
25	c	1.0089	118.792	0.000	0.000	0.000	0.000
26	a	0.9977	-2.493	0.000	0.000	0.000	0.000
26	b	0.0000	0.000	0.000	0.000	0.000	0.000
26	c	1.0021	118.782	0.000	0.000	0.000	0.000
27	a	0.9973	-2.512	0.000	0.000	0.000	0.000
27	b	0.0000	0.000	0.000	0.000	0.000	0.000
27	c	1.0021	118.791	0.000	0.000	0.000	0.000
28	a	0.9976	-2.493	0.447	-26.565	0.407	0.182
28	b	1.0331	-121.177	0.000	0.000	0.000	0.000
28	c	1.0085	118.796	0.000	0.000	0.000	0.000
29	a	0.9974	-2.514	0.446	-29.079	0.398	0.199
29	b	1.0332	-121.171	0.000	0.000	0.000	0.000
29	c	1.0081	118.790	0.000	0.000	0.000	0.000
30	a	0.9977	-2.517	0.000	0.000	0.000	0.000
30	b	1.0332	-121.159	0.000	0.000	0.000	0.000
30	c	1.0076	118.768	0.444	92.203	0.400	0.200
31	a	0.0000	0.000	0.000	0.000	0.000	0.000
31	b	0.0000	0.000	0.000	0.000	0.000	0.000
31	c	1.0015	118.770	0.223	92.205	0.200	0.100
32	a	0.0000	0.000	0.000	0.000	0.000	0.000

32	b	0.0000	0.000	0.000	0.000	0.000	0.000
32	c	1.0011	118.763	0.223	92.198	0.200	0.100
33	a	0.9961	-2.541	0.447	-26.565	0.407	0.181
33	b	0.0000	0.000	0.000	0.000	0.000	0.000
33	c	0.0000	0.000	0.000	0.000	0.000	0.000
34	a	0.0000	0.000	0.000	0.000	0.000	0.000
34	b	0.0000	0.000	0.000	0.000	0.000	0.000
34	c	1.0186	118.880	0.456	92.315	0.415	0.207
35	a	0.9967	-2.388	0.256	2.140	0.255	-0.020
35	b	1.0294	-121.293	0.256	-177.860	0.145	0.220
35	c	1.0110	118.769	0.000	0.000	0.000	0.000
36	a	0.9958	-2.407	0.000	0.000	0.000	0.000
36	b	1.0290	-121.340	0.000	0.000	0.000	0.000
36	c	0.0000	0.000	0.000	0.000	0.000	0.000
37	a	0.9950	-2.423	0.445	-28.988	0.396	0.198
37	b	0.0000	0.000	0.000	0.000	0.000	0.000
37	c	0.0000	0.000	0.000	0.000	0.000	0.000
38	a	0.0000	0.000	0.000	0.000	0.000	0.000
38	b	1.0283	-121.353	0.224	-146.565	0.208	0.098
38	c	0.0000	0.000	0.000	0.000	0.000	0.000
39	a	0.0000	0.000	0.000	0.000	0.000	0.000
39	b	1.0279	-121.361	0.218	-147.926	0.200	0.100
39	c	0.0000	0.000	0.000	0.000	0.000	0.000
40	a	0.9952	-2.424	0.000	0.000	0.000	0.000
40	b	1.0283	-121.339	0.000	0.000	0.000	0.000
40	c	1.0100	118.723	0.000	0.000	0.000	0.000
41	a	0.0000	0.000	0.000	0.000	0.000	0.000
41	b	0.0000	0.000	0.000	0.000	0.000	0.000
41	c	1.0095	118.715	0.221	92.150	0.200	0.100
42	a	0.9936	-2.460	0.225	-29.025	0.200	0.100
42	b	1.0271	-121.390	0.000	0.000	0.000	0.000
42	c	1.0091	118.685	0.000	0.000	0.000	0.000
43	a	0.0000	0.000	0.000	0.000	0.000	0.000
43	b	1.0258	-121.415	0.459	-147.980	0.421	0.210
43	c	0.0000	0.000	0.000	0.000	0.000	0.000
44	a	0.9926	-2.490	0.000	0.000	0.000	0.000
44	b	1.0264	-121.417	0.000	0.000	0.000	0.000
44	c	1.0083	118.654	0.000	0.000	0.000	0.000

45	a	0.9920	-2.502	0.224	-26.565	0.203	0.090
45	b	0.0000	0.000	0.000	0.000	0.000	0.000
45	c	0.0000	0.000	0.000	0.000	0.000	0.000
46	a	0.9916	-2.509	0.225	-29.074	0.200	0.100
46	b	0.0000	0.000	0.000	0.000	0.000	0.000
46	c	0.0000	0.000	0.000	0.000	0.000	0.000
47	a	0.9915	-2.512	0.430	-35.538	0.358	0.232
47	b	1.0253	-121.448	0.430	-155.538	0.365	0.247
47	c	1.0073	118.606	0.430	84.462	0.359	0.243
48	a	0.9913	-2.520	0.853	-38.058	0.688	0.491
48	b	1.0251	-121.454	0.882	-156.992	0.736	0.525
48	c	1.0070	118.596	0.866	83.058	0.710	0.507
49	a	0.9913	-2.520	0.434	-38.058	0.350	0.250
49	b	1.0248	-121.456	0.839	-156.994	0.700	0.500
49	c	1.0069	118.581	0.400	88.837	0.350	0.200
50	a	0.9912	-2.531	0.000	0.000	0.000	0.000
50	b	1.0248	-121.447	0.000	0.000	0.000	0.000
50	c	1.0066	118.570	0.444	92.005	0.400	0.200
51	a	0.9911	-2.539	0.226	-29.104	0.200	0.100
51	b	1.0249	-121.449	0.000	0.000	0.000	0.000
51	c	1.0066	118.574	0.000	0.000	0.000	0.000
52	a	1.0025	-2.246	0.446	-28.811	0.400	0.200
52	b	1.0347	-121.203	0.000	0.000	0.000	0.000
52	c	1.0163	118.649	0.000	0.000	0.000	0.000
53	a	0.9998	-2.424	0.447	-28.989	0.400	0.200
53	b	1.0340	-121.324	0.000	0.000	0.000	0.000
53	c	1.0148	118.517	0.000	0.000	0.000	0.000
54	a	0.9983	-2.527	0.000	0.000	0.000	0.000
54	b	1.0334	-121.398	0.000	0.000	0.000	0.000
54	c	1.0138	118.430	0.000	0.000	0.000	0.000
55	a	0.9981	-2.531	0.223	-29.096	0.199	0.100
55	b	1.0333	-121.407	0.000	0.000	0.000	0.000
55	c	1.0139	118.433	0.000	0.000	0.000	0.000
56	a	0.9981	-2.525	0.000	0.000	0.000	0.000
56	b	1.0332	-121.415	0.216	-147.980	0.200	0.100
56	c	1.0140	118.432	0.000	0.000	0.000	0.000
57	a	0.9953	-2.835	0.000	0.000	0.000	0.000
57	b	1.0307	-121.602	0.000	0.000	0.000	0.000
57	c	1.0112	118.217	0.000	0.000	0.000	0.000

58	a	0.0000	0.000	0.000	0.000	0.000	0.000
58	b	1.0301	-121.615	0.224	-146.565	0.209	0.097
58	c	0.0000	0.000	0.000	0.000	0.000	0.000
59	a	0.0000	0.000	0.000	0.000	0.000	0.000
59	b	1.0297	-121.621	0.217	-148.186	0.200	0.100
59	c	0.0000	0.000	0.000	0.000	0.000	0.000
60	a	0.9889	-3.525	0.226	-30.090	0.200	0.100
60	b	1.0259	-121.997	0.000	0.000	0.000	0.000
60	c	1.0051	117.763	0.000	0.000	0.000	0.000
61	a	0.9889	-3.525	0.000	0.000	0.000	0.000
61	b	1.0259	-121.997	0.000	0.000	0.000	0.000
61	c	1.0051	117.763	0.000	0.000	0.000	0.000
62	a	0.9881	-3.520	0.000	0.000	0.000	0.000
62	b	1.0247	-121.974	0.000	0.000	0.000	0.000
62	c	1.0030	117.750	0.449	91.185	0.402	0.201
63	a	0.9875	-3.509	0.453	-30.074	0.400	0.200
63	b	1.0239	-121.966	0.000	0.000	0.000	0.000
63	c	1.0020	117.741	0.000	0.000	0.000	0.000
64	a	0.9872	-3.487	0.000	0.000	0.000	0.000
64	b	1.0220	-121.935	0.828	-145.017	0.778	0.332
64	c	0.9999	117.710	0.000	0.000	0.000	0.000
65	a	0.9865	-3.497	0.652	-49.246	0.449	0.461
65	b	1.0216	-121.893	0.433	-157.582	0.359	0.258
65	c	0.9969	117.704	0.660	92.261	0.594	0.283
66	a	0.9867	-3.521	0.000	0.000	0.000	0.000
66	b	1.0219	-121.867	0.000	0.000	0.000	0.000
66	c	0.9954	117.702	0.831	92.685	0.750	0.350
67	a	1.0391	-3.773	0.000	0.000	0.000	0.000
67	b	1.0314	-122.178	0.000	0.000	0.000	0.000
67	c	1.0354	117.626	0.000	0.000	0.000	0.000
68	a	1.0376	-3.801	0.216	-30.366	0.200	0.100
68	b	0.0000	0.000	0.000	0.000	0.000	0.000
68	c	0.0000	0.000	0.000	0.000	0.000	0.000
69	a	1.0358	-3.834	0.432	-30.399	0.400	0.200
69	b	0.0000	0.000	0.000	0.000	0.000	0.000
69	c	0.0000	0.000	0.000	0.000	0.000	0.000
70	a	1.0346	-3.858	0.216	-30.423	0.200	0.100
70	b	0.0000	0.000	0.000	0.000	0.000	0.000

70	c	0.0000	0.000	0.000	0.000	0.000	0.000
71	a	1.0339	-3.871	0.433	-30.436	0.400	0.200
71	b	0.0000	0.000	0.000	0.000	0.000	0.000
71	c	0.0000	0.000	0.000	0.000	0.000	0.000
72	a	1.0395	-3.870	0.000	0.000	0.000	0.000
72	b	1.0305	-122.280	0.000	0.000	0.000	0.000
72	c	1.0352	117.507	0.000	0.000	0.000	0.000
73	a	0.0000	0.000	0.000	0.000	0.000	0.000
73	b	0.0000	0.000	0.000	0.000	0.000	0.000
73	c	1.0330	117.467	0.433	90.902	0.400	0.200
74	a	0.0000	0.000	0.000	0.000	0.000	0.000
74	b	0.0000	0.000	0.000	0.000	0.000	0.000
74	c	1.0312	117.432	0.461	90.867	0.425	0.213
75	a	0.0000	0.000	0.000	0.000	0.000	0.000
75	b	0.0000	0.000	0.000	0.000	0.000	0.000
75	c	1.0302	117.413	0.434	90.847	0.400	0.200
76	a	1.0395	-3.935	1.107	-29.721	1.036	0.501
76	b	1.0300	-122.379	1.089	-163.610	0.843	0.739
76	c	1.0358	117.456	0.860	84.462	0.747	0.485
77	a	1.0407	-3.999	0.000	0.000	0.000	0.000
77	b	1.0312	-122.459	0.434	-149.024	0.400	0.200
77	c	1.0367	117.380	0.000	0.000	0.000	0.000
78	a	1.0410	-4.018	0.000	0.000	0.000	0.000
78	b	1.0316	-122.473	0.000	0.000	0.000	0.000
78	c	1.0369	117.362	0.000	0.000	0.000	0.000
79	a	1.0407	-4.033	0.465	-30.598	0.433	0.217
79	b	1.0318	-122.475	0.000	0.000	0.000	0.000
79	c	1.0368	117.371	0.000	0.000	0.000	0.000
80	a	1.0431	-4.079	0.000	0.000	0.000	0.000
80	b	1.0333	-122.533	0.433	-149.098	0.400	0.200
80	c	1.0377	117.255	0.000	0.000	0.000	0.000
81	a	1.0452	-4.155	0.000	0.000	0.000	0.000
81	b	1.0356	-122.565	0.000	0.000	0.000	0.000
81	c	1.0383	117.154	0.000	0.000	0.000	0.000
82	a	1.0461	-4.191	0.428	-30.756	0.400	0.200
82	b	1.0369	-122.594	0.000	0.000	0.000	0.000
82	c	1.0391	117.122	0.000	0.000	0.000	0.000
83	a	1.0473	-4.213	0.000	0.000	0.000	0.000

83	b	1.0380	-122.621	0.000	0.000	0.000	0.000
83	c	1.0399	117.080	0.215	90.515	0.200	0.100
84	a	0.0000	0.000	0.000	0.000	0.000	0.000
84	b	0.0000	0.000	0.000	0.000	0.000	0.000
84	c	1.0357	117.105	0.216	90.540	0.200	0.100
85	a	0.0000	0.000	0.000	0.000	0.000	0.000
85	b	0.0000	0.000	0.000	0.000	0.000	0.000
85	c	1.0345	117.083	0.432	90.517	0.400	0.200
86	a	1.0386	-3.963	0.000	0.000	0.000	0.000
86	b	1.0283	-122.544	0.217	-149.109	0.200	0.100
86	c	1.0372	117.426	0.000	0.000	0.000	0.000
87	a	1.0381	-3.986	0.000	0.000	0.000	0.000
87	b	1.0275	-122.636	0.435	-149.201	0.400	0.200
87	c	1.0378	117.407	0.000	0.000	0.000	0.000
88	a	1.0380	-4.016	0.431	-30.581	0.400	0.200
88	b	0.0000	0.000	0.000	0.000	0.000	0.000
88	c	0.0000	0.000	0.000	0.000	0.000	0.000
89	a	1.0376	-3.981	0.000	0.000	0.000	0.000
89	b	1.0273	-122.683	0.000	0.000	0.000	0.000
89	c	1.0382	117.397	0.000	0.000	0.000	0.000
90	a	0.0000	0.000	0.000	0.000	0.000	0.000
90	b	1.0272	-122.724	0.447	-146.565	0.420	0.186
90	c	0.0000	0.000	0.000	0.000	0.000	0.000
91	a	1.0374	-3.978	0.000	0.000	0.000	0.000
91	b	1.0270	-122.698	0.000	0.000	0.000	0.000
91	c	1.0384	117.381	0.000	0.000	0.000	0.000
92	a	0.0000	0.000	0.000	0.000	0.000	0.000
92	b	0.0000	0.000	0.000	0.000	0.000	0.000
92	c	1.0384	117.329	0.431	90.764	0.400	0.200
93	a	1.0371	-3.984	0.000	0.000	0.000	0.000
93	b	1.0268	-122.714	0.000	0.000	0.000	0.000
93	c	1.0385	117.387	0.000	0.000	0.000	0.000
94	a	1.0364	-3.998	0.432	-30.563	0.400	0.200
94	b	0.0000	0.000	0.000	0.000	0.000	0.000
94	c	0.0000	0.000	0.000	0.000	0.000	0.000
95	a	1.0371	-3.975	0.000	0.000	0.000	0.000
95	b	1.0264	-122.732	0.218	-149.297	0.200	0.100
95	c	1.0387	117.384	0.000	0.000	0.000	0.000

96	a	0.0000	0.000	0.000	0.000	0.000	0.000
96	b	1.0262	-122.737	0.218	-149.302	0.200	0.100
96	c	0.0000	0.000	0.000	0.000	0.000	0.000
97	a	1.0381	-3.825	0.000	0.000	0.000	0.000
97	b	1.0309	-122.200	0.000	0.000	0.000	0.000
97	c	1.0347	117.608	0.000	0.000	0.000	0.000
98	a	1.0379	-3.836	0.431	-30.401	0.400	0.200
98	b	1.0307	-122.208	0.000	0.000	0.000	0.000
98	c	1.0344	117.598	0.000	0.000	0.000	0.000
99	a	1.0382	-3.824	0.000	0.000	0.000	0.000
99	b	1.0298	-122.217	0.434	-148.782	0.400	0.200
99	c	1.0341	117.559	0.000	0.000	0.000	0.000
100	a	1.0384	-3.827	0.000	0.000	0.000	0.000
100	b	1.0298	-122.204	0.000	0.000	0.000	0.000
100	c	1.0337	117.540	0.462	90.975	0.427	0.214
101	a	1.0373	-3.869	0.000	0.000	0.000	0.000
101	b	1.0307	-122.214	0.000	0.000	0.000	0.000
101	c	1.0341	117.598	0.000	0.000	0.000	0.000
102	a	0.0000	0.000	0.000	0.000	0.000	0.000
102	b	0.0000	0.000	0.000	0.000	0.000	0.000
102	c	1.0327	117.571	0.217	91.006	0.200	0.100
103	a	0.0000	0.000	0.000	0.000	0.000	0.000
103	b	0.0000	0.000	0.000	0.000	0.000	0.000
103	c	1.0310	117.540	0.434	90.975	0.400	0.200
104	a	0.0000	0.000	0.000	0.000	0.000	0.000
104	b	0.0000	0.000	0.000	0.000	0.000	0.000
104	c	1.0292	117.506	0.435	90.941	0.400	0.200
105	a	1.0360	-3.911	0.000	0.000	0.000	0.000
105	b	1.0305	-122.258	0.000	0.000	0.000	0.000
105	c	1.0344	117.627	0.000	0.000	0.000	0.000
106	a	0.0000	0.000	0.000	0.000	0.000	0.000
106	b	1.0294	-122.280	0.434	-148.845	0.400	0.200
106	c	0.0000	0.000	0.000	0.000	0.000	0.000
107	a	0.0000	0.000	0.000	0.000	0.000	0.000
107	b	1.0279	-122.308	0.435	-148.873	0.400	0.200
107	c	0.0000	0.000	0.000	0.000	0.000	0.000
108	a	1.0345	-3.981	0.000	0.000	0.000	0.000
108	b	1.0312	-122.271	0.000	0.000	0.000	0.000
108	c	1.0342	117.668	0.000	0.000	0.000	0.000

109	a	1.0304	-4.060	0.434	-30.625	0.400	0.200
109	b	0.0000	0.000	0.000	0.000	0.000	0.000
109	c	0.0000	0.000	0.000	0.000	0.000	0.000
110	a	1.0285	-4.099	0.000	0.000	0.000	0.000
110	b	0.0000	0.000	0.000	0.000	0.000	0.000
110	c	0.0000	0.000	0.000	0.000	0.000	0.000
111	a	1.0277	-4.113	0.218	-30.678	0.200	0.100
111	b	0.0000	0.000	0.000	0.000	0.000	0.000
111	c	0.0000	0.000	0.000	0.000	0.000	0.000
112	a	1.0278	-4.113	0.224	-26.565	0.212	0.088
112	b	0.0000	0.000	0.000	0.000	0.000	0.000
112	c	0.0000	0.000	0.000	0.000	0.000	0.000
113	a	1.0257	-4.152	0.459	-30.717	0.421	0.210
113	b	0.0000	0.000	0.000	0.000	0.000	0.000
113	c	0.0000	0.000	0.000	0.000	0.000	0.000
114	a	1.0253	-4.160	0.218	-30.725	0.200	0.100
114	b	0.0000	0.000	0.000	0.000	0.000	0.000
114	c	0.0000	0.000	0.000	0.000	0.000	0.000
149	a	1.0436	0.000	15.120	159.019	-14.733	-5.650
149	b	1.0436	-120.000	9.840	41.079	-9.714	-3.330
149	c	1.0436	120.000	12.069	-78.209	-11.965	-3.936
151	a	0.9911	-2.539	0.000	0.000	0.000	0.000
151	b	1.0249	-121.449	0.000	0.000	0.000	0.000
151	c	1.0066	118.574	0.000	0.000	0.000	0.000
250	a	0.9977	-2.517	0.000	0.000	0.000	0.000
250	b	1.0332	-121.159	0.000	0.000	0.000	0.000
250	c	1.0076	118.768	0.000	0.000	0.000	0.000
300	a	1.0345	-3.981	0.000	0.000	0.000	0.000
300	b	1.0312	-122.271	0.000	0.000	0.000	0.000
300	c	1.0342	117.668	0.000	0.000	0.000	0.000
450	a	1.0384	-3.827	0.000	0.000	0.000	0.000
450	b	1.0298	-122.204	0.000	0.000	0.000	0.000
450	c	1.0337	117.540	0.000	0.000	0.000	0.000

Current and Power Flow

			Magnitude	Angle	Active	Reactive
1	2	a	0.000	0.000	0.00000	0.00000
1	2	b	0.215	-146.878	0.20004	0.10003
1	2	c	0.000	0.000	0.00000	0.00000

2	1	a	0.000	0.000	0.00000	0.00000
2	1	b	0.215	33.120	-0.20000	-0.10000
2	1	c	0.000	0.000	0.00000	0.00000
8	13	a	13.370	-20.109	12.87210	4.35139
8	13	b	9.414	-138.549	9.30406	2.99152
8	13	c	10.966	102.675	10.77834	3.19497
13	8	a	13.371	159.891	-12.80525	-4.22046
13	8	b	9.414	41.450	-9.29651	-2.94748
13	8	c	10.966	-77.325	-10.73463	-3.12350
101	102	a	0.000	0.000	0.00000	0.00000
101	102	b	0.000	0.000	0.00000	0.00000
101	102	c	1.085	90.970	1.00280	0.50278
102	101	a	0.000	0.000	0.00000	0.00000
102	101	b	0.000	0.000	0.00000	0.00000
102	101	c	1.085	-89.030	-1.00165	-0.50162
101	105	a	1.551	-30.082	1.44378	0.71083
101	105	b	0.869	-148.850	0.80101	0.40173
101	105	c	0.000	-156.669	0.00001	-0.00014
105	101	a	1.551	149.918	-1.44246	-0.70890
105	101	b	0.869	31.149	-0.80120	-0.40109
105	101	c	0.000	23.333	-0.00001	0.00012
102	103	a	0.000	0.000	0.00000	0.00000
102	103	b	0.000	0.000	0.00000	0.00000
102	103	c	0.868	90.961	0.80165	0.40162
103	102	a	0.000	0.000	0.00000	0.00000
103	102	b	0.000	0.000	0.00000	0.00000
103	102	c	0.868	-89.040	-0.80058	-0.40055
103	104	a	0.000	0.000	0.00000	0.00000
103	104	b	0.000	0.000	0.00000	0.00000
103	104	c	0.435	90.945	0.40058	0.20055
104	103	a	0.000	0.000	0.00000	0.00000
104	103	b	0.000	0.000	0.00000	0.00000
104	103	c	0.435	-89.059	-0.40000	-0.20000
105	106	a	0.000	0.000	0.00000	0.00000
105	106	b	0.870	-148.857	0.80122	0.40119
105	106	c	0.000	0.000	0.00000	0.00000
106	105	a	0.000	0.000	0.00000	0.00000
106	105	b	0.870	31.143	-0.80047	-0.40045

```
106    105    c      0.000     0.000   0.00000   0.00000
--------------------------------------------------------------------
105    108    a      1.551   -30.082   1.44246   0.70890
105    108    b      0.000   -24.392  -0.00001  -0.00011
105    108    c      0.000  -156.667   0.00001  -0.00012
--------------------------------------------------------------------
108    105    a      1.551   149.917  -1.44129  -0.70616
108    105    b      0.000   155.608   0.00001   0.00008
108    105    c      0.000    23.334  -0.00001   0.00009
--------------------------------------------------------------------
106    107    a      0.000     0.000   0.00000   0.00000
106    107    b      0.435  -148.870   0.40047   0.20045
106    107    c      0.000     0.000   0.00000   0.00000
--------------------------------------------------------------------
107    106    a      0.000     0.000   0.00000   0.00000
107    106    b      0.435    31.127  -0.40000  -0.20000
107    106    c      0.000     0.000   0.00000   0.00000
--------------------------------------------------------------------
108    109    a      1.551   -30.086   1.44128   0.70623
108    109    b      0.000     0.000   0.00000   0.00000
108    109    c      0.000     0.000   0.00000   0.00000
--------------------------------------------------------------------
109    108    a      1.551   149.914  -1.43656  -0.70146
109    108    b      0.000     0.000   0.00000   0.00000
109    108    c      0.000     0.000   0.00000   0.00000
--------------------------------------------------------------------
108    300    a      0.000    82.535   0.00000  -0.00007
108    300    b      0.000   -24.392  -0.00001  -0.00008
108    300    c      0.000  -156.666   0.00001  -0.00009
--------------------------------------------------------------------
300    108    a      0.000   180.000   0.00000   0.00000
300    108    b      0.000   -90.000   0.00000   0.00000
300    108    c      0.000   -90.000   0.00000   0.00000
--------------------------------------------------------------------
109    110    a      1.117   -29.877   1.03656   0.50146
109    110    b      0.000     0.000   0.00000   0.00000
109    110    c      0.000     0.000   0.00000   0.00000
--------------------------------------------------------------------
110    109    a      1.117   150.122  -1.03492  -0.49982
110    109    b      0.000     0.000   0.00000   0.00000
110    109    c      0.000     0.000   0.00000   0.00000
--------------------------------------------------------------------
9      14     a      0.669   -27.568   0.60990   0.29889
9      14     b      0.000     0.000   0.00000   0.00000
9      14     c      0.000     0.000   0.00000   0.00000
--------------------------------------------------------------------
14     9      a      0.674   152.430  -0.60906  -0.29806
14     9      b      0.000     0.000   0.00000   0.00000
14     9      c      0.000     0.000   0.00000   0.00000
--------------------------------------------------------------------
110    111    a      0.218   -30.672   0.20012   0.10009
```

110	111	b	0.000	0.000	0.00000	0.00000
110	111	c	0.000	0.000	0.00000	0.00000
111	110	a	0.218	149.322	-0.20000	-0.10000
111	110	b	0.000	0.000	0.00000	0.00000
111	110	c	0.000	0.000	0.00000	0.00000
110	112	a	0.900	-29.686	0.83481	0.39973
110	112	b	0.000	0.000	0.00000	0.00000
110	112	c	0.000	0.000	0.00000	0.00000
112	110	a	0.900	150.314	-0.83436	-0.39928
112	110	b	0.000	0.000	0.00000	0.00000
112	110	c	0.000	0.000	0.00000	0.00000
112	113	a	0.677	-30.717	0.62196	0.31151
112	113	b	0.000	0.000	0.00000	0.00000
112	113	c	0.000	0.000	0.00000	0.00000
113	112	a	0.677	149.281	-0.62091	-0.31047
113	112	b	0.000	0.000	0.00000	0.00000
113	112	c	0.000	0.000	0.00000	0.00000
113	114	a	0.218	-30.721	0.20007	0.10005
113	114	b	0.000	0.000	0.00000	0.00000
113	114	c	0.000	0.000	0.00000	0.00000
114	113	a	0.218	149.275	-0.20000	-0.10000
114	113	b	0.000	0.000	0.00000	0.00000
114	113	c	0.000	0.000	0.00000	0.00000
18	35	a	3.263	-30.931	2.86292	1.56298
18	35	b	3.279	-155.831	2.78439	1.92247
18	35	c	2.357	86.832	2.02320	1.26414
35	18	a	3.263	149.069	-2.85738	-1.55426
35	18	b	3.279	24.169	-2.78049	-1.91368
35	18	c	2.357	-93.169	-2.02239	-1.26067
1	149	a	15.120	159.019	-14.62118	-5.41916
1	149	b	9.840	41.079	-9.70858	-3.26929
1	149	c	12.069	-78.209	-11.88868	-3.82250
149	1	a	15.120	-20.981	14.73261	5.64961
149	1	b	9.840	-138.921	9.71369	3.32969
149	1	c	12.069	101.791	11.96471	3.93577
13	52	a	8.000	-13.641	7.89706	1.64590
13	52	b	5.922	-128.357	6.08353	0.78993
13	52	c	6.385	112.467	6.46923	0.72929

```
52     13     a      8.000   166.359  -7.86145  -1.58446
52     13     b      5.922    51.643  -6.07958  -0.76304
52     13     c      6.385   -67.533  -6.45201  -0.69893
----------------------------------------------------------------------
60     67     a      5.806    -5.070   5.73954   0.15481
60     67     b      4.184  -119.234   4.28688  -0.20685
60     67     c      4.615   120.823   4.63193  -0.24768
----------------------------------------------------------------------
67     60     a      5.516   174.930  -5.72990  -0.12980
67     60     b      4.158    60.765  -4.28249   0.22019
67     60     c      4.471   -59.177  -4.62192   0.25816
----------------------------------------------------------------------
97     101    a      1.551   -30.081   1.44437   0.71246
97     101    b      0.869  -148.849   0.80110   0.40202
97     101    c      1.085    90.978   1.00326   0.50305
----------------------------------------------------------------------
101    97     a      1.551   149.918  -1.44378  -0.71083
101    97     b      0.869    31.150  -0.80101  -0.40173
101    97     c      1.085   -89.023  -1.00281  -0.50264
----------------------------------------------------------------------
13     34     a      0.000     0.000   0.00000   0.00000
13     34     b      0.000     0.000   0.00000   0.00000
13     34     c      1.115    92.304   1.01637   0.50885
----------------------------------------------------------------------
34     13     a      0.000     0.000   0.00000   0.00000
34     13     b      0.000     0.000   0.00000   0.00000
34     13     c      1.115   -87.697  -1.01556  -0.50804
----------------------------------------------------------------------
13     18     a      5.496   -29.547   4.90819   2.57456
13     18     b      3.736  -154.840   3.21298   2.15755
13     18     c      3.684    88.773   3.24902   1.88536
----------------------------------------------------------------------
18     13     a      5.496   150.453  -4.88383  -2.51515
18     13     b      3.736    25.159  -3.20968  -2.13519
18     13     c      3.684   -91.228  -3.22757  -1.86776
----------------------------------------------------------------------
11     14     a      0.450   151.928  -0.40492  -0.20246
11     14     b      0.000     0.000   0.00000   0.00000
11     14     c      0.000     0.000   0.00000   0.00000
----------------------------------------------------------------------
14     11     a      0.450   -28.070   0.40514   0.20267
14     11     b      0.000     0.000   0.00000   0.00000
14     11     c      0.000     0.000   0.00000   0.00000
----------------------------------------------------------------------
10     14     a      0.224   153.435  -0.20386  -0.09534
10     14     b      0.000     0.000   0.00000   0.00000
10     14     c      0.000     0.000   0.00000   0.00000
----------------------------------------------------------------------
14     10     a      0.224   -26.562   0.20392   0.09538
14     10     b      0.000     0.000   0.00000   0.00000
14     10     c      0.000     0.000   0.00000   0.00000
```

15	16	a	0.000	0.000	0.00000	0.00000
15	16	b	0.000	0.000	0.00000	0.00000
15	16	c	0.440	92.291	0.40032	0.20030
16	15	a	0.000	0.000	0.00000	0.00000
16	15	b	0.000	0.000	0.00000	0.00000
16	15	c	0.440	-87.711	-0.40000	-0.20000
15	17	a	0.000	0.000	0.00000	0.00000
15	17	b	0.000	0.000	0.00000	0.00000
15	17	c	0.220	92.303	0.20007	0.10006
17	15	a	0.000	0.000	0.00000	0.00000
17	15	b	0.000	0.000	0.00000	0.00000
17	15	c	0.220	-87.701	-0.20000	-0.10000
18	19	a	0.895	-27.728	0.80792	0.38412
18	19	b	0.000	0.000	0.00000	0.00000
18	19	c	0.000	0.000	0.00000	0.00000
19	18	a	0.895	152.272	-0.80704	-0.38325
19	18	b	0.000	0.000	0.00000	0.00000
19	18	c	0.000	0.000	0.00000	0.00000
18	21	a	1.340	-27.393	1.21300	0.56805
18	21	b	0.461	-147.780	0.42529	0.21271
18	21	c	1.331	92.210	1.20437	0.60362
21	18	a	1.340	152.606	-1.21289	-0.56663
21	18	b	0.461	32.217	-0.42531	-0.21276
21	18	c	1.331	-87.791	-1.20319	-0.60248
1	3	a	0.000	0.000	0.00000	0.00000
1	3	b	0.000	0.000	0.00000	0.00000
1	3	c	1.118	93.085	1.03481	0.51661
3	1	a	0.000	0.000	0.00000	0.00000
3	1	b	0.000	0.000	0.00000	0.00000
3	1	c	1.118	-86.915	-1.03345	-0.51524
19	20	a	0.447	-26.563	0.40704	0.18325
19	20	b	0.000	0.000	0.00000	0.00000
19	20	c	0.000	0.000	0.00000	0.00000
20	19	a	0.447	153.435	-0.40676	-0.18297
20	19	b	0.000	0.000	0.00000	0.00000
20	19	c	0.000	0.000	0.00000	0.00000
21	22	a	0.000	0.000	0.00000	0.00000
21	22	b	0.461	-147.795	0.42530	0.21287

21	22	c	0.000	0.000	0.00000	0.00000
22	21	a	0.000	0.000	0.00000	0.00000
22	21	b	0.461	32.202	-0.42481	-0.21241
22	21	c	0.000	0.000	0.00000	0.00000
21	23	a	1.340	-27.394	1.21289	0.56663
21	23	b	0.000	-34.861	0.00001	-0.00011
21	23	c	1.331	92.209	1.20319	0.60248
23	21	a	1.340	152.605	-1.21296	-0.56527
23	21	b	0.000	145.141	-0.00001	0.00010
23	21	c	1.331	-87.792	-1.20200	-0.60149
23	24	a	0.000	0.000	0.00000	0.00000
23	24	b	0.000	0.000	0.00000	0.00000
23	24	c	0.444	92.202	0.40047	0.20045
24	23	a	0.000	0.000	0.00000	0.00000
24	23	b	0.000	0.000	0.00000	0.00000
24	23	c	0.444	-87.801	-0.40000	-0.20000
23	25	a	1.340	-27.395	1.21296	0.56527
23	25	b	0.000	-34.859	0.00001	-0.00010
23	25	c	0.888	92.211	0.80153	0.40104
25	23	a	1.340	152.604	-1.21275	-0.56371
25	23	b	0.000	145.142	0.00000	0.00008
25	23	c	0.888	-87.790	-0.80082	-0.40071
25	26	a	0.447	-26.557	0.40739	0.18216
25	26	b	0.000	0.000	0.00000	0.00000
25	26	c	0.444	92.209	0.40042	0.20037
26	25	a	0.447	153.440	-0.40738	-0.18195
26	25	b	0.000	0.000	0.00000	0.00000
26	25	c	0.447	-87.794	-0.40026	-0.20022
25	28	a	0.893	-27.815	0.80536	0.38154
25	28	b	0.000	-34.858	0.00000	-0.00008
25	28	c	0.444	92.212	0.40040	0.20033
28	25	a	0.893	152.184	-0.80525	-0.38104
28	25	b	0.000	145.143	0.00000	0.00006
28	25	c	0.444	-87.790	-0.40025	-0.20031
26	27	a	0.447	-26.560	0.40738	0.18195
26	27	b	0.000	0.000	0.00000	0.00000
26	27	c	0.000	-142.291	0.00000	-0.00002
27	26	a	0.447	153.438	-0.40730	-0.18177

27	26	b	0.000	0.000	0.00000	0.00000
27	26	c	0.000	0.000	0.00000	0.00000
26	31	a	0.000	0.000	0.00000	0.00000
26	31	b	0.000	0.000	0.00000	0.00000
26	31	c	0.447	92.204	0.40026	0.20024
31	26	a	0.000	0.000	0.00000	0.00000
31	26	b	0.000	0.000	0.00000	0.00000
31	26	c	0.447	-87.797	-0.40007	-0.20005
27	33	a	0.447	-26.562	0.40730	0.18177
27	33	b	0.000	0.000	0.00000	0.00000
27	33	c	0.000	0.000	0.00000	0.00000
33	27	a	0.447	153.435	-0.40686	-0.18135
33	27	b	0.000	0.000	0.00000	0.00000
33	27	c	0.000	0.000	0.00000	0.00000
1	7	a	14.689	-20.797	14.22118	5.21916
1	7	b	9.627	-138.744	9.50855	3.16926
1	7	c	10.966	102.675	10.85387	3.30588
7	1	a	14.689	159.203	-14.13729	-5.05628
7	1	b	9.627	41.256	-9.50632	-3.12267
7	1	c	10.966	-77.325	-10.80837	-3.23969
28	29	a	0.446	-29.071	0.39792	0.19907
28	29	b	0.000	-34.857	0.00000	-0.00006
28	29	c	0.444	92.210	0.40025	0.20031
29	28	a	0.446	150.926	-0.39793	-0.19892
29	28	b	0.000	145.144	0.00000	0.00004
29	28	c	0.444	-87.792	-0.40010	-0.20020
29	30	a	0.000	83.661	0.00000	-0.00005
29	30	b	0.000	-34.856	0.00000	-0.00004
29	30	c	0.444	92.208	0.40010	0.20020
30	29	a	0.000	-96.339	0.00000	0.00002
30	29	b	0.000	145.146	0.00000	0.00001
30	29	c	0.444	-87.795	-0.40000	-0.19998
30	250	a	0.000	83.661	0.00000	-0.00002
30	250	b	0.000	-34.854	0.00000	-0.00001
30	250	c	0.000	-143.750	0.00000	-0.00002
250	30	a	0.000	0.000	0.00000	0.00000
250	30	b	0.000	90.000	0.00000	0.00000
250	30	c	0.000	0.000	0.00000	0.00000

31	32	a	0.000	0.000	0.00000	0.00000
31	32	b	0.000	0.000	0.00000	0.00000
31	32	c	0.223	92.201	0.20007	0.10005
32	31	a	0.000	0.000	0.00000	0.00000
32	31	b	0.000	0.000	0.00000	0.00000
32	31	c	0.223	-87.802	-0.20000	-0.10000
15	34	a	0.000	0.000	0.00000	0.00000
15	34	b	0.000	0.000	0.00000	0.00000
15	34	c	0.659	-87.705	-0.60039	-0.30036
34	15	a	0.000	0.000	0.00000	0.00000
34	15	b	0.000	0.000	0.00000	0.00000
34	15	c	0.659	92.295	0.60058	0.30055
35	36	a	0.445	-28.982	0.39655	0.19853
35	36	b	0.441	-147.228	0.40833	0.19858
35	36	c	0.000	0.000	0.00000	0.00000
36	35	a	0.445	151.014	-0.39625	-0.19824
36	35	b	0.441	32.767	-0.40831	-0.19820
36	35	c	0.000	0.000	0.00000	0.00000
35	40	a	2.609	-34.337	2.20619	1.37589
35	40	b	2.605	-155.168	2.22680	1.49494
35	40	c	2.357	86.831	2.02239	1.26067
40	35	a	2.609	145.662	-2.20376	-1.37244
40	35	b	2.605	24.831	-2.22550	-1.49151
40	35	c	2.357	-93.169	-2.02129	-1.25778
36	37	a	0.445	-28.986	0.39625	0.19824
36	37	b	0.000	0.000	0.00000	0.00000
36	37	c	0.000	0.000	0.00000	0.00000
37	36	a	0.445	151.012	-0.39599	-0.19800
37	36	b	0.000	0.000	0.00000	0.00000
37	36	c	0.000	0.000	0.00000	0.00000
36	38	a	0.000	0.000	0.00000	0.00000
36	38	b	0.441	-147.233	0.40831	0.19820
36	38	c	0.000	0.000	0.00000	0.00000
38	36	a	0.000	0.000	0.00000	0.00000
38	36	b	0.441	32.766	-0.40810	-0.19800
38	36	c	0.000	0.000	0.00000	0.00000
38	39	a	0.000	0.000	0.00000	0.00000
38	39	b	0.218	-147.922	0.20007	0.10005
38	39	c	0.000	0.000	0.00000	0.00000

39	38	a	0.000	0.000	0.00000	0.00000
39	38	b	0.218	32.074	-0.20000	-0.10000
39	38	c	0.000	0.000	0.00000	0.00000
3	4	a	0.000	0.000	0.00000	0.00000
3	4	b	0.000	0.000	0.00000	0.00000
3	4	c	0.433	93.011	0.40016	0.20016
4	3	a	0.000	0.000	0.00000	0.00000
4	3	b	0.000	0.000	0.00000	0.00000
4	3	c	0.433	-86.991	-0.40000	-0.20000
40	41	a	0.000	0.000	0.00000	0.00000
40	41	b	0.000	0.000	0.00000	0.00000
40	41	c	0.221	92.154	0.20007	0.10005
41	40	a	0.000	0.000	0.00000	0.00000
41	40	b	0.000	0.000	0.00000	0.00000
41	40	c	0.221	-87.850	-0.20000	-0.10000
40	42	a	2.609	-34.338	2.20376	1.37244
40	42	b	2.605	-155.169	2.22550	1.49151
40	42	c	2.137	86.280	1.82123	1.15772
42	40	a	2.609	145.662	-2.20113	-1.36893
42	40	b	2.605	24.831	-2.22437	-1.48793
42	40	c	2.137	-93.721	-1.82039	-1.15552
42	43	a	0.000	0.000	0.00000	0.00000
42	43	b	0.459	-147.977	0.42135	0.21088
42	43	c	0.000	0.000	0.00000	0.00000
43	42	a	0.000	0.000	0.00000	0.00000
43	42	b	0.459	32.020	-0.42089	-0.21044
43	42	c	0.000	0.000	0.00000	0.00000
42	44	a	2.385	-34.839	2.00113	1.26893
42	44	b	2.151	-156.699	1.80302	1.27705
42	44	c	2.137	86.279	1.82039	1.15552
44	42	a	2.385	145.161	-1.99965	-1.26650
44	42	b	2.151	23.301	-1.80237	-1.27533
44	42	c	2.137	-93.721	-1.81954	-1.15359
44	45	a	0.449	-27.822	0.40279	0.19067
44	45	b	0.000	0.000	0.00000	0.00000
44	45	c	0.000	0.000	0.00000	0.00000
45	44	a	0.449	152.177	-0.40262	-0.19050
45	44	b	0.000	0.000	0.00000	0.00000

45	44	c	0.000	0.000	0.00000	0.00000
44	47	a	1.940	-36.459	1.59686	1.07583
44	47	b	2.151	-156.699	1.80237	1.27533
44	47	c	2.137	86.279	1.81954	1.15359
47	44	a	1.940	143.540	-1.59562	-1.07413
47	44	b	2.151	23.300	-1.80118	-1.27303
47	44	c	2.137	-93.722	-1.81870	-1.15094
45	46	a	0.225	-29.071	0.20007	0.10005
45	46	b	0.000	0.000	0.00000	0.00000
45	46	c	0.000	0.000	0.00000	0.00000
46	45	a	0.225	150.926	-0.20000	-0.10000
46	45	b	0.000	0.000	0.00000	0.00000
46	45	c	0.000	0.000	0.00000	0.00000
47	48	a	0.853	-38.057	0.68795	0.49152
47	48	b	0.882	-156.992	0.73565	0.52558
47	48	c	0.866	83.059	0.70995	0.50728
48	47	a	0.853	141.942	-0.68782	-0.49130
48	47	b	0.882	23.008	-0.73551	-0.52536
48	47	c	0.866	-96.942	-0.70988	-0.50706
47	49	a	0.658	-34.991	0.55010	0.35017
47	49	b	0.839	-156.988	0.70029	0.50026
47	49	c	0.844	90.509	0.75018	0.40049
49	47	a	0.658	145.007	-0.55000	-0.35002
49	47	b	0.839	23.010	-0.69999	-0.49991
49	47	c	0.844	-89.492	-0.75011	-0.40007
49	50	a	0.226	-29.089	0.20000	0.10002
49	50	b	0.000	-27.191	-0.00001	-0.00009
49	50	c	0.444	92.014	0.40011	0.20007
50	49	a	0.226	150.907	-0.20002	-0.09999
50	49	b	0.000	152.810	0.00000	0.00006
50	49	c	0.444	-87.988	-0.40001	-0.19994
3	5	a	0.000	0.000	0.00000	0.00000
3	5	b	0.000	0.000	0.00000	0.00000
3	5	c	0.685	93.132	0.63328	0.31509
5	3	a	0.000	0.000	0.00000	0.00000
5	3	b	0.000	0.000	0.00000	0.00000
5	3	c	0.685	-86.870	-0.63262	-0.31443
50	51	a	0.226	-29.093	0.20002	0.09999

50	51	b	0.000	-27.190	0.00000	-0.00006
50	51	c	0.000	-159.697	0.00001	-0.00006
51	50	a	0.226	150.904	-0.20000	-0.09997
51	50	b	0.000	152.810	0.00000	0.00004
51	50	c	0.000	20.303	-0.00001	0.00004
51	151	a	0.000	91.566	0.00000	-0.00003
51	151	b	0.000	-27.190	0.00000	-0.00004
51	151	c	0.000	-159.697	0.00001	-0.00004
151	51	a	0.000	0.000	0.00000	0.00000
151	51	b	0.000	0.000	0.00000	0.00000
151	51	c	0.000	-90.000	0.00000	0.00000
52	53	a	7.570	-12.757	7.46145	1.38446
52	53	b	5.922	-128.357	6.07958	0.76304
52	53	c	6.385	112.467	6.45201	0.69893
53	52	a	7.570	167.243	-7.44579	-1.35767
53	52	b	5.922	51.643	-6.07670	-0.74971
53	52	c	6.385	-67.534	-6.44363	-0.68301
53	54	a	7.142	-11.754	7.04579	1.15767
53	54	b	5.922	-128.357	6.07670	0.74971
53	54	c	6.385	112.466	6.44363	0.68301
54	53	a	7.142	168.246	-7.03727	-1.14320
54	53	b	5.922	51.643	-6.07433	-0.74146
54	53	c	6.385	-67.534	-6.43854	-0.67259
54	55	a	0.223	-29.087	0.19927	0.09961
54	55	b	0.216	-147.969	0.20002	0.10004
54	55	c	0.000	-155.577	0.00000	-0.00004
55	54	a	0.223	150.909	-0.19924	-0.09960
55	54	b	0.216	32.025	-0.20002	-0.10002
55	54	c	0.000	24.423	0.00000	0.00002
54	57	a	6.929	-11.205	6.83799	1.04359
54	57	b	5.718	-127.629	5.87431	0.64142
54	57	c	6.385	112.466	6.43854	0.67263
57	54	a	6.929	168.795	-6.82252	-1.00383
57	54	b	5.718	52.370	-5.86110	-0.61886
57	54	c	6.385	-67.534	-6.42439	-0.64700
55	56	a	0.000	95.950	0.00000	-0.00002
55	56	b	0.216	-147.975	0.20002	0.10002
55	56	c	0.000	-155.577	0.00000	-0.00002

56	55	a	0.000	0.000	0.00000	0.00000
56	55	b	0.216	32.020	-0.20000	-0.10000
56	55	c	0.000	-90.000	0.00000	0.00000
57	58	a	0.000	0.000	0.00000	0.00000
57	58	b	0.441	-147.361	0.40909	0.19740
57	58	c	0.000	0.000	0.00000	0.00000
58	57	a	0.000	0.000	0.00000	0.00000
58	57	b	0.441	32.638	-0.40888	-0.19720
58	57	c	0.000	0.000	0.00000	0.00000
57	60	a	6.929	-11.205	6.82252	1.00383
57	60	b	5.305	-126.023	5.45200	0.42146
57	60	c	6.385	112.466	6.42439	0.64700
60	57	a	6.929	168.795	-6.79057	-0.91573
60	57	b	5.305	53.977	-5.42918	-0.38216
60	57	c	6.385	-67.535	-6.39047	-0.59252
58	59	a	0.000	0.000	0.00000	0.00000
58	59	b	0.217	-148.183	0.20005	0.10004
58	59	c	0.000	0.000	0.00000	0.00000
59	58	a	0.000	0.000	0.00000	0.00000
59	58	b	0.217	31.814	-0.20000	-0.10000
59	58	c	0.000	0.000	0.00000	0.00000
5	6	a	0.000	0.000	0.00000	0.00000
5	6	b	0.000	0.000	0.00000	0.00000
5	6	c	0.461	92.983	0.42548	0.21285
6	5	a	0.000	0.000	0.00000	0.00000
6	5	b	0.000	0.000	0.00000	0.00000
6	5	c	0.461	-87.019	-0.42525	-0.21262
60	61	a	0.000	91.336	0.00000	-0.00004
60	61	b	0.000	-39.854	0.00001	-0.00004
60	61	c	0.000	-148.894	0.00000	-0.00004
61	60	a	0.000	-90.000	0.00000	0.00000
61	60	b	0.000	-90.000	0.00000	0.00000
61	60	c	0.000	90.000	0.00000	0.00000
60	62	a	1.090	-41.360	0.85103	0.66096
60	62	b	1.253	-149.276	1.14229	0.58906
60	62	c	1.939	92.224	1.75854	0.84024
62	60	a	1.090	138.632	-0.85029	-0.66070
62	60	b	1.253	30.716	-1.14080	-0.58905
62	60	c	1.939	-87.781	-1.75515	-0.83833

62	63	a	1.090	-41.368	0.85029	0.66070
62	63	b	1.253	-149.284	1.14080	0.58905
62	63	c	1.491	92.530	1.35272	0.63712
63	62	a	1.090	138.627	-0.84964	-0.66058
63	62	b	1.253	30.711	-1.13975	-0.58885
63	62	c	1.491	-87.474	-1.35148	-0.63641
63	64	a	0.652	-49.197	0.44964	0.46058
63	64	b	1.253	-149.289	1.13975	0.58885
63	64	c	1.491	92.526	1.35148	0.63641
64	63	a	0.652	130.787	-0.44930	-0.46083
64	63	b	1.253	30.700	-1.13733	-0.58865
64	63	c	1.491	-87.483	-1.34893	-0.63457
64	65	a	0.652	-49.213	0.44930	0.46083
64	65	b	0.432	-157.521	0.35921	0.25704
64	65	c	1.491	92.517	1.34893	0.63457
65	64	a	0.652	130.768	-0.44907	-0.46074
65	64	b	0.432	22.444	-0.35891	-0.25755
65	64	c	1.491	-87.494	-1.34495	-0.63284
65	66	a	0.000	86.491	0.00000	-0.00023
65	66	b	0.000	-31.880	0.00000	-0.00025
65	66	c	0.831	92.700	0.75112	0.35032
66	65	a	0.000	0.000	0.00000	0.00000
66	65	b	0.000	0.000	0.00000	0.00000
66	65	c	0.831	-87.315	-0.75000	-0.35000
67	68	a	1.296	-30.408	1.20369	0.60368
67	68	b	0.000	0.000	0.00000	0.00000
67	68	c	0.000	0.000	0.00000	0.00000
68	67	a	1.296	149.592	-1.20222	-0.60221
68	67	b	0.000	0.000	0.00000	0.00000
68	67	c	0.000	0.000	0.00000	0.00000
67	72	a	2.906	23.614	2.68088	-1.38885
67	72	b	3.092	-107.219	3.08071	-0.82311
67	72	c	3.222	134.643	3.19030	-0.97639
72	67	a	2.906	-156.386	-2.67967	1.39397
72	67	b	3.092	72.781	-3.07664	0.82789
72	67	c	3.222	-45.358	-3.18765	0.98279
67	97	a	1.982	-30.146	1.84534	0.91497
67	97	b	1.304	-148.820	1.20178	0.60292

67	97	c	1.547	90.983	1.43163	0.71824
97	67	a	1.982	149.853	-1.84442	-0.91242
97	67	b	1.304	31.179	-1.20144	-0.60220
97	67	c	1.547	-89.017	-1.43083	-0.71728
68	69	a	1.080	-30.417	1.00222	0.50221
68	69	b	0.000	0.000	0.00000	0.00000
68	69	c	0.000	0.000	0.00000	0.00000
69	68	a	1.080	149.583	-1.00082	-0.50080
69	68	b	0.000	0.000	0.00000	0.00000
69	68	c	0.000	0.000	0.00000	0.00000
7	8	a	14.471	-20.693	13.93729	4.95628
7	8	b	9.627	-138.744	9.50632	3.12267
7	8	c	10.966	102.675	10.80837	3.23969
8	7	a	14.471	159.306	-13.88321	-4.85150
8	7	b	9.627	41.256	-9.50411	-3.09155
8	7	c	10.966	-77.325	-10.77834	-3.19497
69	70	a	0.649	-30.429	0.60082	0.30080
69	70	b	0.000	0.000	0.00000	0.00000
69	70	c	0.000	0.000	0.00000	0.00000
70	69	a	0.649	149.570	-0.60022	-0.30021
70	69	b	0.000	0.000	0.00000	0.00000
70	69	c	0.000	0.000	0.00000	0.00000
70	71	a	0.433	-30.434	0.40022	0.20021
70	71	b	0.000	0.000	0.00000	0.00000
70	71	c	0.000	0.000	0.00000	0.00000
71	70	a	0.433	149.564	-0.40000	-0.20000
71	70	b	0.000	0.000	0.00000	0.00000
71	70	c	0.000	0.000	0.00000	0.00000
72	73	a	0.000	0.000	0.00000	0.00000
72	73	b	0.000	0.000	0.00000	0.00000
72	73	c	1.328	90.874	1.22902	0.61634
73	72	a	0.000	0.000	0.00000	0.00000
73	72	b	0.000	0.000	0.00000	0.00000
73	72	c	1.328	-89.127	-1.22690	-0.61421
72	76	a	2.906	23.614	2.67967	-1.39397
72	76	b	3.092	-107.219	3.07664	-0.82789
72	76	c	2.443	156.737	1.95863	-1.59913
76	72	a	2.906	-156.386	-2.67793	1.39690

76	72	b	3.092	72.780	-3.07371	0.83277
76	72	c	2.443	-23.263	-1.95839	1.60183
73	74	a	0.000	0.000	0.00000	0.00000
73	74	b	0.000	0.000	0.00000	0.00000
73	74	c	0.895	90.860	0.82690	0.41421
74	73	a	0.000	0.000	0.00000	0.00000
74	73	b	0.000	0.000	0.00000	0.00000
74	73	c	0.895	-89.141	-0.82568	-0.41299
74	75	a	0.000	0.000	0.00000	0.00000
74	75	b	0.000	0.000	0.00000	0.00000
74	75	c	0.434	90.850	0.40033	0.20031
75	74	a	0.000	0.000	0.00000	0.00000
75	74	b	0.000	0.000	0.00000	0.00000
75	74	c	0.434	-89.153	-0.40000	-0.20000
76	77	a	1.876	60.562	0.83952	-1.75980
76	77	b	1.860	-57.275	0.80650	-1.73774
76	77	c	1.862	-177.422	0.81128	-1.74946
77	76	a	1.876	-119.439	-0.83848	1.76268
77	76	b	1.860	122.724	-0.80499	1.74079
77	76	c	1.862	2.577	-0.80964	1.75201
76	86	a	0.783	5.815	0.80204	-0.13781
76	86	b	1.392	-129.020	1.42371	0.16575
76	86	c	0.505	157.636	0.39977	-0.33759
86	76	a	0.783	-174.188	-0.80127	0.13805
86	76	b	1.392	50.978	-1.42180	-0.16144
86	76	c	0.505	-22.369	-0.40013	0.33820
77	78	a	1.876	60.561	0.83848	-1.76268
77	78	b	1.923	-44.246	0.40499	-1.94079
77	78	c	1.862	-177.423	0.80964	-1.75201
78	77	a	1.876	-119.439	-0.83813	1.76347
78	77	b	1.923	135.754	-0.40468	1.94167
78	77	c	1.862	2.577	-0.80921	1.75252
78	79	a	0.465	-30.596	0.43326	0.21674
78	79	b	0.000	-28.848	0.00000	-0.00002
78	79	c	0.000	-148.468	0.00000	-0.00002
79	78	a	0.465	149.402	-0.43318	-0.21659
79	78	b	0.000	0.000	0.00000	0.00000
79	78	c	0.000	0.000	0.00000	0.00000

8	12	a	0.000	0.000	0.00000	0.00000
8	12	b	0.215	-147.293	0.20005	0.10003
8	12	c	0.000	0.000	0.00000	0.00000
12	8	a	0.000	0.000	0.00000	0.00000
12	8	b	0.215	32.704	-0.20000	-0.10000
12	8	c	0.000	0.000	0.00000	0.00000
78	80	a	1.942	74.426	0.40487	-1.98021
78	80	b	1.923	-44.246	0.40468	-1.94165
78	80	c	1.862	-177.423	0.80921	-1.75250
80	78	a	1.942	-105.574	-0.40357	1.98459
80	78	b	1.923	135.754	-0.40330	1.94523
80	78	c	1.862	2.576	-0.80663	1.75541
80	81	a	1.942	74.426	0.40357	-1.98459
80	81	b	2.076	-32.621	0.00330	-2.14523
80	81	c	1.862	-177.424	0.80663	-1.75541
81	80	a	1.942	-105.574	-0.40177	1.98921
81	80	b	2.076	147.379	-0.00212	2.14997
81	80	c	1.862	2.575	-0.80396	1.75776
81	82	a	1.942	74.426	0.40177	-1.98921
81	82	b	2.076	-32.621	0.00212	-2.14997
81	82	c	1.993	-158.458	0.20233	-2.05934
82	81	a	1.942	-105.574	-0.40084	1.99109
82	81	b	2.076	147.379	-0.00101	2.15258
82	81	c	1.993	21.542	-0.20134	2.06096
81	84	a	0.000	0.000	0.00000	0.00000
81	84	b	0.000	0.000	0.00000	0.00000
81	84	c	0.648	90.530	0.60162	0.30159
84	81	a	0.000	0.000	0.00000	0.00000
84	81	b	0.000	0.000	0.00000	0.00000
84	81	c	0.648	-89.473	-0.60039	-0.30037
82	83	a	2.095	85.787	0.00084	-2.19109
82	83	b	2.076	-32.621	0.00101	-2.15258
82	83	c	1.993	-158.458	0.20134	-2.06096
83	82	a	2.095	-94.213	0.00000	2.19355
83	82	b	2.076	147.379	0.00000	2.15490
83	82	c	1.993	21.542	-0.20000	2.06271
84	85	a	0.000	0.000	0.00000	0.00000
84	85	b	0.000	0.000	0.00000	0.00000
84	85	c	0.432	90.520	0.40039	0.20037

85	84	a	0.000	0.000	0.00000	0.00000
85	84	b	0.000	0.000	0.00000	0.00000
85	84	c	0.432	-89.483	-0.40000	-0.20000
86	87	a	0.783	5.812	0.80127	-0.13805
86	87	b	1.190	-125.423	1.22180	0.06144
86	87	c	0.505	157.631	0.40013	-0.33820
87	86	a	0.783	-174.191	-0.80081	0.13826
87	86	b	1.190	54.576	-1.22098	-0.05947
87	86	c	0.505	-22.372	-0.40024	0.33848
87	88	a	0.505	36.245	0.40019	-0.33856
87	88	b	0.000	0.000	0.00000	0.00000
87	88	c	0.000	0.000	0.00000	0.00000
88	87	a	0.505	-143.756	-0.40000	0.33875
88	87	b	0.000	0.000	0.00000	0.00000
88	87	c	0.000	0.000	0.00000	0.00000
87	89	a	0.431	-30.551	0.40061	0.20030
87	89	b	0.811	-112.922	0.82098	-0.14053
87	89	c	0.505	157.628	0.40024	-0.33848
89	87	a	0.431	149.447	-0.40042	-0.20027
89	87	b	0.811	67.076	-0.82067	0.14116
89	87	c	0.505	-22.374	-0.40034	0.33866
89	90	a	0.000	0.000	0.00000	0.00000
89	90	b	0.527	-83.588	0.42046	-0.34164
89	90	c	0.000	0.000	0.00000	0.00000
90	89	a	0.000	0.000	0.00000	0.00000
90	89	b	0.527	96.411	-0.42019	0.34191
90	89	c	0.000	0.000	0.00000	0.00000
8	9	a	1.110	-27.749	1.01111	0.50010
8	9	b	0.000	0.000	0.00000	0.00000
8	9	c	0.000	0.000	0.00000	0.00000
9	8	a	1.110	152.251	-1.00990	-0.49889
9	8	b	0.000	0.000	0.00000	0.00000
9	8	c	0.000	0.000	0.00000	0.00000
89	91	a	0.431	-30.553	0.40042	0.20027
89	91	b	0.436	-149.292	0.40021	0.20049
89	91	c	0.505	157.626	0.40034	-0.33866
91	89	a	0.431	149.444	-0.40033	-0.20027
91	89	b	0.436	30.706	-0.40013	-0.20034

91	89	c	0.505	-22.376	-0.40033	0.33882
91	92	a	0.000	0.000	0.00000	0.00000
91	92	b	0.000	0.000	0.00000	0.00000
91	92	c	0.505	157.620	0.40033	-0.33878
92	91	a	0.000	0.000	0.00000	0.00000
92	91	b	0.000	0.000	0.00000	0.00000
92	91	c	0.505	-22.382	-0.40000	0.33910
91	93	a	0.431	-30.556	0.40033	0.20027
91	93	b	0.436	-149.294	0.40013	0.20034
91	93	c	0.000	-148.470	0.00000	-0.00005
93	91	a	0.431	149.442	-0.40023	-0.20019
93	91	b	0.436	30.704	-0.40013	-0.20021
93	91	c	0.000	31.530	0.00000	0.00003
93	94	a	0.431	-30.561	0.40022	0.20021
93	94	b	0.000	0.000	0.00000	0.00000
93	94	c	0.000	0.000	0.00000	0.00000
94	93	a	0.432	149.437	-0.40000	-0.20000
94	93	b	0.000	0.000	0.00000	0.00000
94	93	c	0.000	0.000	0.00000	0.00000
93	95	a	0.000	78.283	0.00000	-0.00002
93	95	b	0.436	-149.296	0.40013	0.20021
93	95	c	0.000	-148.470	0.00000	-0.00003
95	93	a	0.000	0.000	0.00000	0.00000
95	93	b	0.436	30.702	-0.40004	-0.20003
95	93	c	0.000	-90.000	0.00000	0.00000
95	96	a	0.000	0.000	0.00000	0.00000
95	96	b	0.218	-149.299	0.20004	0.10003
95	96	c	0.000	0.000	0.00000	0.00000
96	95	a	0.000	0.000	0.00000	0.00000
96	95	b	0.218	30.698	-0.20000	-0.10000
96	95	c	0.000	0.000	0.00000	0.00000
97	98	a	0.431	-30.384	0.40005	0.19997
97	98	b	0.434	-148.766	0.40033	0.20018
97	98	c	0.462	90.994	0.42757	0.21424
98	97	a	0.431	149.614	-0.40001	-0.19988
98	97	b	0.434	31.232	-0.40027	-0.20009
98	97	c	0.462	-89.009	-0.42752	-0.21415
98	99	a	0.000	82.662	0.00001	-0.00012

98	99	b	0.434	-148.768	0.40027	0.20009
98	99	c	0.462	90.991	0.42752	0.21415
99	98	a	0.000	-97.337	-0.00001	0.00008
99	98	b	0.434	31.227	-0.39999	-0.19991
99	98	c	0.462	-89.014	-0.42752	-0.21383
99	100	a	0.000	82.663	0.00001	-0.00008
99	100	b	0.000	-24.372	-0.00001	-0.00009
99	100	c	0.462	90.986	0.42752	0.21383
100	99	a	0.000	-97.337	0.00000	0.00006
100	99	b	0.000	155.629	0.00001	0.00006
100	99	c	0.462	-89.017	-0.42742	-0.21364
100	450	a	0.000	82.663	0.00000	-0.00006
100	450	b	0.000	-24.371	-0.00001	-0.00006
100	450	c	0.000	-156.705	0.00001	-0.00007
450	100	a	0.000	0.000	0.00000	0.00000
450	100	b	0.000	0.000	0.00000	0.00000
450	100	c	0.000	90.000	0.00000	0.00000